PhD Thesis

Environmental Engineering Program

Anaerobic digestion and bioelectrochemical systems combination for energy and nitrogen recovery optimisation

Míriam Cerrillo Moreno

Supervised by:

Dr. August Bonmatí Blasi and Dr. Marc Viñas Canals

Barcelona, July 2016

El Dr. August BONMATI BLASI i el Dr. Marc VIÑAS CANALS del GIRO unitat mixta IRTA-UPC,

CERTIFIQUEM:

Que na Míriam Cerrillo Moreno ha realitzat sota la nostra direcció el treball titulat "*Anaerobic digestion and bioelectrochemical systems combination for energy and nitrogen recovery optimisation*", presentat en aquesta memòria, i que constitueix la seva Tesi Doctoral per optar al Grau de Doctor per la Universitat Politècnica de Catalunya.

I perquè es tingui coneixement i consti als efectes oportuns, presentem al Programa de Doctorat d'Enginyeria Ambiental de l`Institut de Recerca en Ciència i Tecnologia de la Sostenibilitat, l`esmentada Tesi Doctoral, signant el present certificat a

Caldes de Montbui, Juliol de 2016

Dr. August Bonmatí Blasi Dr. Marc Viñas Canals

Als meus pares, al meu germà

Al Javi, a la Júlia i al Joan

"*Science is not perfect. It's often misused; it's only a tool, but it's the best tool we have. Self-correcting, ever-changing, applicable to everything; with this tool, we vanquish the impossible*."

Carl Sagan

AGRAÏMENTS

Mai hagués pensat quan vaig acabar Ciències Ambientals al 2002, quan vaig decidir que ja havia estudiat prou, que bastants anys després tornaria a trepitjar la universitat. Ni molt menys que quan vaig arribar al GIRO per fer un treball de final de carrera acabaria començant aquesta història que ara està arribant a la seva fi... i tot això no hauria estat possible sense el recolzament de molta gent.

En primer lloc voldria agrair molt especialment als meus directors de tesi tota la seva dedicació, ànims i suport. A l'August Bonmatí, per haver-me proposat iniciar aquest camí i haver-me convençut (tot i els meus dubtes inicials); per trobar sempre el moment per respondre les meves preguntes i mantenir la meva motivació. Al Marc Viñas, per guiar-me pel món de la microbiologia i fer-me pensar sempre una mica més enllà.

Gràcies també al Xavier Flotats, tutor, per la seva disponibilitat i per fer les trobades en congressos i jornades tan enriquidores. També al Josep Illa, per les aportacions a les reunions del projecte i els seus suggeriments per millorar un dels articles de la tesi.

Durant tots aquests anys ha estat molt important per mi el suport dels meus companys del GIRO... Jordi, Edu, Eva, Victor, Belen, Joan, Francesc, Marta, Josep, Pau... igualment tota la gent que ha passat per allà en pràctiques, TFM, TFG, etc... Judit, Lluis, Eudald... que seria una llista molt llarga! Entre tots han fet la meva estada en el GIRO molt agradable i m'han ajudat a desconnectar en cada esmorzar o dinar que he passat amb ells. Sense oblidar-me de totes les celebracions d'aniversaris tan apetitoses! Ni dels comiats: Jordi, Rim, Arantxa, Susana, Maycoll... Especialment vull agrair a l'Ana tot el que m'ha ensenyat sobre el món dels sistemes bioelectroquímics, perquè haver estat amb ella els primers mesos m'ha facilitat molt els meus inicis en el doctorat. Gràcies per tots els consells, ets una gran persona! A la Miriam per tot el que m'ha ensenyat al laboratori de micro, per la seva paciència i per animar-me amb les noves tècniques que tant respecte em feien! I a la Laura Burgos i la Laura Tey, que m'han recolzat als laboratoris amb les analítiques i muntatges, i s'han preocupat tant per mi ;).

Igualment he d'agrair a la meva família, als meus pares pel seu suport; al meu germà, Javier, per haver-me descobert el món de la investigació i ser un exemple a seguir. Al meu marit Javier, que sempre està al meu costat: ara et toca a tu. I als meus petits, la Júlia i el Joan, que m'han fet seguir endavant cada dia amb la seva alegria i energia. Us estimo!

The author thanks the Secretariat for Universities and Research of the Ministry of Economy and Knowledge of the Catalan Government for the FI PhD grant (2013FI_B 00014).

Table of contents

Index of figures

Index of tables

Glossary.....i

List of abbreviations.....iii

Summary.....v

Resumen.....vii

Resum.....ix

CHAPTER 1. General Introduction 1

1.1 Waste management and energy and products recovery..... 3

1.2 Anaerobic digestion for wastes management..... 3

1.2.1 Metabolic steps and microbial populations involved in AD..... 4

1.2.2 Temperature range, pH and inhibitory substances..... 6

1.2.3 Treatment of complex substrates 6

1.3 Bioelectrochemical systems for the treatment of waste streams..... 7

1.3.1 Fundamentals of voltage generation in MFCs 10

1.3.2 Overpotentials.....11

1.3.3 Microbial mechanisms for external transfer of electrons 13

1.3.4 The microbial communities in BES 14

1.3.5 BES as systems to recover nitrogen.....16

1.3.6 Methane potential as renewable energy source 18

1.3.7 BES as systems for obtaining methane.....19

1.4 Combination of AD/BES for organic wastes valorisation 21

1.4.1 System stability and robustness.....22

1.4.2 AD/MFC reactors configurations.....23

1.4.3 AD/MEC reactors configurations.....24

1.5 References.....25

CHAPTER 2. Objectives and Thesis outline 33

2.1 Objectives 35

2.2 Research chronology and scope of the Thesis 36

2.3 Thesis outline 37

CHAPTER 3. Materials and methods 41

3.1 Reactor configuration 43

3.1.1 MFC and MEC 43

3.1.2 MEC with a methanogenic biocathode 45

3.1.3 Anaerobic digester (AD) 47

3.1.4 Stripping and absorption system 48

3.1.5 Upflow anaerobic sludge blanket reactor (UASB) 50

3.2 Analytical methods 51

3.2.1 pH 51

3.2.2 Alkalinity 51

3.2.3 Total and volatile solids 51

3.2.4 Chemical oxygen demand 52

3.2.5 Ammonium nitrogen 52

3.2.6 Total kjeldahl nitrogen 53

3.2.7 Volatile fatty acids 53

3.2.8 Anions and cations determination 54

3.2.9 Biogas composition 54

3.2.10 Dissolved methane 54

3.2.11 Anaerobic biodegradability tests (ABT) 55

3.2.12 Specific methanogenic activity (SMA) 55

3.3 Electrochemical calculations and techniques 56

3.4 System performance calculations and indices 56

3.4.1 Removal efficiencies 56

3.4.2 Charge transport 56
3.4.3 Electrochemical efficiencies....57
3.5 Statistical analysis....58
3.6 Microbial community analysis....58
3.6.1 Total DNA extraction 58
3.6.2 Simultaneous total DNA and RNA extraction and complementary DNA (cDNA) synthesis....58
3.6.3 Quantitative PCR assay (qPCR)....59
3.6.4 High Throughput Sequencing (454-Pyrosequencing) of total eubacterial and archaeal community....59
3.6.5 High throughput sequencing (MiSeq, Illumina) of total eubacteria and archaeal community....60
3.6.6 Biodiversity evaluation and statistical analyses....61
3.7 References....61
CHAPTER 4. Comparative assessment of raw and digested pig slurry treatment in bioelectrochemical systems 63
Abstract....65
4.1 Introduction....67
4.2 Materials and methods 69
4.2.1 Experimental set-up 69
4.2.2 Reactors operation 69
4.2.3 Analyses and calculations 71
4.3 Results and discussion....72
4.3.1 Performance of the BES....72
4.3.2 Microbial community assessment....78
4.4 Conclusions....89
4.5 References....89

CHAPTER 5. Anaerobic digestion instability by organic and nitrogen overloads: polishing of effluents by coupling a microbial fuel cell 93

Abstract 95

5.1 Introduction 97

5.2 Materials and methods 98

5.2.1 Experimental set-up 98

5.2.2 Reactor operation 99

5.2.3 Analyses and calculations 100

5.3 Results and discussion 101

5.3.1 MFC performance under AD instability: assays with VFA pulses in the feed 101

5.3.2 MFC performance under AD stable and inhibited states 102

5.3.3 Microbial community analysis 105

5.4 Conclusions 113

5.5 References 113

CHAPTER 6. Removal of volatile fatty acids and ammonia recovery from unstable anaerobic digesters with a microbial electrolysis cell 117

Abstract 119

6.1 Introduction 120

6.2 Materials and methods 121

6.2.1 Experimental set-up 121

6.2.2 Reactor operation 122

6.2.3 Analyses and calculations 123

6.3 Results and discussion 123

6.3.1 Stable feeding with digested pig slurry (Phase 1) 123

6.3.2 Punctual VFA pulses (Phase 2) 125

6.3.3 Punctual mixed VFA pulses (Phase 3) 127

6.3.4 Continuous daily base mixed VFA pulses (Phase 4) 129

6.4 Conclusions 132

6.5 References....132

CHAPTER 7. Overcoming organic and nitrogen overload in thermophilic anaerobic digestion of pig slurry by coupling a microbial electrolysis cell....135

Abstract....137

7.1 Introduction....139

7.2 Materials and methods....140

7.2.1 Experimental set-up....140

7.2.2 Reactors operation....141

7.2.3 Analyses and calculations....142

7.3 Results and discussion....143

7.3.1 Performance of the AD independent operation....143

7.3.2 Performance of the AD-MEC combined system in series operation....146

7.3.3 Performance of the AD-MEC combined system with recirculation loop....148

7.3.4 Microbial community assessment....149

7.4 Conclusions....157

7.5 References....157

CHAPTER 8. Unravelling the active microbial community in a thermophilic anaerobic digester-microbial electrolysis cell coupled system under different conditions....161

Abstract....163

8.1 Introduction....165

8.2 Materials and methods....166

8.2.1 Experimental set-up....166

8.2.2 Reactors operation....166

8.2.3 Analyses and calculations....167

8.3 Results and discussion....168

8.3.1 Inhibition of the AD with the suppression of the recirculation loop (Phase 1)....168

8.3.2 Recovery of the AD after restarting the recirculation loop (Phase 2)....170

8.3.3 Microbial community assessment....171

8.4 Conclusions....180
8.5 References....180
CHAPTER 9. Assessment of active methanogenic archaea in a methanol-fed upflow anaerobic sludge blanket reactor....183
Abstract....185
9.1 Introduction....187
9.2 Materials and methods....188
9.2.1 Experimental set-up....188
9.2.2 Reactor operation....188
9.2.3 Analyses and calculations....189
9.3 Results and discussion....190
9.3.1 Operation performance....190
9.3.2 Metabolic pathways and granular sludge activity....191
9.3.3 Microbial community assessment....192
9.4 Conclusions....200
9.5 References....200
CHAPTER 10. Start-up of electromethanogenic microbial electrolysis cells with two different biomass inocula....203
Abstract....205
10.1 Introduction....206
10.2 Materials and methods....207
10.2.1 Experimental set-up....207
10.2.2 Reactor operation....207
10.2.3. Analyses and calculations....208
10.3 Results and discussion....209
10.3.1 Operation performance....209
10.3.2 Evaluation of the electromethanogenic MEC as a biogas upgrading technology....211
10.3.3 Microbial community assessment....212

10.4 Conclusions....220
10.5 References....220
CHAPTER 11. Anaerobic digestion and electromethanogenic microbial electrolysis cell integrated system: increased stability and recovery of ammonia and methane....223
Abstract....225
11.1 Introduction....227
11.2 Materials and methods....228
11.2.1 Experimental set-up....228
11.2.2 Reactor operation....228
11.2.3 Analyses and calculations....229
11.3 Results and discussion....231
11.3.1 Performance of the AD independent operation....231
11.3.2 Performance AD-MEC combined system in series operation....233
11.3.3 Performance AD-MEC combined system with recirculation loop....234
11.3.4 Biocathode operation performance....234
11.3.3 Microbial community assessment....235
11.4 Conclusions....244
11.5 References....244
CHAPTER 12. General conclusions....247
12.1 General conclusions....249
12.2 Future work....252

Index of figures

Figure 1.1 Schematic representation of the process of anaerobic digestion (adapted from Villano et al., 2012). SAO: Syntrophic acetate oxidation. 4

Figure 1.2 Schematic representation of an MFC (left) and a MEC (right) (Villano et al., 2012)..... 8

Figure 1.3 Schematic representation of the reaction produced in a biocathode (Villano et al., 2012). 9

Figure 1.4 Representation of different kinds of bacteria in an anodic biofilm including exoelectrogens that transfer electrons by direct contact (green), produce nanowires (purple) and use endogenous mediators (blue). Other non-exoelectrogenic bacteria that live from the products generated by other bacteria (brown) or possibly use nanowires or mediators produced by other microorganisms may be also present (Logan, 2009). 14

Figure 1.5 Schematic representation of the three main routes (A, B and C) of syntrophic interactions in MECs (Lu and Ren, 2016). 15

Figure 1.6 Schematic representation of a methane producing MEC (Villano et al., 2010).....19

Figure 1.7 Ecological parameters of functional stability (Hashsham et al., 2000). 23

Figure 2.1 Graphical abstract of the assays performed in each Chapter.....39

Figure 3.1 Pictures of the materials for BES construction: a) methacrylate frames; b) cation exchange membrane (CEM); c) carbon felt; d) stainless steel mesh. 44

Figure 3.2 Pictures of the MFC. 44

Figure 3.3 a) Scheme and b) picture of the MEC; c) picture of the potentiostat. 45

Figure 3.4 Picture of the granular graphite used as anode and cathode in the MEC BC1 and BC2. 46

Figure 3.5 a) Scheme and b) picture of the anaerobic digester. 47

Figure 3.6 a) Scheme and b) picture of the stripping and absorption system connected to the MEC (right side).....49

Figure 3.7 a) Scheme and b) picture of the UASB; c) detail of the granular biomass.....50

Figure 3.8 Picture of the serum bottles used for SMA test.....55

Figure 4.1 Current density (j) and COD and ammonium removals obtained in the three experimental runs of MFC operation mode with an external resistance of 100 Ω and fed with (a) raw and (b) digested

pig slurry, and in MEC operation mode poising the anode at -200 mV vs. SHE fed with (c) raw and (d) digested pig slurry. ▲COD removal, ■ Ammonium removal, ▪ ▪ Current density.....73

Figure 4.2 (a) COD and (b) ammonium removal efficiency for MFC operation mode after 24 h with the different external resistances (R_{ext}) assayed and (c) COD and (d) ammonium removal efficiency for MEC operation mode after 48 h poising the anode at the different potentials (E_{anode}) assayed. Raw pig slurry in black, digested pig slurry in light grey and AD-MFC or AD-MEC integrated system in dark grey. Significance of the differences among values in the same resistance/potential is represented by lowercase; and among different resistance/potential with the same feeding solution, by uppercase. 74

Figure 4.3 Comparison of the total charge production (Q^-) to the transport of charge in the form of specific ions transferred to the cathode compartment in MFC mode after 24 h with the different external resistances (R_{ext}) assayed and using (a) raw pig slurry and (b) digested pig slurry, and in MEC operation mode after 48 h poising the anode at the different potentials (E_{anode}) assayed using (c) raw pig slurry and (d) digested pig slurry. Q^-, in dotted bars; Na^+, in black bars; K^+, in light grey; NH_4^+, in striped bars; Ca^{2+}, in dark grey bars; and Mg^{2+}, in white bars.....78

Figure 4.4 Rarefaction curves for MFC and MEC anode and raw and digested pig slurry samples regarding (a) Eubacterial and (b) Archaeal community. Inoculum, dark blue; MFC, red; Raw pig slurry, green; Digested pig slurry, purple; and MEC, light blue. 79

Figure 4.5 Taxonomic assignment by means RDP Bayesian classifier of 454-pyrosequencing reads from massive 16SrRNA libraries of Eubacteria in the inoculum, and anode under MFC and MEC mode at the a) phylum b) family levels. Relative abundance was defined as the number of reads (sequences) affiliated with any given taxon divided by the total number of reads per sample. Phylogenetic groups with a relative abundance lower that 1% were categorised as “others”.....81

Figure 4.6 Taxonomic assignment by means RDP Bayesian classifier of 454-pyrosequencing reads from massive 16SrRNA libraries of Eubacteria of raw and digested pig slurry at the a) phylum b) family levels. Relative abundance was defined as the number of reads (sequences) affiliated with any given taxon divided by the total number of reads per sample. Phylogenetic groups with a relative abundance lower that 1% were categorised as “others”. 84

Figure 4.7 Correspondence Analysis for inoculum, MFC and MEC anode samples regarding (a) Eubacterial and (b) Archaeal community.....85

Figure 4.8 Taxonomic assignment by means of RDP Bayesian classifier of 454-pyrosequencing reads from massive 16SrRNA libraries of Archaea in the inoculum, and anode from MFC and MEC mode at family levels. Relative abundance was defined as the number of reads (sequences) affiliated with any given

taxon divided by the total number of reads per sample. Phylogenetic groups with a relative abundance lower that 1% were categorised as “others”. 87

Figure 4.9 Taxonomic assignment by means of RDP Bayesian classifier of 454-pyrosequencing reads from massive 16SrRNA libraries of Archaea of raw and digested pig slurry at family levels. Relative abundance was defined as the number of reads (sequences) affiliated with any given taxon divided by the total number of reads per sample. Phylogenetic groups with a relative abundance lower that 1% were categorised as “others”.....87

Figure 5.1 a) Current density and b) VFA concentration and pH in the anode compartment obtained in Phase 1 during the pure and mixed VFA pulses. Arrows show when each pulse was performed. 102

Figure 5.2 Current density and COD and ammonium removal efficiencies obtained in Phase 2. 103

Figure 5.3 VFA concentration in a) the influent and b) the effluent in Phase 2.....105

Figure 5.4 Gene copy numbers for *16S* rRNA and *mcrA* genes and ration between them, of the initial and final MFC anode biofilm (MFCi and MFCf, respectively), and the MFC influent in Phase 1. 106

Figure 5.5 Rarefaction curves for initial (MFC_i) and final (MFC_f) MFC anode samples and the digested pig slurry in Phase 1 regarding (a) Eubacterial and (b) Archaeal community.....108

Figure 5.6 Taxonomic assignment of sequencing reads from Eubacterial community of the initial and final MFC anode biofilm (MFCi and MFCf, respectively), and the MFC influent of Phase 1, at a) phylum b) family levels. Relative abundance was defined as the number of reads (sequences) affiliated with any given taxon divided by the total number of reads per sample. Phylogenetic groups with a relative abundance lower that 1% were categorised as “others”. 110

Figure 5.7 Taxonomic assignment of sequencing reads from Archaeal community of the initial and final MFC anode biofilm (MFCi and MFCf, respectively), and the MFC influent of Phase 1, at family level. Relative abundance was defined as the number of reads (sequences) affiliated with any given taxon divided by the total number of reads per sample. Phylogenetic groups with a relative abundance lower that 1% were categorised as “others”. 111

Figure 5.8 Correspondence Analysis for initial (MFC_i) and final (MFC_f) MFC anode samples and the 3 AD influents (AD-Ph1, AD-Ph2a and AD-Ph2b) regarding (a) Eubacterial and (b) Archaeal community. 112

Figure 6.1 Current density during Phase 1, of stable feeding with digested pig slurry. 124

Figure 6.2 Current density, VFA concentration, ammonium removal and anode and cathode pH obtained in Phase 2 during the VFA pulses of (a) 250 and 500 mg of acetate, (b) 500 mg of propionate and (c) 500 mg of butyrate. Arrows show when each pulse was performed. 127

Figure 6.3 Current density, VFA concentration, ammonium removal and anode and cathode pH obtained in Phase 3 during the mixed VFA pulses of (a) 500 mg of acetate and 500 mg of propionate and (b) 1000 mg of acetate, 200 mg of propionate and 85 mg of butyrate. Arrows show when each pulse was performed. 129

Figure 6.4 Current density, VFA concentration, ammonium removal and anode and cathode pH obtained in Phase 4, during daily pulses of 1000 mg of acetate, 200 mg of propionate and 85 mg of butyrate. Arrows show when each pulse was performed. 131

Figure 7.1 Scheme of the set up of the AD-MEC combined system coupled to the stripping and absorption unit. 141

Figure 7.2 Performance of the AD regarding (a) COD removal efficiency; (b) methane productivity; (c) IA:TA ratio; (d) VFA concentration; and (e) free ammonia concentration (FAN) and pH. 145

Figure 7.3 Performance of the MEC regarding (a) Current density; (b) ammonium removal efficiency; and (c) VFA concentration in the effluent. 147

Figure 7.4 Gene copy numbers for *16S rRNA* and *mcrA* genes and ration between them, of the effluent of the AD at the five phases, and initial and final MEC anode biofilm (MECi and MECf, respectively)....150

Figure 7.5 Taxonomic assignment of sequencing reads from Eubacterial community of the effluent of the AD at the five phases, and initial and final MEC anode biofilm (MECi and MECf, respectively), at a) phylum b) family levels; and c) from Archaeal community at family level. Relative abundance was defined as the number of reads (sequences) affiliated with any given taxon divided by the total number of reads per sample. Phylogenetic groups with a relative abundance lower that 1% were categorised as "others". 152

Figure 7.6 Correspondence Analysis for initial (MEC_i) and final (MEC_f) MEC anode samples and the 5 phases AD samples (AD-Ph1 to AD-Ph5) regarding (a) Eubacterial and (b) Archaeal community. 155

Figure 8.1 Performance of the AD regarding (a) COD removal efficiency; (b) methane production; (c) VFA concentration; and (d) IA:TA ratio. 169

Figure 8.2 Performance of the MEC regarding current density and COD and ammonium removal efficiency (phase 2). 171

Figure 8.3 Gene copy numbers for 16S rRNA and mcrA genes and ratio between them of DNA and cDNA (gene expression), of the effluent of the AD at the end of Phases 1 and 2 and the initial and final MEC anode biofilm (MECi and MECf, respectively). 172

Figure 8.4 Taxonomic assignment of sequencing reads from Eubacterial community of the effluent of the AD at the end of Phases 1 (Ph1) and 2 (Ph2) and the initial and final MEC anode biofilm (MECi and MECf, respectively) for DNA and cDNA, at a) phylum b) family levels. Relative abundance was defined as the number of reads (sequences) affiliated with any given taxon divided by the total number of reads per sample. Phylogenetic groups with a relative abundance lower that 1% were categorised as "others". 173

Figure 8.5 Taxonomic assignment of sequencing reads from Archaeal community of the effluent of the AD at the end of Phases 1 (Ph1) and 2 (Ph2) and the initial and final MEC anode biofilm (MECi and MECf, respectively) for DNA and cDNA at family level. Relative abundance was defined as the number of reads (sequences) affiliated with any given taxon divided by the total number of reads per sample. Phylogenetic groups with a relative abundance lower that 1% were categorised as "others". 175

Figure 8.6 Correspondence Analysis of the effluent of the AD at the end of Phases 1 (Ph1) and 2 (Ph2) and the initial and final MEC anode biofilm (MECi and MECf, respectively) for DNA and cDNA samples regarding (a) Eubacteria and (b) Archaea community. 179

Figure 9.1 Gene copy numbers for *16S* rRNA and *mcr*A genes and ratio between them of DNA and mRNA (cDNA), of the initial inoculum and the biomass of the UASB at the end of Phases 1 (acetate feeding) and 3 (methanol feeding). 193

Figure 9.2 Taxonomic assignment of sequencing reads from Eubacterial community of the initial inoculum and the biomass of the UASB at the end of Phases 1 (acetate feeding) and 3 (methanol feeding) for genomic DNA and RNA (cDNA) level , at a) phylum b) family levels. Relative abundance was defined as the number of reads (sequences) affiliated with any given taxon divided by the total number of reads per sample. Phylogenetic groups with a relative abundance lower that 1% were categorised as "others". 195

Figure 9.3 Taxonomic assignment of sequencing reads from Archaeal community of the initial inoculum and the biomass of the UASB at the end of Phases 1 (acetate feeding) and 3 (methanol feeding) for genomic DNA and RNA (cDNA) at family level. Relative abundance was defined as the number of reads (sequences) affiliated with any given taxon divided by the total number of reads per sample. Phylogenetic groups with a relative abundance lower that 1% were categorised as "others". 196

Figure 9.4 Correspondence Analysis of the initial inoculum and the biomass of the UASB at the end of Phases 1 (acetate feeding) and 3 (methanol feeding) for DNA and cDNA samples regarding (a) Eubacteria and (b) Archaea community. 199

Figure 10.1 Current density profiles obtained for (a) BC1 and (b) BC2. 209

Figure 10.2 Cyclic voltammograms obtained for BC1 and BC2 at the start (BC1i and BC2i) and the end (BC1f and BC2f) of the assay. 211

Figure 10.3 Gene copy numbers and transcripts of *16S* rRNA and *mcr*A genes from initial inoculum of BC1 and BC2 (i) and the final enrichment on each biocathode (f). 212

Figure 10.4 Taxonomic assignment of sequencing reads from Eubacterial community of the inoculum of BC1 and BC2 and the final sample of each cathode for DNA (total population) and cDNA (active populations), at a) phylum b) family levels. Relative abundance was defined as the number of reads (sequences) affiliated with any given taxon divided by the total number of reads per sample. Phylogenetic groups with a relative abundance lower that 1% were categorised as "others". 214

Figure 10.5 Taxonomic assignment of sequencing reads from Archaeal community of the inoculum of BC1 and BC2 and the final sample of each cathode for DNA (total population) and cDNA (active populations) at family level. Relative abundance was defined as the number of reads (sequences) affiliated with any given taxon divided by the total number of reads per sample. Phylogenetic groups with a relative abundance lower that 1% were categorised as "others". 216

Figure 10.6 Correspondence Analysis (CA) of the inoculum of BC1 and BC2 and the final sample of each cathode for 16SrDNA and 16SrRNA (cDNA) regarding (a) Eubacteria and (b) Archaea community on the basis of MiSeq-16S based profile (OTU level). 219

Figure 11.1 Performance of the AD regarding (a) COD removal efficiency; (b) methane production; (c) VFA concentration; and (d) IA:TA ratio. 232

Figure 11.2 Current density profile obtained during the operation of the MEC. Data corresponding to the unstable period (shaded) was not considered for calculations. 233

Figure 11.3 Cyclic voltammograms of the MEC after the cathode inoculation (t=0 d) and at the end of Phase 2 and 3 ((t=78 d and t=222 d, respectively). 235

Figure 11.4 Gene copy numbers for *16S* rRNA and *mcr*A genes and ratio between them of DNA and cDNA, of the AD effluent at the end of Phases 1, 2 and 3, and the biofilm harboured on the anode and cathode of the MEC at the end of Phase 2 and 3. 236

Figure 11.5 Taxonomic assignment of sequencing reads from Eubacterial community of the AD effluent at the end of Phases 1, 2 and 3, and the biofilm harboured on the anode and cathode of the MEC at the end of Phase 2 and 3 for DNA and cDNA, at a) phylum and b) family levels. Relative abundance was defined as the number of reads (sequences) affiliated with any given taxon divided by the total number of reads per sample. Phylogenetic groups with a relative abundance lower that 1% were categorised as "others". 238

Figure 11.6 Taxonomic assignment of sequencing reads from Archaeal community of the AD effluent at the end of Phases 1, 2 and 3, and the biofilm harboured on the anode and cathode of the MEC at the end of Phase 2 and 3 for DNA and cDNA, at family level. Relative abundance was defined as the number of reads (sequences) affiliated with any given taxon divided by the total number of reads per sample. Phylogenetic groups with a relative abundance lower that 1% were categorised as "others". 240

Figure 11.7 Correspondence Analysis of the AD effluent at the end of Phases 1, 2 and 3, and the biofilm harboured on the anode and cathode of the MEC at the end of Phase 2 and 3 for DNA and cDNA samples regarding (a) Eubacteria and (b) Archaea community. 243

Index of tables

Table 4.1 Characterisation of raw and digested pig slurry used as feedings in the AD and the BES. Abbreviations: MFC: microbial fuel cell, MEC: microbial electrolysis cell, AD: anaerobic digestion, COD: chemical oxygen demand, N-NH4+: ammonium nitrogen, TS: total solids, VS: volatile solids.....70

Table 4.2 Conditions tested in MFC and MEC operation modes. Abbreviations: MFC: microbial fuel cell, MEC: microbial electrolysis cell, OCV: open circuit voltage; R_{ext} (external resistance); E_{anode} (anode potential).....71

Table 4.3 Coulombic Efficiency and CH_4 production efficiency obtained in the different assays. Abbreviations: CE: coulombic efficiency, MFC: microbial fuel cell, MEC: microbial electrolysis cell, R_{ext} (external resistance), E_{anode} (anode potential).....76

Table 4.4 Diversity index for Eubacterial and Archaeal community of the inoculum, MFC and MEC mode and raw and digested pig slurry. Data normalised to the sample with the lowest number of reads (2115 and 867 for eubacterial and archaeal, respectively). Abbreviations: OTU: operational taxonomic unit, MFC: microbial fuel cell, MEC: microbial electrolysis cell, SD: standard deviation. (mean±SD).....80

Table 4.5 Eubacterial microbial community enriched in MFC (microbial fuel cell) and MEC (microbial electrolysis cell) mode (percentage of total 16S rRNA reads).....82

Table 4.6 Archaeal microbial community enriched in MFC (microbial fuel cell) and MEC (microbial electrolysis cell) mode (percentage of total 16S rRNA reads).....88

Table 5.1 Characterisation of the digested pig slurries used as feeding in the MFC.....98

Table 5.2 Operational conditions for de MFC reactor during the series of pure and mixed VFA pulses in Phase 1.....99

Table 5.3 Diversity index for Eubacterial and Archaeal community of the MFC anode and MFC influent in Phase 1 samples (average±SD). Data normalised to the sample with the lowest number of reads (17049 and 16875 for eubacterial and archaeal, respectively).....107

Table 6.1 Characterisation of digested pig slurry and the final solution used as feeding in the MEC. 122

Table 6.2 Operational conditions for the MEC reactor during the series of VFA pulses. 123

Table 7.1 Characterisation of the diluted pig slurry used as feeding solution in the anaerobic digester (AD) in Phase 1 and Phases 2 to 5 (n=number of samples).....142

Table 7.2 Operational conditions for the AD reactor and the MEC. 142

Table 7.3 Summary of the parameters for the AD and the MEC reactors in the different phases (n=number of samples). Results for the AD correspond to the stable period of each phase. n.a.; data not available as the stripping and absorption system was disconnected. 144

Table 7.4 Diversity index for Eubacterial and Archaeal community of the MEC anode and AD effluent samples (mean±standard deviation). Data normalised to the sample with the lowest number of reads (16872 and 19235 for eubacterial and archaeal, respectively). 151

Table 7.5 Operational taxonomic units (OTUs) of eubacterial microbial community that were not detected in the initial microbial electrolysis cell (MEC) sample (MECi) but were present in the anaerobic digester and enriched in the final MEC sample (MECf) after the AD-MEC integrated operation (percentage of total 16S rRNA reads). 154

Table 7.6 Operational taxonomic units (OTUs) of eubacterial microbial community that were not detected in the anaerobic digester (AD) before the connection of the recirculation loop (AD-Ph2) but were present in the microbial electrolysis cell (MEC) and enriched in the final AD sample (AD-Ph5) after the AD-MEC integrated operation (percentage of total 16S rRNA reads). 154

Table 7.7 Operational taxonomic units (OTUs) most abundant of eubacterial microbial community in the final microbial electrolysis cell (MEC) sample (MECf) shared with the final sample of the anaerobic digester (AD-Ph5) (percentage of total 16S rRNA reads). 154

Table 7.8 Operational taxonomic units (OTUs) most abundant of archaeal microbial community in the final microbial electrolysis cell (MEC) sample (MECf) shared with the final sample of the anaerobic digester (AD-Ph5) (percentage of total 16S rRNA reads). 157

Table 8.1 Characterisation of the diluted pig slurry used as feeding in the anaerobic digester (AD) (n=number of samples). 167

Table 8.2 Operational conditions for the AD reactor. 167

Table 8.3 Diversity index for Eubacterial and Archaeal community of the effluent of the AD at the end of Phases 1 and 2 and the initial and final MEC anode biofilm (MECi and MECf, respectively) (mean±standard deviation). Data normalised to the sample with the lowest number of reads (36854 and 62211 for eubacteria and archaea, respectively). 177

Table 9.1 Operational conditions for the UASB reactor. 189

Table 9.2 Average performance of the UASB reactor in the different operational phases. 190

Table 9.3 Specific methanogenic activity (SMA) of the inoculum and Phase 1 and 3 granular sludge fed with different substrates. n.d: not determined. 191

Table 9.4 Diversity index for Eubacteria and Archaea community of the inoculum and the biomass of the UASB at the end of Phases 1 (acetate feeding) and 3 (methanol feeding) for DNA and cDNA samples (mean±standard deviation). Data normalised to the sample with the lowest number of reads (50466 and 66226 for eubacterial and archaeal, respectively). 197

Table 10.1 Performance of BC1 and BC2 (average±standard deviation).....210

Table 10.2 Diversity indices for Eubacteria and Archaeal community of the inoculums and the final biofilm of BC1 and BC2 (BC1f and BC2f, respectively) for 16S rRNA (cDNA) and 16S rDNA (DNA) massive libraries (mean±standard deviation). Data normalised to the sample with the lowest number of reads (104277 and 93126 for eubacterial and archaeal, respectively).....218

Table 11.1 Characterisation of the raw pig slurry used as feeding solution in the anaerobic digester (AD) in Phase 1 and Phases 2 and 3 (n=number of samples; mean±standard deviation). 229

Table 11.2 Operational conditions for the AD reactor and the MEC (mean±standard deviation). 229

Table 11.3 Summary of the main parameters for the AD and the MEC reactors in the different phases. Results for the AD correspond to the stable period of each phase (mean±standard deviation).....231

Table 11.4 Diversity index for Eubacteria and Archaea community of the AD effluent at the end of Phases 1, 2 and 3, and the biofilm harboured on the anode and cathode of the MEC at the end of Phase 2 and 3 for DNA and cDNA samples (mean±standard deviation). Normalised to the lowest number of reads (56424 and 59671 for eubacteria and archaea, respectively) 242

Glossary

Anaerobic digestion (AD): wastewater treatment in which microorganisms convert biodegradable material into methane in the absence of oxygen.

Anode: electrode of an electrochemical system at which an oxidation reaction takes place.

Biocathode (BC): cathode of a BES in which reduction reactions are catalysed by microorganisms.

Bioelectrochemical System (BES): electrochemical bioreactor in which active microorganisms catalyse oxidation and/or reduction reactions at an electrode surface.

Biofilm: community of microorganisms growing embedded within a self-produced matrix of extracellular polymeric substances on a solid support.

Complementary DNA (cDNA): double-stranded DNA synthesised from a single stranded RNA (e.g., messenger RNA (mRNA))

Coulombic efficiency (CE): amount of coulombs captured in electrical current generation relative to the maximum possible assuming complete oxidation of the substrate.

Cathode: electrode of an electrochemical system at which reduction reaction takes place.

Cationic exchange membrane (CEM): type of membrane that is selectively permeable to cations.

Chemical oxygen demand (COD): measure of the amount of organic compounds in water. Corresponds with the amount of oxygen needed to completely oxidise the organic compounds to carbon oxide.

Counter electrode: electrode that serves as a source or sink for electrons so that current can be passed from the external circuit through the cell.

Cyclic voltammetry (CV): electrochemical technique used to characterise electron transfer processes in which a cyclic potential sweep is imposed on the working electrode, while monitoring the response of the system in terms of current intensity.

Diffusion: net movement of a substrate by gradient of concentration.

Electromotive force (EMF): difference between the cathodic and the anodic potentials, which is positive for spontaneous processes and negative for nonspontaneous processes.

Extracellular electron transfer: process in which electrons derived from the oxidation of electron donors are transferred out of the cell to reduce an electron acceptor.

Electrogenic bacteria: microorganisms which are capable of either donating electrons to or accepting electrons from an electrode.

Intermediate alkalinity (IA): measure of the concentration of VFA of a sample, obtained with the titration from pH 5.75 to 4.3.

Microbial fuel cell (MFC): bioelectrochemical system in which the chemic energy stored in organic compounds is directly converted into electrical energy.

Microbial electrolysis cell (MEC): bioelectrochemical system in which value-added products can be generated by applying an electric voltage.

Migration: motion of charged species as a result of an electric field.

Nanowire: electrically conductive appendages that electrogenic bacteria use for extracellular electron transfer.

Messenger RNA (mRNA): RNA molecule that convey genetic information from DNA to the ribosome, where they specify the amino acid sequence of the protein products of gene expression

Partial alkalinity (PA): measure of bicarbonate concentration, obtained with the titration from the original pH of a sample to pH 5.75.

Potentiostat: electronic hardware required to set a specific potential for an electrode, control a three electrode cell and run most electroanalytical experiments.

Reference electrode: electrode with a stable and well-known electrode potential.

Standard hydrogen electrode (SHE): redox electrode which forms the basis of the thermodynamic scale of oxidation-reduction potentials. By convention, it is zero at all temperatures to allow the comparison with all other electrode reactions.

Total alkalinity (TA): alkalinity which corresponds to partial alkalinity (PA) plus intermediate alkalinity (IA).

Two-chamber cell BES: bioelectrochemical system with a membrane that separates the anode and the cathode chambers.

Working electrode: electrode in an electrochemical system on which the reaction of interest is occurring.

List of abbreviations

16S rRNA	Small subunit of the ribosomal RNA
A	Ampere
ABT	Anaerobic biodegradability test
AD	Anaerobic digestion
AD-MEC	Anaerobic digestion-microbial electrolysis cell integrated system
AD-MFC	Anaerobic digestion-microbial fuel cell integrated system
BC	Biocathode
BES	Bioelectrochemical System
BLAST	Basic local alignment search tool
C	Coulomb
CA	Correspondence analysis
cDNA	Complementary DNA
CE	Coulombic efficiency
CEM	Cationic exchange membrane
COD	Chemical oxygen demand
CODs	Soluble chemical oxygen demand
CSTR	Continuous stirred tank reactor
CV	Cyclic voltammetry
DGGE	Denaturing gradient gel electrophoresis
DIET	Direct interspecies electron transfer
E	Potential
EDTA	Ethylenediaminetetraacetic acid
EE_e	Energy efficiency relative to electrical input
EE_s	Energy efficiency relative to the energy content of the substrate
EE_{e+s}	Energy efficiency relative to electrical input and the energy content of the substrate
EET	External electron transfer
EMF	Electromotive force
F	Faraday's constant (96485 C mol^{-1}_{e-})
FAN	Free ammonia concentration
FID	Flame ionisation detector
HRT	Hydraulic retention time
I	Current intensity
IA	Intermediate alkalinity

IC	Ionic chromatography
MFC	Microbial fuel cell
MEC	Microbial electrolysis cell
mRNA	Messenger RNA
NLR	Nitrogen loading rate
$N\text{-}NH_4^+$	Ammonium nitrogen
NTK	Total kjeldahl nitrogen
OCV	Open circuit voltage
OLR	Organic loading rate
OTU	Operational taxonomic unit
PA	Partial alkalinity
R_{cat}	Cathodic recovery efficiency
PCR	Polymerase chain reaction
Q^+	Transport of positive charges in the form of cations through the cation exchange membrane
Q^+	Transport of negative charges in the form of electrons through the electric circuit
QIIME	Quantitative insights into microbial ecology
qPCR	Quantitative polymerase chain reaction
RDP	Ribosomal database project
R_{ext}	External resistance
rRNA	Ribosomal RNA
SAO	Syntrophic acetate oxidation
SAOB	Syntrophic acetate-oxidising bacteria
SHE	Standard hydrogen electrode
SMA	Specific methanogenic activity
TA	Total alkalinity
TAN	Total ammonia nitrogen
TCD	Thermal conductivity detector
TS	Total solids
UASB	Upflow anaerobic sludge blanket
VFA	Volatile fatty acid
VS	Volatile solids
VSS	Volatile suspended solids
Ω	Ohm

Summary

Anaerobic digestion (AD) is a widespread technology for treating high strength waste streams, such as livestock manure. Faced with its many advantages, such as energy recovery in the form of biogas, the AD has some limitations: i) high nutrient concentrations in effluents (especially nitrogen and phosphorus); ii) process instability against organic or nitrogen overloads, or the presence of inhibitors; and iii) the need for pre-processing of biogas to increase its methane content for using it as renewable energy for certain uses, such as injection into the natural gas grid or being used as fuel for transport. Therefore, it is necessary to implement strategies to keep the AD process and effluent quality under control, and increase the amount of energy recovered in the system.

Bioelectrochemical systems (BES) have the versatility to be combined with AD for its optimisation. They are bioreactors in which the oxidation and/or reduction reactions are catalysed by microorganisms on the surface of an electrode and generally produced in two compartments separated by an ion exchange membrane.

In this Thesis the combination of AD-BES technology has been studied with the aim of increasing energy recovery and recover nitrogen from a complex waste stream such as pig slurry. Two-chambered cells with cation exchange membrane operated both in microbial fuel cell (MFC) and microbial electrolysis cell mode (MEC) have been used.

In the first part of the Thesis integration of BES technology with AD was studied to improve system stability, the quality of the effluent and recovery of nitrogen. Firstly, batch tests were performed using an MFC and a MEC to compare the operation with fresh and digested pig slurry in both systems regarding the reduction of organic load and ammonium recovery for its reuse. Subsequently, both cells were operated continuously with digestate and their ability to absorb specific organic overloads was checked by simulating a malfunction of the AD by performing volatile fatty acids pulses in the anode chambers. Next, a lab-scale AD was connected in series with both cells and was subjected to an organic and nitrogen overload, which caused inhibition process. The MEC and MFC functioned as suitable systems for maintaining the quality of the effluent, reducing the residual organic load of the digestate and recovering ammonium. In addition, a recirculation loop between the AD and the MEC allowed stabilising the inhibited AD. Afterwards, the effectiveness of the recirculation loop for maintaining the operation of the AD was checked by its temporary interruption and subsequent reconnection. Total and active microbial populations of the reactors were analysed during the different phases to study their evolution during periods of inhibition and recirculation.

In the second part of the Thesis the implementation of the MEC technology for the enrichment of the biogas produced in the AD, through the establishment of a biofilm on the

cathode of the MEC capable of converting CO_2 to methane, was studied to increase energy recovery of the system. First, an up-flow anaerobic sludge blanket reactor (UASB) was operated with the objective of obtaining biomass enriched in methanogenic archaea to be inoculated into the cathode of a MEC. Two MECs were set up to compare their operation with two different inocula (biomass enriched in the UASB and anaerobic granular biomass) and the evolution of the microbial population. Finally, AD-MEC-biocathode technology was integrated into a system where the digestate was refined in the anode chamber of the MEC and recirculated to control AD inhibition by organic and nitrogen overload; ammonia was recovered from the digestate thanks to its transfer to the cathode chamber; and CO_2 introduced into the cathode chamber was transformed into methane to increase the calorific value of biogas.

The work developed in this Thesis has revealed at lab-scale that BES systems have the versatility to be combined with the AD and improve its operation, the effluent quality and energy recovery and nitrogen.

Resumen

La digestión anaerobia (DA) es una tecnología ampliamente extendida para el tratamiento de corrientes residuales de alta carga orgánica, como pueden ser los residuos ganaderos. Frente a sus múltiples ventajas, como la recuperación de energía en forma de biogás, la DA presenta algunas limitaciones: i) elevadas concentraciones de nutrientes en los efluentes (especialmente nitrógeno y fósforo); ii) inestabilidad del proceso frente a sobrecargas orgánicas o nitrogenadas, o la presencia de productos inhibidores; y iii) necesidad de un procesado previo del biogás para aumentar su contenido en metano para su aprovechamiento como energía renovable para determinados usos, como su inyección en la red de gas natural o la utilización como combustible para el transporte. Por lo tanto, será necesario implementar estrategias que permitan mantener el proceso de DA y la calidad de los efluentes bajo control, y aumentar la cantidad de energía recuperada en el sistema.

Los sistemas bioelectroquímicos (BES) presentan una gran versatilidad para ser combinados con la DA para su optimización. Se trata de bioreactores en los que las reacciones de oxidación y/o reducción están catalizadas por microorganismos sobre la superficie de un electrodo y generalmente producidas en dos compartimentos separados por una membrana de intercambio iónico.

En esta Tesis se ha estudiado la combinación de DA con la tecnología BES con el objetivo de aumentar la recuperación de energía y recuperar nitrógeno de una corriente residual compleja como son los purines porcinos. Se han utilizado celdas de doble compartimento con membrana de intercambio catiónico operadas tanto en modo de celda de combustible microbiana (microbial fuel cell, MFC) como en modo celda de electrólisis microbiana (microbial electrolysis cell, MEC).

En la primera parte de la Tesis se estudió la integración de la tecnología BES con la DA para mejorar la estabilidad del sistema, la calidad del efluente y la recuperación de nitrógeno. En primer lugar se realizaron ensayos en discontinuo con una MFC y una MEC para comparar la operación con purín de cerdo fresco y digerido en ambos sistemas respecto a la reducción de carga orgánica y recuperación de amonio para su posterior reutilización. Posteriormente, ambas celdas fueron operadas en continuo con digerido y se comprobó su capacidad para absorber sobrecargas orgánicas puntuales, simulando un mal funcionamiento del DA mediante pulsos de ácidos grasos volátiles en las cámaras anódicas. A continuación, un DA a escala de laboratorio fue conectado en serie con ambas celdas y fue sometido a una sobrecarga orgánica y nitrogenada que provocó la inhibición del proceso. La MFC y la MEC funcionaron como sistemas adecuados para mantener la calidad del efluente, reduciendo la carga orgánica residual del digerido y recuperando amonio. Además, un circuito de recirculación entre el DA y

la MEC permitió estabilizar el DA inhibido. Finalmente, la efectividad del circuito de recirculación para el mantenimiento de la operación del DA fue comprobada, mediante su interrupción temporal y posterior reconexión. La población microbiana total y activa de los reactores fue analizada durante las diferentes fases para estudiar su evolución durante los períodos de inhibición y recirculación.

En la segunda parte de la Tesis se estudió la aplicación de la tecnología MEC para el enriquecimiento del biogás producido en la DA, gracias al establecimiento de un biofilm en el cátodo de la MEC capaz de convertir CO_2 en metano, aumentando la recuperación de energía del sistema. En primer lugar se operó un reactor anaerobio de lecho fluidificado ascendente (up-flow anaerobic sludge blanket, UASB) con el objetivo de obtener biomasa enriquecida en archaeas metanogénicas, para posteriormente ser inoculada en el cátodo de una MEC. Se pusieron en marcha dos celdas MEC para comparar su operación con dos inóculos diferentes (biomasa enriquecida en el UASB y biomasa granular anaerobia) y la evolución de la población microbiana. Finalmente, la tecnología DA-MEC-biocátodo fue integrada en un sistema en el que el digerido era refinado en la cámara anódica de la MEC y recirculado al DA para controlar la inhibición por sobrecarga orgánica y nitrogenada; el amonio era recuperado del digerido por transferencia a la cámara catódica; y el CO_2 introducido en la cámara catódica era transformado en metano para aumentar el poder calorífico del biogás.

El trabajo desarrollado en esta Tesis ha permitido comprobar a escala de laboratorio que los sistemas BES presentan una gran versatilidad para ser combinados con la DA y mejorar su operación, la calidad del efluente y la recuperación de energía y nitrógeno.

Resum

La digestió anaeròbia (DA) és una tecnologia àmpliament estesa per al tractament de corrents residuals d'alta càrrega orgànica, com poden ser els residus ramaders. Davant els seus múltiples avantatges, com la recuperació d'energia en forma de biogàs, la DA presenta algunes limitacions: i) elevades concentracions de nutrients en els efluents (especialment nitrogen i fòsfor); ii) inestabilitat del procés enfront de sobrecàrregues orgàniques o nitrogenades, o la presència de productes inhibidors; i iii) necessitat d'un processament previ del biogàs per augmentar el seu contingut en metà per al seu aprofitament com a energia renovable per a determinats usos, com la injecció a la xarxa de gas natural o la utilització com a combustible per al transport. Per tant, caldrà implementar estratègies que permetin mantenir el procés de DA i la qualitat dels efluents sota control, i augmentar la quantitat d'energia recuperada en el sistema.

Els sistemes bioelectroquímics (BES) presenten una gran versatilitat per ser combinats amb la DA per a la seva optimització. Es tracta de bioreactors en què les reaccions d'oxidació i/o reducció estan catalitzades per microorganismes sobre la superfície d'un elèctrode i generalment produïdes en dos compartiments separats per una membrana d'intercanvi iònic.

En aquesta tesi s'ha estudiat la combinació de DA amb la tecnologia BES amb l'objectiu d'augmentar la recuperació d'energia i recuperar nitrogen d'un corrent residual complex com són els purins porcins. S'han utilitzat cel·les de doble compartiment amb membrana d'intercanvi catiònic operades tant en mode de cel·la de combustible microbiana (microbial fuel cell, MFC) com en mode cel·la d'electròlisi microbiana (microbial electrolysis cell, MEC).

A la primera part de la tesi es va estudiar la integració de la tecnologia BES amb la DA per millorar l'estabilitat del sistema, la qualitat de l'efluent i la recuperació de nitrogen. En primer lloc es van realitzar assajos en discontinu amb una MFC i una MEC per comparar l'operació amb purí de porc fresc i digerit en els dos sistemes pel que fa a la reducció de càrrega orgànica i recuperació l'amoni per a la seva posterior reutilització. Posteriorment, ambdues cel·les van ser operades en continu amb digerit i es va comprovar la seva capacitat per absorbir sobrecàrregues orgàniques puntuals, simulant un mal funcionament del DA mitjançant polsos d'àcids grassos volàtils en les càmeres anòdiques. Després, un DA a escala de laboratori va ser connectat en sèrie amb les dues cel·les i va ser sotmès a una sobrecàrrega orgànica i nitrogenada que va provocar la inhibició del procés. La MFC i la MEC van funcionar com a sistemes adequats per mantenir la qualitat de l'efluent, reduint la càrrega orgànica residual del digerit i recuperant amoni. A més, un circuit de recirculació entre el DA i la MEC va permetre estabilitzar el DA inhibit. Finalment, l'efectivitat del circuit de recirculació per al manteniment de l'operació del DA va ser comprovada, mitjançant la seva interrupció temporal i posterior

reconnexió. La població microbiana total i activa dels reactors va ser analitzada durant les diferents fases per estudiar la seva evolució durant els períodes d'inhibició i recirculació.

A la segona part de la tesi es va estudiar l'aplicació de la tecnologia MEC per a l'enriquiment del biogàs produït en la DA, gràcies a l'establiment d'un biofilm en el càtode de la MEC capaç de convertir CO_2 en metà, augmentant la recuperació d'energia del sistema. En primer lloc es va operar un reactor anaerobi de llit fluïdificat ascendent (up-flow anaerobic sludge blanket, UASB) amb l'objectiu d'obtenir biomassa enriquida en archaees metanogèniques, per posteriorment ser inoculada en el càtode d'una MEC. Es van posar en marxa dues cel·les MEC per comparar la seva operació amb dos inòculs diferents (biomassa enriquida en el UASB i biomassa granular anaeròbia) i l'evolució de la població microbiana. Finalment, la tecnologia DA-MEC-biocàtode va ser integrada en un sistema en què el digerit era refinat a la cambra anòdica de la MEC i recirculat al DA per controlar la inhibició per sobrecàrrega orgànica i nitrogenada; l'amoni era recuperat del digerit per transferència a la càmera catòdica; i el CO_2 introduït a la cambra catòdica era transformat en metà per augmentar el poder calorífic del biogàs.

El treball desenvolupat en aquesta tesi ha permès comprovar a escala de laboratori que els sistemes BES presenten una gran versatilitat per ser combinats amb la DA i millorar la seva operació, la qualitat de l'efluent i la recuperació d'energia i nitrogen.

CHAPTER 1

General introduction

1.1 Waste management and energy and products recovery

Fossil fuels cover around 80% of the world energy demand, while 7% is covered by nuclear energy and 13% by renewable sources (Goldemberg and Johansson, 2004). The increasing global demand for fossil fuels, their tendency to be scarcer, and the need to control the greenhouse gas emissions when using them are demanding new strategies for energy production (Schiermeier et al., 2008). Renewable energy production can be achieved through different ways, such as biomass, solar, wind or hydroelectric energies, all of them alternatives to fossil fuels.

An alternative to conventional refineries for clean and renewable energy production is the biorefinery. Biorefineries can recover nutrients and other products of interest from energetic crops, organic wastes and other waste fluxes (Schiermeier et al., 2008). This concept goes beyond the philosophy of petrochemical refineries, including sustainable management practices and closed cycle processes whenever possible. The goal is to mimic the natural carbon cycle, of global scale. But there are also natural cycles for water and, at local scale, for minerals, especially nitrogen, phosphorus and potassium, all essential nutrients for agriculture.

Wastes, whether domestic, industrial, agricultural or from livestock are a great opportunity to recover water, energy, chemical products and nutrients, and have a big potential for application in biorefineries (Foster-Carneiro et al., 2013). Therefore it is necessary to develop technologies capable of recovering the energy and resources contained in waste fluxes. To reduce the energy investment and to avoid depletion of natural resources, there is a need to recover the resources available in the wastewater and to transform in the coming years present wastewater treatment plants to resource recovery facilities and waste biorefineries (Nancharaiah et al., 2016).

1.2 Anaerobic digestion for wastes management

Anaerobic digestion (AD), which consists in the microorganism catalysed conversion of organic substrates into a mixture of gases (biogas) –mainly methane and carbon dioxide- under anoxic conditions is a well-established energy recovering technology in terms of performance and economic feasibility and one of the most attractive technologies to produce sustainable energy from wastes (Kleerebezem and van Loosdrecht, 2007). However, this technology does not modify the total content of N in the digestates, and thus needs to be combined with other processes for N removal or recovery (Foresti et al., 2006). The combination of the AD process with ammonia stripping with its subsequent absorption in an acid solution (Bonmatí and Flotats, 2003a; Laureni et al., 2013), thermal concentration of the digestate (Bonmatí and Flotats, 2003b) or chemical precipitation of ammonium and phosphate as struvite (Cerrillo et al., 2015)

has previously been studied, but despite these combined processes being feasible, few full scale applications exist so far.

On the other hand, the AD process, especially when it is performed at thermophilic range, can be sensitive to several substances that may be present in the waste stream, such as ammonia (Yenigün and Demirel, 2013), long chain fatty acids (Palatsi et al., 2009), sulphide, light metal ions (Na, K, Mg, Ca and Al), heavy metals and organic compounds such as chlorophenols or halogenated aliphatics (Chen et al., 2008; Kroeker et al., 1979). In case of inhibition of the AD, an increase of volatile fatty acids (VFA) content in the effluent will take place, and an additional system to maintain the effluent quality will be needed.

1.2.1 Metabolic steps and microbial populations involved in AD

Methane production in anaerobic digesters is the final step in a series of biochemical reactions (Figure 1.1) which can be grouped in six different processes (Anderson et al., 2003):

1. Hydrolysis of biopolymers
2. Fermentation of amino acids and sugars.
3. Anaerobic oxidation of alcohols and long chain fatty acids.
4. Anaerobic oxidation of intermediary products, such as volatile acids, except acetate.
5. Conversion of acetate to methane.
6. Conversion of hydrogen to methane.

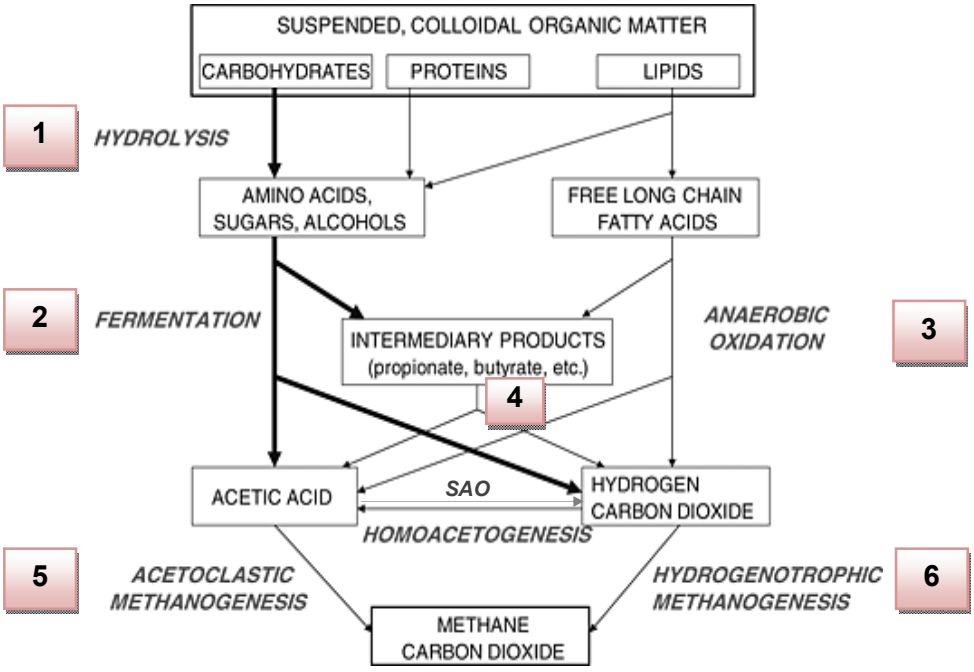

Figure 1.1 Schematic representation of the process of anaerobic digestion (adapted from Villano et al., 2012). SAO: Syntrophic acetate oxidation.

Each step is catalysed by different groups of microorganisms, each with a specific role in the overall process. The bacterial consortium involved in the anaerobic digestion process and the relationships between the groups are described below.

The first bacterial group is composed by hydrolytic bacteria that break down lipids, complex polymeric molecules (such as proteins and carbohydrates) and particulate organic matter into simpler soluble components such as short chain fatty acids, glycerol, peptides, amino acids, oligosaccharides and sugars.

The second group is designated as acid-forming bacteria and is divided into acidogenic (organic acid forming) and acetogenic (acetate forming) bacteria. These bacteria convert the end-products of the first group into the key substrates of methanogenesis (acetate, hydrogen, carbon dioxide) and a number of intermediary products such as formate, propionate, butyrate, etc. Syntrophic acetate oxidising bacteria (SAO) can oxidise acetate to produce hydrogen and CO_2 only when their products are subsequently utilised by the hydrogen-scavenging methanogens (Schnürer et al., 1999).

The sequence is completed with a third group of microorganisms, methanogenic archaea, which consume the end-products of the second group of bacteria and convert them into methane and carbon dioxide. Methanogenic archaea include two main different groups, called acetoclastic methanogenic archaea and hydrogenotrophic methanogenic archaea. A third group is composed by methylotrophic methanogenic archaea, which can dismutate methylamines and methanol for growth but cannot catabolise acetate, dimethylsulphide, H_2/CO_2 or formate. Methanogenic archaea are strict anaerobes and form methane as an end product of their metabolism. In the anaerobic process methane production is considered the slowest step. In addition, since methanogens are more active in the pH range of 6.5-8.0, they are very sensitive to low buffered environments against acidification caused by the products of acetogenic and acidogenic bacteria. Although methane production in the digesters from acetate represents 70%, only two genera of methanogens include species that are capable of using acetate, *Methanosaeta* and *Methanosarcina*. Besides acetate, *Methanosarcina spp*. is also able to utilise methanol, methylamine and sometimes CO_2 and H_2 as growth substrates. These two genera have different physiology of growth; *Methanosaeta* is a filamentous organism, while *Methanosarcina* generally grows in aggregates that consist of many individual cells, each surrounded by a thick wall (Anderson et al., 2003).

A significant amount of methane produced in anaerobic digesters, up to 30% of the total, is produced by hydrogenotrophic and methylotrophic archaea. These methanogens reduce carbon dioxide, formate, methanol and methylamine using hydrogen produced by fermentation by bacteria and hydrolytic acidogenics in earlier stages of anaerobic digestion (Anderson et al., 2003).

1.2.2 Temperature range, pH and inhibitory substances

Usually anaerobic digestion is performed in two different ranges of temperature, defined as mesophilic, with optimal temperature of 30-37 °C; and thermophilic, with optimal temperature of 55-60 °C. The thermophilic temperature regime has advantages such as a higher production rate of methane than in mesophilic regime, the possibility of using higher organic loadings and lower sludge production. However, it has some disadvantages such as less stability than mesophilic reactors, higher energy requirement for heating the reactor and increased production of VFA in the effluent (Angelidaki and Ahring, 1994).

The optimal pH range is between 6.5 and 7.8. The pH of the reactor may be affected by the consumption and production of ammonia and VFA, production of sulphur from the reduction of sulphate or sulphite, and the conversion of organic carbon to methane and carbon dioxide. The presence of compounds such as metals, VFA, oxygen, sulphur or ammonia can also produce toxicity or inhibition in anaerobic reactors. In the case of inhibition by high concentrations of ammonium, very frequent in the treatment of high strength waste such as livestock manure, significant differences in what the inhibitory concentration is have been reported (Siles et al., 2010). Some methanogenic strains are inhibited at 4.2 $g_{N\text{-}NH4+}$ L^{-1}, while others are resistant to ammonia levels above 10 $g_{N\text{-}NH4+}$ L^{-1} (Jarrell et al., 1987). Hashimoto (1986) found ammonia inhibition of about 2.5 $g_{N\text{-}NH4+}$ L^{-1} for both mesophilic and thermophilic digesters, when the reactors were not previously acclimated to high ammonia content. In fact, AD process is very complex, harbouring different mechanisms such as antagonism, synergy, acclimatisation and complexion that can significantly affect the methanogenesis inhibition phenomenon (Chen et al., 2008). It may also be attributable to differences in substrates and concentrations of inoculum, environmental conditions such as temperature and pH, and periods of acclimatisation (Angelidaki and Ahring, 1994).

1.2.3 Treatment of complex substrates

Anaerobic digestion of complex substrates, such as organic waste, stands out as a strategy for bio-energy recovery. But the AD of protein rich waste, such as livestock manure, waste from fish processing, fermentation industry waste or sludge is often affected by the accumulation of acid and ammonium (Lü et al., 2013). When anaerobic digesters are inhibited by VFA accumulation it is difficult to restore the process because methanogens are highly sensitive to the presence of high VFA concentrations and low pH. The concentration of VFA is recognised as a mechanism of selective pressure that strongly influences the structure of the community, by promoting for example the methanogenic activity of *Methanosarcina*, and even can lead to a change in the metabolic pathway. The transformation of acetate, as the dominant

intermediary in the AD of organic matter, into methane can occur in two ways. The first one is acetoclastic methanogenesis, which is carried out by *Methanosarcinaceae* or *Methanosaetaceae*. The second process includes two reactions, syntrophic acetate oxidation (SAO organisms) to H_2 and CO_2 and the subsequent conversion of these products to methane by hydrogenotrophic methanogenic specific populations. Although globally it is assumed that most (up 67%) of produced methane comes directly from acetate, acetoclastic methanogens are more sensitive than hydrogenotrophic methanogens to compounds such as ammonia and heavy metals, and recent studies have found that the SAO metabolic pathway is significant under thermophilic conditions or stress due to high ammonia or VFA concentrations (Schnürer et al., 1999; Hao et al., 2011).

Given the high variability of substrates that can be used in AD, and the different problems that may arise in the operation, it is interesting to find mechanisms to keep the process under control, to increase the resilience mechanisms, and optimise the production of biogas. The AD treatment is a key treatment for complex wastes since it provides many benefits when combined with a process for nutrients recovering such as stripping, composting or membrane filtration, etc., and/or recover the residual energy, such as the combination with a microbial fuel cell (Min and Angelidaki, 2008).

1.3 Bioelectrochemical systems for the treatment of waste streams

Bioelectrochemical Systems (BES) use microorganisms attached to one or both bioelectrode(s) to catalyse the oxidation and/or reduction reactions (Figure 1.2). A BES is called microbial fuel cell (MFC) when electrical energy from the oxidation of organic matter is obtained, and microbial electrolysis cell (MEC) when electric power is supplied externally to promote non thermodynamically spontaneous reactions (Hamelers et al., 2010). These systems have emerged as a highly versatile technology that allows to join the treatment of wastewater to the generation of chemicals and energy carriers (Pant et al., 2012).

In the anodic compartment of an MFC, the organic matter is oxidised by microbial populations, including exoelectrogenic populations, which are electrochemically active. The electrons generated in this oxidation are not transferred to a soluble terminal acceptor of electrons (O_2, NO_3^-, SO_4^{2-}, Fe^{3+}, CO_2), but are derived to the anode (insoluble electron acceptor external from microbe cells). This transfer can occur both through components associated with the membrane and through soluble electron mediators or nanowires of microbial origin (Gorby et al., 2006; Kim, Chae et al., 2008). From the anode, electrons are conducted through an external circuit, which is connected to an external resistance, to the cathode, where they are consumed during the reduction of molecular oxygen to form water. The balance of charge between the two compartments is maintained because there is a simultaneous transport of ions

(cations such as H^+, Na^+, K^+, and other anions such as Cl^-) through the ion exchange membrane. The voltage difference between the two compartments is the electromotive force (emf) that allows the flow of electrons. This process is not totally efficient, since in the microbial community the processes of respiration and fermentation of microorganisms compete for the electrons of the substrate. The efficiency of an MFC is largely determined by the energy losses of the reactions expressed as overpotentials, and to which degree the electrons produced are derived to the desired product, expressed as coulombic efficiency (Hamelers et al., 2010). But in addition to energy production, another objective of these systems can also be the treatment or recovery of contaminants such as nitrates, sulphides and sulphates.

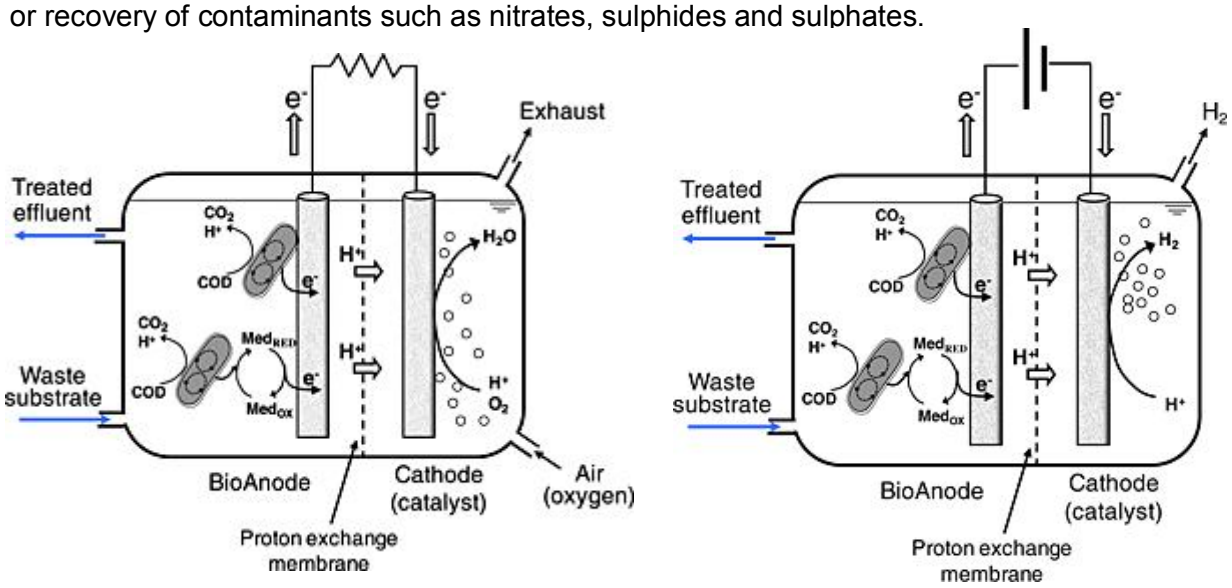

Figure 1.2 Schematic representation of an MFC (left) and a MEC (right) (Villano et al., 2012).

In a MEC, in the same way as in an MFC, electro-active microorganisms use a solid anode as terminal electron acceptor for the oxidation of organic substrates up to carbon dioxide while simultaneously releasing protons to the solution. The electrons flow from the anode to the cathode through an external circuit while the protons diffuse to the cathode compartment through a membrane separating the two compartments. At the cathode, in the presence of a suitable (bio)catalyst, the electrons combine with a soluble electron acceptor (Figure 1.3), generating a target product (Rabaey and Rozendal, 2010). The main difference with an MFC is that the MEC requires an external power supply to ensure that the cathode reaction is thermodynamically favourable. In the case of MEC systems, the main objective is to generate products of interest such as hydrogen or methane, which in this particular case are produced in the cathodic compartment.

So far various substrates have been studied as potential energy sources to generate electricity in MFCs, including carbohydrates (e.g. glucose, sucrose, starch and cellulose), volatile fatty acids (e.g. formate, acetate and butyrate), alcohols (e.g. methanol and ethanol),

amino acids and proteins. The use of organic wastewater is an attractive alternative to the use of pure compounds, allowing the treatment of residual flows while generating renewable energy. It has been demonstrated the ability to use a wide range of complex substrates to maintain the production of electricity in MFCs, such as oxalate (Bonmatí et al., 2013), domestic wastewater (Liu et al., 2004), swine wastewater (Min et al., 2005), wastewater from paper recycling or the production of beer, or the effluent of anaerobic digesters, as reviewed by Pant et al. (2010). This compatibility between the influent of BESs and the effluent of conventional anaerobic digesters makes MFCs suitable as a polishing treatment after the AD; or methane producing MECs to be a promising technology to extract additional energy (in the form of methane) of the residual organic matter contained in the effluent of AD systems.

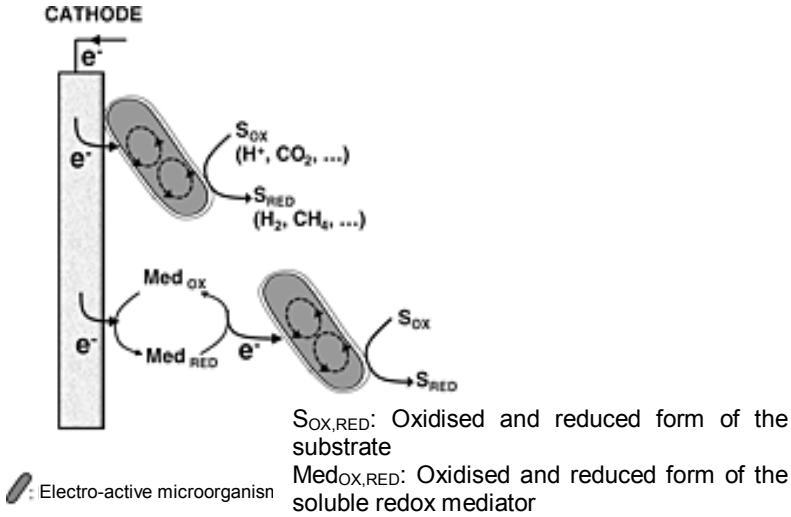

Figure 1.3 Schematic representation of the reaction produced in a biocathode (Villano et al., 2012).

Different from manure treatment in AD, an MFC generates electric current directly, and a gas containing mainly carbon dioxide and traces of CH_4. The MFCs have potential advantages of performance and operation over other technologies currently used for the production of electricity from organic matter. First, the direct conversion of electrical energy contained in the substrate theoretically allows high conversion efficiencies. Secondly, the MFCs operate efficiently at room temperature and even lower and can treat low organic matter content fluxes. And thirdly, an MFC does not require a subsequent combustion of biogas because it is rich in carbon dioxide and not in methane or molecular hydrogen and it usually has no useful energy content (Rabaey and Verstraete, 2005).

Although initially the main interest of BESs was the ability to produce electricity with MFCs, the attention of the scientific community is now focusing on other options a priori more attractive. In recent years BESs are standing for their complementary role to anaerobic digestion system, since the coupling of the two systems may allow recovering and/or producing products of interest.

1.3.1 Fundamentals of voltage generation in MFCs

In an MFC electricity is generated only if the overall reaction is thermodynamically favourable. The reaction can be evaluated in terms of Gibbs free energy expressed in Joules (J), which is a measure of the maximum amount of work that can be derived from a reaction, calculated as:

$$\Delta G_r = \Delta G_r^o + RT\ln(II) \qquad (1.1)$$

where ΔG_r (J) is the Gibbs free energy for specific conditions, ΔG^o_r is the Gibbs free energy under standard conditions normally defined as 298.15 K, 1 bar pressure and a concentration of 1 M for all species, R (8.31447 J mol^{-1} K^{-1}) is the gas universal constant, T (K) is the absolute temperature and II (no units) is the reaction quotient calculated as the product activity divided by that of the reagents. The Gibbs standard free energy is calculated from the tabulated energies of formation for different organic compounds in water (Logan et al., 2006).

For MFC calculations, it is more appropriate to assess the reaction in terms of electromotive force of the cell (emf) E_{emf} (V), defined as the difference of potential between the cathode and the anode. This is related with the work, W (J), produced by the cell:

$$W = E_{emf}\, Q = -\Delta G_r \qquad (1.2)$$

where $Q = nF$ is the load transferred in the reaction expressed in Coulombs (C), which is determined by the number of electrons exchanged in the reaction, n is the number of electrons per reacted mol, and F is the Faraday constant (9.64853 x 10^4 C mol^{-1}). Combining these two equations it gives:

$$E_{emf} = -\Delta G_r/(nF) \qquad (1.3)$$

If all the reactions are evaluated in standard conditions, II = 1, then:

$$E^o_{emf} = -\Delta G^o_r/(nF) \qquad (1.4)$$

where E^o_{emf} (V) is the standard electromotive force of the cell. Then we can use the above equations to express the overall reaction in terms of potentials:

$$E_{emf} = E^o_{emf} + (RT/nF)\ln(II) \qquad (1.5)$$

The advantage of Eq. 1.5 (Nernst equation) is that it is positive for a favourable reaction, and directly produces a value of the *emf* of the reaction. The calculated *emf* provides an upper limit for the voltage of the cell; the real potential derived from the MFC will be lower due to the different potential losses that occur (Section 1.3.2).

1.3.2 Overpotentials

The maximum voltage that can be achieved in an MFC (*emf*) is of the order of 1.1 V (Logan et al., 2006). The measured voltages, however, are considerably lower due to various losses. The difference between the voltage measured at the cell and the *emf* is called overpotential and it is the sum of the anode and cathode overpotentials and the ohmic losses of the system.

$$E_{cell} = \mathrm{E}_{emf} - [\sum \eta_{\mathrm{a}} + |\sum \eta_{\mathrm{c}}| + \mathrm{IR}_{\Omega}] \qquad (1.6)$$

where $\Sigma\eta_a$ and $\Sigma\eta_c$ are the anode and cathode overpotentials, respectively, IR_Ω is the sum of all the ohmic losses, which are proportional to the intensity of current generated (I) and the ohmic resistance of the system (R_Ω). The overpotentials of the electrodes are generally dependent on the current and in an MFC can be divided as follows: (i) activation loss; (ii) microbial metabolic losses; and (iii) mass transport or concentration losses.

In an MFC the measured voltage in the cell is normally a linear function of the intensity, and can be described as:

$$E_{cell} = \mathrm{OCV} - \mathrm{IR}_{\mathrm{int}} \qquad (1.7)$$

where IR_{int} is the sum of all the internal losses of the MFC and OCV is the voltage of the cell in the open circuit.

These are the different mentioned overpotentials:

Ohmic losses. The ohmic resistance is the opposition that ions and electrons experiment when they move through an electrochemical system. The more current density and ohmic resistance, the more relevant will ohmic losses in a system be. The two most important kinds of ohmic losses in BESs are: ohmic losses due to the electrolyte and ion exchange membrane (if any) and ohmic losses due to the electrode. The first ones refer to the voltage loss caused by the movement of ions through the anodic and cathodic electrolyte and the membrane, and the second ones refer to the movement of electrons through the electrode and the electrical wiring of a BES.

Ohmic losses can be reduced by minimising the distance between electrodes, using a membrane with low resistance, checking electrical connections and increasing the conductivity of the solution at the maximum tolerated by microorganisms (if feasible). In the case of waste water with low conductivity, electrolyte ohmic losses can be considerable.

Activation losses. Due to the activation energy necessary to produce an oxidation/reduction reaction, activation losses occur during the transfer of electrons from/to a compound that reacts on the surface of the electrode. This compound can be found on the surface of the microorganism, as a mediator in the solution, or as a terminal electron acceptor

reacting at the cathode. Activation losses typically show a strong increase at low current intensities and a steady growth when the current density increases. Low losses can be achieved by increasing the activation of the electrode surface, improving the catalysis of the electrode, increasing the operating temperature, and favouring the establishment of an exoelectrogenic microbial biofilm on the electrode(s).

Bacterial metabolism losses. To generate metabolic energy, bacteria carry electrons from a substrate with low potential (such as acetate, 0.187 V) through the electron transport chain to a terminal electron acceptor (such as oxygen or nitrate) with higher potential (1.23 and 0.80 V, respectively). In an MFC, the anode is the terminal electron acceptor and its potential determines the energy gain of bacteria. The higher the difference between the redox potential of the substrate and the potential of the anode, the higher the possible metabolic energy gain by the bacteria, but the lower the maximum voltage that can be achieved in the MFC. The potential of the anode, however, is affected by the potential of the cathode; this potential difference favours electron transport from the biofilm to the anode and later to the cathode. In order to maximise the voltage of the MFC, the potential of the anode should be kept as low (negative) as possible. But if the potential of the anode is too low, the electron transport will be inhibited and microorganisms will get more energy if the fermentation of the substrate can be carried out.

Concentration losses. Concentration losses occur when the rate of mass transport of a species to or from the electrode limits current production. Concentration losses occur mainly in high current densities due to a limited mass transfer by diffusion of chemical species to the surface of the electrode. The anode concentration losses are caused by a limited discharge of oxidised species from the surface of the electrode or a limited supply of reduced species to the electrode. This increases the ratio of oxidised and reduced species at the electrode surface, which can cause an increase in the potential of the electrode. At the cathode the opposite effect can take place, causing a drop of potential. In poorly agitated systems, diffusion gradients in the liquid can occur (Logan et al., 2006).

The Butler-Volmer equation can be used to predict the current intensity resulting from overpotential when there are not mass transfer limitations:

$$i = i_0 \left[e^{-\alpha f \eta} - e^{(1-\alpha) f \eta} \right] \qquad (1.8)$$

where i is the current (A), η is the overpotential (V), the coefficient $f = F / (RT)$, F is the Faraday constant, R is the gas constant and T is the temperature (K), and the transfer coefficient α is a dimensionless parameter with values between 0 and 1, often estimated as 0.5; i_0 (A) is the current exchanged, which can be written as:

$$i_0 = FAk^0 C_0^{*(1-\alpha)} C_R^{*\alpha} \qquad (1.9)$$

where C_R and C_0 are the oxidised and reduced compounds concentrations (mol cm^{-3}), respectively, A is the area of the electrode (cm^2) and k_0 is the standard heterogeneous rate constant (cm sec^{-1}).

1.3.3 Microbial mechanisms for external transfer of electrons

In order to optimise the different applications of BESs it is necessary to understand how microorganisms exchange electrons with the electrode surface. So far two main methods for extracellular electron transfer (EET) have been identified: direct electron transfer from bacteria physically attached to an electrode, and indirect transfer of electrons from bacteria that are not physically attached to the electrode (Rabaey et al., 2007) (Figure 1.4). These processes are not mutually exclusive, and microorganisms may be able to use several of these mechanisms simultaneously.

Regarding the direct transfer between bacteria and electrode, it can occur in two ways. First, it can be caused by physical contact between the structures of the outer membrane of the microbial cell and the surface of the electrode. These external structures are also attached to the internal structures of the organism, allowing the electrons to be transported from the interior of the cell through the cell wall directly to the electrode. And secondly, the electrons can be transferred between the electrode and the microorganism through appendages of 10 nm diameter and up to several thousand nanometres in length (nanowires) extending from the outer membrane of the microorganisms and attached to the electrode (Franks et al., 2010). Since the nanowires can extend tens of microns, microorganisms which are placed far from the electrode can maintain direct contact with it or with other cells. The direct electron transfer was first proposed as a transfer mechanism for *Shewanella putrefaciens* MR-1 (Kim et al., 1999), but later it was also demonstrated the use of indirect electron transfer with mediators (Marsili et al., 2008). Other microorganisms which are believed to transfer electrons directly to the surface of the anode include *Shewanella s*pp., *Aeromonas hydrophila*, *Clostridium* spp., *Rhodoferax ferrireducens*, *Desulfobulbus propionicus* and *Geobacter spp. Geobacter spp* and *Shewanella spp* would also be capable of producing nanowires (Franks et al., 2010). Direct interspecies electron transfer (DIET) between different bacteria and archaea has also recently been described (Summers et al., 2010).

Indirect electron transfer between the electrode and the microorganism is produced through long range electron shuttles or mediator compounds that can be naturally present in the environment (waste water, for example), or be produced by bacteria. The electrons are transported first to the surface of the bacterial cell and mediators or shuttle compounds collect

and transport them to the electrode. Some mediators producing bacteria are *Shewanella spp*., *Pseudomonas spp* and *Geothrix fermentans* (Franks et al., 2010).

It is essential to continue to deepen the knowledge of the biology of extracellular transfer of electrons and direct interspecies electron transfer (DIET) mechanisms for future developments in the field of BESs technology (both bioanodes and biocathodes).

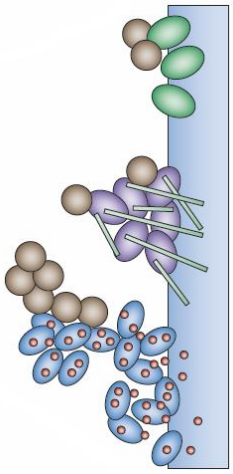

Figure 1.4 Representation of different kinds of bacteria in an anodic biofilm including exoelectrogens that transfer electrons by direct contact (green), produce nanowires (purple) and use endogenous mediators (blue). Other non-exoelectrogenic bacteria that live from the products generated by other bacteria (brown) or possibly use nanowires or mediators produced by other microorganisms may be also present (Logan, 2009).

1.3.4 The microbial communities in BES

There are a wide variety of microorganisms that can be found in association with electrodes in a BES, depending on operating conditions such as inoculum and the type of substrate used (Sotres et al., 2015b; 2016b; Logan and Regan, 2006; Pant et al., 2010). The generation of electricity has been demonstrated in four of the five classes of *Proteobacteria* (*α-, β-, γ- or δ-proteobacteria*), as well as *Firmicutes* and *Acidobacteria phyla* (Logan, 2009; Logan and Regan, 2006). The most active electrochemical species described in BESs biofilms are iron-reducing bacteria such as *Shewanella* and *Geobacter* (Yang et al., 2012), but the diversity of microbial communities present in exoelectrogenic processes seems to be much more complex.

It is likely that not all the microorganisms that are associated to the anode biofilm interact directly with it, but interaction may be indirectly through other electrode community members (Franks and Nevin, 2010). For example, *Brevibacillus spp. PTH1* was detected as an abundant member of a community in an MFC, but its electricity production was low unless co-cultured with *Pseudomonas spp* or the supernatant of an MFC (Pham et al. 2008).

Most known exoelectrogenic bacteria can only extract electrons from simple organic substrates such as volatile fatty acids (VFAs) and alcohols to produce current, so they require the cooperation of polymer-degrading bacteria (fermenters) to firstly break down the complex polymers such as cellulose and protein to simple and usable organics. Figure 1.5 shows three main routes of syntrophic interactions in MECs, and they include (A) interactions between the aforementioned fermentative bacteria and exoelectrogens, with the first group converting complex substrates into simpler organics for the second group to generate current; (B) interactions among fermentative bacteria, homoacetogens, and exoelectrogens. H_2 derived from fermentation or electrolysis is used to reduce CO_2 by homoacetogens to acetate ($HCO_3^- + 2H_2 + 0.5H^+ \longleftrightarrow 0.5CH_3COO^- + 2H_2O$), which then can be oxidised by exoelectrogens; and (C) interactions between fermentative bacteria and methanogens. Fermentation products, acetate or H_2 can be used by methanogens for CH_4 production (Lu and Ren, 2016).

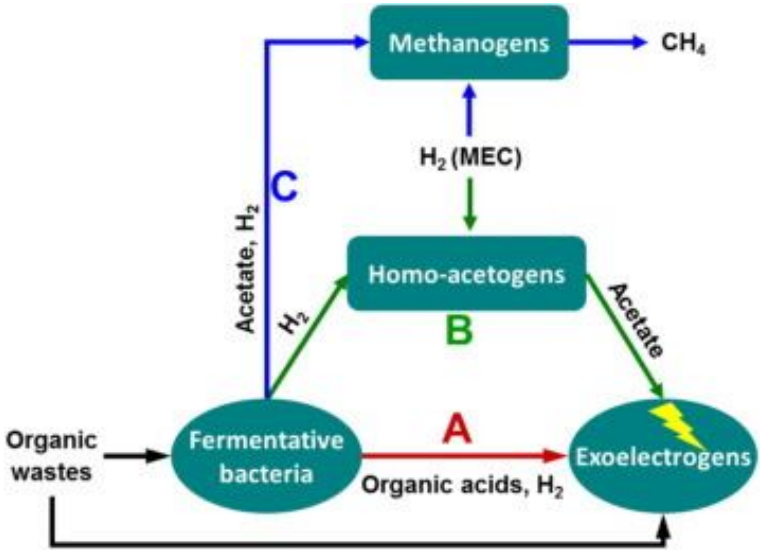

Figure 1.5 Schematic representation of the three main routes (A, B and C) of syntrophic interactions in MECs (Lu and Ren, 2016).

The higher power densities were achieved by inoculating the MFC's anode with a rich and diverse source of bacteria, such as wastewater or sewage sludge. However, the power densities achieved are typically more dependent on the specific architecture of the reactor, the ion exchange membrane materials used (Sotres et al., 2015b), the distance between the electrodes and the conductivity of the MFC solution, rather than on the specific microbial populations (Logan et al., 2006).

Regarding microbial community assessment of complex biofilms attached to BES electrodes (bioanode and biocathode), high throughput sequencing (454-pyrosequencing, MiSeq and Ion Torrent platforms) of massive gene libraries of *16S rRNA* are arising as

emerging techniques to cope with the low sensitivity of former culture-independent techniques such as DGGE or cloning libraries, enabling the identification of less abundant members of the community, while eliminating the cloning bias, but not this of the previous step of PCR (Yates et al., 2012).

In addition more efforts focused on RNA-based studies are needed to distinguish active microbial key players from total community composition to gain insight on main microbial mechanisms that are taking place on the BES biofilms. New emerging techniques such as metatranscriptomic and metagenomics can provide valuable information about the active pathways and gene expression, as well as identifying those key genes and microbial species to be further monitored in the future.

1.3.5 BES as systems to recover nitrogen

A phenomenon described in MFCs equipped with cation exchange membranes is the diffusion of cations, such as ammonium, to maintain the balance of charges between the anode compartment, where protons are produced, and the cathode compartment, where they are consumed (even against a concentration gradient). Because the MFC anolyte always contains mineral salts and buffer in concentrations several times higher than that of protons (typically 10^5 times), these ions are the predominant species in maintaining the charge balance in detriment of protons, resulting in a pH gradient between anolyte and catholyte (Rozendal et al., 2006; 2008).

Several studies have been conducted to determine how the nitrogen is transported through the membrane of the MFC. Kim, Zuo et al. (2008) examined the balance of nitrogen during pig wastewater treatment with a single and two-chambered MFC. For the cathode-air system, the results suggested that N losses were increased due to volatilisation of ammonia as a result of a high pH near the cathode. In the two-chambered MFC, the nitrogen losses in the anode compartment were mainly due to the diffusion of ions through the membrane and subsequent stripping due to the injection of air into the cathode compartment. The transport through the membrane increased with the increased electricity generation.

Taking advantage of this phenomenon, Cord-Ruwisch et al. (2011) developed a strategy for using ammonium as a proton shuttle between the anode and cathode compartments, trapping and recovering ammonia volatilised by stripping of ammonium transferred to the catholyte from the anode compartment and subsequent absorption in an acid solution. This mechanism avoided having to add reagents to maintain the pH of the anode at suitable levels for biological activity. Later, Cheng et al. (2013) modified this ammonium recycling system using the hydrogen generated in the cell to perform the stripping. Kuntke et al. (2011) worked with synthetic water and measured the transport of cations to the cathode of an MFC in order to

recover the ammonia and determined that the high ammonium transport through the cation exchange membrane achieved was motivated by the charges exchange process. Ammonium was transferred to the cathode compartment through both diffusion flux (which allows the transport until it achieves a balance of ammonium concentrations between the anode and cathode compartments) and migration flux (caused by charge production). Later, Kuntke et al. (2012) showed that the same process could be done with wastewater with high nitrogen load, such as urine. In addition, they found a linear relationship between charge and ammonium transport produced in the experiments. Regardless of the concentration of ammonium, 30% of the produced charge was used to for the transport of ammonium to the cathode compartment. Desloover et al. (2012) studied the flux of ammonium between the anode and cathode compartment using an electrochemical cell applying voltage to the system and determined that under optimum conditions and working with synthetic solution the ammonium transfer efficiency was of 96%. Working with digestate the achieved efficiency was of 41%. The ammonium dissolved in the cathode could be recovered later by stripping and absorption, with a 100% efficiency. Later, Sotres et al. (2015a) found that the diffusion of ammonium between both chambers of an MFC fed in continuous mode was independent of the concentration of $N\text{-}NH_4^+$ of the influent and that the operation of the MFC was not affected by the high concentration of ammonium used in the feed. It was also reported that the recovery of ammonia in an MFC fed with liquid fraction of manure through stripping was feasible. Haddadi et al. (2013) studied the effect of ammonium diffusion and the behaviour of the anode pH on the recovery of ammonia in a MEC. In this study, the transport of ammonium through a cation exchange membrane represented approximately 61% of the coulombs produced, since there were other cations in the medium. Deducing ammonium transported by diffusion, ammonium transported due to migration to ensure the electroneutrality represented 34% of the total balance of charge. Zhang, Zhu et al. (2013) worked in batch with an MFC with three compartments, to study the transport of ammonium to the cathode compartment. It was reported that the increase in the voltage of the cell increased the speed of migration of ammonium. The efficiency of ammonium migration stood at 97.0±2%. The diffusion of ammonium through the membrane when voltage was not applied was of 30±2%. The diffused ammonium was later removed from the cathode compartment by simultaneous nitrification and denitrification. Clauwaert et al. (2007) reported the removal of nitrate by denitrificant microorganisms in the cathode of an MFC operated with acetate, without the need for external power. Subsequent results showed that the removal of nitrogen may be combined with MFC technology with simultaneous production of energy (Virdis et al. 2008). Sotres et al. (2016) worked with a dual-compartment MFC with synthetic feed, noting that 24% of ammonium migrated through the cation exchange membrane and was subsequently nitrificated at the cathode compartment. The prevalence of concomitant

phylotypes belonging to nitrifying (*Nitrosomonas*) and denitrifying bacteria in the cathode chamber was determined, which could explain the presence of active processes of nitrification and denitrification and the loss of nitrogen detected in the overall balance of the MFC. Finally, it was showed that it was feasible to conduct a sequentially nitrification-denitrification process using intermittent aeration in the cathode chamber.

These latter systems seek to achieve the removal of nitrogen from the waste water stream, and there are many articles published about it (Kelly and He, 2014), while the MFC coupling to a stripping system allows for the more environmentally suitable tool of nitrogen recovery for subsequent reuse as fertiliser, for example, also avoiding the potential production of nitrogen oxides during the process of denitrification. Fertiliser nitrogen is chiefly obtained by converting atmospheric nitrogen to ammonia nitrogen in industry by the Haber–Bosch process (Fowler et al., 2013). It combines nitrogen and hydrogen at high temperature (400–600 ºC) and high pressure (20–40 MPa) using an iron catalyst. This process is so energy intensive that it consumes between 1% and 2% of the energy generated per year globally. Moreover, hydrogen required for this reaction is processed from natural gas and carbon dioxide is the by-product (Nancharaiah et al., 2016).

In this frame, BESs emerge as interesting systems to be coupled to an anaerobic digestion process, since ammonia is not removed in the conventional anaerobic digestion treatment, but generated from organic nitrogen, making it necessary to find a complementary system that allows recovering or removing the nitrogen content in the effluent.

1.3.6 Methane potential as renewable energy source

In the context of energy sources scarcity and the need of finding alternatives to fossil fuels to produce energy without releasing new carbon to the atmosphere, actual investigation lines are focused in more sustainable methods for obtaining energy, and in renewable fuels which could be stored and used for transport, heating or chemical synthesis (Cheng et al., 2009). Renewable energy carriers with no carbon or neutral in their release of carbon to the atmosphere (they do not contribute with new CO_2) are of especial interest. Although renewable energy production based on actual technology is still not economically competitive in comparison with the fossil fuel based production, there is a decrease in costs in the last decades due to technological development. In this sense, biotechnological processes catalysed by microorganisms (such as microbial electrolysis cells reactors) are of increasing interest for their use for the production of liquid and gaseous renewable biofuels. Among the latter, biomethane and biohydrogen have a great potential because they are energy carriers and can be stored and have diverse applications such as transport, heating, electricity or even chemical products production (Villano et al., 2012).

Although hydrogen has as advantage that it can be used directly in fuel cells to produce electricity, obtaining water as the only waste, storage systems and adequate infrastructures still have to be developed in the coming decades to allow its use in transport and decentralised electricity production. Instead, methane needs a pre-treatment in order to be used but can be stored and distributed with the existing natural gas infrastructure. Furthermore, its use for energy production and heat is a mature technology, since it has been produced in anaerobic digestion processes for decades. Using methane as transport fuel has also a significant potential, since NO_x emissions, particles and other emissions related with fossil fuels utilisation would be reduced.

1.3.7 BES as systems for obtaining methane

In conventional BESs, a biocathalysed anode is combined with an abiotic cathode containing a catalyst suitable to carry out the objective reaction. Recently BESs with microbial biocathodes are emerging as a way to achieve low cost cathode catalysts and provide more opportunities for commercial applications (Franks and Nevin, 2010).

So far there have been very few studies that have investigated the application of MEC technology for methane production. A methane producing MEC consists of a compartment where anodic oxidation reaction takes place, producing CO_2, protons and electrons (Figure 1.6). The electrons are driven to the anode and flow through an external electrical circuit to the cathode while the protons and ions migrate through the membrane to the cathode compartment to keep electroneutrality. At the cathode, CO_2, protons and electrons are used to produce methane. The cathode reaction is catalysed by electrochemically active microorganisms, the hydrogenotrophic methanogens (Cheng et al., 2009). The reaction is thermodynamically unfavourable, so power is needed to make it possible.

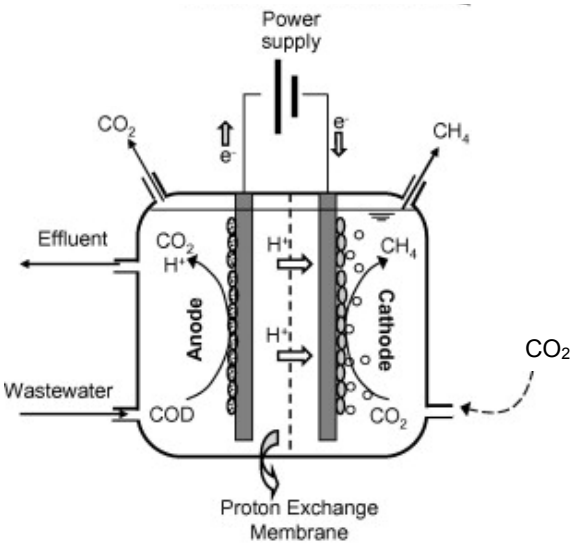

Figure 1.6 Schematic representation of a methane producing MEC (Villano et al., 2010).

The ability of microorganisms to produce methane from CO_2 reduction using an electrode as a direct donor of electrons has been demonstrated for the first time a few years ago (Cheng et al., 2009), so microorganisms can be used at the cathode of a MEC to produce methane gas from electricity at much higher speeds than those that can be obtained via evolution of hydrogen gas in a non-catalysed electrode. The hydrogenotrophic methanogens can catalyse the production of methane from CO_2 in MECs by two mechanisms of extracellular electron transfer: direct (electrons are taken directly from the electrode and are used to reduce CO_2 to methane) or indirect (with intermediate hydrogen production (Cheng et al., 2009; Villano et al., 2010)). The equations corresponding to both processes are shown in Eq. 1.10 (Cheng et al., 2009) and Eq. 1.10 (Logan et al., 2008) and 1.11 (Van Eerten et al., 2012), respectively.

$$CO_2 + 8\ H^+ + 8\ e^- \rightarrow CH_4 + 2\ H_2O \quad (E_{cat} = -0.24\ V\ vs.\ NHE) \qquad (1.10)$$

$$2\ H^+ + 2\ e^- \rightarrow H_2 \quad (E_{cat} = -0.41\ V\ vs.\ NHE) \qquad (1.11)$$

$$CO_2 + 4\ H_2 \rightarrow CH_4 + 2\ H_2O \qquad (1.12)$$

In standard conditions, the reaction of Eq. 1.10 requires a theoretical voltage of -0.244 V (vs. standard hydrogen electrode, SHE) at pH 7, but it is usually affected by quite high overpotentials that can be reduced using a microbial biocathode. Villano et al. (2010) found that methane production in a BES with mineral medium in batch could be achieved with simple carbon cathodes polarised at potential more negative than -650 mV vs. SHE in the presence of a hydrogenotrophic methanogenic culture. They showed that at cathode potentials in the investigated range (-650 to -900 mV), only part of the methane was produced via extracellular electron transfer processes; the rest was produced biologically through hydrogenotrophic methanogenesis. This study revealed that the extracellular electron transfer rate was heavily dependent on the potential of the cathode. The results of Clauwaert and Verstraete (2009) with a membraneless MEC indicated that it could be used as a viable treatment for AD effluent, since methane was produced with a low organic load and at environment temperature. In a later study, Villano et al. (2011) described the batch operation of a MEC at room temperature with mineral medium, consisting of a bioanode enriched with *Geobacter sulfurreducens* and a methane producing biocathode. The MEC was successfully started up by sequentially controlling the potential of the anode and the cathode in values that favoured the establishment of an active methanogenic biocathode (-850 mV vs SHE) and an acetate oxidant bioanode (500 mV vs SHE), respectively.

Cheng et al. (2011) worked with a new design of MEC, called bioelectrochemical rotative contactor, which through regular 180º rotation made the anode work as a cathode and vice versa. This operation favoured the growth of a biofilm that could catalyse both the anodic oxidation of acetate and the methanogenesis conducted by the cathode.

Recently, Jiang et al. (2013) studied a BES constructed to produce simultaneously CH_4 and CH_3COOH through direct and indirect extracellular electron transfer with CO_2 as the only carbon source. They showed that methane production grew almost linearly as the cathode potential became more negative, between -850 and -950 mV. At more negative potential, CH_3COOH began to accumulate.

1.4 Combination of AD/BES for organic wastes valorisation

Anaerobic digestion is limited, among other factors, by the susceptibility of methanogenic microorganisms to toxic compounds, the necessity of operating at temperatures generally above 35 ºC, the permanence of nutrients in the effluent and the difficulty in removing organic substrates at low residual concentrations (Pham et al., 2006). For this last reason, and with the objective of meeting discharge limits, AD systems require a polishing post-treatment step. Typically this step was performed with active sludge systems, energy consuming and with the concomitant production of considerable amounts of sludge (Villano et al., 2013).

On the other hand, the economic viability of the AD for the treatment of livestock manure depends, among other factors, on the specific methane production per unit of waste. Different strategies have been proposed and developed in order to increase the production of biogas, such as pre-treatments (Bonmatí et al., 2001), the co-digestion with other organic waste (Angelidaki and Ellegaard, 2003), the use of a more efficient configuration of the reactor (Sakar et al., 2009) and operating at thermophilic temperature range (Angelidaki and Ahring, 1994).

Operating at thermophilic temperature range has a positive effect on the anaerobic process, because the growth rates of thermophilic bacteria are 2-3 times larger than their mesophilic counterparts, but otherwise they are more sensitive to the presence of inhibitory substances. The total ammonia nitrogen (TAN) has been described as the main inhibitor in the anaerobic treatment of livestock wastewater. The concentration of non-ionised ammonia (NH_3), which depends on the TAN, pH and temperature, is the active compound that causes inhibition (Angelidaki and Ahring, 1993). Different techniques for removing nitrogen in AD systems have been investigated, such as ion exchange with zeolite (Wang et al., 2011; Tada et al., 2005), stripping (Bonmatí and Flotats, 2003a; Zhang and Jahng, 2010) and co-digestion with carbon-rich substrates (Yen and Brune, 2007), among others. Taking advantage of the phenomenon of transport of ammonium across the cationic membrane, the combination of an AD-BES system that favours this process can be an interesting alternative to reduce ammonia inhibition of AD.

Integration of biological and bioelectrochemical treatment systems in waste biorefinery concepts has a great promise to fully recover and reuse nutrients from waste streams (Nancharaiah et al., 2016).

There are different ways to integrate synergistically AD and BES technologies. MFCs can be used to refine the effluent from the AD in order to produce additional power. This second phase of treatment could also act as a buffer in case of malfunction of the AD and could help to eliminate toxic compounds contained in the anaerobic effluent. Despite these promising opportunities, little attention has been given to hybrid AD/BES systems. The idea of using an integrated configuration of BES and AD technologies for a more efficient bioconversion in waste treatment has been proposed by several authors (Pham et al., 2006; Hawkes at al., 2010; Rosenbaum et al. 2010; Ge et al., 2013; Higgins et al., 2013; Premier et al., 2013), and in recent years BESs are strengthening due to their applications in integrative waste biorefineries (Li et al. 2014; Nancharaiah et al. 2016; Lu and Ren, 2016; Venkata Mohan et al., 2016).

1.4.1 System stability and robustness

Regardless of the dynamics of microbial community in a constant environment, a stable system should have the ability to maintain the stability of the process in response to disturbances. A system with more routes to produce methane, for example, will be functionally more stable than one that is based on a series of interdependent metabolic events. It has been reported that the diversity of the population alone does not lead to the stability of a system. There is a positive relationship between the presence of multiple paths towards the obtaining of a product (parallel processing of a substrate) and theoretical concepts of functional stability in an increased environmental organisation (Briones and Raskin, 2003). The stability of an ecosystem is not the result of the diversity of the population *per se*, but of the functional redundancy, which ensures the presence of a reservoir of species able to perform the same ecological function (Briones and Raskin, 2003).

Hashsham et al. (2000) showed that methanogenic communities in a bioreactor that had a parallel processing of the substrate were functionally more stable in response to a disturbance produced by glucose than communities that processed the substrate predominantly in series. Methanogenic systems are good examples of networks were a number of fermentative, syntrophic and methanogenic populations work together as a community to convert organic substrates into methane.

The functional stability of a system in response to a disturbance can be measured with two main parameters: resistance and resilience (Figure 1.7). The resistance of a community against a product is defined as the maximum accumulation of the product. It is a measure of the

buffer capacity of the community regarding this product. Resilience is defined as the time required for the accumulated product to return to its reference level.

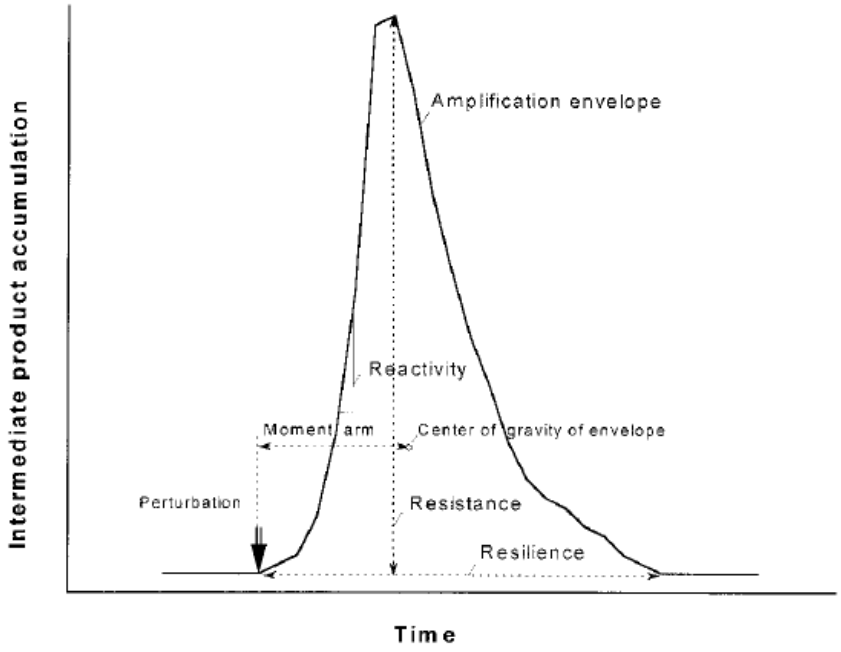

Figure 1.7 Ecological parameters of functional stability (Hashsham et al., 2000).

The notion of stability and robustness in anaerobic reactors is still quite unclear. The robustness can be defined as the capacity of the treatment systems to achieve stable operation under certain environmental and operational conditions. But stability can also be defined in terms of variability of the final product of the process, in this case the effluent. The stability may also be defined as the ability of a system to cope with severe environmental and operational variations (Leitão et al., 2006).

Despite the variety of existing studies on the effect of various parameters on the anaerobic digestion process, there are still aspects unclear on how to improve its stability and reliability in extreme situations. The combination of AD/BES can increase the stability and robustness of the system, diversifying the routes to treat various compounds of waste streams.

1.4.2 AD/MFC reactors configurations

So far, there have been several works studying different AD/MFC configurations. Min and Angelidaki (2008) reported a hybrid AD/MFC system, where the MFC was submerged in the AD reactor, and demonstrated that it could produce energy from domestic wastewaters. Jeong et al. (2008) reported that VFA removal in the AD of organic wastes could accelerate their decomposition to CO_2 and H_2O with an MFC. Zhang et al. (2009) combined an UASB with an MFC and an aerobic filter (BAF) in continuous operation to treat molasses wastewater with

simultaneous obtaining of energy. De Schamphelaire and Verstraete (2009) reported a lab-scale system which conducted the effluent of an AD treating algae biomass to the anode compartment of an MFC. More recently, Weld and Singh (2011) proposed and hybrid AD/MFC that worked in series, with the objective of improving the stability against organic overloads of a thermophilic AD. Higgins et al. (2013) operated an MFC fed with the effluent of an AD working with wastewater, and applying an electric potential to favour the development of exoelectrogenic bacteria. This way, alternative routes to degrade substrates were favoured, such as electrogenic bacteria in case the AD suffered a perturbation that inhibited methanogenesis. Xie et al. (2014) operated an MFC introduced in an anaerobic-anoxic-oxic wastewater treatment, with an increased removal of chemical oxygen demand (COD), nitrogen and phosphorus.

Furthermore, with the connexion of an AD fed with filamentous cyanobacteria biomass to an MFC and its recirculation, it was reported that methane production increased with respect to the AD without recirculation (Inglesby and Fischer, 2012). The improvement in the biogas production achieved in this work was due to the migration of ammonium ions from the digester to the cathodic compartment of the MFC, conducted by the energy production. This phenomenon had been previously demonstrated (Kim, Zuo et al., 2008), as VFA removal in an MFC. And finally, a recent work with synthetic wastewater focused on ammonium recovery with a desalination cell to overcome AD inhibition achieved a 40.8% recovery of ammonium and helped to gradually increase methane productivity back to 83%, compared to the control, 55 days after the inhibition of the AD (Zhang and Angelidaki, 2015).

1.4.3 AD/MEC reactors configurations

Regarding AD/MEC combination, Zhang and Angelidaki (2012) described recently a hybrid system connected to an MFC that produced the required energy for the hydrogen obtaining reaction, where MEC and MFC were submerged in an AD working with synthetic medium. Later, Zhang et al. (2013a, 2013b) studied the effect of Fe^{3+} addition in an AD-MEC to improve VFA removal and achieve an improved AD process. Guo et al. (2013) used a membraneless single chamber MEC to increase hydrogen and methane production in an AD.

The integration of the AD process with BESs seems to be especially interesting when the AD is combined with a methanogenic MEC (Pham et al., 2006; Clauwaert et al., 2008; Villano et al., 2010, 2011). Introducing the biogas produced by an AD in the cathode compartment of a MEC would increase the value of the biogas, which is typically composed of carbon dioxide (25-45 vol.%) and methane (75-55 vol.%), converting the carbon dioxide in additional content of methane. Conventionally, CO_2 is removed when biogas is purified with an aqueous solution which contents chemical products (hydroxide, ammines, etc.). Instead, a

methane producing MEC not only reduces CO_2 content of the biogas, but also converts the CO_2 into additional methane (Van Eerten-Jansen et al., 2012).

So far, the combination of MEC with AD for methane production has been poorly investigated. Villano et al. (2013) operated a methane producing MEC fed with synthetic solution in continuous mode. The cathode compartment was bubbled with a gas mixture containing carbon dioxide, simulating the biogas obtained in the AD. These findings suggest that MEC can be used to treat low organic load wastewater, with good energy efficiency and reduced sludge production. Therefore, further research is needed on the applicability of the MEC system for the enrichment of the biogas generated by the AD.

In spite of all the studies performed so far regarding BESs applications, further assessment of the combination with AD as a strategy to recover ammonium, increase the quality of the effluent and the stability of the system, and optimise energy recovery has to be undertaken. Furthermore, it is necessary to increase the knowledge on microbial communities present and metabolically active on BESs electrodes and AD rectors under different conditions, in order to understand their performance and stability.

1.5 References

Anderson, K., Sallis, P., Uyanik, S. 2003. Anaerobic treatment processes. In The Handbook of Water and Wastewater Microbiology. San Diego, Calif. Academic Press.

Angelidaki, I., Ahring, B.K. 1993. Thermophilic anaerobic digestion of livestock waste: effect of ammonia. *Applied Microbiology and Biotechnology*, **38**, 560-564.

Angelidaki, I., Ahring, B.K. 1994. Anaerobic thermophilic digestion of manure at different ammonia loads: effect of temperature. *Water Research*, **28**, 727-731.

Angelidaki, I., Ellegaard, L. 2003. Codigestion of manure and organic wastes in centralized biogas plants. *Applied Biochemistry and Biotechnology*, **109**, 95-105.

Bonmatí, A. 2001. Usos de l'energia tèrmica per a la millora del procés de digestió anaeròbia de purins de porc i per a la recuperació de productes d'interès. PhD Thesis. Universitat de Lleida, Lleida, p. 141.

Bonmatí, A., Flotats, X. 2003a. Air stripping of ammonia from pig slurry: characterisation and feasibility as a pre- or post- treatment to mesophilic anaerobic digestion. *Waste Management*, **23**, 261-272.

Bonmatí, A., Flotats, X. 2003b. Pig slurry concentration by vacuum evaporation: influence of previous mesophilic anaerobic process. *Journal of the Air and Waste Management Association*, **53**, 21-31.

Bonmatí, A., Sotres, A., Mu, Y., Rozendal, R., Rabaey, K. 2013. Oxalate degradation in a bioelectrochemical system: Reactor performance and microbial community characterization. *Bioresource Technology*, **143**, 147–153.

Briones, A., Raskin, L. 2003. Diversity and dynamics of microbial communities in engineered environments and their implications for process stability. *Current Opinion in Biotechnology*, **14**, 270-276.

Cerrillo, M., Palatsi, J., Comas, J., Vicens, J., Bonmatí, A. 2015. Struvite precipitation as a technology to be integrated in a manure anaerobic digestion treatment plant – Removal efficiency, crystal characterisation and agricultural assessment. *Journal of Chemical Technology & Biotechnology*, **90**, 1135-1143.

Chen, Y., Cheng, J.J., Creamer, K.S. 2008. Inhibition of anaerobic digestion process: a review. *Bioresource Technololy*, **99**, 4044–4064.

Cheng, S., Xing, D., Call, D.F., Logan, B.E. 2009. Direct biological conversion of electrical current into methane by electromethanogenesis. *Environmental Science & Technology*, **43**(10), 3953–3958.

Cheng, K.Y., Ho, G., Cord-Ruwisch, R. 2011. Novel methanogenic rotatable biolectrochemical system operated with polarity inversion. *Environmental Science & Technology*, **45**, 796-802.

Cheng, K.Y., Kaksonen, A.H., Cord-Ruwisch, R. 2013. Ammonia recycling enables sustainable operation of bioelectrochemical systems. *Bioresource Technology*, **143**, 25-31.

Clauwaert, P., Rabaey, K., Aelterman, P., Deschamphelaire, L., Pham, T.H., Boeckx, P., Boon, N., Verstraete, W. 2007. Biological denitrification in microbial fuel cells. *Environmental Science & Technology*, **41**, 3354-3360.

Clauwaert, P., Toledo, R., Van der Ha, D., Crab, R., Verstraete, W., Hu, H., Udert, K. M., Rabaey, K. 2008. Combining biocatalyzed electrolysis with anaerobic digestion. *Water Science and Technology*, **57**, 575-579.

Clauwaert, P., Verstraete, W. 2009. Methanogenesis in membraneless microbial electrolysis cells. *Applied Microbiology and Biotechnology*, **82**, 829-836.

Cord-Ruwisch, R., Law, Y., Cheng, K. T. 2011. Ammonium as a sustainable proton shuttle in bioelctochemical systems. *Bioresource Technology*, **102**, 9691-9696.

De Schamphelaire, L., Verstraete, W. 2009. Revival of the biological sunlight-to-biogas energy conversion system. *Biotechnology and Bioengineering*, **103**, 296-304.

Desloover, J., Woldeyohannis, A. A., Verstraete, W., Boon, N., Rabaey, K. 2012. Electrochemical resource recovery from digestate to prevent ammonia toxicity during anaerobic digestion. *Environmental Science & Technology*, **46**, 12209-12216.

Foresti, E., Zaiat, M., Vallero, M. 2006. Anaerobic processes as the core technology for sustainable domestic wastewater treatment: Consolidated applications, new trends, perspectives, and challenges *Reviews in Environmental Science and Bio/Technology*, **5**, 3-19.

Foster-Carneiro, T., Berni, M., Dorileo, I., Rostagno, M.A. 2013. Biorefinery study of availability of agricultura residues and wastes for integrated biorefineries in Brazil. *Resources, Conservation and Recycling*, **77**, 78-88.

Fowler, D., Coyle, M., Skiba, U., Sutton, M.A., Cape, J.N., Reis, S., Sheppard, L.J., Jenkins, A., Grizzetti, B., Galloway, J.N., Vitousek, P., Leach, A., Bouwman, A.F., Butterbach-Bahl, K., Dentener, F.,

Stevenson, D., Amann, M., Voss, M., 2013. The global nitrogen cycle in the twenty-first century. *Philosophical Transactions of the Royal Society B*. **368** (1621), 20130164.

Franks, A.E., Malvankar, N., Nevin, K.P. 2010. Bacterial biofilms: the powerhouse of a microbial fuel cell. Biofuels, **1**, 589–604.

Franks, A.E., Nevin, K.P. 2010. Microbial fuel cells, a current review. *Energies*, **3**, 899-919.

Ge, Z., Zhang, F., Grimaud, J., Hurst, J., He, Z. 2013. Long-term investigation of microbial fuel cells treating primary sludge or digested sludge. *Bioresource Technology*, **136**, 509-514.

Gorby, Y.U., Yanina, S., McLean, J.S., Rosso, K.M., Moyles, D., Dohnalkova, A., Beveridge, T.J., Chang, I.S., Kim, B.H., Culley, D.E., Reed, D.S., Romine, M.F., Saffarine, D.A., Hill, E.A., Elias, D.A., Kennedy, D.W., Pinchuk, G., Watanabe, K., Ishii, S., Logan, B.E., Nealson, K.H., Fredrickson, J.K. 2006. Electrically conductive bacterial nanowires produced by *Shewanella oneidensis* strain MR-1 and other microorganisms. *PNAS*. **103**(30), 11358-11363.

Goldemberg, J., Johansson, T.B. 2004. World Energy Assessment Overview: 2004 Update, United Nations Development Programme, New York.

Guo, X., Liu, J., Xiao, B. 2013. Bioelectrochemical enhancement of hydrogen and methane production from the anaerobic digestion of sewage sludge in single-chamber membrane-free microbial electrolysis cells. *International Journal of Hydrogen Energy*, **38**, 1342-1347.

Haddadi, S., Elbeshbishy, E., Lee, H-S. 2013. Implication of diffusion and significance of anodic pH in nitrogen-recovering microbial electrochemical cells. *Bioresource Technology*, **142**, 562-569.

Hamelers, H.V.M., Heijne, A.T., Sleutels, T.H.J.A., Jeremiasse, A.W., Strik, D.P.B.T.B., Buisman, C.J.N. 2010. New applications and performance of bioelectrochemical systems. *Applied Microbiology and Biotechnology*, **85**, 1673-1685.

Hao, L-P., Lü, F., He, P-J., Li, L., Shao, L-M. 2011. Predominant contribution of syntrophic acetate oxidation to thermophilic methane formation at high acetate concentrations. *Environmental Science and Technology*, **45**, 508–513.

Hashimoto, G. 1986. Ammonia inhibition of methanogenesis from cattle wastes. *Agricultural Wastes*, **17**, 241–261.

Hashsham, S.A., Fernandez, A.S., Dollhopf, S.L., Dazzo, F.B., Hickey, R.F., Tiedje, J.M., Criddle, C.S. 2000. Parallel processing of substrate correlates with grater functional stability in methanogenic bioreactor communities perturbed by glucose. *Applied and Environmental Microbiology*, **66**, 4050-4057.

Hawkes, F.R., Kim, J.R., Kyazze, G., Premier, G.C. 2010. Feedstocks for BES conversion. In Bioelectrochemical Systems: from extracellular electron transfer to biotechnological application. IWA, 488 pp, 369-392.

Higgins, S.R., Lopez, R.J., Pagaling, E., Yan, T., Cooney, M.J. 2013. Towards a hybrid anaerobic digester-microbial fuel cell integrated energy recovery system: An overview of the development of an electrogenic biofilm. *Enzyme and Microbial Technology*, **52**, 344-351.

Inglesby A.E., Fischer A.C. 2012. Enhanced methane yields from anaerobic digestion of Arthrospira maxima biomass in an advanced flow-through reactor with an integrated recirculation loop microbial fuel cell. *Energy and Environmental Science*, **5**, 7996-8006.

Jarrell, K.F., Saulnier, M., Ley, A. 1987. Inhibition of methanogenesis in pure cultures by ammonia, fatty acids, and heavy metals, and protection against heavy metal toxicity by sewage sludge. *Canadian Journal of Microbiology*, **33**, 551–555.

Jeong, C.M., Dal, J., Choi, R., Ahn, Y., Chang, H.N. 2008. Removal of volatile fatty acids (VFA) by microbial fuel cell with aluminum electrode and microbial community identification with *16S* rRNA sequence. *Korean Journal of Chemical Engineering*, **25**, 535-541.

Jiang, Y., Su, M., Zhang, Y., Zhan, G., Tao, Y., Li, D. 2013. Bioelectrochemical systems for simultaneously production of methane and acetate from carbon dioxide at relatively high rate. *International Journal of Hydrogen Energy*, **38**, 3497-3502.

Kelly, P.T., He, Z. 2014. Nutrients removal and recovery in bioelectrochemical systems: A review. *Bioresource Technology*, **153**, 351-360.

Kim, H.J., Hyun, M.S., Chang, I.S., Kim, B.H. 1999. A microbial fuel cell type lactate biosensor using a metal-reducing bacterium, *Shewanella putrefaciens*. J. Microbiol. Biotech. **9**, 365–367.

Kim, I.S., Chae, K., Choi, M., Vestraete, W. 2008. Microbial Fuel Cells: recent advances, bacterial communities and application beyond electricity generation. *Environmental Engineer Research*, **13**, 51-65.

Kim, J.R., Zuo, Y., Regan, J.M., Logan, B.E. 2008. Analysis of ammonia loss mechanisms in microbial fuel cells treating animal wastewater. *Biotechnology and Bioengineering*, **99**, 1120–1127.

Kleerebezem, R., van Loosdrecht, M.C.M. 2007. Mixed culture biotechnology for bioenergy production. *Current Opinion in Biotechnology*, **18**, 207–212.

Kroeker, E.J., Schulte, D.D., Sparling, A.B., Lapp, H.M. 1979. Anaerobic treatment process stability. *Journal Water Pollution Control Federation*, **51**(4), 718-727.

Kuntke, P., Geleji, M., Bruning, H., Zeeman, G., Hamelers, H.V.M., Buisman, C.J.N. 2011. Effects of ammonium concentration and charge exchange on ammonium recovery from high strength wastewater using a microbial fuel cell. *Bioresource Technology*, **102**, 4376-4382.

Kuntke, P., Śmiech, K.M., Bruning, H., Zeeman, G., Saakes, M., Sleutels, T.H.J.A., Hamelers, H.V.M., Buisman, C.J.N. 2012. Ammonium recovery and energy production from urine by a microbial fuel cell. *Water Research*, **46**, 2627-2636.

Laureni, M., Palatsi, J., Llovera, M., Bonmatí, A. 2013. Influence of pig slurry characteristics on ammonia stripping efficiencies and quality of the recovered ammonium-sulfate solution. *Journal of Chemical Technology & Biotechnology*, **88**(9), 1654-1662.

Leitão, R.C., van Haandel, A.C, Zeeman, G., Lettinga, G. 2006. The effects of operational and environmental variations on anaerobic wastewater treatment systems: A review. *Bioresource Technology*, **97**, 1105–1118.

Li, W-W., Yu, H-Q., He, Z. 2014. Towards sustainable wastewater treatment by using microbial fuel cells-centered technologies. *Energy & Environmental Science*, **7**, 911-924.

Liu, H., Ramnarayanan, R., Logan, B. E. 2004. Production of electricity during wastewater treatment using a single chamber microbial fuel cell. *Environmental Science and Technology*, **38**, 2281-2285.

Logan, B.E. 2009. Exoelectrogenic bacteria that power microbial fuel cells. *Nature Reviews*, **7**, 375-381.

Logan, B. E., Hamelers, B., Rozendal, R., Schröder, U., Keller, J., Freguia, S., Aelterman, P., Verstraete, W., Rabaey, K. 2006. Microbial fuel cells: methodology and technology. *Environmental Science and Technology*, **40**, 5181–5192.

Logan, B. E., Regan, J. M. 2006. Electricity-producing bacterial communities in microbial fuel cells. *Trends in Microbiology*, **14**, 512-518.

Logan, B. E., Call, D., Cheng, S., Hamelers, H.V.M., Sleutels, T.H.J.A., Jeremiasse, A.W., Rozendal, R.A. 2008. Microbial electrolysis cells for high yield hydrogen gas production from organic matter. *Environmental Science and Technology*, **42**, 8630–8640.

Lü, F., Hao, L., Guan, D., Qi, Y., Shao, L., He, P. 2013. Synergetic stress of acids and ammonium on the shift in the methanogenic pathways during thermophilic anaerobic digestion of organics. *Water Research*, **47**, 2297-2306.

Lu, L., Ren, Z.J. 2016. Microbial electrolysis cells for waste biorefinery: A state of the art review. *Bioresource Technology*, **215**, 254-264.

Marsili, E., Baron, D.B., Shikhare, I.D., Coursolle, D., Gralnick, J.A., Bond, D.R. 2008. *Shewanella* secretes flavins that mediate extracellular electron transfer. Proc. Natl Acad. Sci. **105**, 3968–3973.

Min, B., Kim, J., Oh, S., Regan, J. M., Logan, B. 2005. Electricity generation from swine wastewater using microbial fuel cells. *Water Research*, **39**, 4961-4968.

Min, B., Angelidaki, I. 2008. Innovative microbial fuel cell for electricity production from anaerobic reactors. *Journal of Power Sources*, **180**, 641-647.

Munk, B., Bauer, C., Gronauer, A., Lebuhn, M. 2012. A metabolic quotient for methanogenic Archaea. *Water Science and Technology*, **66**(11), 2311-7.

Nancharaiah, Y.V., Venkata Mohan, S., Lens, P.N.L.. 2016. Recent advances in nutrient removal and recovery in biological and bioelectrochemical systems. *Bioresource Technology*, **215**, 173-185.

Palatsi, J., Laureni, M., Andres, M.V., Flotats, X., Nielsen, H.B., Angelidaki, I. 2009. Strategies for recovering inhibition caused by long chain fatty acids on anaerobic thermophilic biogas reactors. *Bioresour Technol*, **100**(20), 4588-96.

Pant, D., Van Bogaert, G., Diels, L., Vanbroekhoven, K. 2010. A review of the substrates used in microbial fuel cells (MFCs) for sustainable energy production. *Bioresource Technology*, **101**, 1533-1543.

Pant, D., Singh, A., Van Bogaert, G., Irving Olsen, S., Singh Nigam, P., Diels, L., Vanbroekhoven, K. 2012. Bioelectrochemical systems (BES) for sustainable energy production and product recovery from organic wastes and industrial wastewaters. *RSC* Adv. **2**(4), 1248–1263.

Pham, T. H., Rabaey, K., Aelterman, P., Clauwaert, P., De Schamphelaire, L., Boon, N. and Verstraete, W. 2006. Microbial fuel cells in relation to conventional anaerobic digestion technology. *Engineering in Life Sciences*, **6**(3), 285-292.

Pham, T.H., Boon, N., Aelterman, P., Clauwaert, P., De Schamphelaire, L., Vanhaecke, L., De Maeyer, K., Hofte, M., Verstraete, W., Rabaey, K. 2008. Metabolites produced by *Pseudomonas* sp. enable a Gram-positive bacterium to achieve extracellular electron transfer. *Applied Microbiology and Biotechnology*, **77**, 1119-1129.

Premier, G.C., Kim J.R., Massanet-Nicolau, J., Kyazze, G., Esteves, S.R.R., Penumathsa, B.K.V., Rodríguez, J., Maddy, J., Dinsdale, R.M., Guwy, A.J. 2013. Integration of biohydrogen, biomethane and bioelectrochemical systems. *Renewable Energy*, **49**, 188-192.

Rabaey, K., Verstraete, W. 2005. Microbial fuel cells: novel biotechnology for energy generation. Trends in Biotechnology, **23**, 291-298.

Rabaey, K., Rodriguez, J., Blackall, L.L., Keller, J., Gross, P., Batstone, D., Verstraete, W., Nealson, K.H. 2007. Microbial ecology meets electrochemistry: electricity driven and driving communities. The ISME Journal, **1**, 9-18.

Rabaey, K., Rozendal, R.A. 2010. Microbial electrosynthesis - revisiting the electrical route for microbial production. *Nature Reviews Microbiology*, **8**, 706-716.

Rosenbaum, M., Agler, M.T., Fornero, J.J., Venkataraman, A., Angenent, L.T. 2010. Integrating BES in the wastewater and sludge treatment line. In Bioelectrochemical Systems: from extracellular electron transfer to biotechnological application. IWA. 488 pp, 393-408.

Rozendal, R.A., Hamelers, H.V.M., Buisman, C.J.N. 2006. Effects of membrane cation transport on ph and microbial fuel cell performance. *Environmental Science and Technology*, **40**, 5206-5211.

Rozendal, R.A., Sleutels, T.H.J.A., Hamelers, H.V.M., Buisman, C.J.N. 2008. Effect of the type of ion exchange membrane on performance, ion transport and ph in biocatalyzed electrolysis of wastewater. *Water Science and Technology*, **57**, 1757-1762.

Sakar, S., Yetilmezsoy, K., Kocak, E. 2009. Anaerobic digestion technology in poultry and livestock waste treatment – a literature review. *Waste Management and Research*, **27**, 3-18.

Schiermeier, Q., Tollefson, J., Scully, T., Witze, A., Morton, O. 2008. Electricity without carbon. *Nature*, **454**, 816-823.

Schnürer, A., Zellner, G., Svensson, B.H. 1999. Mesophilic syntrophic acetate oxidation during methane formation in biogas reactors. *FEMS Microbiology Ecology*, **29**, 249-261.

Siles, J.A., Brekelmans, J., Martín, M.A., Chica, A.F., Martín, A. 2010. Impact of ammonia and sulphate concentration on thermophilic anaerobic digestion. *Bioresource Technology*, **101**, 9040-9048.

Sotres, A., Cerrillo, M., Viñas, M., Bonmatí, A. 2015a. Nitrogen recovery from pig slurry in a two-chambered bioelectrochemical system. *Bioresource Technology*, **194**, 373-382.

Sotres, A., Díaz-Marcos, J., Guivernau, M., Illa, J., Magrí, A., Prenafeta-Boldú, F.X., Bonmatí, A., Viñas, M. 2015b. Microbial community dynamics in two-chambered microbial fuel cells: effect of different ion exchange membranes. *Journal of Chemical Technology & Biotechnology*, **90**(8), 1497-1506.

Sotres, A., Cerrillo, M., Viñas, M., Bonmatí, A. 2016a. Nitrogen removal in a two-chambered microbial fuel cell: establishment of a nitrifying-denitryfying microbial community on an intermittent aerated cathode. *Chemical Engineering Journal*, **284**, 905-916.

Sotres, A., Tey, L., Bonmatí, A., Viñas, M. 2016b. Microbial community dynamics in continuous microbial fuel cells fed with synthetic wastewater and pig slurry. *Bioelectrochemistry*, **111**, 70-82.

Summers, Z.M., Fogarty, H.E., Leang, C., Franks, A.E., Malvankar, N.S., Lovley, D.R. 2010. Direct exchange of electrons within aggregates of an evolved syntrophic coculture of anaerobic bacteria. *Science*, **330**(6009), 1413-1415.

Tada, C., Yang, Y., Hanaoka, T., Sonoda, A., Ooi, K. 2005. Effect of natural zeolite on methane production for anaerobic digestion of ammonium rich organic sludge. *Bioresource Technology*, **96**, 459-464.

Van Eerten-Jansen, M.C.A.A., Heijne, A.T., Buisman, C.J.N., Hamelers, H.V.M. 2012. Microbial electrolysis cells for production of methane from CO_2: long-term performance and perspectives. *International Journal of Energy Research***, 36**, 809–819.

Venkata Mohan, S., Nikhil, G.N., Chiranjeevi, P., Nagendranatha Reddy, C., Rohit, M.V., Naresh Kumar, A., Sarkar, O.. 2016. Waste biorefinery models towards sustainable circular bioeconomy: Critical review and future perspectives. *Bioresource Technology*, **215**, 2-12.

Villano, M., Aulenta, F., Ciucci, C., Ferri, T., Giuliano, A., Majone, M. 2010. Bioelectrochemical reduction of CO_2 to CH_4 via direct and indirect extracellular electron transfer by a hydrogenophilic methanogenic culture. *Bioresource Technology*, **101**, 3085-3090.

Villano, M., Monaco, G., Aulenta, F., Majone, M. 2011. Electrochemically assisted methane production in a biofilm reactor. *Journal of Power Sources*, **196**, 9467-9472.

Villano, M., Aulenta, F., Majone, M. 2012. Perspectives of biofuels production from renewable resources with bioelectrochemical systems. *Asia-Pacific Journal of Chemical Engineering*, **7**, SUPPL. 3: S263-S274.

Villano, M., Scardala, S., Aulenta, F., Majone, M. 2013. Carbon and nitrogen removal and enhanced methane production in a microbial electrolysis cell. *Bioresource Technology*, **130**, 366-371.

Virdis, B., Rabaey, K., Yaun, Z., Keller, J. 2008. Microbial fuel cells for simultaneous carbon and nitrogen removal. *Water Research*, **32**, 3031-3024.

Wang, Q., Yang, Y., Yu, C., Huang, H., Kim, M., Feng, C., Zhang, Z. 2011. Study on a fixed zeolite bioreactor for anaerobic digestion of ammonium-rich swine wastes. *Bioresource Technology*, **102**, 7064-7068.

Weld, R.J., Singh, R. 2011. Functional stability of a hybrid anaerobic digester/microbial fuel cell system treating municipal wastewater. *Bioresource Technology*, **102**, 842-847.

Xie, B., Dong, W., Liu, B. Liu, H. 2014. Enhancement of pollutants removal from real sewage by embedding microbial fuel cell in anaerobic–anoxic–oxic wastewater treatment process. *Journal of Chemical Technology and Biotechnology*, **89**, 448-454.

Yang, Y., Xu, M., Guo, J., Su, G. 2012. Bacterial extracellular electron transfer in bioelectrochemical systems. *Process Biochemistry*, **47**, 1707–1714.

Yates, M.D., Kiely, P.D., Call, D.F., Rismani-Yazdi, H., Bibby, K., Peccia, J., Regan, J.M. and Logan, B.E. 2012. Convergent development of anodic bacterial communities in microbial fuel cells. *The ISME Journal*, **6**, 2002–2013.

Yen, H.-W., Brune, D.E. 2007. Anaerobic co-digestion of algal sludge and waste paper to produce methane. *Bioresource Technology*, **98**, 130-134.

Yenigün, O., Demirel, B. 2013. Ammonia inhibition in anaerobic digestion: A review. *Process Biochemistry*, **48**(5-6), 901-911.

Zhang, Y., Angelidaki, I. 2012. Innovative self-powered submersible microbial electrolysis cell (SMEC) for biohydrogen production from anaerobic reactors. Water Research, **46**, 2727-2736.

Zhang, Y., Angelidaki, I. 2015. Counteracting ammonia inhibition during anaerobic digestion by recovery using submersible microbial desalination cell. Biotechnology and Bioengineering, **112**(7), 1478-1482.

Zhang, L., Jahng, D. 2010. Enhanced anaerobic digestion of piggery wastewater by ammonia stripping: Effects of alkali types. *Hazardous Materials*, **182**, 536-543.

Zhang, J., Zhang, Y., Quan, X., Chen, S., Afzal, S. 2013a. Enhanced anaerobic digestion of organic contaminants containing diverse microbial population by combined microbial electrolysis cell (MEC) and anaerobic reactor under Fe (III) reducing conditions. *Bioresource Technology*, **136**, 273-280.

Zhang, J., Zhang, Y., Quan, X., Chen, S. 2013b. Effects of ferric iron on the anaerobic treatment and microbial biodiversity in a coupled microbial electrolysis cell (MEC) – anaerobic reactor. *Water Research*, **47**, 5719-5728.

Zhang, B., Zhao, H., Zhou, S., Shi, C., Wang, C., Ni, J. 2009. A novel UASB–MFC–BAF integrated system for high strength molasses wastewater treatment and bioelectricity generation. *Bioresource Technology*, **100**, 5687-5693.

Zhang, X., Zhu, F., Chen, L., Zhao, Q., Tao, G. 2013. Removal of ammonia nitrogen from wastewater using an aerobic cathode microbial fuel cell. *Bioresource Technology*, **146**, 161-168.

CHAPTER 2

Objectives and Thesis outline

2.1 Objectives

The main objective of the present PhD Thesis is to study the integration of AD and BES in order to optimise energy production and nitrogen recovery, as well as the resilience of the combined process, during the treatment of a complex waste stream (pig slurry). This objective is divided in the following specific goals:

1. To optimise the energy production of an integrated AD-BES system with ammonia recovery by a stripping and absorption system, both in MFC and MEC mode operation.

   1.1 To assess COD removal and ammonia recovery from raw and digested pig slurry both in MFC and MEC mode in batch operation, and analyse changes in microbial population that take place in each system.

   1.2 To evaluate the performance, microbial evolution and robustness of the integrated AD-MFC system in series operation, against different instability events (VFA, organic and nitrogen overload).

   1.3 To analyse the performance and robustness of the integrated AD-MEC system in series operation, against different instability events.

   1.4 To study the effect of applying different recirculation rates in the integrated AD-MEC/AbsNH_3 system, as a strategy to reduce inhibition phenomena by an organic and nitrogen overload in the thermophilic AD.

   1.5 To assess the effect over active biomass of different operational strategies in an integrated AD-MEC system.

2. To study the conversion of CO_2 into CH_4 by means of an electromethanogenic process operating a MEC with a biocathode in combination with AD.

   2.1 To assess the enrichment process of methanogenic archaea in a UASB reactor.

   2.2 To study the start-up and biomass evolution of two methanogenic MECs using different biocathode inocula.

   2.3 To evaluate the performance and the microbial communities of an integrated AD-MEC/Biocathode for ammonia recovery, biogas upgrading and AD stabilisation.

2.2 Research chronology and scope of the Thesis

The activities of this PhD Thesis were carried out within the framework of the Spanish Ministry of Economy and Competitiveness project (INIA project RTA2012-00096-00-00). The research work was developed at the GIRO group (Integral Management of Organic Waste), from the Institute for Agri-Food Research and Technology (IRTA), under the supervision of Dr. August Bonmatí Blasi and Dr. Marc Viñas Canals. The Thesis was developed within the doctoral program on "Environmental Engineering" at the Universitat Politècnica de Catalunya, Barcelona TECH (UPC) and was financially supported by the Secretariat for Universities and Research of the Ministry of Economy and Knowledge of the Catalan Government with an FI PhD grant (2013FI_B 00014).

The GIRO programme develops new knowledge and technologies in the field of sustainable management of organic wastes produced by the different activity sectors (agricultural, farming, industrial and urban), in an integrated focus of the problematic and transversal technological and management solutions.

In 2010 the research line on Bioelectrochemical Systems (BES) was born aiming to develop a BES technology for the treatment of high strength wastewater, such as pig slurries, focusing in electricity production from organic matter and its simultaneous nitrogen reduction (MICINN project CTM2009-12632). From that work, the first PhD Thesis on bioelectrochemical systems research line was completed in the GIRO group. The research continued with the start of this second PhD Thesis in 2013, focused on the integration of bioelectrochemical systems with anaerobic digestion.

2.3 Thesis outline

This Thesis is divided into twelve chapters. Chapter 1 comprises a general introduction to the topic of waste management, energy and products recovery, focusing in anaerobic digestion, bioelectrochemical systems and the possibilities that arise from the integration of both systems. Chapter 2 presents the main objectives of the Thesis, the research chronology and its scope. In Chapter 3, the reactors setups, and the analytical, electrochemical and microbial community assessment by means of molecular biology techniques followed in this work are described.

The experiments performed and the main results obtained in order to meet the objectives of the Thesis are presented in Chapters 4 to 11. The first part of the Thesis, from Chapter 4 to 8, describes the assays that were carried out with the general objective of optimising the energy production of an integrated AD-BES system with ammonia recovery, both in MFC and MEC mode operation. The second part of the Thesis comprehends Chapters 9, 10 and 11, and describes the experiments performed with the objective of studying the electromethanogenic process (CO_2 conversion into CH_4) operating a MEC with a biocathode in combination with AD. Figure 2.1 presents a graphical abstract of the different assays carried out and the reactors involved in each chapter.

In Chapter 4, batch assays in MFC and MEC mode are described to compare raw and digested pig slurry treatment in BES, regarding COD removal and nitrogen recovery. Furthermore, charge production, its relation with cation transport through the membrane and the influence of the other cations on the ammonium migration flux are also assessed. Finally, the evolution of microbial populations (total eubacteria and archaea) on the anode biofilm, both under MFC and MEC operation mode, are studied to identify potential key players involved in electric current production.

Chapter 5 assesses the stability and robustness of continuous MFC operation to treat digested pig slurry when the AD is submitted to an organic and nitrogen overload, and its feasibility as a strategy to recover ammonia. Changes in the microbial composition of the MFC anode will be evaluated.

In Chapter 6 the stability and robustness of continuous MEC operation in combination with AD, and its feasibility as a strategy to recover ammonia is assessed. VFA pulses were performed in the anode compartment of the MEC in order to simulate AD failure and evaluate the MEC response to punctual and sustained organic overloads.

Chapter 7 describes a strategy to overcome organic and nitrogen overload in thermophilic AD by coupling a MEC, either to polish the effluent and to stabilise the AD by establishing a loop configuration to recirculate the effluent. A stripping and absorption unit is

connected to the system in order to recover ammonia. Microbial community dynamics have been assessed in both reactors (AD and anode from MEC) to understand the reactor set-up effects, as well as microbial resilience at different operational conditions, even under an inhibited AD operation.

In Chapter 8 the effect of suppressing the recirculation loop in a stable integrated AD-MEC system is evaluated. The microbial population evolution of the AD-MEC integrated system is analysed, under inhibited and stable operation of the AD, regarding presence of predominant eubacteria and archaea in the biomass, but also regarding the metabolically active populations by means of using simultaneous DNA and RNA-based methods.

Chapter 9 details the operation of an upflow anaerobic sludge blanket reactor (USAB) fed with methanol with the main objective of enriching the biomass in methanogenic archaea, in order to obtain inoculum for the biocathodes operated in the following Chapters. The evolution of the microbial community is evaluated in terms of composition (DNA) and activity (RNA) by using quantitative PCR (qPCR) and high throughput sequencing (MiSeq) of 16S rDNA and 16S rRNA, besides specific methanogenic activity batch tests.

Chapter 10 assesses the performance of the biocathode of two lab-scale MECs to convert CO_2 into CH_4 as a technology for upgrading the biogas produced in anaerobic digesters, comparing two different inocula: i) a mixture of biomass from the anode of a MEC and anaerobic granular sludge; ii) biomass enriched in the methanol-fed UASB operated in Chapter 9. The evolution of total and active microbial population harboured on the biocathodes is analysed quantitatively and qualitatively with the techniques used in the previous chapters.

Chapter 11 presents the combination of AD and electromethanogenic MEC as an integrated system to increase thermophilic AD stability under an organic and nitrogen overload, recover ammonia and increase the methane content of the biogas produced by the AD. The evolution of total and active microbial community of the AD and the MEC bioelectrodes (both the anode and the cathode) is evaluated.

Finally, Chapter 12 summarises the main conclusions drawn from this work and outlines some directions for future research.

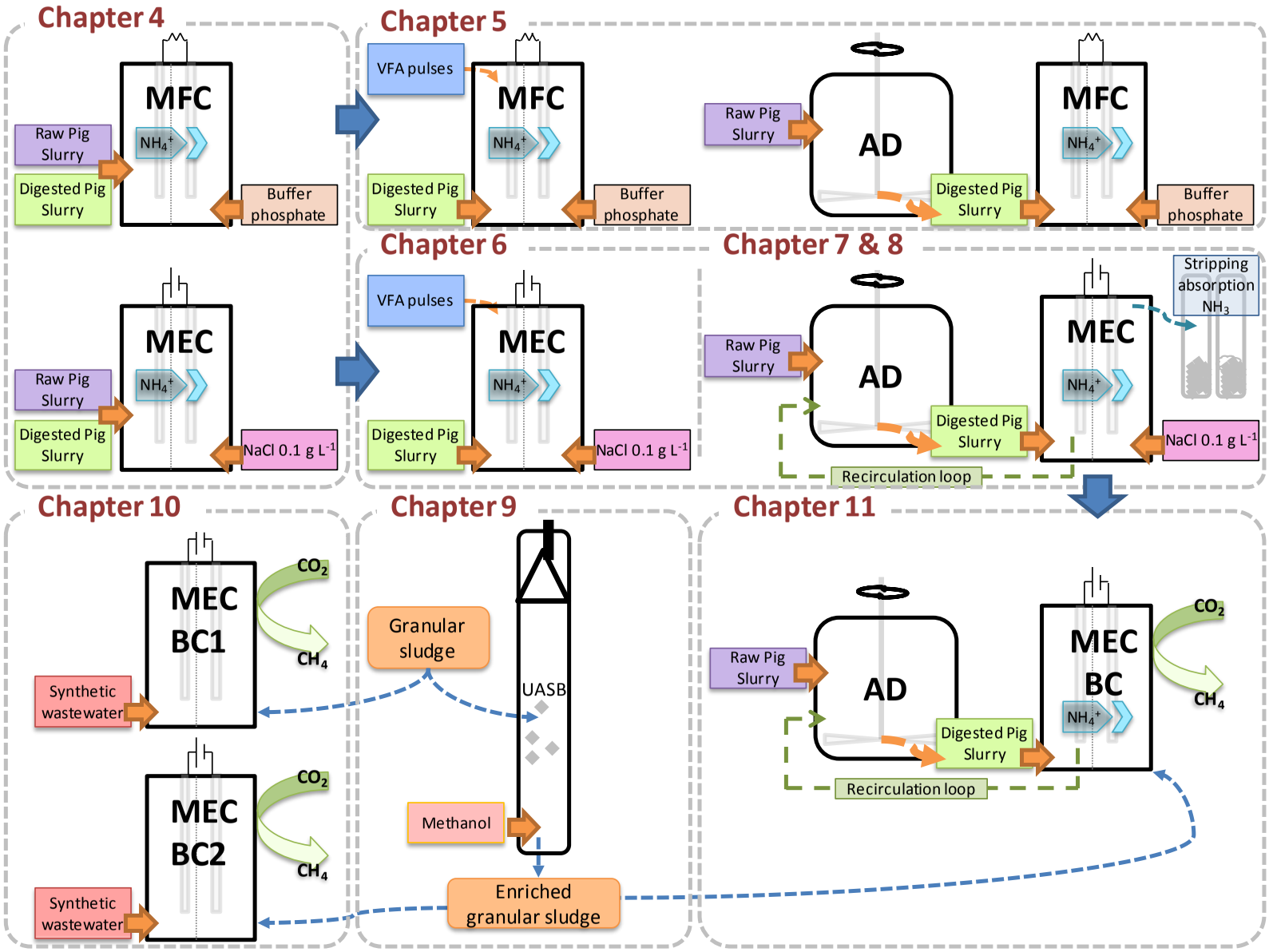

Figure 2.1 Graphical abstract of the assays performed in each Chapter.

CHAPTER 3

Materials and methods

This Chapter describes the materials and methods used for the development of the Thesis, organised in five Sections: 3.1 Reactor configuration; 3.2 Analytical methods; 3.3 Electrochemical calculations and techniques; 3.4 System performance calculations and indices; and 3.5 Microbial community analysis. The specific methodology of the different experiments will be described in each Chapter.

3.1 Reactor configuration

Reactors with different configurations have been used in this Thesis. BESs operated in MFC (Chapters 4 and 5) and MEC mode (Chapters 4, 6, 7 and 8) are described in Section 3.1.1. MECs with a biocathode, described in Section 3.1.2, have been used in Chapters 10 and 11. The anaerobic digester (AD) operated in Chapters 5, 7, 8 and 11 is described in Section 3.1.3. The stripping and absorption unit used in Chapter 7 is described in Section 3.1.4. Finally, the main characteristics of the UASB operated in Chapter 9 are described in Section 3.1.5.

3.1.1 MFC and MEC

A pair of identical two chambered cells were constructed in methacrylate (Figure 3.1a), with the anode and cathode compartments (0.14 x 0.12 x 0.03 m^3) separated by a cation exchange membrane (CEM) (dimensions: 14 x 12 cm; Ultrex CMI-7000, Membranes International Inc., Ringwood, NJ, USA; Figure 3.1b). A carbon felt was used as anode (dimensions: 14 x 12 cm; thickness: 3.18 mm; Alfa Aesar GmbH & Co KG, Karlsruhe, Germany; Figure 3.1c); and a 304 stainless steel mesh was used as cathode (dimensions: 14 x 12 cm; mesh width: 150 μm; wire thickness: 112 μm; Feval Filtros, Spain). An A304 stainless steel mesh was used as electron collector in each compartment (dimensions: 14 x 12 cm; mesh width: 6 x 6 mm; wire thickness: 1 mm; Feval Filtros, S.L., Barcelona, Spain; Figure 3.1d). Prior to its use, and in order to remove all impurities from the carbon felt, it was sequentially soaked in acetone and nitric acid for 3 h and later rinsed in deionised water, as elsewhere described (Zhu et al., 2011). An Ag/AgCl reference electrode (Bioanalytical Systems, Inc., USA) was inserted in the anode compartment (+197 mV vs. SHE (all potential values hereafter in this Thesis are referred to SHE)).

One of the BESs was operated in MFC mode (Chapters 4 and 5; Figure 3.2), and the other one was operated in MEC mode (Chapters 4, 6, 7 and 8; Figure 3.3). The anode of each cell was connected to the cathode through a potentiostat (VSP, Bio-Logic, Grenoble, France; Figure 3.3c) in a three-electrode mode for data monitoring and poising of the anode potential (working electrode) when operating in MEC mode. The potentiostat was connected to a personal computer which recorded electrode potentials and current densities every 5 minutes using EC-Lab software V10.32 (Bio-Logic, Grenoble, France).

The anodic chamber of each cell was inoculated with a 30 mL (volatile suspended solids content of 2 g L^{-1}) resuspension of an MFC anode biofilm which had been operated with raw pig slurry (Sotres et al., 2015) and was stored submerged in pig slurry at +4 ºC for 2 months. The resuspension was done by vortex mixing during 10 minutes in a 50 mL tube containing 10 cm^2 of the carbon felt used as anode and 35 mL of Ringer 1/4 sterilised solution. The feeding solution for the MFC cathode chamber contained (per litre of deionised water): KH_2PO_4, 3 g; and Na_2HPO_4, 6 g. Aerobic conditions were maintained in the cathode (MFC) supplying air at a flow rate of 2 L min^{-1}. The catholyte for the MEC consisted of NaCl 0.1 g L^{-1}. Both the anode and the cathode compartment solutions were mixed continuously recirculating them with an external pump.

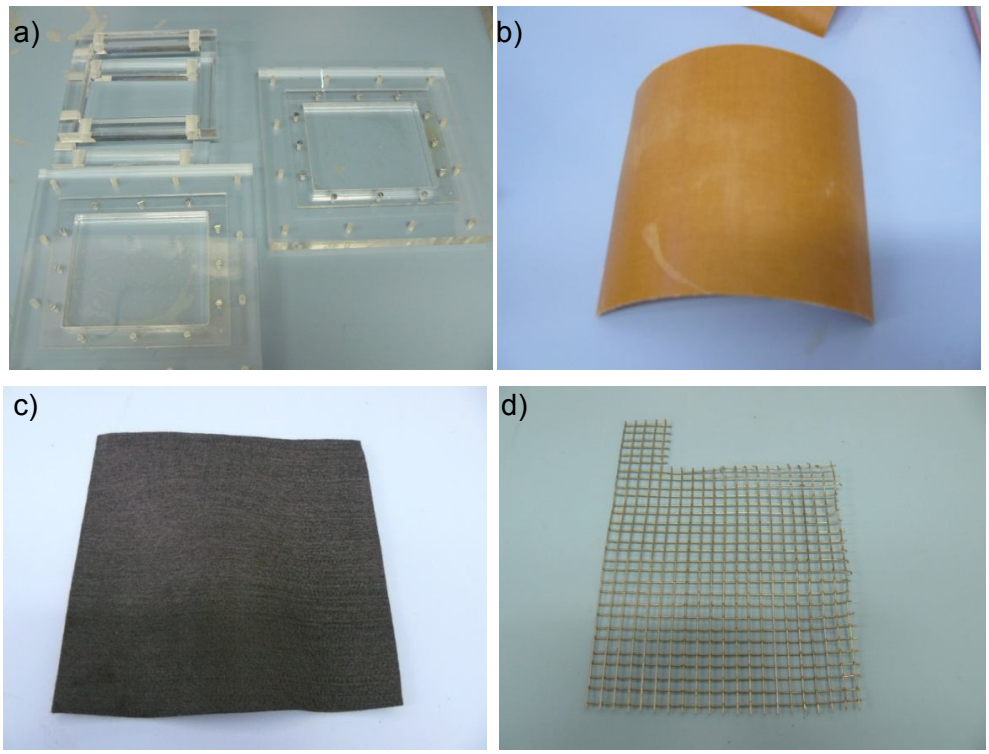

Figure 3.1 Pictures of the materials for BES construction: a) methacrylate frames; b) cation exchange membrane (CEM); c) carbon felt; d) stainless steel mesh.

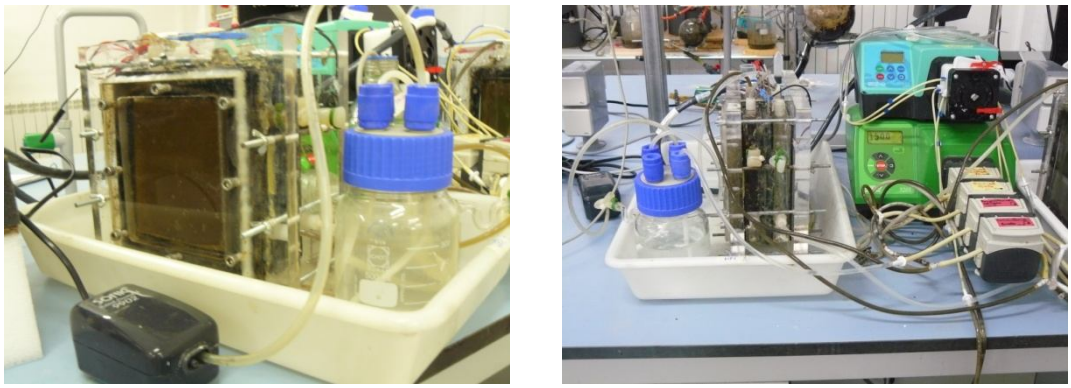

Figure 3.2 Pictures of the MFC.

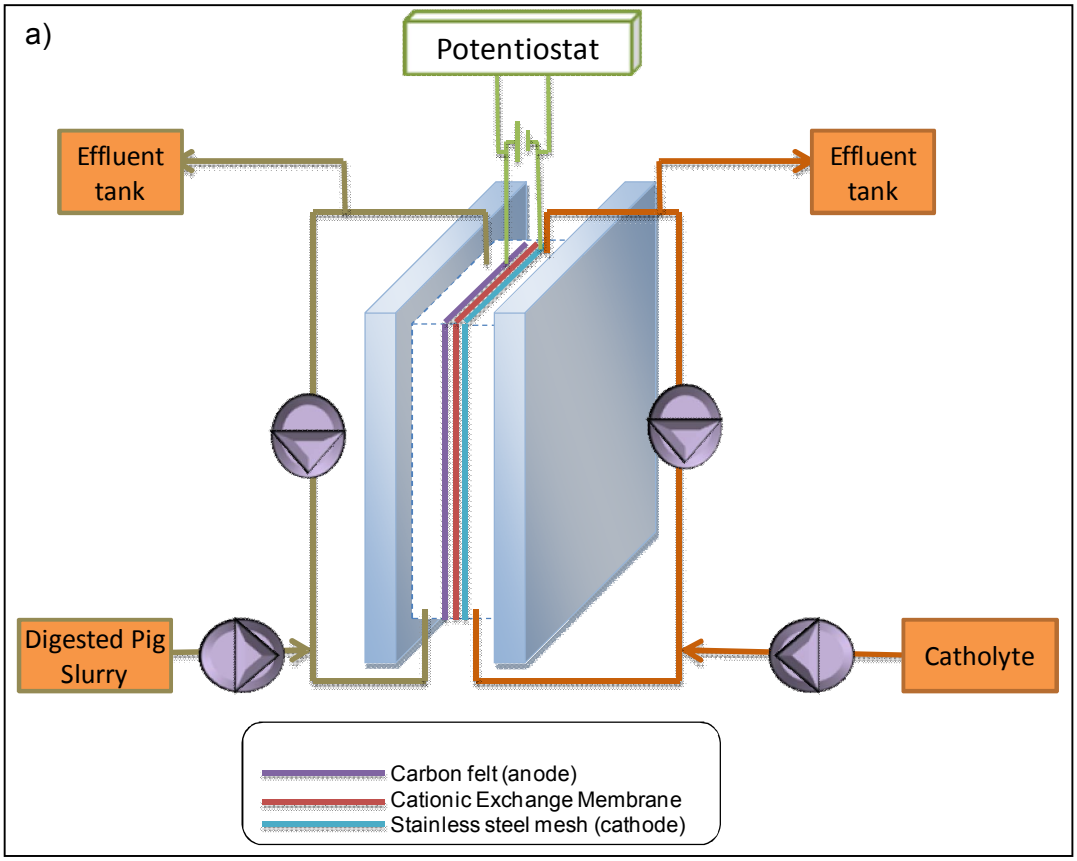

Figure 3.3 a) Scheme and b) picture of the MEC; c) picture of the potentiostat.

3.1.2 MEC with a methanogenic biocathode

Three MECs with methanogenic biocathode have been operated in this Thesis. All of them were identical two chamber cell (0.5 L each compartment) constructed using methacrylate, with the anode and cathode compartments (0.14 x 0.12 x 0.03 m^3) separated by a CEM as described in Section 3.1.1.

Two of the MECs (BC1 and BC2) were operated, both the anode and the cathode compartment, with synthetic medium (Chapter 10). In this case, each chamber was filled with

granular graphite with diameter ranging from 1 to 5 mm (Typ 00514, enViro-cell Umwelttechnik GmbH, Oberursel, Germany; Figure 3.4) to act as electrodes (anode and cathode), remaining 265 mL of net volume in each compartment. Prior to being used, in order to remove metals and organic residues, granular graphite was sequentially submerged in HCl (37%) and NaOH (1M) each for 24 hours, and then rinsed in deionised water and dried at 100 ºC (Sotres et al., 2016).

The third methanogenic MEC was operated with digested pig slurry in the anode compartment (Chapter 11). The MEC described in Section 3.1.1 was modified in order to convert it in a MEC with a methanogenic biocathode. The anode electrode, a carbon felt, was used as it was from the previous operation, while the cathode chamber was filled with granular graphite with diameter ranging from 1 to 5 mm as described for BC1 and BC2. The electrodes inoculation procedures are described in each Chapter.

An A304 stainless steel mesh was used as electron collector in each compartment for all the cells, and the anode of each cell was connected to the cathode through a potentiostat with a personal computer as described in Section 3.1.1.

The cathode potential (working electrode) was poised at -800 mV vs SHE, being the anode the counter electrode. An Ag/AgCl reference electrode (+197 mV vs. SHE; Bioanalytical Systems, Inc., USA) was inserted in the cathode compartment.

In BC1 and BC2 the anode compartment feeding solutions contained (per litre of deionised water): 2.9 g L^{-1} of CH_3COONa; NH_4Cl, 0.87 g; $CaCl_2$, 14.7 mg; KH_2PO_4, 3 g; Na_2HPO_4, 6 g; $MgSO_4$, 0.246 g; and 1 mL L^{-1} of a trace elements solution. As stated above, the third MEC was operated with digested pig slurry in the anode compartment The cathode compartment feeding solution of the three MECs had the same composition as the BC1 and BC2 anode solution, but replacing the carbon source (CH_3COONa) with 5 g L^{-1} of $NaHCO_3$ (as CO_2 is mainly present as HCO_3^- at pH 7). The solution of trace mineral contained (per litre of deionised water): $FeCl_3 \cdot H_2O$, 1.50 g; H_3BO_3, 0.15 g; $CuSO_4 \cdot 5H_2O$, 0.03 g; KI, 0.18 g; $MnCl_2 \cdot 4H_2O$, 0.12 g; $Na_2MoO_4 \cdot 2H_2O$, 0.06 g; $ZnSO_4 \cdot 7H_2O$, 0.12 g; $CoCl_2 \cdot 6H_2O$, 0.15 g; $NiCl_2 \cdot 6H_2O$, 0.023 g; EDTA, 10 g.

Figure 3.4 Picture of the granular graphite used as anode and cathode in the MEC BC1 and BC2.

3.1.3 Anaerobic digester (AD)

A lab-scale continuous stirred tank reactor (CSTR) was used to study its performance when treating pig slurry at a thermophilic temperature range (Chapters 5 to 8 and 11). The anaerobic digester (AD) consisted of a cylindrical glass reactor (25 cm diameter) with a 4 L working volume (Figure 3.5). The digester was fitted with a heat jacket with hot water circulating to keep the temperature at 55 ºC. Thermophilic conditions were chosen since AD is more sensitive to the presence of inhibitors such as ammonia at this range of temperature. A temperature probe was fitted into de reactor lid for temperature monitoring. Continuous mixing was also supplied using an overhead stirrer. A gas counter was used to measure biogas production (µFlow, Bioprocess Control AB, Sweden). The digester was initially inoculated with 2,550 mL (64% of the AD volume) of the effluent of another lab scale thermophilic AD fed with sewage sludge from a wastewater treatment plant.

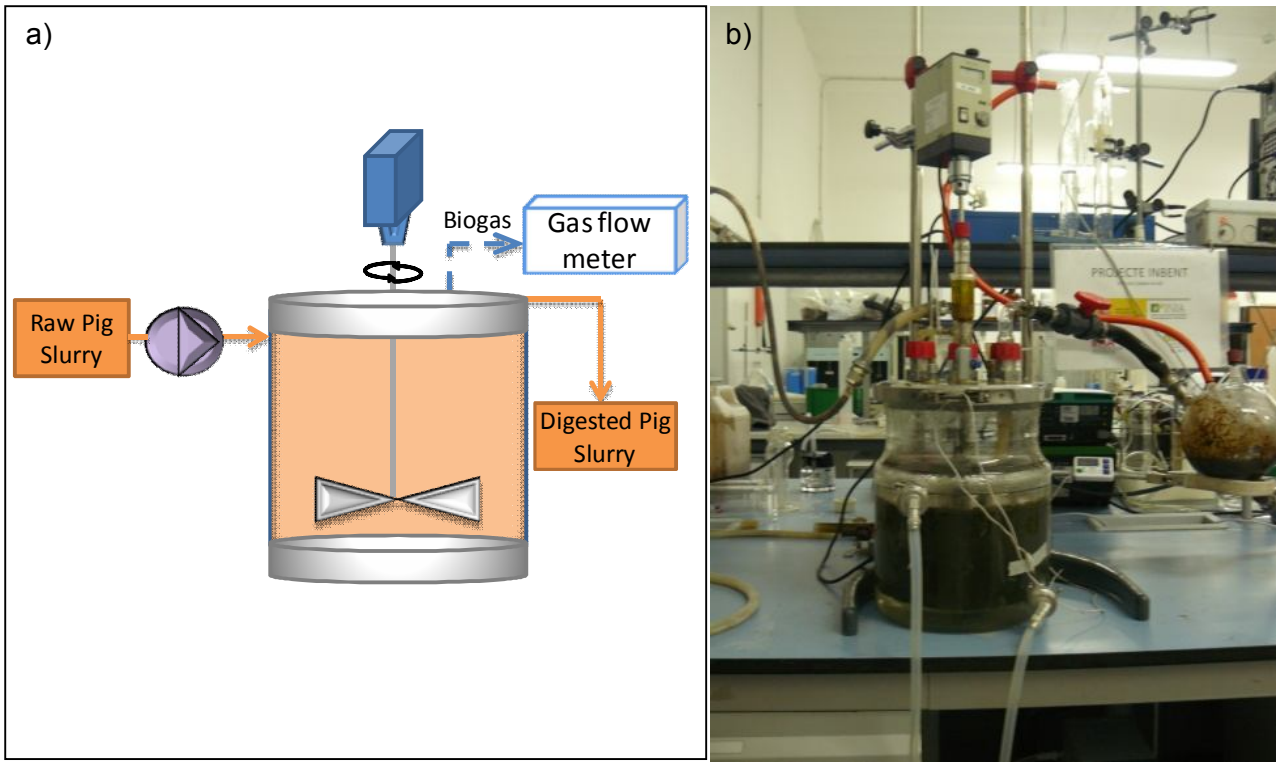

Figure 3.5 a) Scheme and b) picture of the anaerobic digester.

3.1.4 Stripping and absorption system

A stripping and absorption system was used to recover the ammonium transferred from the anode to the cathode compartment (Chapter 7; Figure 3.6). It consisted of two glass columns (70 cm height; 7 cm $Ø_{external}$; 5.5 cm $Ø_{internal}$) filled with glass rings (5-7 mm length). The cathode effluent was initially conducted to the top of the stripping column, and later circulated through the filling towards the bottom while air was pumped in the opposite direction. The air leaving the top of the column was directed to the absorption column, which was filled with an acidic solution (H_2SO_4, 10% v/v).

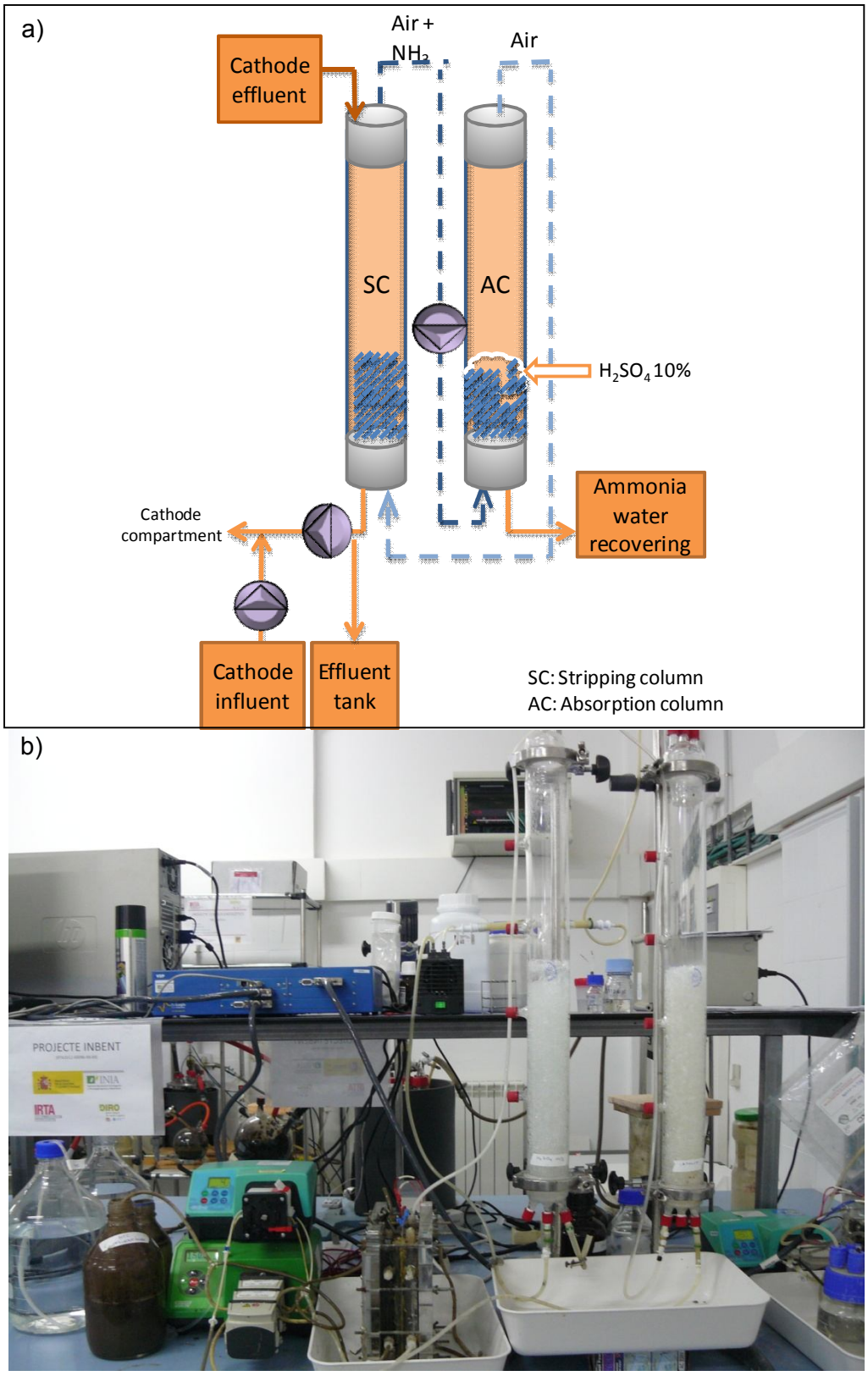

Figure 3.6 a) Scheme and b) picture of the stripping and absorption system connected to the MEC (right side).

3.1.5 Upflow anaerobic sludge blanket reactor (UASB)

A lab-scale UASB reactor with a working volume of 0.5 L was used in Chapter 9 (Figure 3.7). The reactor was constructed with glass and equipped with a water jacket to maintain the temperature at mesophilic conditions (35 ºC). Peristaltic pumps were used to control the influent feed rate and the recirculation rate. The reactor was inoculated with 100 mL of anaerobic granular sludge (volatile suspended solids content, VSS, of 59.60 g kg^{-1}) taken from a full-scale UASB reactor processing fruit juice wastewater (Mollerussa, Spain), which had been stored at 4 ºC until its utilisation in this study.

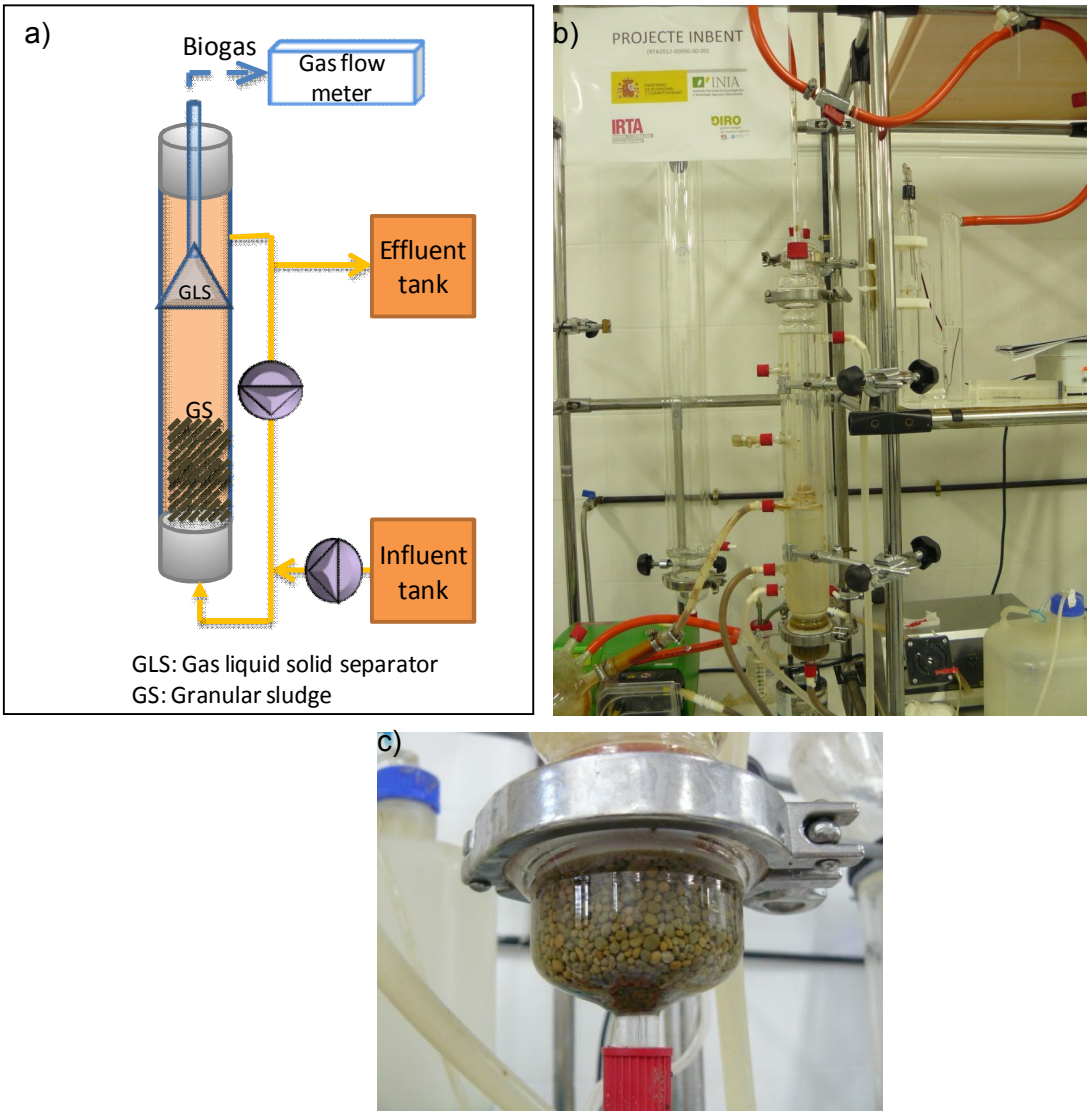

Figure 3.7 a) Scheme and b) picture of the UASB; c) detail of the granular biomass.

3.2 Analytical methods

3.2.1 pH

The pH of the bulk solution in each experiment was measured using a Crison 2000 pHmeter.

3.2.2 Alkalinity

Total alkalinity (TA) was determined according to standard methods (APHA, 2005) through titration to pH 4.3 with H_2SO_4 0.5 N. Partial alkalinity (PA, titration from the original pH sample to pH 5.75, an alkalinity which corresponds roughly to bicarbonate alkalinity) was determined to obtain intermediate alkalinity (IA, titration from 5.75 to 4.3, approximately the VFA alkalinity) (Ripley et al., 1986).

Alkalinity is expressed in calcium carbonate units according to the following equations:

$$\text{TA } (mg_{CaCO3}\ L^{-1}) = \frac{V_{4.3} \cdot N_{H_2SO_4}}{V_{sample}} \cdot 50 \qquad (3.1)$$

$$\text{PA } (mg_{CaCO3}\ L^{-1}) = \frac{V_{5.75} \cdot N_{H_2SO_4}}{V_{sample}} \cdot 50 \qquad (3.2)$$

$$\text{IA } (mg_{CaCO3}\ L^{-1}) = \text{TA} - \text{PA} \qquad (3.3)$$

where $V_{4.3}$, $V_{5.75}$, and V_{sample} correspond to the volume of acid consumed for the titration to pH 4.3 and 5.75 and the sample volume, respectively; and N the acid normality.

The IA:TA ratio was used as a tool to monitor anaerobic digestion, considering that the process was stable when the IA:TA was below 0.3.

3.2.3 Total and volatile solids

Total (TS) and volatile solids (VS) were determined according to standard methods (APHA, 2005). TS were obtained drying a well homogenised sample in a stove at 105 ºC for 24 h to constant weight, and are calculated with the following equation:

$$TS(\%) = 100 - \frac{W_w - W_d}{W_w - T} \cdot 100 \qquad (3.4)$$

Next, the sample is calcined at 550 ºC in the muffle during 3.5 hours and weighed. The weight difference between the TS and the obtained ashes is the VS content.

$$VS(\%) = 100 - \frac{W_d - W_a}{W_d - T} \cdot 100 \qquad (3.5)$$

where W_w, W_d, W_a and T are the weight (g) of the wet sample, the dry sample, the ashes and the capsule, respectively.

3.2.4 Chemical oxygen demand

Chemical oxygen demand (COD) was analysed according to an optimised standard method (Noguerol et al., 2012). The sample was oxidised with 1.5 mL of digestion reagent (potassium dichromate, 0.5 N, mercury sulphate and sulphuric acid 95-97%) and 1.5 mL of catalyst (silver sulphate 1%, and sulphuric acid 95-97%) and digested at 150 ºC for 2 h in a digester (Hach Lange LT 200). Dichromate concentration was measured colorimetrically (spectrophotometer Hach Lange DR 2800). For soluble COD measurement the samples were previously filtered through a 0.45 µm pore diameter Nylon syringe filter (Scharlau, S.L.).

3.2.5 Ammonium nitrogen

Ammonium (N-NH_4^+) was analysed according to standard methods (APHA, 2005) with a Büchi B-324 distiller (Büchi Labortechnic AG, Switzerland) and a Metrohm 702 SM autotitrator (Metrohm, Switzerland).

The analysis is based on the transformation, in liquid medium, of the ammonium ion (NH_4^+) into ammonia (NH_3), in the presence of a base such as sodium hydroxide (NaOH, 40%). NH_3 is distilled, and recovered latter as NH_4^+ in a known volume of boric acid (2%), obtaining ammonium borate. Finally, the solution was titrated with HCl 0.1N. NH_4^+ in the sample is quantified with the following equation:

$$N - NH_4^+ (mg\, kg_{W_w}^{-1}) = \cdot \frac{(V_1 - V_0) \cdot 14 \cdot 1000 N_{HCl}}{W_w} \qquad (3.6)$$

where V_1 and V_0 are the volumes of HCl consumed in sample and control titration (mL), respectively; N_{HCl} is the normality of the HCl used for the titration; and W_w is the sample wet weight (g).

3.2.6 Total kjeldahl nitrogen

Total kjeldahl nitrogen (NTK) was determined according to standard methods (APHA, 2005). The sample was digested in a 300 mL glass Kjeldahl tube with 10 mL of sulphuric acid (96%) and a catalyst (Kjeltab) in a Büchi K-437 block digester at 180 ºC for 60 min and at 350 ºC for 60 min. Afterwards, the sample was distilled and titrated as described for ammonium nitrogen determination (Section 3.2.5).

NTK in the sample is quantified with the following equation:

$$NTK(mg\,kg_{W_w}^{-1}) = \frac{(V_1 - V_0)\cdot 14\cdot 1000 N_{HCl}}{W_w} \qquad (3.7)$$

where V_1 and V_0 are the volumes of HCl consumed in sample and control titration (mL), respectively; N_{HCl} is the normality of the HCl used for the titration; and W_w is the sample wet weight (g).

Free ammonia concentration was calculated from the equilibrium relationship:

$$[NH_3] = \frac{[T\text{-}NH_3]}{\left(1+\frac{H^+}{k_a}\right)} \qquad (3.8)$$

where $[NH_3]$ and $[T\text{-}NH_3]$ are respectively the free and the total ammonia (NTK) concentrations, and k_a the dissociation constant with a value of $38.3\cdot10^{-10}$ at 55 °C.

3.2.7 Volatile fatty acids

Volatile fatty acids (VFAs) -acetic, propionic, iso and n-butyric, iso and n-valeric, iso and n-caproic and heptanoic acids- were quantified with a VARIAN CP-3800 (Varian, USA) gas chromatograph equipped with a TRB-FFAP (free fatty acids phase) column and a flame ionisation detector (FID). A sample of 1 µL was automatically injected (autosampler VARIAN CP-8400) by means of a gas tight syringe (10 µL Hamilton 701 N) at a temperature of 250 ºC under split conditions. The carrier gas was helium with a split ratio of 1/30, and a flux of 40 mL min^{-1}. The column temperature was set to 40 ºC for 1 min, followed by a first increase of 25 ºC min^{-1} until a stable value of 95 ºC was reached, then 10 ºC min^{-1} up to 125 ºC and finally 30 ºC min^{-1} up to 215 ºC. The oven and detector temperatures were set at 40 and 300 ºC, respectively, with 300 mL min^{-1} air and 30 mL min^{-1} hydrogen gas supplied. The run time was 9.5 min.

3.2.8 Anions and cations determination

Anion concentration (Cl^-, NO_3^-, NO_2^-, PO_4^{3-}, SO_4^{2-}) was measured by ionic chromatography (IC) with a 861 Advanced Compact IC (Metrohm, Switzerland) using a Metrosep A Supp 4-250 (Metrohm, Switzerland) column and a CO_2 suppressor. The eluent consisted of 1.8 mmol $NaCO_3$ L^{-1} and 1.7 mmol $NaHCO_3$ L^{-1}.

Cations (Na^+, K^+, Ca^{+2}, Mg^{+2}) were measured with a 790 Personal IC (Metrohm, Switzerland) and Metrosep C2 column (Metrohm, Switzerland), using as eluent 4 mmol $C4H_6O_6$ L^{-1} (tartaric acid) and 0.75 mmol pyridine-2,6-dicarboxylic acid L^{-1}.

Prior to the IC analysis, samples were diluted and filtrated with nylon (0.45 mm) and BonElut JR C18 micro filters (Varian, USA). Samples were injected automatically (863 Compact Autosampler, Metrohm, Switzerland).

3.2.9 Biogas composition

Methane in the samples was determined using a VARIAN CP-3800 (Varian, USA) gas chromatograph equipped with a Hayesep® Q packed column (matrix 80/100) and a thermal conductivity detector (TCD). A sample of 200 µL was manually injected by means of a gas tight syringe (500 µL Hamilton Sampleblock Syringe) at a temperature of 180 ºC. The carrier gas was helium, with a flux of 45 mL min^{-1}. The oven and detector temperatures were set at 90 and 180 ºC, respectively.

3.2.10 Dissolved methane

Methane production in the BES was calculated through the determination of dissolved methane in solution (Alberto et al. 2000). Around 2.5 mL anolyte samples were collected with a 5 mL syringe and injected with a needle in a 5 mL vacutainer. The vacutainers were shaken vigorously for 30 s and then allowed to stand for 1 h. Headspace gas was analysed for CH_4 using a VARIAN CP-3800 (Varian, USA) gas chromatograph (Section 3.2.9). Dissolved CH_4 was computed using the equation:

$$X_L = \frac{C_{CH_4} \cdot MV_{CH_4} \cdot MW_{CH_4} \cdot (V_T - V_L + \propto V_L) \cdot 1000}{V_L} \qquad (3.9)$$

where X_L is the concentration of CH_4 (mg L^{-1}) in the solution, C_{CH4} is the concentration of CH_4 (%) in the headspace 1 h after shaking, MV_{CH4} is the molar volume of CH_4 at 25 ºC (0.041 mol L^{-1}), MW_{CH4} is the molecular weight of CH_4 (16 g mol^{-1}), V_T is the volume (mL) of the vacutainer, V_L is the volume (mL) of the solution, and α is the water:air partition coefficient at 25 ºC (0.03).

3.2.11 Anaerobic biodegradability tests (ABT)

In order to know the biodegradability of the remaining organic matter of the digestates used as feed solution for the BES or the pig slurry used to feed the AD, anaerobic biodegradability tests (ABT) of the substrates were performed. ABT were performed in serum bottles (120 mL) in duplicate according to Soto et al. (1993) and Angelidaki et al. (2009). The serum bottles were filled with 50 g of a solution composed of the inoculum (5 g_{VSS} L^{-1}), substrate (5 g_{COD} L^{-1}), macronutrients and micronutrients and bicarbonate (1 $g_{NaHCO3-}$ $g_{CODadded}^{-1}$). Digested sludge from a mesophilic lab-scale anaerobic digester was used as inoculum. A control, in duplicate without digestate substrate was included in the setup. The bottles were sealed with rubber stoppers and capped with aluminium crimp caps. The headspace was purged with N_2 for 5 min in order to remove O_2. The bottles were incubated at 37±2 ºC for 40 days. Methane production was monitored by periodically taking a gas sample (0.2 mL) from the head space with a gas-tight syringe and analysing the gas composition by gas chromatography equipped with a TCD detector (Section 3.2.9).

3.2.12 Specific methanogenic activity (SMA)

The SMA of the anaerobic granular sludge of the UASB (figure 3.8) was evaluated at 36 ºC in serum bottles (120 mL) in duplicate (Angelidaki et al. 2009; Silvestre et al. 2015; Soto et al. 1993). Acetate, a VFA mix (acetate/propionate/butyrate, 70/20/10), methanol and H_2 were used as substrates. The serum bottles were filled with 50 mL of a solution composed of the granular sludge (5 g_{VSS} L^{-1}), substrate (5 g_{COD} L^{-1}), macronutrients, micronutrients and bicarbonate (1 $g_{NaHCO3-}$ $g_{CODadded}^{-1}$). A control duplicate without medium was included in the setup. The bottles were sealed with rubber stoppers and capped with aluminium crimp caps. The headspace was purged during 5 min with N_2 in order to remove O_2. Methane production was monitored by periodically taking a gas sample (0.2 mL) from the head space with a gas-tight syringe and analysing the gas composition by gas chromatography (Section 3.2.9). The SMA was calculated from the linear increase in the CH_4 concentration in the beginning of the experiments, when no lag phase was observed, divided by the amount of VSS.

Figure 3.8 Picture of the serum bottles used for SMA test.

3.3 Electrochemical calculations and techniques

The current density (A m^{-2}) of the MECs was calculated as the quotient between the intensity recorded by the potentiostat (A) and the area of the anode (m^2). In the case of BC1 and BC2 (Chapter 10), current density was normalised to the net volume of the anode compartment (A m^{-3}). For the MFC, current density was obtained according to $I=V/(R \cdot a)$, where V (V) is the cell voltage, R (Ω) is the resistance and a (m^2) is the area of the anode in contact with the anode bulk solution.

Cyclic voltammetries (CV) in turnover conditions, i.e. in the presence of substrate, were performed using a potentiostat (VSP, Bio-Logic, Grenoble, France) at different times of operation of the biocathodes, in order to study the electroactive microbial biofilms developed on the cathodes. The same three-electrode configuration used for the MECs operation was maintained for the set up of the CV. The start (E_i) and vertex (E_f) potentials were -800 and +400 mV *vs* SHE, respectively, and the scan rate was set at 1 mV s^{-1}.

3.4 System performance calculations and indices

3.4.1 Removal efficiencies

In batch assays (Chapter 4), ammonium and COD removal efficiency were calculated as the ratio of the difference between initial and final concentrations in the bulk solution in each assay and its initial concentration. The flux of N-NH_4^+ from the anode to the cathode (g N-NH_4^+ d^{-1} m^{-2}) was calculated as the difference between the initial and final concentration, divided by the volume of the anode compartment, the time of the batch (day) and the surface of the cationic exchange membrane (m^2).

Ammonium and COD removal efficiencies in the BESs in continuous operation were calculated as the ratio of the difference between the anode influent and effluent concentrations and the influent concentration.

3.4.2 Charge transport

When calculating charge, Q, in the batch assays of Chapter 4 a distinction was made between transport of negative charges in the form of electrons through the electric circuit, Q^-, and transport of positive charges in the form of the dominantly present cation species in the system (Na^+, K^+, NH_4^+, Ca^{2+}, and Mg^{2+}), through the membrane, Q^+. Total charge production, Q^-, expressed in coulombs (C) was determined by integrating current over time. Transport of positive charges in the form of cation species in the system through the membrane, Q^+, expressed in coulombs (C) was determined as follows:

$$Q^{+} = \sum_{cat} ((x^{cat,t} - x^{cat,0}) V z^{cat} F) \quad (3.10)$$

with $x^{cat,t}$ the molar concentration of the cation species at the end of an experimental run expressed in mol L^{-1} (M), $x^{cat,0}$ the molar concentration of the cation species at the start of an experimental run expressed in mol L^{-1} (M), V the cathode chamber liquid volume expressed in litres (L), z^{cat} the valence of the cation species, and F the Faraday constant (96485 C mol^{-1}).

3.4.3 Electrochemical efficiencies

The Coulombic efficiency (CE), or the fraction of electrons obtained from the consumption of COD that are available for current generation or methane production at the biocathodes (Equation 3.11), the energy efficiency relative to electrical input recovered as methane (EE_e, Equation 3.12), the energy efficiency relative to the energy content of the substrate (EE_s, Equation 3.13) and the energy efficiency with respect to the energy input and the energy in the substrate (EE_{e+s}, Equation 3.14) were calculated as:

$$CE = \frac{M \int_0^t I \, dt}{F \, b \, q \, \Delta COD} \quad (3.11)$$

$$EE_e = \frac{n_{CH_4} \Delta G_{CH_4}}{\int_0^t I \, E_{ap} dt} \quad (3.12)$$

$$EE_s = \frac{n_{CH_4} \Delta G_{CH_4}}{n_S \Delta G_S} \quad (3.13)$$

$$EE_{e+s} = \frac{n_{CH_4} \Delta G_{CH_4}}{\int_0^t I \, E_{ap} dt + n_S \Delta G_S} \quad (3.14)$$

where M is the molecular weight of the final electron acceptor, I is the current (A), F is Faraday's constant, b is the number of electrons transferred per mole of O_2, q is the volumetric influent flow rate (L d^{-1}), ΔCOD is the difference in the influent and effluent COD (g L^{-1}), n_{CH4} are the moles of produced methane, ΔG_{CH4} is the molar Gibbs free energy of CH_4 oxidation by oxygen to carbon dioxide (-817.97 kJ mol^{-1}), E_{ap} is the applied voltage calculated as the difference between the cathode and anode potentials (V), n_S are the moles of acetate consumed and ΔG_S is the molar Gibbs free energy of acetate oxidation to carbon dioxide (-844.61 kJ mol^{-1}).

Finally, the cathodic methane recovery efficiency (R_{cat}), defined as the fraction of electrons reaching the cathode that are recovered as methane, was calculated as:

$$R_{cat} = \frac{8\,F\,n_{CH_4}}{\int_0^t I\,dt} \qquad (3.15)$$

CH_4 production efficiency was calculated as the ratio between the COD contained in the CH_4 and the total removed COD.

3.5 Statistical analysis

Data were analysed using one-way analysis of variance (ANOVA). Whenever significant differences of means were found, the Tukey test at a 5% significance level was performed for separation of means. Statistical analysis was performed using the R software package (R project for statistical computing, http://www.r-project.org).

3.6 Microbial community analysis

3.6.1 Total DNA extraction

Total DNA was extracted in triplicate from known weights of each sample (mainly graphite granule, carbon felt and AD sludge/granule) following a bead-beating protocol by means of the PowerSoil® DNA Isolation Kit (MoBio Laboratories Inc., Carlsbad, CA, USA), according to the manufacturer's instructions.

3.6.2 Simultaneous total DNA and RNA extraction and complementary DNA (cDNA) synthesis

Simultaneous total genomic DNA and RNA (including rRNA) were extracted in triplicate from known weights of each sample with the PowerMicrobiome™ RNA Isolation Kit (MoBio Laboratories Inc., Carlsbad, CA, USA), according to manufacturer's instructions. Purified mRNA and rRNA were obtained by removal of co-extracted DNA with DNase I incubation (provided in the kit) at 25 ºC for 10 min and inactivation of DNase I with EDTA 50 mM (Thermo Scientific Fermentas, USA) at 75 ºC during 5 min. Reverse transcription step PCR (RT-PCR) for cDNA synthesis from the obtained RNA was performed by using PrimeScript™ RT Reagent Kit (Takara Bio Inc., Japan). The reaction was carried out in a final volume of 30 µL which contained 15 µL of purified RNA, 6 µL of PrimeScript™ buffer, 1.5 µL of retrotranscriptase mix, 1.5 µL of Random 6 mers and 6 µL of RNase Free dH_2O. Henceforth, the term cDNA or 16S rRNA is used to refer to the extracted RNA or 16S rRNA gene amplicons from cDNA as a

measure of gene expression and microbial activity, whereas DNA or 16S rDNA terms are used referring to the extracted genomic DNA and 16S rRNA gene amplicons from DNA.

3.6.3 Quantitative PCR assay (qPCR)

Total and expressed gene copy numbers of eubacterial *16S rRNA* gene and *mcrA* gene (methanogenic archaeal methyl coenzyme-M reductase) were quantified by means of quantitative real-time PCR (qPCR). Each sample was analysed in triplicate by means of the three independent DNA extracts. The analysis was carried out by using Brilliant II SYBR Green qPCR Master Mix (Stratagene, La Jolla, CA, USA) in a Real-Time PCR System Mx3000P (Stratagene) operated with the following protocol: 10 min at 95 ºC, followed by 40 cycles of denaturation at 95 ºC for 30 s, annealing for 30 s at 55 ºC and 54 ºC (for *16S rRNA* and *mcrA* gene, respectively), extension at 72 ºC for 45 s, and fluorescence capture at 80 ºC for 30 s and 15 s (for *16S rRNA* and *mcrA* gene, respectively). The specificity of PCR amplification was determined by observations on a melting curve and gel electrophoresis profile. A melting curve analysis, to detect the presence of primer dimmers, was performed after the final extension, increasing the temperature from 55 to 95 ºC at heating rates of 0.5 ºC each 10 s. Image capture was performed at 80 ºC to exclude fluorescence from the amplification of primer dimmers. Each reaction was performed in 10 µL volumes containing 1 µL of DNA template, 200 nmol L^{-1} of each *16S rRNA* primer, 600 nmol L^{-1} of each *mcrA* primer, 5 µL of the ready reaction mix, and 30 nmol L^{-1} of ROX reference dye. The primer set for eubacterial population was 341F (5′-CCTACGGGAGGCAGCAG-3′) and 518R (5′-ATTACCGCGGCTGCTGG-3′). The primer set for archaeal *mcrA* gene was ME1F (5′-GCMATGCARATHGGWATGTC-3′) and ME3R (5′-TGTGTGAASCCKACDCCACC-3′); both primer pairs were purified by HPLC. The standard curves were performed with the following reference genes: a *16S rRNA* gene from *Desulfovibrio vulgaris* ssp. *vulgaris* ATCC 29579, and a *mcrA* gene fragment obtained from *Methanosarcina barkeri* DSM 800, both inserted in a TOPO TA vector (Invitrogen Ltd, Paisley, UK). All reference genes were quantified by NanoDrop 1000 (Thermo Scientific). Ten-fold serial dilutions of known copy numbers of the plasmid DNA, in the range of 10^2 to 10^9 copies for *16S rRNA* gene and in the range of 10 to 10^8 copies for *mcrA* gene, were subjected to a qPCR assay in duplicate to generate the standard curves. All results were processed by MxPro QPCR Software (Stratagene).

3.6.4 High Throughput Sequencing (454-Pyrosequencing) of total eubacterial and archaeal community

The specific steps for 16S-based eubacteria and archaea 454-Pyrosequencing analysis were carried out as follows: sequencing step of massive bar-coded *16S rRNA* gene libraries,

targeting eubacterial region V1-V3 *16S rRNA* and archaeal region V3-V4, was performed at MR DNA (www.mrdnalab.com, Shallowater, TX, USA) on a 454 FLX Titanium (Roche Diagnostics, Branford, CT, USA) equipment. In summary, diluted DNA extracts (1:10) were used as a template for PCR. Each DNA (two independent total DNA extracts per sample) was amplified separately with both the eubacteria and archaea *16S rRNA* set of primers containing unique multiplex identifier (MID) tags recommended by Roche Diagnostics (Roche Diagnostics, 2009). For eubacteria libraries the primer sets were 27F (5'-AGRGTTTGATCMTGGCTCAG–3') and 519R (5'-GTNTTACNGCGGCKGCTG-3'), while the archaeal sets of primers were 349F (5'-GYGCASCAGKCGMGAAW-3') and 806R (5'–GGACTACVSGGGTATCTAAT-3').

The obtained reads were compiled in FASTq files for further bioinformatics processing. Trimming of the *16S rRNA* barcoded sequences into libraries was carried out using QIIME software version 1.8.0 (Caporaso et al., 2010b). Quality filtering of the reads was performed at Q25 quality, prior to grouping into Operational Taxonomic Units (OTUs) at a 97% sequence homology cutoff. The following steps were performed using QIIME: Denoising, using a Denoiser (Reeder and Knight, 2010). Reference sequences for each OTU (OTU picking up) were obtained via the first method of UCLUST algorithm (Edgar, 2010). PyNAST was used for sequence alignment (Caporaso et al., 2010a) and ChimeraSlayer for chimera detection (Haas et al., 2011). OTUs were then taxonomically assigned using the Ribosomal Database Project (RDP training set 14) Naïve Bayesian Classifier (http://rdp.cme.msu.edu) and compiled into each taxonomic level with a bootstrap cutoff value of 80% (Cole et al. 2009; Wang et al., 2007). Data obtained from pyrosequencing datasets were deposited in the Sequence Read Archive of the National Centre for Biotechnology Information (NCBI, USA). The accession numbers for each study are specified in the corresponding Chapters.

3.6.5 High throughput sequencing (MiSeq, Illumina) of total eubacteria and archaeal community

The specific steps followed during MiSeq analysis of massive libraries of 16S rDNA and 16S rRNA both for eubacteria and archaea were carried out as follows. Massive bar-coded *16S rRNA* gene libraries (16S rDNA and 16S rRNA) targeting eubacterial region V1-V3 *16S rRNA* and archaeal region V3-V4 were sequenced utilising MiSeq equipment (Illumina, San Diego, CT, USA). Each DNA or cDNA was amplified separately (16S rDNA and 16S rRNA respectively) with both *16S*-based eubacteria and archaea sets of primers. For eubacteria libraries the primer sets were 27F (5'-AGRGTTTGATCMTGGCTCAG–3') and 519R (5'-GTNTTACNGCGGCKGCTG-3'), while the archaeal sets of primers were 349F (5'-GYGCASCAGKCGMGAAW-3') and 806R (5'–GGACTACVSGGGTATCTAAT-3'). Sequencing step was performed at MR DNA (www.mrdnalab.com, Shallowater, TX, USA) on a MiSeq

instrument following the manufacturer's guidelines. The obtained reads were compiled in FASTq files for further bioinformatics processing, following the steps described in Section 3.6.4. All data obtained from sequencing datasets were submitted to the Sequence Read Archive of the National Center for Biotechnology Information (NCBI, USA). The accession numbers for each study are specified in the corresponding Chapters.

3.6.6 Biodiversity evaluation and statistical analyses

To evaluate the diversity of the samples, the number of OTUs, the inverted Simpson index, Shannon index, Goods coverage and Chao1 richness estimator were calculated using Mothur software v.1.34.4 (http://www.mothur.org) (Schloss et al., 2009). All estimators were normalised to the lower number of reads among the different samples. Statistical multivariate analyses (covariance-based Principal Component Analyses (PCA) and correspondence analysis (CA)) on the OTUs abundance matrix of Eubacterial and Archaeal OTUs distribution were performed. The obtained samples and OTUs scores were depicted in a 2D biplot, which represented the phylogenetic assignment of the predominant OTUs (relative abundance above 1%). Statistical multivariate correspondence analysis (CA) of 454-Pyrosequencing or MiSeq OTU relative distribution data was performed by means XLSTAT 2014 software (Addinsoft, Paris, France).

3.7 References

Alberto, M.C.R., Arah, J.R.M., Neue, H.U., Wassmann, R., Lantin, R.S., Aduna, J.B., Bronson, K.F. 2000. A sampling technique for the determination of dissolved methane in soil solution. *Chemosphere - Global Change Science*, **2**(1), 57-63.

Angelidaki, I., Alves, M., Bolzonella, D., Borzacconi, L., Campos, J.L., Guwy, A.J., Kalyuzhnyi, S., Jenicek, P., van Lier, J.B. 2009. Defining the biomethane potential (BMP) of solid organic wastes and energy crops: a proposed protocol for batch assays. *Water Sci Technol*, **59**(5), 927-34.

APHA. 2005. *Standard methods for the examination of water and wastewater. 21th ed*. American Public Health Association, American Water Works Association, and Water Pollution Control Federation, Washington, D.C.

Caporaso, J.G., Bittinger, K., Bushman, F.D., DeSantis, T.Z., Andersen, G.L., Knight, R. 2010a. PyNAST: a flexible tool for aligning sequences to a template alignment. *Bioinformatics*, **26**(2), 266-267.

Caporaso, J.G., Kuczynski, J., Stombaugh, J., Bittinger, K., Bushman, F.D., Costello, E.K., Fierer, N., Gonzalez Peña, A., Goodrich, J.K., Gordon, J.I., A Huttley, G., Kelley, S.T., Knights, D., Koenig, J.E., Ley, R.E., Lozupone, C.A., McDonald, D., Muegge, B.D., Pirrung, M., Reeder, J., Sevinsky, J.R., Turnbaugh, P.J., Walters, W.A., Widmann, J., Yatsunenko, T., Zaneveld, J., Knight, R. 2010b. QIIME allows analysis of high-throughput community sequencing data. *Nature Methods*, **7**, 335–336.

Cole, J.R., Wang, Q., Cardenas, E., Fish, J., Chai, B., Farris, R.J., Kulam-Syed-Mohideen, A.S., McGarrell, D.M., Marsh, T., Garrity, G.M., Tiedje, J.M. 2009. The Ribosomal Database Project: improved alignments and new tools for rRNA analysis. *Nucleic Acids Research*, **37**(suppl 1), D141-D145.

Edgar, R.C. 2010. Search and clustering orders of magnitude faster than BLAST. *Bioinformatics*, **26**(19), 2460-1.

Haas, B.J., Gevers, D., Earl, A.M., Feldgarden, M., Ward, D.V., Giannoukos, G., Ciulla, D., Tabbaa, D., Highlander, S.K., Sodergren, E., Methé, B., DeSantis, T.Z., The Human Microbiome, C., Petrosino, J.F., Knight, R., Birren, B.W. 2011. Chimeric 16S rRNA sequence formation and detection in Sanger and 454-pyrosequenced PCR amplicons. Genome Research, **21**(3), 494-504.

Noguerol, J., Rodríguez-Abalde, A., Romero, E., Flotats, X., 2012. Determination of Chemical Oxygen Demand in Heterogeneous Solid or Semisolid Samples Using a Novel Method Combining Solid Dilutions as a Preparation Step Followed by Optimized Closed Reflux and Colorimetric Measurement. *Analytical Chemistry*. **84**, 5548−5555.

Reeder, J., Knight, R. 2010. Rapidly denoising pyrosequencing amplicon reads by exploiting rank-abundance distributions. *Nature Methods*, **7**(9), 668-669.

Ripley, L.E., Boyle, W.C., Converse, J.C. 1986. Improved alkalimetric monitoring for anaerobic digestion of high-strength wastes. Journal (Water Pollution Control Federation), **58**(5), 406-411.

Schloss, P.D., Westcott, S.L., Ryabin, T., Hall, J.R., Hartmann, M., Hollister, E.B., Lesniewski, R.A., Oakley, B.B., Parks, D.H., Robinson, C.J., Sahl, J.W., Stres, B., Thallinger, G.G., Van Horn, D.J., Weber, C.F. 2009. Introducing mothur: open-source, platform-independent, community-supported software for describing and comparing microbial communities. Applied and Environmental Microbiology, **75**(23), 7537-7541.

Silvestre, G., Bonmatí, A., Fernández, B. 2015. Optimisation of sewage sludge anaerobic digestion through co-digestion with OFMSW: Effect of collection system and particle size. *Waste Management*, **43**, 137-143.

Soto, M., Méndez, R., Lema, J.M. 1993. Methanogenic and non-methanogenic activity tests. Theoretical basis and experimental set up. *Water Research*, **27**(8), 1361-1376.

Sotres, A., Cerrillo, M., Viñas, M., Bonmatí, A. 2015. Nitrogen recovery from pig slurry in a two-chambered bioelectrochemical system. *Bioresource Technology*, **194**, 373-382.

Sotres, A., Cerrillo, M., Viñas, M., Bonmatí, A. 2016. Nitrogen removal in a two-chambered microbial fuel cell: establishment of a nitrifying-denitrifying microbial community on an intermittent aerated cathode. *Chemical Engineering Journal*, **284**, 905-916.

Zhu, N., Chen, X., Zhang, T., Wu, P., Li, P., Wu, J. 2011. Improved performance of membrane free single-chamber air-cathode microbial fuel cells with nitric acid and ethylenediamine surface modified activated carbon fiber felt anodes. *Bioresource Technology*, **102**(1), 422-426.

Wang, Q., Garrity, G.M., Tiedje, J.M., Cole, J.R. 2007. Naïve bayesian classifier for rapid assignment of rRNA sequences into the new bacterial taxonomy. Applied and Environmental Microbiology, **73**(16), 5261-5267.

CHAPTER 4

Comparative assessment of raw and digested pig slurry treatment in bioelectrochemical systems

Part of the content of this chapter was published as:

Cerrillo, M., Oliveras, J., Viñas, M., Bonmatí, A. 2016. Comparative assessment of raw and digested pig slurry treatment in bioelectrochemical systems. *Bioelectrochemistry*, **110**, 69-78. doi: 10.1016/j.bioelechem.2016.03.004

Abstract

Both raw and anaerobically digested pig slurries were investigated in batch assays in two chambered bioelectrochemical systems (BES) run in Microbial Fuel Cell (MFC) and Microbial Electrolysis Cell (MEC) mode. Chemical Oxygen Demand (COD) removal, nitrogen recovery, cation transport and anode microbial population evolution were assessed. The Anaerobic Digestion-MEC (AD-MEC) integrated system achieved the highest COD removal (60% in 48h); while the maximum NH_4^+ removal efficiency (40%, with an ammonia flux of 8.86 g $N\text{-}NH_4^+$ d^{-1} m^{-2}) was achieved in MFC mode fed with digested pig slurry in 24 h. On the other hand, the high pH (12.1) achieved in MEC mode (NaCl solution as catholyte), could favour ammonium recovery in a subsequent stripping and absorption process. Ammonia was the main cation involved in maintaining the electroneutrality between both compartments. Regarding microbial population, *Desulfuromonadaceae*, a known family of exoelectrogenic bacteria, was enriched under MEC mode, whereas hydrogenotrophic and methylotrophic methanogen phylotypes belonging to *Thermoplasmatales* were also favoured against acetotrophic *Methanosaetaceae*. From these results, the integration of anaerobic digestion in BES seems to be an interesting alternative for the treatment of complex substrates, since a polished effluent can be obtained and ammonium can be simultaneously recovered for further reuse as fertiliser.

4.1 Introduction

The increasing global demand for fossil fuels, their tendency to be scarcer, and the need to control the greenhouse effect gases produced when using them, are demanding new strategies for energy production. Biorefineries aiming to obtain clean and renewable energy recovering nutrients and other products of interest from energetic cultures, organic wastes and other waste fluxes are an alternative to conventional refineries (Schiermeier et al., 2008). Anaerobic digestion (AD), which consists in the microorganism catalysed conversion of organic substrates into a mixture of gases (biogas) –mainly methane and carbon dioxide- is a well-established energy recovering technology in terms of performance and economic feasibility and one of the most attractive technologies to produce sustainable energy from wastes (Kleerebezem and van Loosdrecht, 2007). However, this technology does not modify the total content of N in the digestates, and thus needs to be combined with other processes for N removal or recovery. The combination of the AD process with ammonia stripping with its subsequent absorption in an acid solution (Bonmatí and Flotats, 2003a; Laureni et al., 2013), thermal concentration of the digestate (Bonmatí et al., 2003; Bonmatí and Flotats, 2003b) or chemical precipitation of ammonium and phosphate as struvite (Cerrillo et al., 2015) has previously been studied, but despite these combined processes being feasible, few full scale applications exist nowadays.

Bioelectrochemical systems (BES) operated in microbial fuel cell (MFC) mode, or microbial electrolysis cell (MEC) mode -when electric energy is produced or energy is supplied to promote nonspontaneous reactions, respectively- can also be coupled to AD in order to improve its performance and the quality of the effluent (Hamelers et al., 2010). These systems have revealed themselves to be a highly versatile technology allowing for the coupling of wastewater treatments to the production of chemical compounds and energy carriers (Pant et al., 2012).

A wide range of complex substrates have been studied as possible energy sources for BES, such as domestic (Liu et al., 2004), slaughterhouse (Katuri et al., 2012), or swine (Min et al., 2005) wastewater, or anaerobic digester sludge (Ge et al., 2013). The compatibility between the influent of a BES and the AD effluent makes both MFC and MEC operation suitable as a polishing step once the AD process has ended, or as a system to absorb organic compound peaks should any operational problems in the AD reactor arise.

In a two chamber BES with a cation exchange membrane configuration, electrons produced during the oxidation of organic matter in the anode chamber are conducted through an external circuit to the cathode; as a result, and in order to maintain charge electroneutrality between both compartments, protons produced in the anode as a result of organic matter

oxidation diffuse through the cation exchange membrane to the cathode compartment, where, for instance, they are combined with oxygen to produce molecular water. However, other cations, such as ammonia, are usually present in the anode compartment in a higher concentration than protons (typically 10^5 times) and are the predominant species involved in maintaining the charge balance, resulting in a pH gradient between anolyte and catholyte (Rozendal et al., 2008). This fact can be exploited to remove or recover nutrients, such as ammonium, from waste flux. There are some experiences focused on removing ammonia from the cathode compartment using different configurations (Zhang et al., 2013), and even simultaneous nitrification and denitrification processes through intermittent aeration of the cathode have been achieved (Sotres et al., 2016). The possibility of recovering ammonium from the cathode compartment adding a subsequent step of stripping and absorption (Cord-Ruwisch et al., 2011; Kim et al., 2008; Kuntke et al., 2012; Sotres et al., 2015a) to later reuse it as a cleaner fertiliser, is especially interesting since nutrient recovery is favoured instead of nutrient removal and fertiliser production from raw materials.

Despite this previous work, performed in a synthetic medium, swine wastewater or urine, there is a lack of comprehensive studies focused on chemical oxygen demand (COD) and ammonia removal from complex waste flux in BES when treating digestates compared with the treatment of the raw substrates, to be able to evaluate if the AD-BES combination is a suitable treatment strategy. Furthermore, an analysis of the microbial population that develops in the anode of the BES is also needed to better understand its performance when working with digestates in different operational modes (MFC and MEC).

In the present Chapter, BES operation in combination with AD was investigated in batch assays in order to improve COD removal and nitrogen recovery from a complex waste substrate such as pig slurry, compared to raw pig slurry treatment in BES. Furthermore, charge production, its relation with cation transport through the membrane and the influence of the other cations on the ammonium migration flux was also assessed. Finally, the evolution of microbial populations (total eubacteria and archaea) on the anode biofilm, both under MFC and MEC operation mode, was studied to identify potential key players involved in electric current production.

4.2 Materials and methods

4.2.1 Experimental set-up

A pair of identical two chambered cells described in Section 3.1.1 were used, one of them operated in MFC mode and the second one in MEC mode. Two feedings were used in the anode compartment: i) raw pig slurry, and ii) digested pig slurry obtained from a thermophilic (55 ºC) 2 L lab-scale continuous stirred tank reactor. Both the raw pig slurry and the effluent of the AD were sieved to remove particles larger than 125 μm previous to being used as feed for the BES (Table 4.1).

4.2.2 Reactors operation

The AD was fed in continuous mode with the raw pig slurries previously specified (Table 4.1) with a hydraulic retention time (HRT) fixed at 5 d, and an organic loading rate (OLR) of 2.26 g COD L^{-1} d^{-1}. The reactor ran for 3 months and, once the steady state of operation regarding COD removal and biogas production was achieved, the effluent of the AD was collected during 3 weeks and homogenised in order to be used as substrate for the BES (hereafter referred to as digested pig slurry). The digested pig slurry was stored at -20 ºC for further utilisation. Samples of the BES substrate were taken in every experimental run to assure that its characteristics remained stable.

The MFC was operated under six different conditions (Table 4.2). In the first three assays, raw pig slurry was used as feeding, and the MFC was operated using two different external resistances (100 Ω and 500 Ω) and in open circuit to investigate diffusion driven processes. In the second set of assays, digested pig slurry was used as feeding. The MEC was operated under eight different conditions (Table 4.2), fixing the anode potential at -200, -100 and 0 mV vs. SHE, and in open circuit, using raw pig slurry in the first stage, and later repeating the same conditions with digested pig slurry. Both cells were operated at room temperature (~ 23-25 ºC).

Prior to every experimental run, the anode and the cathode compartment of each cell were filled with 0.5 L of the correspondent solution and emptied completely at the end of each run; repeating this procedure every 24 h and 48 h in the MFC and the MEC (according to the duration of the current density peaks in each mode), respectively, in order to perform three batches for every condition. Samples were taken from the anode and the cathode compartment at different times during the run -three samples for the MFC experiments, and four samples for the MEC experiments.

Table 4.1 Characterisation of raw and digested pig slurry used as feedings in the AD and the BES. Abbreviations: MFC: microbial fuel cell, MEC: microbial electrolysis cell, AD: anaerobic digestion, COD: chemical oxygen demand, N-NH4+: ammonium nitrogen, TS: total solids, VS: volatile solids.

Parameter	AD Reactor feeding	MEC/MFC feeding	
	Raw pig slurry	Raw pig slurry (sieved 125 µm)	Digested pig slurry (sieved 125 µm)
pH (-)	7.98	7.98	8.12
Alkalinity (g_{CaCO3} L^{-1})	3.5	3.5	3.6
COD (mg_{O2} kg^{-1})	14 585	6 512	7 951
$N\text{-}NH_4^+$ (mg L^{-1})	997	857	872
TS (%)	1.74	0.78	0.83
VS (%)	1.04	0.37	0.42
NH_4^+ (mg L^{-1})		1 102	1 121
NH_4^+ (mM)		61.2	62.3
Na^+ (mg L^{-1})		359	383
Na^+ (mM)		15.6	16.7
Mg^{2+} (mg L^{-1})		14	9
Mg^{2+} (mM)		0.6	0.4
Ca^{2+} (mg L^{-1})		3 272	3 219
Ca^{2+} (mM)		81.8	80.5
K^+ (mg L^{-1})		1 093	1 045
K^+ (mM)		28.0	26.8
PO_4^{3-} (mg L^{-1})		9 713	8 315
PO_4^{3-} (mM)		102.2	87.5

Table 4.2 Conditions tested in MFC and MEC operation modes. Abbreviations: MFC: microbial fuel cell, MEC: microbial electrolysis cell, OCV: open circuit voltage; R_{ext} (external resistance); E_{anode} (anode potential).

Operation mode	**Catholyte**	**Feeding**	**R_{ext} (Ω) (MFC mode) E_{anode} (mV) (MEC mode)**
MFC	Phosphate buffer solution	Raw Pig Slurry	100
			500
			OCV
		Digested Pig Slurry	100
			500
			OCV
MEC	NaCl solution	Raw Pig Slurry	-200
			-100
			0
			OCV
		Digested Pig Slurry	-200
			-100
			0
			OCV

4.2.3 Analyses and calculations

Samples of the feeding solutions and the anode effluent were characterised for chemical oxygen demand (COD), total and volatile solids (TS and VS), alkalinity, volatile fatty acids (VFA), ammonium N-NH_4^+, pH and anion and cation concentrations, besides dissolved methane in the anode effluent. Cathode samples were characterised for ammonium N-NH_4^+, pH and anion and cation concentrations. All the analyses were performed following the methods described in Section 3.2.

Current density, coulombic efficiency (CE), CH_4 production efficiency, COD and ammonium removal efficiencies, ammonium flux, transport of negative (Q^-) and positive charges (Q^+) were determined as described in Section 3.4.

To determine the effect the shift from MFC to MEC mode had on the microbial population (total eubacteria and archaea) harboured on the anode, bacterial communities present in the feedings (raw and digested pig slurry) and attached to the anode under MFC and MEC mode at the end of the experiments (after 2 and 4 months of operation, respectively) were analysed by 454-Pyrosequencing. Total DNA extraction and 454-Pyrosequencing were performed following the methods described in Section 3.6.1 and 3.6.4, respectively. Data obtained from pyrosequencing datasets were deposited in the Sequence Read Archive of the

National Center for Biotechnology Information (NCBI) under study accession number SRP062261, for eubacterial and archaeal populations.

The evaluation of the diversity of the samples and statistical multivariate analyses were performed following Section 3.6.6.

4.3 Results and discussion

4.3.1 Performance of the BES

4.3.1.1 Current density and removal efficiencies of the MFC batch experiments

The profiles of the current density generated, and the COD and ammonium removal efficiencies corresponding to the three batches performed in MFC mode with an external resistance of 100 Ω are shown in Figures 4.1a and 4.1b. As it can be seen, the response of the three batches is very similar, achieving 250 mA m^{-2} and 225 mA m^{-2} peak current densities, when respectively fed with raw and digested pig slurry. Similar results were obtained using an external resistance of 500 Ω (data not shown); although in this case the maximum current densities were 70 and 60 mA m^{-2}, respectively. These current densities are in the same range as in other studies that also used swine wastewater in a MFC (Min et al., 2005). As expected, the current density decreased with respect to the increasing external resistance according to Ohm's law. Interestingly, although COD removal started in the first hours and continued for more than 24 hours, current generation became minimal 10 hours after fresh substrate addition, since less biodegradable organic matter may be available. This behaviour was also observed when studying COD removals in a single chamber MFC treating domestic wastewater with a soluble COD of 223 mg L^{-1} (Zhang et al., 2015). In that study, graphite fibre brush was used as anode, and the applied external resistances were 1000 Ω and 100 Ω.

Results of the MFC operation (Figure 4.2a and 4.2b) showed that there were no statistically significant differences in COD removal when working with an open or closed circuit (17-21% and 7-12% with raw and digested pig slurry, respectively). These data indicate that microorganisms attached to the anode or in suspension may be using final electron acceptors present in the medium. Lower COD removals when using digested pig slurry can be expected, since organic matter present in the effluent of an AD can be less biodegradable. A decrease in COD removal was also reported when changing from raw to digested primary sludge (Ge et al., 2013). Nevertheless, if the integrated AD-MFC system is taken into account, the overall COD removal efficiency would be of around 50% (final average COD of 7160 mg O_2 kg^{-1}). Furthermore, almost all ammonium transport produced in this MFC is promoted by diffusion, probably due to the low current densities achieved, with removal efficiencies of 32-35% and 32-

40% for raw and digested pig slurry, respectively. This behaviour was also observed by Kuntke et al. (2012), who reported that, at low current densities, ammonia diffusion was the dominant ammonium transport mechanism. Zhang et al. (2013) also reported high ammonium diffusion in their system in batch mode when no voltage was applied, achieving 30% when working with a synthetic solution.

Initial pH of the raw pig slurry was in a range of 7.9-8.1, a result which is very similar to the final pH range of 7.8-8.2. In the case of the catholyte, the initial pH of 7.1 was maintained at the end of each batch. For digested pig slurry, the initial pH of 8.1-8.2 remained in a range of 7.9-8.3 at the end of the assays. Regarding the catholyte, it remained around 7.3. These stable values are explained because a buffer phosphate was being used as a catholyte.

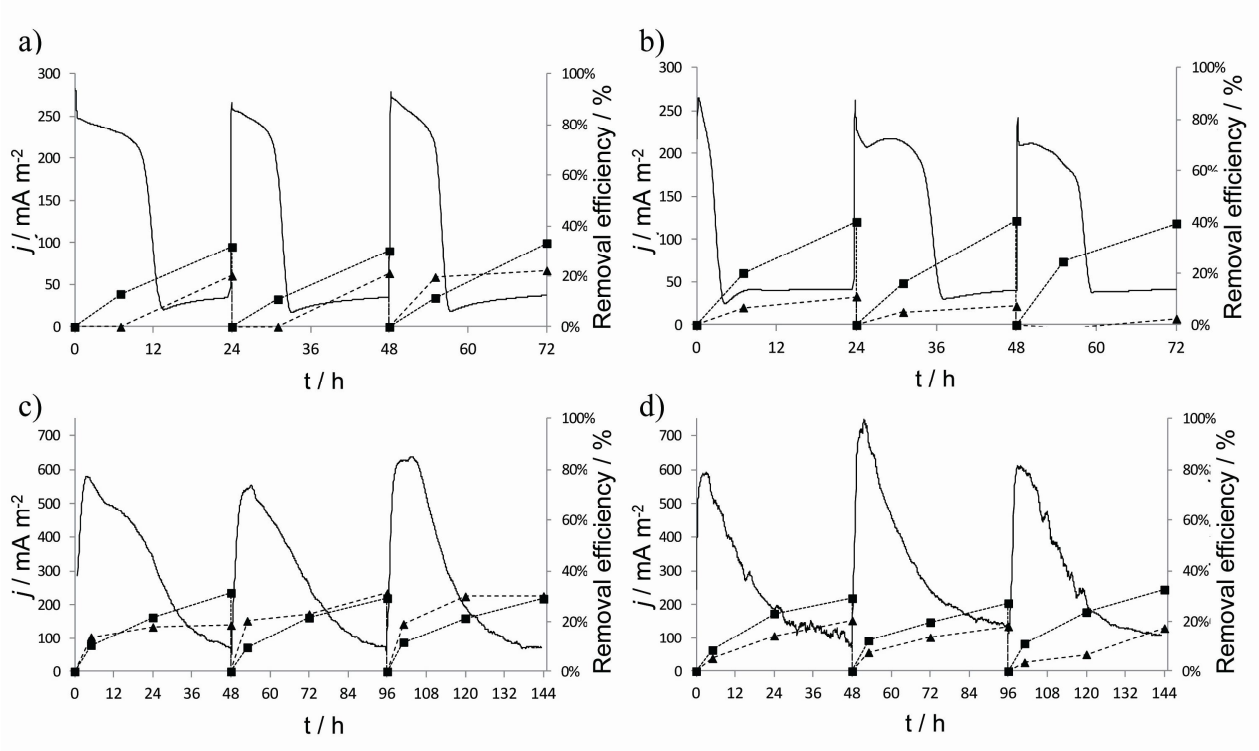

Figure 4.1 Current density (j) and COD and ammonium removals obtained in the three experimental runs of MFC operation mode with an external resistance of 100 Ω and fed with (a) raw and (b) digested pig slurry, and in MEC operation mode poising the anode at -200 mV vs. SHE fed with (c) raw and (d) digested pig slurry. ▲COD removal, ■ Ammonium removal, ⎯ Current density.

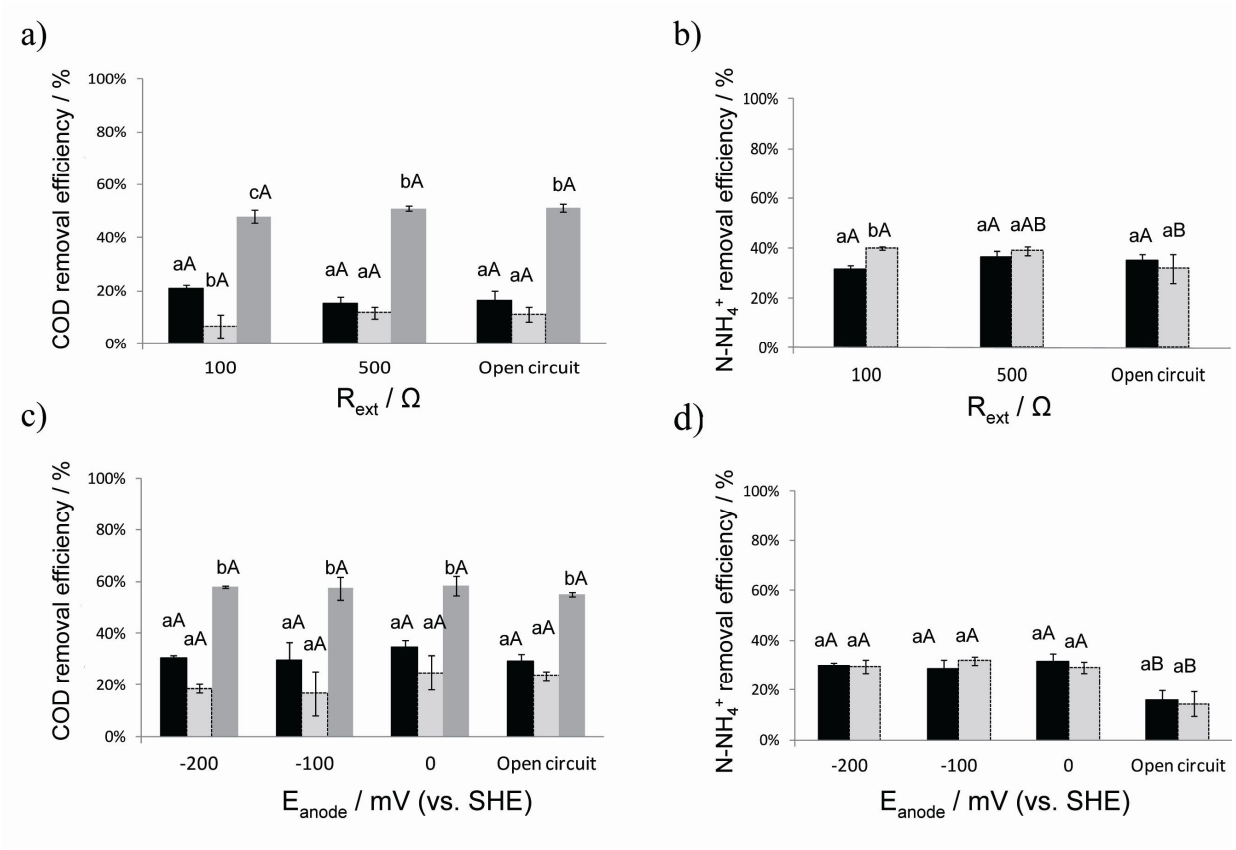

Figure 4.2 (a) COD and (b) ammonium removal efficiency for MFC operation mode after 24 h with the different external resistances (R_{ext}) assayed and (c) COD and (d) ammonium removal efficiency for MEC operation mode after 48 h poising the anode at the different potentials (E_{anode}) assayed. Raw pig slurry in black, digested pig slurry in light grey and AD-MFC or AD-MEC integrated system in dark grey. Significance of the differences among values in the same resistance/potential is represented by lowercase; and among different resistance/potential with the same feeding solution, by uppercase.

4.3.1.2 Current density and removal efficiencies of the MEC batch experiments

The profiles of the generated current density and COD and ammonium removal efficiencies corresponding to the three sequential batches performed in MEC mode poising the anode at -200 mV vs. SHE, using raw and digested pig slurry are shown in Figures 4.1c and 4.1d, respectively. The MEC showed maximum current densities of 600, 750 and 700 mA m^{-2} poising the anode at -200, -100 and 0 mV vs. SHE, respectively, when it was fed with raw pig slurry; similar results for the three sequential batches were achieved when it was fed with digested pig slurry (data not shown). There were no statistically significant differences in COD removal when working with an open or closed circuit, neither when feeding with raw nor digested pig slurry (29-35% and 17-25% respectively), but an overall COD removal of nearly 60% was achieved in combination with the AD (final average COD of 6080 mg O_2 kg^{-1}) (Figure 4.2c). Ammonium removal was maximum when feeding with raw pig slurry and poising the anode potential at 0 mV vs. SHE (31%, with a final N-NH_4^+ of 606 mg L^{-1}), two-fold higher than

the ammonium transferred from the anode to the cathode compartment in an open circuit mode (16%) (Figure 4.2d). Ammonia diffusion values in an open circuit are similar to those obtained in other studies, with a 13% achieved in batch assays lasting 120 h with a synthetic solution (Haddadi et al., 2013). The same study achieved a 2.5 fold increase when the anode potential was fixed at -0.2 V vs. SHE. Also around 30% of ammonia was recovered in continuous assays fed with urine (Kuntke et al., 2014) and 29% of ammonia was recovered in 56 h batch assays using pig slurry as anolyte and a NaCl solution in the cathode when applying 0.6 V to an abiotic two-chamber cell (Sotres et al., 2015a). The same study showed that ammonia recovering was improved by using a NaCl solution instead of a buffer in the cathode, even in an open circuit, reaching removal efficiencies of 50%.

Contrary to the behaviour observed in MFC mode, pH evolution in the assays fed with raw pig slurry showed a decreasing tendency during the assay, achieving a final pH in the range of 7.0-7.3, except in the open circuit assays, were pH was maintained around 8. In the case of the catholyte, pH increased from 9.1 to around 10.8-12.1 at the end of the batches, and remained under 10 in open circuit assays, since a NaCl instead of a buffer solution was used. For digested pig slurry, the final pH in the anode and cathode compartments showed similar values to the ones obtained with raw pig slurry, both in a closed and open circuit. In spite of anodic acidification due to cation transport to the cathode compartment and proton accumulation in the anode, pH was still suitable for microorganism growth, thanks to the buffering capacity of the pig slurry. On the other hand, the high pH achieved in the cathode compartment is highly convenient for ammonia recovering, since it can drive ammonium to ammonia gas favouring a subsequent stripping and absorption process (Sotres et al., 2015a).

To sum up, the results revealed that COD removal was improved by integrating AD and BES technologies and, furthermore, ammonia content of the AD effluent can be recovered and could maybe be reused as an alternative fertiliser, integrating a stripping and absorption unit in the system.

4.3.1.3 Coulombic efficiency and methane production

Coulombic and methane production efficiencies are shown in Table 4.3. Assays in MEC mode presented higher CE than in MFC mode, with a maximum of 18.2% and, in both operation modes, the highest CEs were achieved when digested pig slurry was used. Furthermore, in MFC mode, higher CEs were achieved when the lowest external resistance was applied. Other studies have reported that, in general, CE was a function of substrate concentration and circuit resistance, and an increasing circuit resistance or substrate concentration results in a decrease in CE, because it is difficult to recover electrons from substrates with higher external resistances (Zhang et al., 2015). The thus obtained CEs are quite low, but this is to be expected as the

feedings are complex substrates and other electron acceptors may be present. Other studies have shown similar CEs with complex substrates, reporting a CE range of 3-12% using local domestic wastewater as substrate (Liu et al., 2004), 8% using swine wastewater in a single chambered MFC (Min et al., 2005), or a range of 12-18% using digestate from grass silage in a MFC (Catal et al., 2011). Interestingly, the MFC displayed a higher methane production than the MEC, and accumulated methane, though it only accounted for 1% of COD removal in MEC mode, this being lower than data previously described (Gao et al., 2014). The percentage of COD removal converted to methane increased up to 3-7% in MFC mode. The highest methane production in MFC mode may be related to the lower potentials of the anode in the MFC (<-300 mV) with respect to the MEC, as a previous study found that the lower the anode potential the higher the methane production (Bonmatí et al., 2013). Furthermore, methane production slightly increased in the MEC mode as the fixed anode potential was decreased, although the differences found were not statistically significant.

Table 4.3 Coulombic Efficiency and CH_4 production efficiency obtained in the different assays. Abbreviations: CE: coulombic efficiency, MFC: microbial fuel cell, MEC: microbial electrolysis cell, R_{ext} (external resistance), E_{anode} (anode potential).

Operation mode	Feeding	R_{ext} (Ω) (MFC mode) E_{anode} (mV) (MEC mode)	CE (%)	CH_4 production efficiency (%)
MFC	Raw Pig Slurry	100	2.2±0.4%	7±3%
		500	1.1±0.6%	7±1%
	Digested Pig Slurry	100	4±3%	3±2%
		500	1.3±0.3%	4.2±0.4%
MEC	Raw Pig Slurry	-200	8.0±0.2%	0.7±0.2%
		-100	9±2%	0.3±0.1%
		0	7±2%	0.2±0.1%
	Digested Pig Slurry	-200	12±3%	1.0±0.1%
		-100	18±8%	0.9±0.0%
		0	11±3%	0.9±0.2%

4.3.1.4 Charge and cation transfer

It is well known that the flux through a membrane can be the result of diffusion (caused by a concentration gradient) or migration (caused by the charge transport and balance) (Kuntke et al., 2011; Rozendal et al., 2008). Comparison of the total charge production in the form of electrons relative to the transport of charge in the form of cations through the cationic membrane of each condition assayed is shown in Figure 4.3. In the case of the MFC operation (Figure 4.3a and 4.3b), since that the intensities produced were quite low, the amount of

electrons transferred was negligible with respect to positive charges, thus achieving approximately the same cation transport both in an open or closed circuit. Sodium was the most transferred cation, despite it being initially found in a lower concentration in the anode than in the buffer solution of the cathode. In this study the most abundant cation was calcium (3200 mg L^{-1}), followed by ammonium (1100 mg L^{-1}) and potassium (1090 mg L^{-1}), being sodium the one found in less concentration (360 mg L^{-1}). These results differ from the obtained by Kuntke et al. (2011), who reported that in an MFC the order in which cations were transported corresponded to the concentration of the ions in the anode compartment ($NH_4^+ \geq Na^+ > K^+ > Ca^{2+} >> Mg^{2+}$). These differences can be due to the fact that a synthetic solution was used for the anode in that study and the use of different catholytes. Regarding MEC operation, Figures 4.3c and 4.3d show a clear increase in cation transport through the membrane when applying different potentials to the system with respect to the open circuit assay. Although in the latter case there is already some cation transport, it improves in parallel to the negative charge increase, being ammonia the predominant cation involved in maintaining electroneutrality. As an example, when using digested pig slurry in MEC mode, ammonia accounted for 64, 55 and 45% of the total amount of cations transferred when the anode was fixed at 0, -100 and -200 mV, respectively. When the amount of cations transferred in an open circuit assay was subtracted, results showed that ammonia accounted for 63, 67 and 53% of the migrated positive charge when the anode was respectively fixed at 0, -100 and -200 mV. Other studies have obtained similar results, reporting that 30-50% of the charge transferred was neutralised by ammonium migration when using synthetic wastewater and real urine (Haddadi et al., 2013). Sodium and potassium cations accounted for nearly the rest charge transferred when using fresh pig slurry, while calcium was favoured with respect to sodium when using the digested one. The obtained results are the consequence of the coordinated effect of a variety of driving forces. Apart from gradient concentration between both compartments, the different mobility of each cation when subjected to an electric field may have also had an impact in the obtained results. Mobility depends on the hydrodynamic radius of the ion (taking into account the hydrating water molecules it carries when moving), its charge and the viscosity of the medium. This way, NH_4^+ and K^+ have the same ionic mobility ($7.62 \cdot 10^{-8}$ m^2 s^{-1} V^{-1} in water at 298 K), while Na^+, Mg^{2+} or Ca^{2+} have lower ones ($5.19 \cdot 10^{-8}$, $5.50 \cdot 10^{-8}$ and $6.17 \cdot 10^{-8}$ m^2 s^{-1} V^{-1}, respectively) (Atkins and de Paula, 2013). Finally, the organic matter and solids content of the raw and digested pig slurry, as well as the presence of other cations, may affect the migration patterns that have been observed with synthetic solutions. Diffusion numbers in the MFC also differ from those obtained in the MEC because of the use of different catholytes, a phosphate buffer and a NaCl solution, respectively. Although a higher flux was expected in MEC mode due to the concentration

gradient (only 39 mg L^{-1} of sodium was present at the beginning of the batch in the cathode compartment), it was finally lower than the obtained in MFC mode using a phosphate buffer.

In summary, the results obtained show that diffusion flux was predominant in the MFC operation because of the low generated intensities while migration promoted by electron transport was the main phenomenon driving the cation flux through the membrane in MEC. The differences between both systems, as observed in an open circuit, could be explained by the difference in the catholytes used in each one.

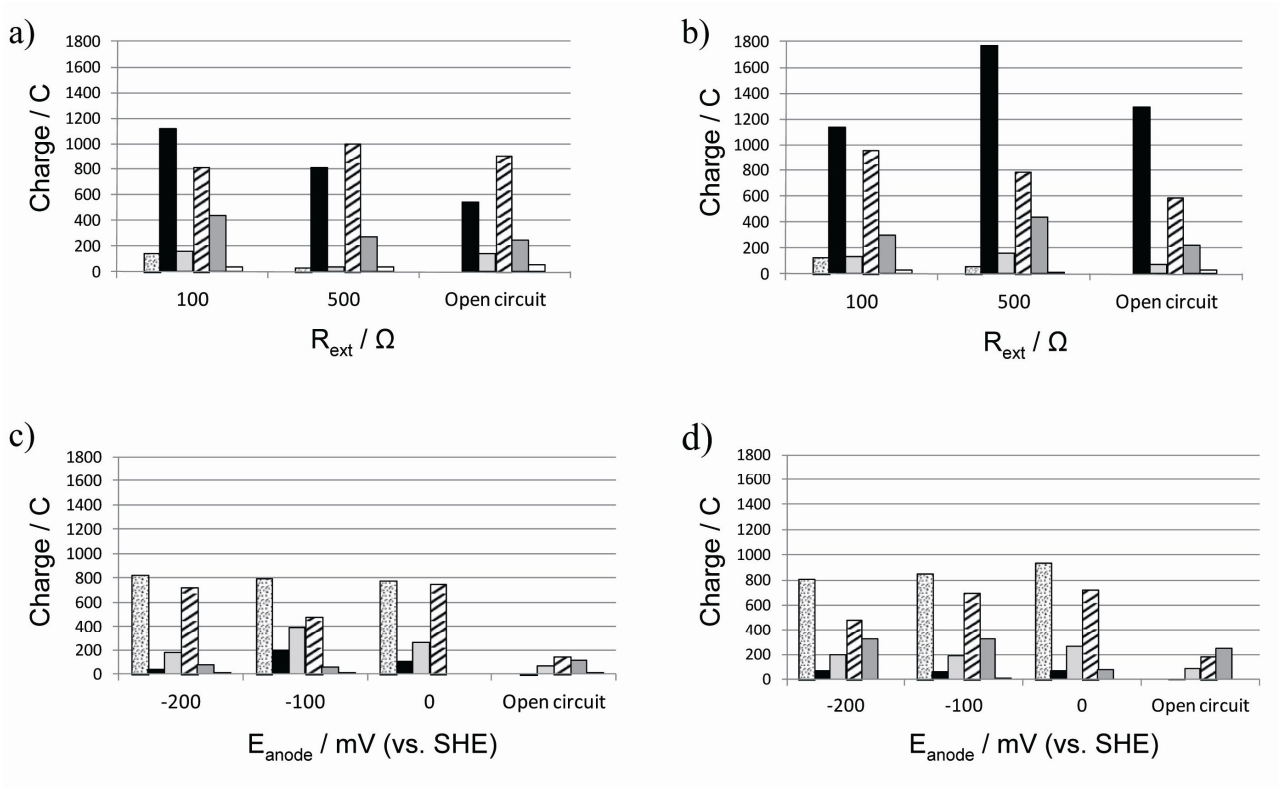

Figure 4.3 Comparison of the total charge production (Q^-) to the transport of charge in the form of specific ions transferred to the cathode compartment in MFC mode after 24 h with the different external resistances (R_{ext}) assayed and using (a) raw pig slurry and (b) digested pig slurry, and in MEC operation mode after 48 h poising the anode at the different potentials (E_{anode}) assayed using (c) raw pig slurry and (d) digested pig slurry. Q^-, in dotted bars; Na^+, in black bars; K^+, in light grey; NH_4^+, in striped bars; Ca^{2+}, in dark grey bars; and Mg^{2+}, in white bars.

4.3.2 Microbial community assessment

The microbial community structure of the inoculum and the samples taken from the carbon felt of the MEC and MFC reactors at the end of the assays was characterised by pyrotag 16SrRNA gene-based pyrosequencing analysis focused on the total eubacterial and archaeal *16S* rRNA gene. 3089, 2115 and 3223 reads and coverage of 0.97, 0.96 and 0.96 were obtained for eubacterial in the inoculum, MFC and MEC anode samples, respectively (Table 4.4). Regarding archaeal community, 1985, 8469 and 4598 reads were obtained for the inoculum, MFC and MEC anode samples, respectively, and coverage of 0.98 for all three

samples. Figure 4.4 shows the rarefaction curves, with all samples closer to approaching a plateau when plotting OTUs vs. the number of *16S* rRNA.

a)

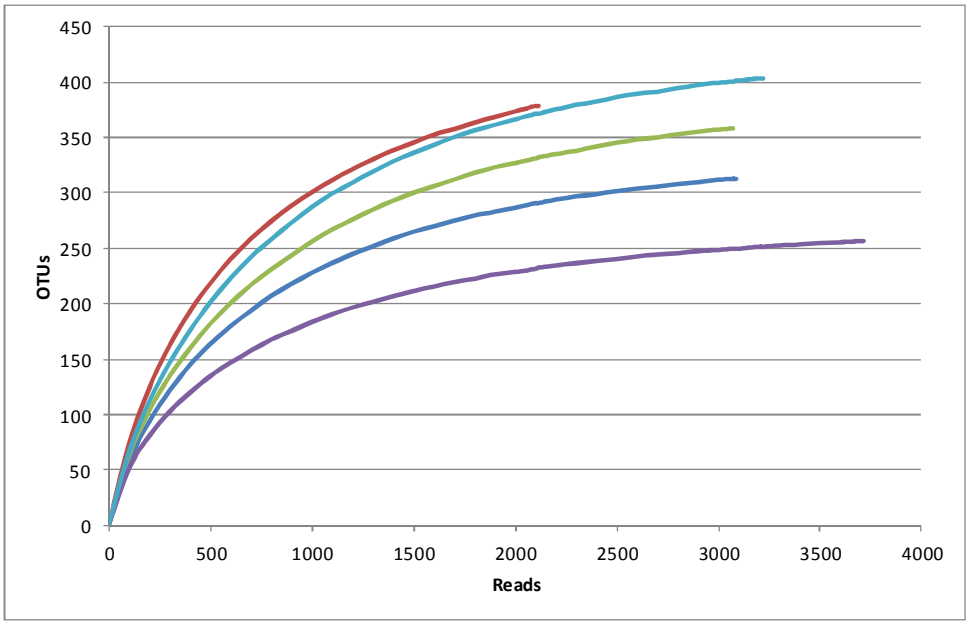

b)

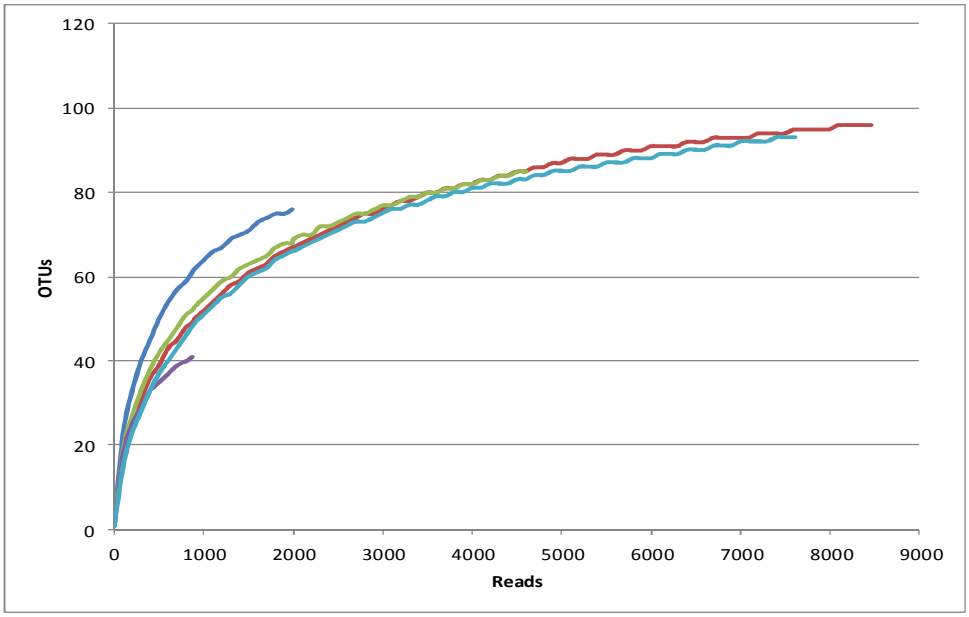

Figure 4.4 Rarefaction curves for MFC and MEC anode and raw and digested pig slurry samples regarding (a) Eubacterial and (b) Archaeal community. Inoculum, dark blue; MFC, red; Raw pig slurry, green; Digested pig slurry, purple; and MEC, light blue.

Table 4.4 Diversity index for Eubacterial and Archaeal community of the inoculum, MFC and MEC mode and raw and digested pig slurry. Data normalised to the sample with the lowest number of reads (2115 and 867 for eubacterial and archaeal, respectively). Abbreviations: OTU: operational taxonomic unit, MFC: microbial fuel cell, MEC: microbial electrolysis cell, SD: standard deviation. (mean±SD).

	Reads	Coverage	OTUs	Inverted Simpson	Shannon	Chao
Eubacteria						
Inoculum	3089	0.97±0.00	291.18±4.03	31.31±1.12	4.57±0.02	329.40±10.90
MFC	2115	0.96±0.00	379.00±0.00	99.96±0.00	5.31±0.00	448.05±0.00
MEC	3223	0.96±0.00	371.43±4.71	43.54±2.05	5.00±0.02	421.11±13.42
Pig slurry	3068	0.96±0.00	331.60±4.42	58.09±1.73	4.89±0.02	378.63±12.31
Digested pig slurry	3713	0.97±0.00	232.65±4.02	28.73±0.93	4.29±0.02	263.78±10.86
Archaea						
Inoculum	1985	0.98±0.00	60.91±2.84	5.48±0.22	2.48±0.04	78.48±10.74
MFC	8469	0.98±0.00	49.62±3.51	3.67±0.19	2.10±0.05	74.57±16.06
MEC	4598	0.98±0.00	52.43±3.33	3.57±0.16	2.00±0.06	73.05±13.66
Pig slurry	867	0.99±0.00	41.00±0.00	3.65±0.00	2.07±0.00	57.50±0.00
Digested pig slurry	7605	0.98±0.00	47.74±3.84	4.14±0.18	1.99±0.05	73.81±17.37

Figure 4.5 and Table 4.5 show that the three dominant eubacterial *phyla* identified in the inoculum sample, *Proteobacteria*, *Bacteroidetes* and *Firmicutes,* were also the dominant ones in both the MEC and MFC anodes, although in the MFC mode an enrichment in *Bacteroidetes* took place. *Proteobacteria* and *Firmicutes* are the predominant *phyla* found on the anode in several MFC systems regardless of MFC configuration, inoculums or substrate (Bonmatí et al., 2013; Sotres et al., 2015a; Sotres et al., 2015b). *Delta-Proteobacteria* members were present, although the well known electrogenic *Geobacter sulfurreducens* was not detected. A recent study on a MFC working with pig slurry identified *G. sulfurreducens* on the anode by means of fluorescence in situ hybridisation (FISH), although it was not detected by polymerase chain reaction–denaturing gradient gel electrophoresis (PCR–DGGE) (Vilajeliu-Pons et al., 2015). When complex organic compounds serve as fuel in BES, it is expected that microorganisms fermenting these substrates into simpler molecules to be also present in the anode microbial community (Jung and Regan, 2007). Although these fermentative microorganisms may have little or no capacity for electron transfer to the anode, their metabolism has a key role to power BES. At the family level, results in Figure 4.5b and Table 4.5 revealed the dominance of *Desulfuromonadaceae*, *Clostridiaceae* and *Porphyromonadaceae* in MFC and MEC samples, with a clear enrichment of 2 OTUs belonging to the *Desulfuromonadaceae* family (8 and 18 %

of relative predominance, respectively) with respect to the inoculum, where they were not detected.

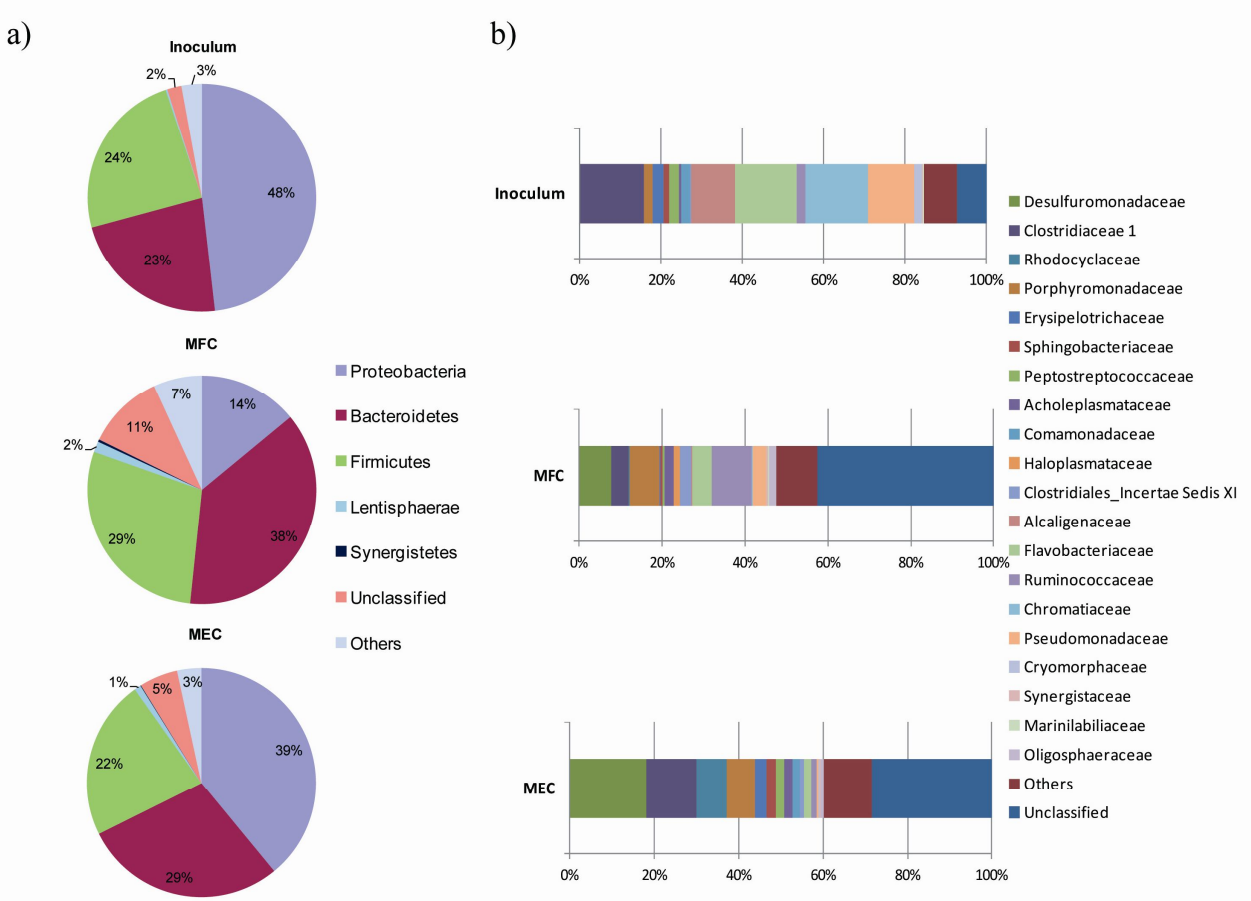

Figure 4.5 Taxonomic assignment by means RDP Bayesian classifier of 454-pyrosequencing reads from massive 16SrRNA libraries of Eubacteria in the inoculum, and anode under MFC and MEC mode at the a) phylum b) family levels. Relative abundance was defined as the number of reads (sequences) affiliated with any given taxon divided by the total number of reads per sample. Phylogenetic groups with a relative abundance lower that 1% were categorised as “others”.

Table 4.5 Eubacterial microbial community enriched in MFC (microbial fuel cell) and MEC (microbial electrolysis cell) mode (percentage of total 16S rRNA reads).

Phylum	MFC (% reads)	MEC (% reads)	Class	MFC (% reads)	MEC (% reads)	Order	MFC (% reads)	MEC (% reads)	Family	MFC (% reads)	MEC (% reads)	Genus	MFC (% reads)	MEC (% reads)
Bacteroidetes	15.11	16.12	*Bacteroidia*	1.88	1.60	*Bacteroidales*	1.88	1.60	*Porphyromonadaceae*	1.12	1.07	*Proteiniphilum*	0.56	0.52
									Prevotellaceae	0.75	0.52	*Paraprevotella*	0.75	0.52
Proteobacteria	7.74	26.84	*β -Proteobacteria*	0.05	6.53	*Rhodocyclales*	0.05	2.87	*Rhodocyclaceae*	0.05	2.87	*Thauera*	0.05	0.92
												Sterolibacterium	0	1.94
						Hydrogenophilales	0	1.02	*Hydrogenophilaceae*	0	1.02	*Thibacillus*	0	1.02
						Gallionellales	0	0.80	*Gallionellaceae*	0	0.80	*Sideroxydans*	0	0.80
						Burkholderiales	0	0.43	*Comamonadaceae*	0	0.43	*Simplicispira*	0	0.43
			ε -Proteobacteria	0	0.43	*Campylobacterales*	0	0.43	*Helicobacteraceae*	0	0.43	*Sulfurimonas*	0	0.43
			γ -Proteobacteria	0.14	1.63									
			δ -Proteobacteria	7.56	17.81	*Desulfuromonadales*	7.56	17.07	*Desulfuromonadaceae*	7.56	17.07	*Desulfuromonas*	7.56	17.07
						Desulfobacterales	0	0.74	*Desulfobacteraceae*	0	0.74			
Firmicutes	4.55	12.63	*Clostridia*	2.11	11.03	*Clostridiales*	2.11	11.03	*Clostridiaceae*	2.02	8.97	*Clostridium*	1.83	8. 23
									Peptostreptococcaceae	0.09	0.92	*Clostridium XI*	0.09	0.92
									Peptococcaceae	0	1.14	*Thermincola*	0	1.14
			Erysipelotrichia	0.14	1.42	*Erysipelotrichales*	0.14	1.42	*Erysipelotrichaceae*	0.14	1.42	*Turicibacter*	0.14	1.42
Cloacimonetes	1.03	0.86	*Candidatus Cloacamonas*	1.03	0.86									
Lentisphaerae	0.23	0.55	*Oligosphaeria*	0.23	0.55	*Oligosphaerales*	0.23	0.55	*Oligosphaeraceae*	0.23	0.55	*Oligosphaera*	0.23	0.55

Regarding microbial diversity, the inverted Simpson, Shannon and Chao1 indices showed that the sample of the anode in MFC was the most diverse one (99.96, 5.31 and 448.05 respectively), even if the anode potential was lower (<-300 mV) than the different potentials assayed in the MEC. A higher diversity is expected with higher anode potentials, as only those microorganisms capable of utilising minimal energy for growth, respiring at low anode potentials efficiently with minimal energy loss, can live at low potentials (Torres et al., 2009). However, the specific conditions applied in our study could have promoted more syntrophic metabolic interactions that could explain a higher diversity at lower potentials. MEC sample indices were 43.54, 5.00 and 421.11, respectively; while for the inoculum they were 31.31, 4.57 and 329.40, thus displaying enrichment in diversity during the BES operation (Table 4.4). In order to know the background populations that could have been provided by the feedings, samples from both the raw and the digested pig slurry were also analysed. The dominant *phyla* in raw pig slurry were *Bacteroidetes* (33%) and *Firmicutes* (46%), while in digested pig slurry *Proteobacteria* represented 44% of the eubacterial population and *Firmicutes* did 46%. At family level, Clostridiaceae accounted for 26 and 15% for the population of raw and digested pig slurry, respectively, followed by *Porphyromonadaceae* in raw (7%) and *Pseudomonadaceae* in digested pig slurry (39%) (Figure 4.6). Indeed, a low relative predominance of OTUs belonging to *Desulfuromonadaceae* (below 0.11% in digested slurry) was revealed in the feedings.

Correspondence multivariate analysis performed on OTUs' relative distribution among samples indicated that biofilms from the MEC and MFC anodes clustered together, and close to the raw pig slurry sample, while the inoculum and the digested pig slurry samples were clearly separated, indicating that the BESs had been enriched in certain groups such as *Desulfuromondaceae*, with a special relevance of one OTU (13), due to the operation conditions (Figure 4.7a).

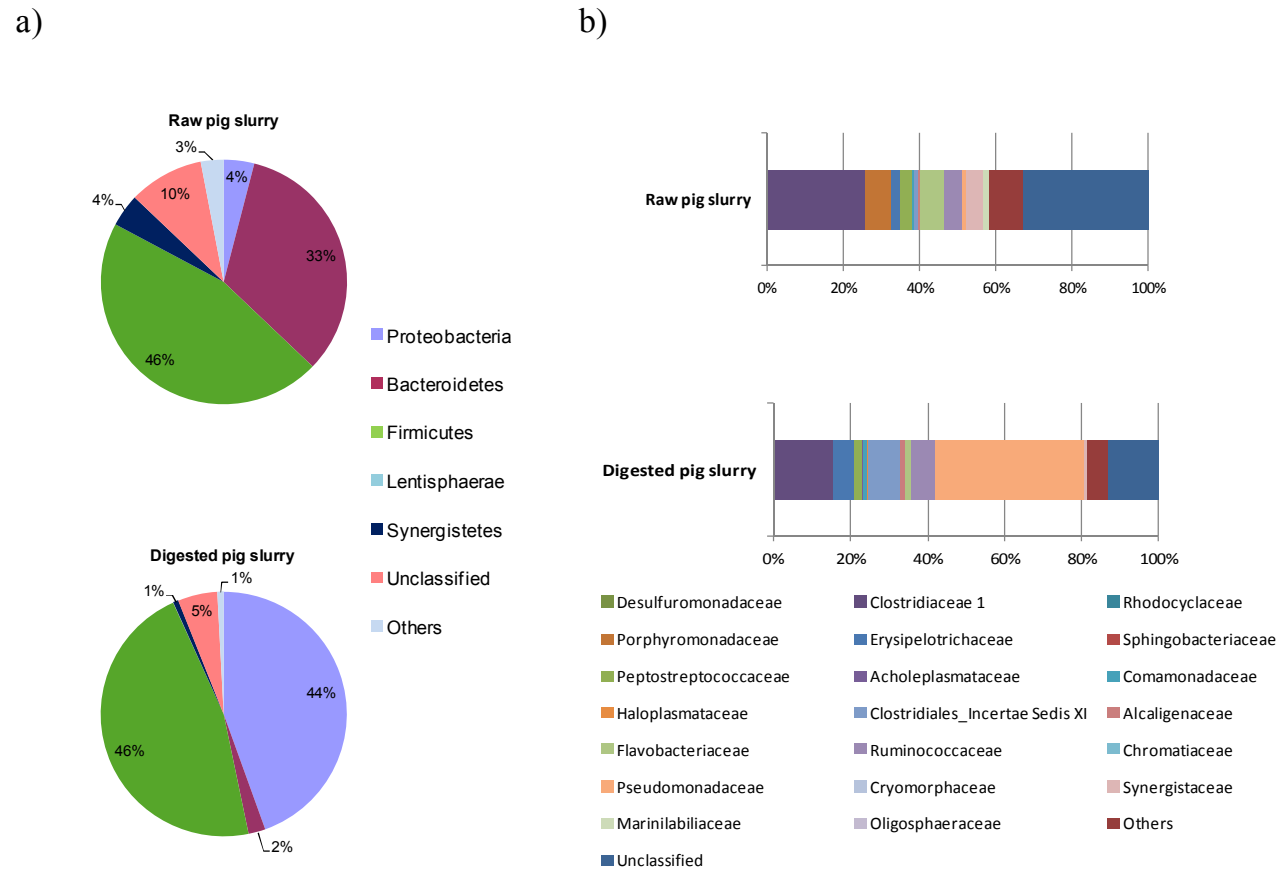

Figure 4.6 Taxonomic assignment by means RDP Bayesian classifier of 454-pyrosequencing reads from massive 16SrRNA libraries of Eubacteria of raw and digested pig slurry at the a) phylum b) family levels. Relative abundance was defined as the number of reads (sequences) affiliated with any given taxon divided by the total number of reads per sample. Phylogenetic groups with a relative abundance lower that 1% were categorised as “others”.

a)

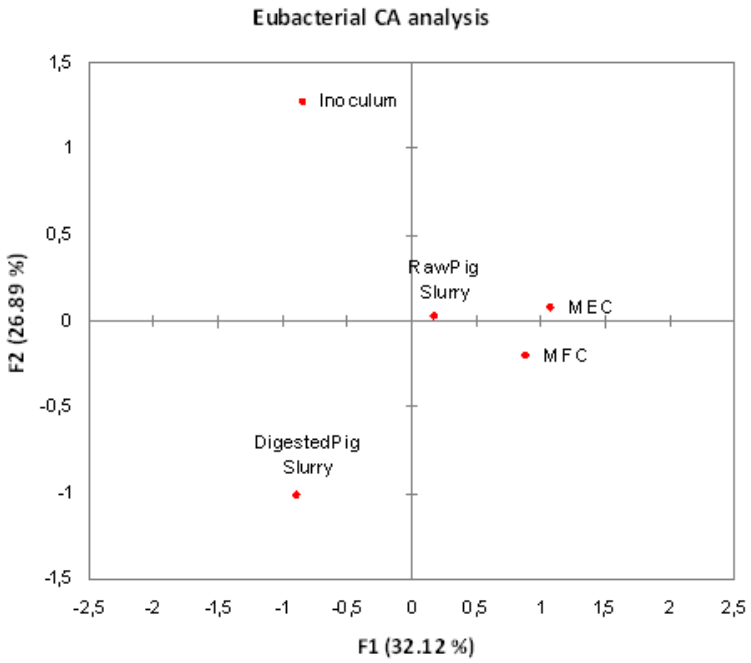

b)

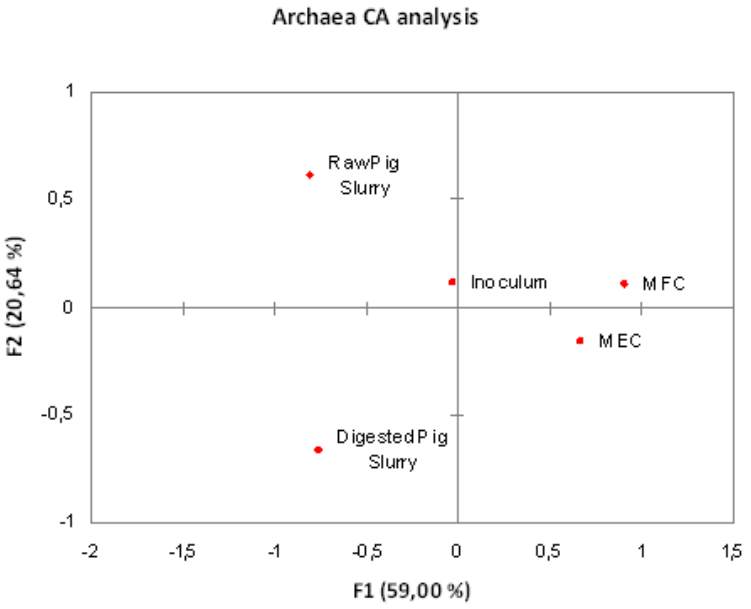

Figure 4.7 Correspondence Analysis for inoculum, MFC and MEC anode samples regarding (a) Eubacterial and (b) Archaeal community.

Regarding archaeal population, Figure 4.8 and Table 4.6 show an important enrichment in the *Thermoplasmatales* family on the anode of both BES reactors with respect to the inoculum, representing 83, 61 and 41%, respectively. *Thermoplasmata* is a novel group of methylotrofic methanogenic archaea that has so far been scarcely described, and which reduces methanol with hydrogen (Paul et al., 2012) and might also use methylamines as methanogenic substrate (Borrel et al., 2014). It has been described in anaerobic digesters (Nelson et al., 2011), in pig slurry (Petersen et al., 2014) and in MFC anodes in previous studies (Sotres et al., 2015a; Sotres et al., 2015b). It has been found that this group was enriched in an UASB with high NH_4^+ concentrations when de OLR was increased (Chen et al., 2014), which also agrees with the rich ammonia substrates used in this study. The acetotrophic *Methanosaetaceae* decreased its relative abundance from 41% in the inoculum down to 11 and 13% in MFC and MEC anode, respectively, which may reflect the importance of acetate as an anodic substrate. Recently it has been reported that also methanogenic archaea can accept electrons from a solid donor or through direct interspecies electron transfer to reduce carbon dioxide to methane (Cheng et al., 2009; Rotaru et al., 2014) though its role in BES processes still needs to be studied in depth. Furthermore, *Methanosaetaceae* has been described as a more sensitive microorganism to high ammonia concentrations (Zhang et al., 2014). This can explain the shift towards the *Thermoplasmatales* family, although in a previous study the *Methanosaetaceae* family has been detected with a relative abundance of over 50% at the anodes of BESs working in MEC and MFC mode with pig slurries with high ammonium concentrations (Sotres et al., 2015a). Regarding archaea composition, raw and digested pig slurries were richer in *Methanosaetaceae,* representing 56 and 54%, respectively (Figure 4.9). Regarding microbial diversity, the sample of the inoculum was the most diverse one (5.48 (inverted Simpson), 2.48 (Shannon) and 78 (Chao-1)) when compared to the anode biofilm from MFC and MEC mode (Table 4.4). Correspondence analysis for archaeal population indicated that biofilms from the MEC and MFC anodes clustered together, as in the case of eubacterial population, but in this case they were close to the inoculum sample, while the raw and the digested pig slurry samples were clearly separated (Figure 4.7b). OTU 4, related to *Thermoplasmatales*, was the predominant one, since it was enriched both in MFC and MEC.

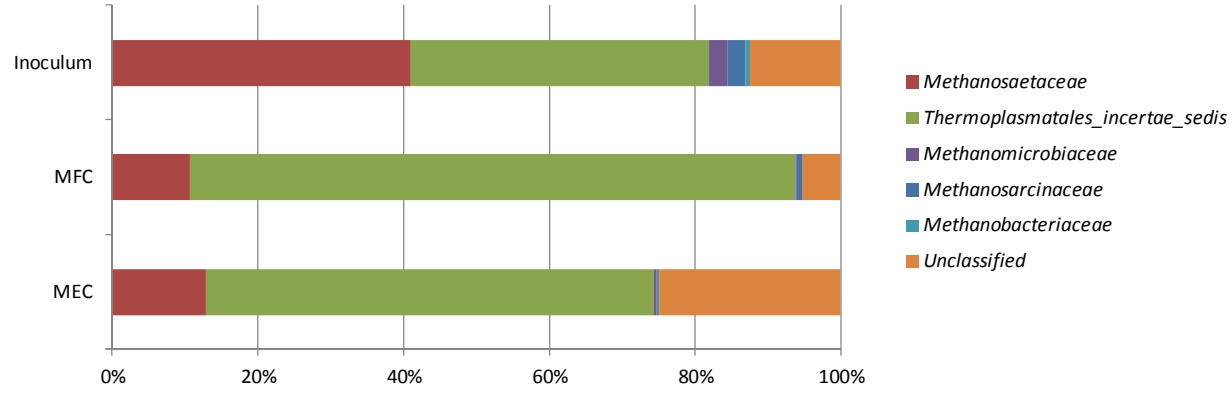

Figure 4.8 Taxonomic assignment by means of RDP Bayesian classifier of 454-pyrosequencing reads from massive 16SrRNA libraries of Archaea in the inoculum, and anode from MFC and MEC mode at family levels. Relative abundance was defined as the number of reads (sequences) affiliated with any given taxon divided by the total number of reads per sample. Phylogenetic groups with a relative abundance lower that 1% were categorised as "others".

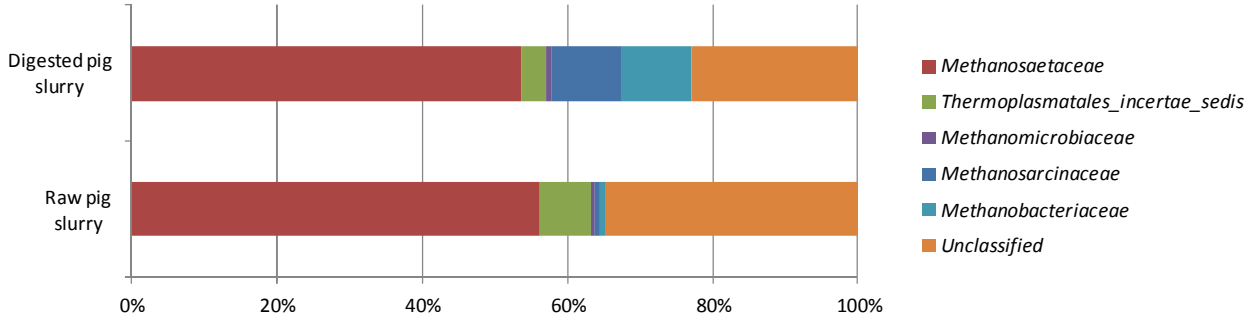

Figure 4.9 Taxonomic assignment by means of RDP Bayesian classifier of 454-pyrosequencing reads from massive 16SrRNA libraries of Archaea of raw and digested pig slurry at family levels. Relative abundance was defined as the number of reads (sequences) affiliated with any given taxon divided by the total number of reads per sample. Phylogenetic groups with a relative abundance lower that 1% were categorised as "others".

Table 4.6 Archaeal microbial community enriched in MFC (microbial fuel cell) and MEC (microbial electrolysis cell) mode (percentage of total 16S rRNA reads).

Phylum	MFC (% reads)	MEC (% reads)	Class	MFC (% reads)	MEC (% reads)	Order	MFC (% reads)	MEC (% reads)	Family	MFC (% reads)	MEC (% reads)	Genus	MFC (% reads)	MEC (% reads)
Euryarchaeota	94.30	74.69	*Thermoplasmata*	81.56	58.95	*Thermoplasmatales*	77.04	58.34	*Thermoplasmatales_incertae_sedis*	77.0	58.34	*Thermogymnomonas*	77.0	58.34
			Methanomicrobia	11.29	13.09	*Methanosarcinales*	11.09	12.82	*Methanosaetaceae*	10.4	12.69	*Methanosaeta*	10.4	12.69
									Methanosarcinaceae	0.63	0.13	*Methanosarcina*	0.36	0.13
												Methanimicrococcus	0.27	0
						Methanomicrobiales	0.20	0.28	*Methanomicrobiaceae*	0.20	0.28	*Methanoculleus*	0.20	0.20
												Methanogenium	0	0.08
			Methanobacteria	0	0.09	*Methanobacteriales*	0	0.09	*Methanobacteriaceae*	0	0.09	*Methanobrevibacter*	0	0.09
Crenarchaeota	0.07	1.08	*Thermoprotei*	0.07	1.08									

4.4 Conclusions

Batch assays performed with raw and digested pig slurry in MEC and MFC showed that, although COD removals were higher when feeding with raw slurry, NH_4^+ removal efficiencies increased when feeding with digested pig slurry. The AD-MEC integrated system achieved the highest COD removal (60%) and the maximum NH_4^+ removal efficiency obtained was 40% (in MFC mode fed with digested pig slurry). The high pH achieved under MEC mode (>10), using a NaCl solution as catholyte, could favour ammonium recovering in a subsequent stripping and absorption process. In the positive charge transport through the cation exchange membrane, ammonia was the main cation involved in maintaining electroneutrality between the two compartments. Finally, the microbial community assessment revealed that *Desulfuromonadaceae* was highly enriched in MEC mode, and that phylotypes belonging to the potential methylotrofic-hydrogenotrophic methanogen *Thermoplasmatales* were also favoured against acetotrophic *Methanosaetaceae*. Consequently, it can be concluded that BES operation in combination with anaerobic digestion is an interesting alternative for the treatment of complex substrates, since a polished effluent can be obtained and ammonium can be recovered for its reuse as fertiliser.

4.5 References

Atkins, P., de Paula, J. 2013. Elements of Physical Chemistry. 6th ed. Oxford University Press, Oxford.

Bonmatí, A., Campos, E., Flotats, X. 2003. Concentration of pig slurry by evaporation: anaerobic digestion as the key process. *Water Science and Technology*, **48**(4), 189-94.

Bonmatí, A., Flotats, X. 2003a. Air stripping of ammonia from pig slurry: characterisation and feasibility as a pre- or post-treatment to mesophilic anaerobic digestion. *Waste Management*, **23**(3), 261-272.

Bonmatí, A., Flotats, X. 2003b. Pig slurry concentration by vacuum evaporation: influence of previous mesophilic anaerobic digestion process. *Journal of the Air & Waste Management Association*, **53**(1), 21-31.

Bonmatí, A., Sotres, A., Mu, Y., Rozendal, R.A., Rabaey, K. 2013. Oxalate degradation in a bioelectrochemical system: Reactor performance and microbial community characterization. *Bioresource Technology*, **143**(0), 147-153.

Borrel, G., Parisot, N., Harris, H., Peyretaillade, E., Gaci, N., Tottey, W., Bardot, O., Raymann, K., Gribaldo, S., Peyret, P., O'Toole, P., Brugere, J.-F. 2014. Comparative genomics highlights the unique biology of Methanomassiliicoccales, a Thermoplasmatales-related seventh order of methanogenic archaea that encodes pyrrolysine. *BMC Genomics*, **15**(1), 679.

Catal, T., Cysneiros, D., O'Flaherty, V., Leech, D. 2011. Electricity generation in single-chamber microbial fuel cells using a carbon source sampled from anaerobic reactors utilising grass silage. *Bioresource Technology*, **102**(1), 404-410.

Cerrillo, M., Palatsi, J., Comas, J., Vicens, J., Bonmatí, A. 2015. Struvite precipitation as a technology to be integrated in a manure anaerobic digestion treatment plant – Removal efficiency, crystal characterisation and agricultural assessment. *Journal of Chemical Technology & Biotechnology*, **90**, 1135-1143.

Chen, Z., Wang, Y., Li, K., Zhou, H. 2014. Effects of increasing organic loading rate on performance and microbial community shift of an up-flow anaerobic sludge blanket reactor treating diluted pharmaceutical wastewater. *Journal of Bioscience and Bioengineering*, **118**(3), 284-288.

Cheng, S., Xing, D., Call, D.F., Logan, B.E. 2009. Direct biological conversion of electrical current into methane by electromethanogenesis. *Environmental Science & Technology*, **43**(10), 3953-3958.

Cord-Ruwisch, R., Law, Y., Cheng, K.Y. 2011. Ammonium as a sustainable proton shuttle in bioelectrochemical systems. *Bioresource Technology*, **102**(20), 9691-9696.

Gao, Y., Ryu, H., Santo Domingo, J.W., Lee, H.-S. 2014. Syntrophic interactions between H2-scavenging and anode-respiring bacteria can improve current density in microbial electrochemical cells. *Bioresource Technology*, **153**(0), 245-253.

Ge, Z., Zhang, F., Grimaud, J., Hurst, J., He, Z. 2013. Long-term investigation of microbial fuel cells treating primary sludge or digested sludge. *Bioresource Technology*, **136**(0), 509-514.

Haddadi, S., Elbeshbishy, E., Lee, H.-S. 2013. Implication of diffusion and significance of anodic pH in nitrogen-recovering microbial electrochemical cells. *Bioresource Technology*, **142**(0), 562-569.

Hamelers, H.M., Heijne, A., Sleutels, T.J.A., Jeremiasse, A., Strik, D.B.T.B., Buisman, C.N. 2010. New applications and performance of bioelectrochemical systems. *Applied Microbiology and Biotechnology*, **85**(6), 1673-1685.

Jung, S., Regan, J. 2007. Comparison of anode bacterial communities and performance in microbial fuel cells with different electron donors. *Applied Microbiology and Biotechnology*, **77**(2), 393-402.

Katuri, K.P., Enright, A.-M., O'Flaherty, V., Leech, D. 2012. Microbial analysis of anodic biofilm in a microbial fuel cell using slaughterhouse wastewater. *Bioelectrochemistry*, **87**, 164-171.

Kim, J.R., Zuo, Y., Regan, J.M., Logan, B.E. 2008. Analysis of ammonia loss mechanisms in microbial fuel cells treating animal wastewater. *Biotechnology and Bioengineering*, **99**(5), 1120-1127.

Kleerebezem, R., van Loosdrecht, M.C.M. 2007. Mixed culture biotechnology for bioenergy production. *Current Opinion in Biotechnology*, **18**(3), 207-212.

Kuntke, P., Geleji, M., Bruning, H., Zeeman, G., Hamelers, H.V.M., Buisman, C.J.N. 2011. Effects of ammonium concentration and charge exchange on ammonium recovery from high strength wastewater using a microbial fuel cell. *Bioresource Technology*, **102**(6), 4376-4382.

Kuntke, P., Sleutels, T.H.J.A., Saakes, M., Buisman, C.J.N. 2014. Hydrogen production and ammonium recovery from urine by a Microbial Electrolysis Cell. *International Journal of Hydrogen Energy*, **39**(10), 4771-4778.

Kuntke, P., Smiech, K.M., Bruning, H., Zeeman, G., Saakes, M., Sleutels, T.H.J.A., Hamelers, H.V.M., Buisman, C.J.N. 2012. Ammonium recovery and energy production from urine by a microbial fuel cell. *Water Research*, **46**(8), 2627-2636.

Laureni, M., Palatsi, J., Llovera, M., Bonmatí, A. 2013. Influence of pig slurry characteristics on ammonia stripping efficiencies and quality of the recovered ammonium-sulfate solution. *Journal of Chemical Technology & Biotechnology*, **88**(9), 1654-1662.

Liu, H., Ramnarayanan, R., Logan, B.E. 2004. Production of electricity during wastewater treatment using a single chamber microbial fuel cell. *Environmental Science & Technology*, **38**(7), 2281-2285.

Min, B., Kim, J., Oh, S., Regan, J.M., Logan, B.E. 2005. Electricity generation from swine wastewater using microbial fuel cells. *Water Research*, **39**(20), 4961-4968.

Nelson, M.C., Morrison, M., Yu, Z. 2011. A meta-analysis of the microbial diversity observed in anaerobic digesters. *Bioresource Technology*, **102**(4), 3730-3739.

Pant, D., Singh, A., Van Bogaert, G., Irving Olsen, S., Singh Nigam, P., Diels, L., Vanbroekhoven, K. 2012. Bioelectrochemical systems (BES) for sustainable energy production and product recovery from organic wastes and industrial wastewaters. *RSC Advances*, **2**(4), 1248-1263.

Paul, K., Nonoh, J.O., Mikulski, L., Brune, A. 2012. "Methanoplasmatales," Thermoplasmatales-related archaea in termite guts and other environments, are the seventh order of methanogens. *Applied and Environmental Microbiology*, **78**(23), 8245-8253.

Petersen, S.O., Højberg, O., Poulsen, M., Schwab, C., Eriksen, J. 2014. Methanogenic community changes, and emissions of methane and other gases, during storage of acidified and untreated pig slurry. *Journal of Applied Microbiology*, **117**(1), 160-172.

Rotaru, A.-E., Shrestha, P.M., Liu, F., Shrestha, M., Shrestha, D., Embree, M., Zengler, K., Wardman, C., Nevin, K.P., Lovley, D.R. 2014. A new model for electron flow during anaerobic digestion: direct interspecies electron transfer to Methanosaeta for the reduction of carbon dioxide to methane. *Energy & Environmental Science*, **7**(1), 408-415.

Rozendal, R.A., Sleutels, T.H., Hamelers, H.V., Buisman, C.J. 2008. Effect of the type of ion exchange membrane on performance, ion transport, and pH in biocatalyzed electrolysis of wastewater. *Water Science & Technology*, **57**(11), 1757-62.

Schiermeier, Q., Tollefson, J., Scully, T., Witze, A., Morton, O. 2008. Energy alternatives: electricity without carbon. *Nature*, **454**, 816-823.

Sotres, A., Cerrillo, M., Viñas, M., Bonmatí, A. 2015a. Nitrogen recovery from pig slurry in a two-chambered bioelectrochemical system. *Bioresource Technology*, **194**, 373-382.

Sotres, A., Cerrillo, M., Viñas, M., Bonmatí, A. 2016. Nitrogen removal in a two-chamber microbial fuel cell: establishment of a nitrifying-denitrying microbial community on an intermittent aerated cathode. *Chemical Engineering Journal*, **284**, 905-916.

Sotres, A., Díaz-Marcos, J., Guivernau, M., Illa, J., Magrí, A., Prenafeta-Boldú, F.X., Bonmatí, A., Viñas, M. 2015b. Microbial community dynamics in two-chambered microbial fuel cells: effect of different ion exchange membranes. *Journal of Chemical Technology & Biotechnology*, **90**(8), 1497-1506.

Torres, C.I., Krajmalnik-Brown, R., Parameswaran, P., Marcus, A.K., Wanger, G., Gorby, Y.A., Rittmann, B.E. 2009. Selecting anode-respiring bacteria based on anode potential: phylogenetic, electrochemical, and microscopic characterization. *Environmental Science & Technology*, **43**(24), 9519-9524.

Vilajeliu-Pons, A., Puig, S., Pous, N., Salcedo-Dávila, I., Bañeras, L., Balaguer, M.D., Colprim, J. 2015. Microbiome characterization of MFCs used for the treatment of swine manure. *Journal of Hazardous Materials*, **288**, 60-68.

Zhang, C., Yuan, Q., Lu, Y. 2014. Inhibitory effects of ammonia on methanogen mcrA transcripts in anaerobic digester sludge. *FEMS Microbiology Ecology*, **87**(2), 368-77.

Zhang, X., He, W., Ren, L., Stager, J., Evans, P.J., Logan, B.E. 2015. COD removal characteristics in air-cathode microbial fuel cells. *Bioresource Technology*, **176**(0), 23-31.

Zhang, X., Zhu, F., Chen, L., Zhao, Q., Tao, G. 2013. Removal of ammonia nitrogen from wastewater using an aerobic cathode microbial fuel cell. *Bioresource Technology*, **146**(0), 161-168.

CHAPTER 5

Anaerobic digestion instability by organic and nitrogen overloads: digestate polishing by coupling a microbial fuel cell

Part of the content of this chapter is in preparation to be submitted for publication as:

Cerrillo, M., Viñas, M., Bonmatí, A. Anaerobic digestion instability by organic and nitrogen overloads: polishing of effluents by coupling a microbial fuel cell.

Abstract

Bioelectrochemical systems have been recently proposed as a polishing step of anaerobic digestion (AD). They can also be useful to overcome AD instability in case of anaerobic digestion inhibition and volatile fatty acids (VFA) accumulation, while recovering ammonia. Continuous assays with a microbial fuel cell (MFC) fed with digested pig slurry were performed to evaluate its operation during malfunction periods of the AD reactor and its feasibility as a strategy to recover ammonia, either by introducing VFA pulses in the MFC or by inducing the AD inhibition. A microbial community assessment was performed to study MFC changes over its operation when it was fed with digestate. The MFC achieved COD removal efficiencies of 50% during the AD inhibition, reaching a maximum of ammonium removal of 31% (11.19 g_N m^{-2} d^{-1}), while during stable operation of AD the COD removed in the serial MFC was 10-20%. High throughput 16S rRNA gene based sequencing assessment revealed anode biofilm different from feeding digestates, with a reduction in the microbial population diversity in the anode after a 182-day-operation period with digested pig slurry. Main enriched populations in the anode belonged to Bacteroidetes (*Flavobacteriaceae), Chloroflexi* (fermentative bacteria *Anaerolineaceae), Methanosarcinaceae* and hydrogenotrophic methanogens belonging to *Methanobacteriaceae.* An MFC has proven to be a reliable technology to complement the AD operation, improve the effluent quality and recover ammonia, especially during AD inhibition.

5.1 Introduction

Microbial fuel cells (MFCs) are bioelectrochemical devices with a wide range of applications, from power sources to biosensors (Abrevaya et al., 2015). MFCs have proven recently as a promising technology to be combined with anaerobic digestion (AD), mainly as a polishing strategy to increase the quality of the effluent, either by reducing its organic matter content or by removing nutrients. MFCs have been used to polish the effluent of two-stage biogas process (Fradler et al., 2014), hydrogen production fermentors (Sharma and Li, 2010) or up-flow anaerobic sludge blanket reactors (UASB) (Zhang et al., 2009), working with different kind of substrates, such as landfill leachate (Tugtas et al., 2013), wastewater from potato-processing industries (Durruty et al., 2012), sludge (Ge et al., 2013), pig slurry (Chapter 4; Cerrillo et al., 2016a) or molasses wastewater (Zhang et al., 2009).

MFCs can be particularly useful when the AD suffers from inhibition, as a buffer system to complement the AD process until its recovery. It is well known that the AD process, especially when it is performed at thermophilic temperature range, can be sensitive to several substances that may be present in the waste stream, such as ammonia (Yenigün and Demirel, 2013), long chain fatty acids (Palatsi et al., 2009), sulphide, light metal ions (Na, K, Mg, Ca and Al), heavy metals and organic compounds such as chlorophenols or halogenated aliphatics (Chen et al., 2008; Kroeker et al., 1979). In case of inhibition of the AD, an increase of VFA content in the effluent will take place, and a system such as a MFC to maintain them at low concentrations will be needed.

Apart from the utility of MFCs as a system to reduce VFA, it has been applied in the recovery of ammonium, since in two chamber systems there is a flux of cations through the cation exchange membrane from the anode to the cathode compartment in order to maintain electroneutrality. A subsequent step of stripping and absorption will allow for the recovery of the ammonia in order to reuse it as a fertiliser (Chapter 4; Cerrillo et al., 2016a; Cord-Ruwisch et al., 2011; Kim et al., 2008; Kuntke et al., 2012; Sotres et al., 2015a). This application is particularly interesting, since AD does not modify total N content of digestates, and thus it needs to be combined with other processes for N removal or recovery, especially when working with high strength wastewater such as livestock manure. Recently, a hybrid system consisting of a submersible microbial desalination cell and a continuous stirred tank reactor has been developed for counteracting ammonia inhibition during AD with simultaneous in-situ ammonia recovery and electricity production, when working with synthetic wastewater (Zhang and Angelidaki, 2015).

The combination of a thermophilic AD with an MFC under perturbation has been previously evaluated, by the addition of a severe acetic acid load (Weld and Singh, 2011). But MFCs performance against an AD destabilisation has not been studied in depth, neither its

influence in ammonia recovery. In Chapters 6 and 7 work performed under microbial electrolysis cell (MEC) mode, thus applying a low amount of energy to the system to boost the process, will show that VFA accumulation in pig slurry digestate can be removed in a MEC reactor while recovering ammonium, and that a higher performance of the MEC is achieved when the AD is under unstable or inhibited states. Therefore, it is interesting to assess whether this behaviour is also achieved under a producing energy MFC without additional external energy in terms of reactor sustainability.

Furthermore, the combination of the AD with the MFC systems may modify the anode biofilm biomass, both due to a continuous allocthonous biomass from digestate and to anodophilic enrichment on the anode. Therefore, the evolution of the microbial population in these conditions is a field that needs a deep study to gain insight on the stability of microbial biofilms established on the anode material in BES reactors. In Chapter 7 it will be shown a reduction in the anode biodiversity when integrating pig slurry AD with a MEC system (Cerrillo et al., 2016b), but more data is needed to understand these changes with a MFC system when no additional energy is provided to the BES.

The main aim of this study is to assess the performance of an MFC operated in combination with a pig slurry thermophilic AD, as a system to overcome AD destabilisation and inhibition periods due to organic and nitrogen overloads. Effluent quality will be assessed in terms of chemical oxygen demand (COD), VFA and ammonium removal. Also changes in the microbial composition of the MFC anode will be evaluated.

5.2 Materials and methods

5.2.1 Experimental set-up

The MFC reactor was the same two chamber cell used in the previous Chapter, and described in Section 3.1.1. The assays were performed after the batch assays carried out in Chapter 4. Digested pig slurry was used as feeding solution in the anode compartment (Table 5.1). The feeding solution for the MFC cathode chamber contained (per litre of deionised water): KH_2PO_4, 3 g; Na_2HPO_4, 6 g (pH of the buffer of 9.1).

Table 5.1 Characterisation of the digested pig slurries used as feeding in the MFC.

Parameter	Phase 1	Phase 2a	Phase 2b
pH (-)	8.21 ± 0.05	7.85 ± 0.03	7.74 ± 0.03
COD (g_{O2} kg^{-1})	26.04 ± 3.73	15.13 ± 2.46	34.43 ± 7.43
N-NH_4^+ (g L^{-1})	2.05 ± 0.04	1.29 ± 0.07	2.41 ± 0.34
TS (%)	1.37 ± 0.10	1.05 ± 0.02	1.93 ± 0.51
VS (%)	0.83 ± 0.10	0.62 ± 0.03	1.18 ± 0.33

5.2.2 Reactor operation

The MFC was operated in continuous for 182 days with a hydraulic retention time (HRT) of 34 h. The stability of the AD-MFC integrate operation was assessed in two different experiments, using digestate from two different sources. Table 5.1 shows the main characteristics of the feeding solutions.

In a first block of experiments, Phase 1, the MFC was fed for 40 days with the digestate from a pig slurry mesophilic AD plant with a HRT of 40 days (Vila-Sana, Lleida, Spain), previously filtered through a stainless steel sieve of 125 µm and diluted with tap water (1:2) to obtain the desired COD. The OLR of the MFC anode compartment was set at 18.22 g_{COD} L^{-1} d^{-1}, similar to the one used in a latter work in MEC mode (Chapter 6). As a preliminary evaluation of the performance of the MFC under a punctual overload episode of the AD system, a series of pulses of diverse pure and mixed VFA were performed (Table 5.2). Samples were taken from the anode and the cathode compartment previous to the pulse, and at time 1, 4, 7 and 24 h after the pulse.

Table 5.2 Operational conditions for de MFC reactor during the series of pure and mixed VFA pulses in Phase 1.

Day	VFA addition (mg)			Added COD (mg)
	Acetate	Propionate	Butyrate	
1-7	0	0	0	-
8	250	0	0	267
9 ,14 and 15	500	0	0	534
19 and 20	0	500	0	757
21 and 28	500	500	0	1291
29 and 33	1000	200	85	1525

The second block of experiments, Phase 2a and 2b, started a week after the last pulse of Phase 1. The MFC was fed during 142 days with the effluent of a 4 L lab-scale thermophilic AD described in Section 3.1.3, fed with pig slurry with a HRT of 10 days, in order to assess its performance under a real inhibited AD effluent. During Phase 2a, the MFC was fed for 80 days with the effluent of the AD performing in a stable state, while during Phase 2b (62 days) the effluent resulted from the AD destabilised by an organic and nitrogen overload. Previously to feed the MFC, the AD effluent was filtered through a stainless steel sieve of 125 µm. The resulting OLR of the MFC anode compartment was of 10.59±1.78 and 24.10±5.20 g_{COD} L^{-1} d^{-1} in Phase 2a and 2b, respectively, and a nitrogen loading rate (NLR) of 0.90±0.05 and 1.84±0.06 g_N L^{-1} d^{-1}, respectively. All the assays were performed at room temperature (~ 23 ºC).

5.2.3 Analyses and calculations

Samples of the feeding solutions and the anode effluent were characterised for chemical oxygen demand (COD), total and volatile solids (TS and VS), alkalinity, volatile fatty acids (VFA), ammonium N-NH_4^+ and pH, besides dissolved methane in the anode effluent. Cathode samples were characterised for ammonium N-NH_4^+ and pH. All the analyses were performed following the methods described in Section 3.2.

In order to know the biodegradability of the remaining organic matter of the digestates used as feed solution to the MFC, anaerobic biodegradability tests (ABT) of the two different digestates used during Phase 2 were performed as described in Section 3.2.11.

Current density, coulombic efficiency (CE), COD and ammonium removal efficiencies and ammonium flux were determined as described in Section 3.4.

The bacterial communities attached to the anode material in the MFC at the beginning and the end of the experiments, and the ones present in the digested pig slurry in Phase 1, were analysed by culture-independent molecular techniques such as quantitative real-time PCR (qPCR) and high throughput *16S rRNA* gene sequencing (MiSeq, Illumina). The microbial diversity and structure of the MFC influent (digestate) in Phase 2a and 2b will be described later as part of Chapter 7, defined there as Phase 1 and Phase 2, respectively. Briefly, that study showed that Pseudomonadaceae (20%), and Clostridiaceae (20%) were the predominant eubacteria families in Phase 2a and 2b, respectively, while Methanobacteriaceae was the predominant archaea family (98%) in both digestates.

Total DNA extraction, qPCR and high throughput *16S rRNA* gene sequencing (MiSeq, Illumina) were performed following the methods described in Section 3.6.1, 3.6.3, and 3.6.5, respectively. The standard curve parameters of the qPCRs performed had a high efficiency, and were as follows (for *16S rRNA* and *mcrA*, respectively): slope of -3.407 and -3.591; Y-intercept of 39.26 and 39.48; correlation coefficient of 0.999 and 0.998; efficiency of 97 and 90%. Data obtained from sequencing datasets were deposited in the Sequence Read Archive of the National Center for Biotechnology Information (NCBI) under study accession number SRP070839, for eubacterial and archaeal populations.

The evaluation of the diversity of the samples and statistical multivariate analyses were performed following Section 3.6.6.

5.3 Results and discussion

5.3.1 MFC performance under AD instability: assays with VFA pulses in the feed

In order to test the performance of the MFC when an AD instability even occurred, the MFC was fed with the digested plus different pulses of VFA to simulate the composition of the digestate under these periods (Table 5.2). During the first 7 days of Phase 1, before any VFA pulse was performed, the MFC produced a current density in a range of 100-300 mA m^{-2}. When the pulses of VFA started to be applied, the current density was maintained at around 150 mA m^{-2}, and although some current peaks were registered, a clear correspondence between the VFA introduction and an increase in the current density could not be established (Figure 5.1a). After each VFA pulse, the VFA concentration showed a fast decrease, returning to the values existing before the VFA addition in less than 24 h, and the pH of the bulk solution in the anode compartment was maintained in a range of 7.3-8.8, thus appropriate for the microbial activity (Figure 5.2a). In a latter work, using a MEC, the response to the VFA addition fitted properly with each pulse after 24h, obtaining an increase in the current density after the addition of COD (Chapter 6). This behaviour is in concordance with the low coulombic efficiencies achieved when working with MFC (11-18%) compared to the obtained in MEC mode (1-4%) (Chapter 4; Cerrillo et al., 2016a). Independently from the energy recovery, these results show that the MFC can absorb punctual increases in VFA, without showing signs of destabilisation.

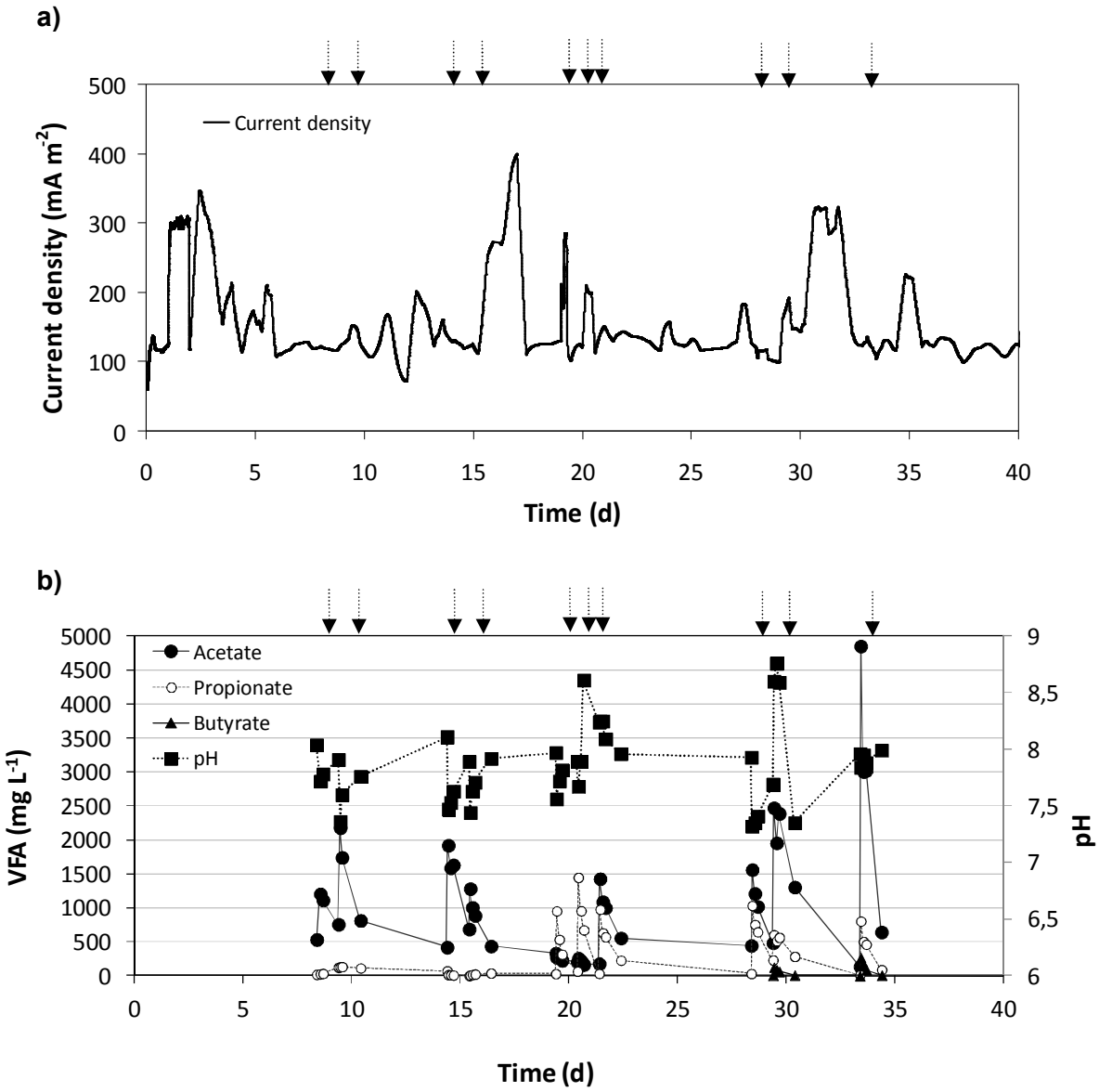

Figure 5.1 a) Current density and b) VFA concentration and pH in the anode compartment obtained in Phase 1 during the pure and mixed VFA pulses. Arrows show when each pulse was performed.

5.3.2 MFC performance under AD stable and inhibited states

During Phase 2a, the MFC was fed with the effluent of a lab-scale thermophilic AD at steady state operation. The current density was in average 121 mA m^{-2}. At the start of this period, the COD removal efficiency in the MFC was as high as 48%, and gradually decreased to values between 10 and 20% at the end of the period (Figure 5.2), since the COD of the influent gradually decreased from 18.70 to 12.50 g L^{-1}, showing an improvement in the performance of the AD. At the end of Phase 2a, the COD of the MFC effluent was of 10.06 g kg^{-1}, representing a removal of 1.57 g_{COD} L^{-1} d^{-1}. The overall COD removal for the AD-MFC combined system would be of around 70%. Results of the anaerobic biodegradability assay showed that the

maximum biodegradability in 62 days of the digestate utilised in Phase 2a was of 53%, similar to the COD removal efficiency of the MFC in this phase, with lower HRT than the time used in the anaerobic biodegradability assays. Average CE was 1.07±0.59%, much lower than the obtained in batch experiments with digested pig slurry and the same reactor and external resistance (100 Ω) (Chapter 4; Cerrillo et al., 2016a). The conversion of COD to methane only represented between 0.5-3.5% of the electron losses in this MFC, accordingly to the dissolved methane detected in the samples. So other complex processes are taking part in the anode compartment, and other electron acceptors may be present in the substrate, reducing the amount of electrons reaching the electric circuit. The ammonium removal efficiency during this phase oscillated between 12 and 27%, with a $N\text{-}NH_4^+$ concentration in the effluent at the end of this phase of 1.03 g L^{-1}, representing a flux of $N\text{-}NH_4^+$ through the CEM of 4.76 g_N m^{-2} d^{-1}. Previous assays performed in batch mode MFC with the same external resistance achieved a flux of 8.86 g_N m^{-2} d^{-1}, although working with a lower COD and ammonia concentration; in that case, it was also found that ammonia transport in open circuit was as high as the obtained in closed circuit, so all ammonium transport was being produced by diffusion (Chapter 4; Cerrillo et al., 2016a). Although nitrogen removal rates obtained in other studies so far range between 2.94 and 162.18 g_N m^{-2} d^{-1} (Rodriguez Arredondo et al., 2015), the removal rate in this study is similar to the 3.3 g_N m^{-2} d^{-1} value obtained working with urine with an MFC working at higher current density (500 mA m^{-2}) and also a 3 times higher concentration of N in the influent (4050 mg_N L^{-1}) (Kuntke et al., 2012). Increasing the electron recovery efficiency of the MFC system will allow to have a higher current density and more ammonia could be recovered.

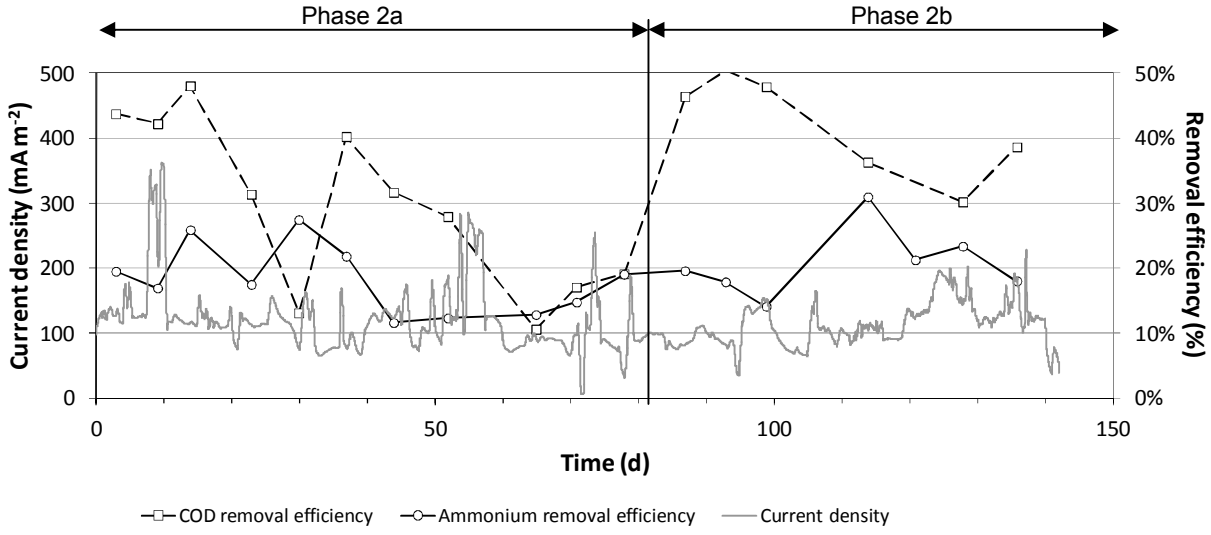

Figure 5.2 Current density and COD and ammonium removal efficiencies obtained in Phase 2.

On day 80 the influent was changed (Table 5.1), shifting to the effluent obtained from an inhibited AD as a result of an increase in the organic and nitrogen loading rates (Phase 2b). As a response, the MFC showed an increase in the COD removal efficiency up to values of 50%, stabilising around 30-40%. At the end of Phase 2b, the COD of the MFC effluent was of 25.20 g L^{-1}, representing a removal of 5.04 g_{COD} L^{-1} d^{-1}, a 3.2 fold increase with respect to Phase 2a (when the OLR was half of the one in Phase 2b). The anaerobic biodegradability tests (ABT) showed a maximum biodegradability of the MFC influent used in this phase of 81%. The increase with respect to the value obtained for the influent in the previous phase is in concordance with a destabilisation of the AD. The MFC maximum COD removal efficiency is 62% of the achieved in the ABT, so a longer HRT would help to achieve higher removal efficiencies in the MFC. Average CE was 0.30±0.06%, a third part of the obtained in the previous phase, pointing out that in spite of a higher COD removal, an increase in the current density was not achieved. A previous study has found that an increase in the organic loading rate is not always followed by a significant increase in current generation, since the increase in the loading rate needs to be accompanied by a decrease of the external resistance in order to increase the continuous current generation (Aelterman et al., 2008). Methane production in the MFC during Phase 2b was lower than in the previous phase, representing between 0.3-0.9% of the removed COD. On the other hand, the ammonium removal efficiency remained in a range of 14-31%, slightly higher than in the previous phase (12-27%). The $N\text{-}NH_4^+$ concentration in the effluent at the end of this phase was of 2.23 g L^{-1}, representing a flux of $N\text{-}NH_4^+$ through the CEM of 11.19 g_N m^{-2} d^{-1}, which was a two-fold higher value than the one obtained in Phase 2a, and approaching the flux obtained in a similar reactor running in MEC mode with equivalent OLR and NLR (Chapter 7; Cerrillo et al., 2016b). In spite of the increase of COD of the influent and the removal rate, the average current density was similar to the previous phase (112 mA m^{-2}), so migration force may have a low influence on ammonia transfer through the CEM. Ammonia transport by diffusion may still have an important role in this system, probably due to the exchange of cations with the cathodic buffer and favoured in Phase 2b by the 2-fold higher ammonium concentration in the influent.

Figure 5.3 shows the VFA concentration both of the influent and the effluent of the MFC. At the end of Phase 2a the removal efficiency for acetate established in a range of 50-80% (with a concentration in the effluent of 155-387 mg L^{-1}), achieving 100% removal for propionate, thus polishing the effluent of the AD and removing the residual VFA concentration of the digestate. During Phase 2b, an increase in the VFA of the influent was observed, especially acetate and propionate, as a result of the destabilisation of the AD. The reduction of the VFA concentration in the MFC at the end of this period was of 52-64% for acetate and 55-70% for propionate. Minor VFA such as iso- and n-butyrate, and iso- and n-valerate, were reduced in a 68-70%, 92-

98%, 71-77% and 87-100%, respectively, maintaining the acetic equivalent average VFA concentration under 2000 mg L^{-1} in spite of being the influent concentration in a range of 4200-6500 mg L^{-1}. The MFC is able to polish the AD effluent when the reactor is under inhibition, being the integration of both systems a valuable approach to maintain the effluent quality.

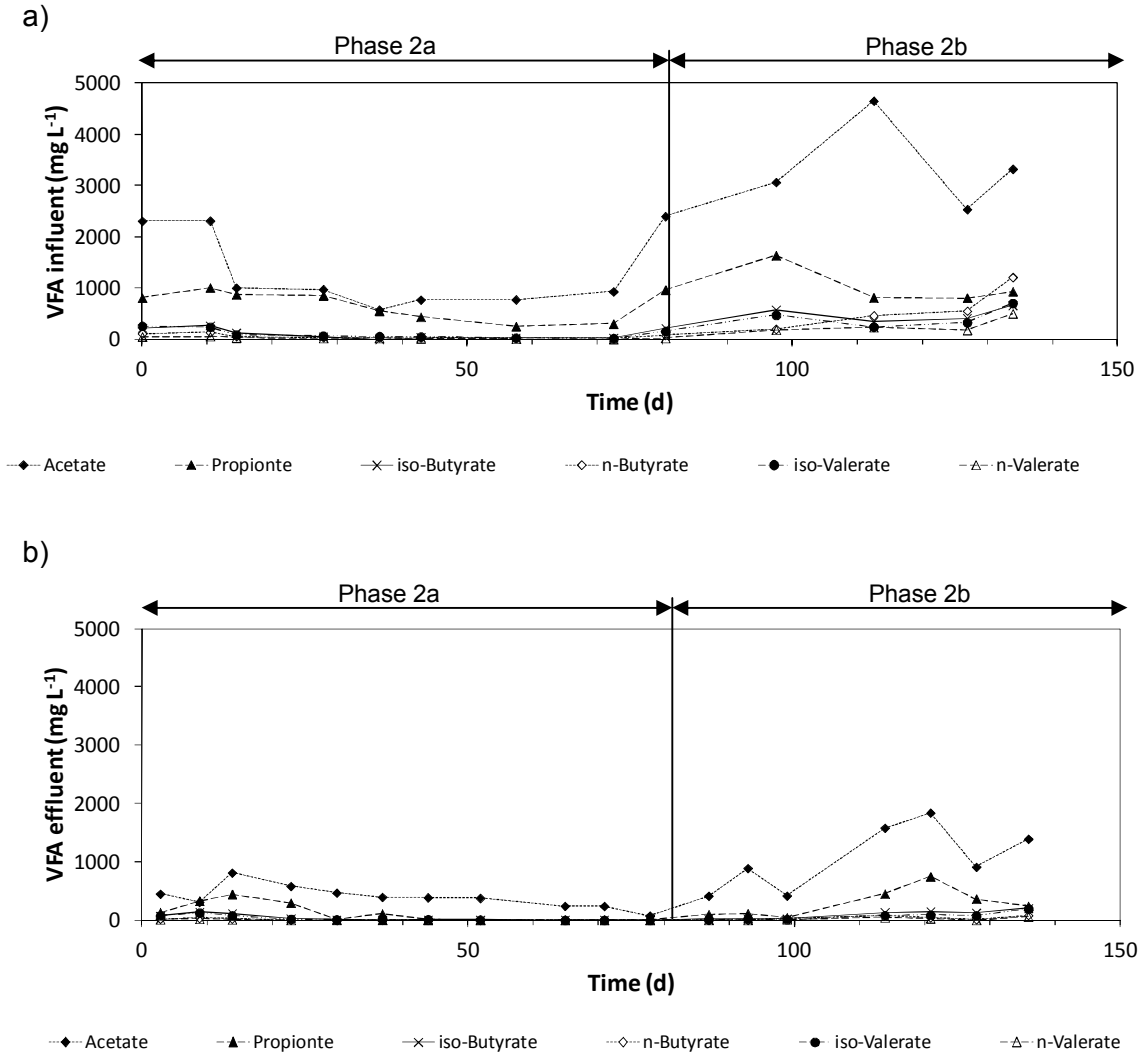

Figure 5.3 VFA concentration in a) the influent and b) the effluent in Phase 2.

5.3.3 Microbial community analysis

The evolution of the anodic microbial community of the MFC due to the integrated operation with the AD was studied by means of qPCR and high throughput sequencing.

Quantitative evolution of total eubacteria and archaeal methanogenic populations attached to the anode material as biofilm is shown in Figure 5.4. After 182 days of MFC operation (at the end of phase 2b), the eubacterial population suffered a 33 fold decrease, while archaeal population was reduced 3.6 times, being relatively enriched and accounting for 1.5% of total bacterial community, but maintained the same order of magnitude. This slight reduction

in methanogenic populations may explain the reduction in methane production during Phase 2b. On the other hand, the decrease in eubacteria and archaea populations may be due to the increase in the NLR in the last phase, since some microbial populations may be sensible to the high ammonia concentration of the influent. Concentrations of free ammonia nitrogen (FAN) above 900 mg L^{-1} were reached during Phase 2b, and at these levels the first signs of inhibition may occur according to previous studies (Angelidaki and Ahring, 1993; Hansen et al., 1998).

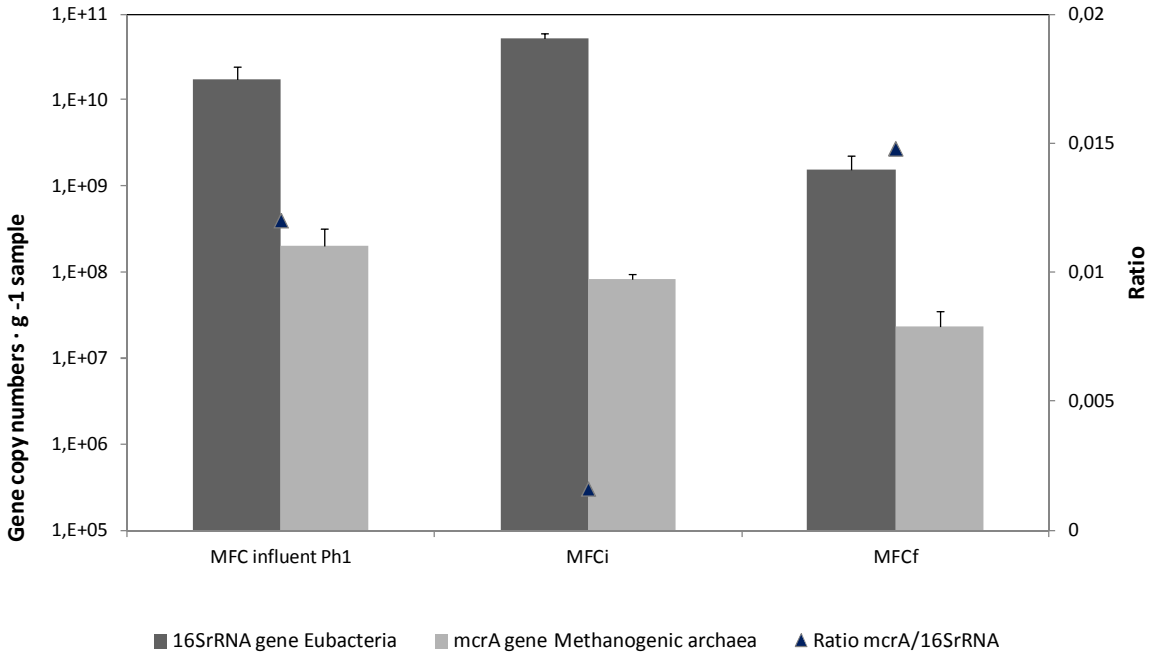

Figure 5.4 Gene copy numbers for *16S* rRNA and *mcrA* genes and ration between them, of the initial and final MFC anode biofilm (MFCi and MFCf, respectively), and the MFC influent in Phase 1.

Regarding high throughput 16S rRNA gene sequencing assessment (MiSeq analysis), the reads, ranging from 34632 to 16875 reads per sample, and the coverage obtained for bacteria and archaeal community for each sample are shown in Table 5.3. Figure 5.5 shows rarefaction curves, with all the samples near to approach a plateau when plotting OTUs vs. the number of *16S* rRNA, concomitant to high coverage values (99-100%) (Table 5.3). Regarding the eubacterial diversity, the inverted Simpson, Shannon and Chao-1 indices showed that the sample of the MFC at the start of the assays was the most diverse one (36.63, 4.75 and 820.25, respectively), while the MFC anode biofilm at the end of the assays was the less diverse one (8.01, 3.03 and 591.25, respectively) (Table 5.3). With respect to the archaeal diversity, different results were obtained depending on the index taken into account (Table 5.3). Inverted Simpson index showed the highest diversity in the case of the initial sample of the MFC anode biofilm, being followed by the final sample and the AD effluent. Shannon index identified the final anode

biofilm as the sample with the highest diversity, followed by the initial anode biofilm. However by using Inverted Simpson index, which is more sensitive to samples with low diversity (i.e. Archaea), it was revealed that the diversity of archaeal community on the anode was maintained throughout phase 2 period, being higher than those harboured in the inflow digestate. Chao-1 revealed complex eubacterial populations in all samples (anode and digestate) ranging from 591 to 820 OTUs, whereas Archaeal community was quite less complex accounting for 62 to 94 OTUs. These diversity and richness results are in concordance with the study performed in Chapter 7 that also showed a reduction of the BES biodiversity after being operated with digested pig slurry (Cerrillo et al., 2016b).

Table 5.3 Diversity index for Eubacterial and Archaeal community of the MFC anode and MFC influent in Phase 1 samples (average±SD). Data normalised to the sample with the lowest number of reads (17049 and 16875 for eubacterial and archaeal, respectively).

	Reads	**Coverage**	**OTUs**	**Inverted Simpson**	**Shannon**	**Chao**
Eubacteria						
MFC_i	17049	0.99±0.00	713.00±0.00	36.63±0.00	4.75±0.00	820.25±0.00
MFC_f	26308	0.99±0.00	453.12±6.54	8.01±0.06	3.03±0.01	591.25±28.39
$Influent_{Ph1}$	23555	0.99±0.00	689.01±6.36	15.66±0.17	4.30±0.01	819.02±23.00
Archaea						
MFC_i	128381	1.00±0.00	68.61±3.81	2.30±0.01	1.19±0.01	94.25±16.95
MFC_f	16875	1.00±0.00	51.00±0.00	2.13±0.00	1.41±0.00	62.14±0.00
$Influent_{Ph1}$	34632	1.00±0.00	56.63±2.58	1.64±0.01	1.03±0.01	74.68±14.40

(a)

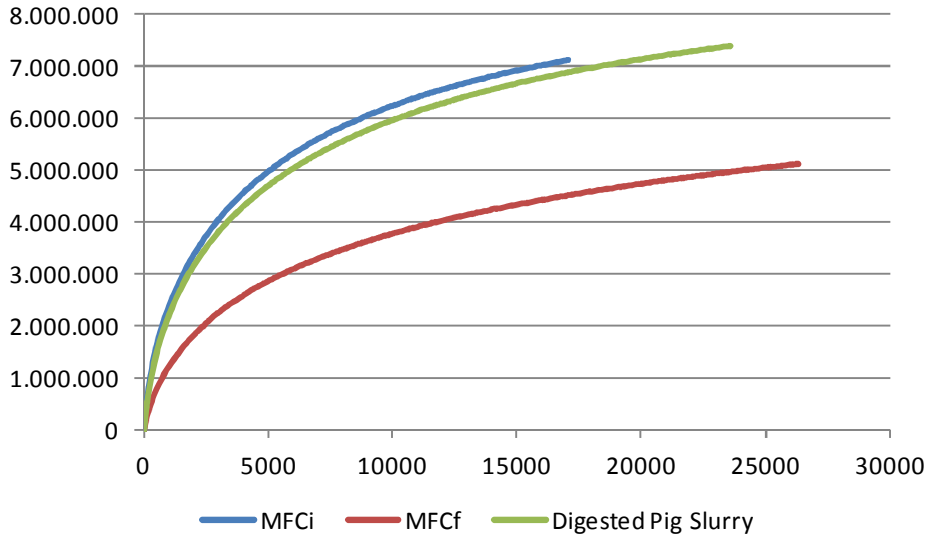

(b)

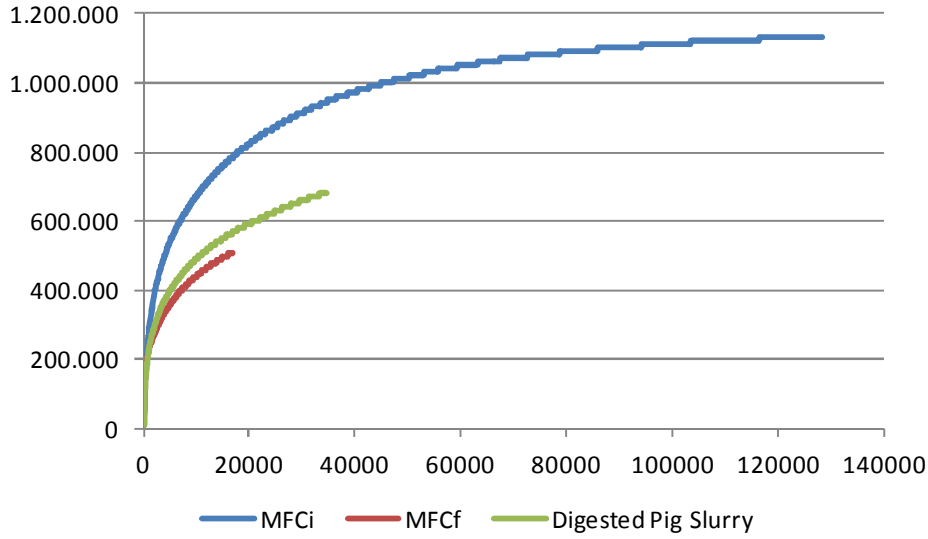

Figure 5.5 Rarefaction curves for initial (MFC_i) and final (MFC_f) MFC anode samples and the digested pig slurry in Phase 1 regarding (a) Eubacterial and (b) Archaeal community.

The dominant eubacterial *phylum* identified in the anode biofilm sample of the MFC at the start of Phase 1 was *Bacteroidetes* (40%), followed by *Firmicutes* (20%) and *Proteobacteria* (14%). These *phyla* are also the predominant ones in previous studies (Bonmatí et al., 2013; Mei et al., 2015; Sotres et al., 2015a; Sotres et al., 2015b) and in Chapter 7. At the end of the experiment (Phase 2b), *Bacteroidetes* increased its relative abundance in the anode up to 66%, concomitant to an increase of a minor *phylum* at the initial biofilm, *Chloroflexi* (17%), and the decrease of *Firmicutes* (8%) and *Proteobacteria* (below 0.5%). Regarding the eubacterial community, the influent (digestate) in Phase 1 and the anode biofilm were closely similar at the

start of the experiments (Figure 5.6). The anode compartment of the MFC had been fed previously in batch mode with digested pig slurry for 2 months as described in Chapter 4. At family level, the digestate in Phase 1 was dominated, as in the case of the MFC biofilms, by *Flavobacteriaceae* (24%). Indeed, *Flavobacteriaceae* (13%) was the predominant one at the initial biofilm, followed by three families with the same relative abundance, *Desulfuromonadaceae*, *Porphyromonadaceae* and *Acholeplasmataceae* (8%). The anode biofilm in MFC at the end of the experiment (Phase 2b) showed 2.6 fold increase of *Flavobacteriaceae* (34%, within the phylum *Bacteroidetes*), while *Anaerolineaceae* family, mainly *Longilinea* sp., (harbouring well known fermentative bacteria belonging to phylum *Chloroflexi*) increased from 1 to 17%, probably due to a higher bioavailability of fermentative substrates on the digestate from unstable anaerobic digester (Phase 2b). Both families have been identified in the anode of a MEC in the study performed in Chapter 7, as well as *Anaerolineaceae* in the anode of a MFC (Bonmatí et al., 2013). 32% and 36% of the OTUs of the initial and final biofilm of the MFC were unclassified at family level and belonged mainly to *Bacteroidetes* and *Firmicutes* phyla, representing 47 and 34% of the unclassified OTUs in the initial MFC biofilm, respectively, and 81% and 15% in the final one. These OTUs that cannot be assigned to a known family may be novel taxa or be still poorly defined in RDP database.

Regarding archaea population, *Methanomassiliicoccaceae* (49%) and *Methanotrichaceae* ("*Methanosaetaceae*") (45%) were the predominant families in the anode of the MFC at the start of the experiments (Figure 5.7). A clear shift was observed after the experiments of VFA pulses and inhibited AD feeding, showing a clear enrichment of *Methanosarcinaceae* family (70%), when in the initial anode it only represented 2% of the population. Also *Methanobacteriaceae* family, which was under 0.5% in the initial MFC biofilm, increased to 9% at the final sample. Both families are classified as hydrogenotrophic methanogens, being *Methanosarcinaceae* able to generate methane also by means of the aceticlastic way. On the other hand, Methanotrichaceae ("*Methanosaetaceae"*) is strictly aceticlastic. Previous studies have stated that *Methanosarcina* sp. *s*eems to be more tolerant towards ammonium stress than other methanogens, particularly *Methanosaeta* sp. (De Vrieze et al., 2012). So the increase in the NLR of the MFC may have favoured the increase in relative abundance of the first one. Interestingly, Methanosarcinaceae was not a predominant group in the MFC influent, neither in Phase 1, dominated by *Methanotrichaceae* (78%), nor in Phase 2, dominated by the genus *Methanothermobacter* (98%) belonging to *Methanobacteriaceae* family, as was also described later in Chapter 7.

a)

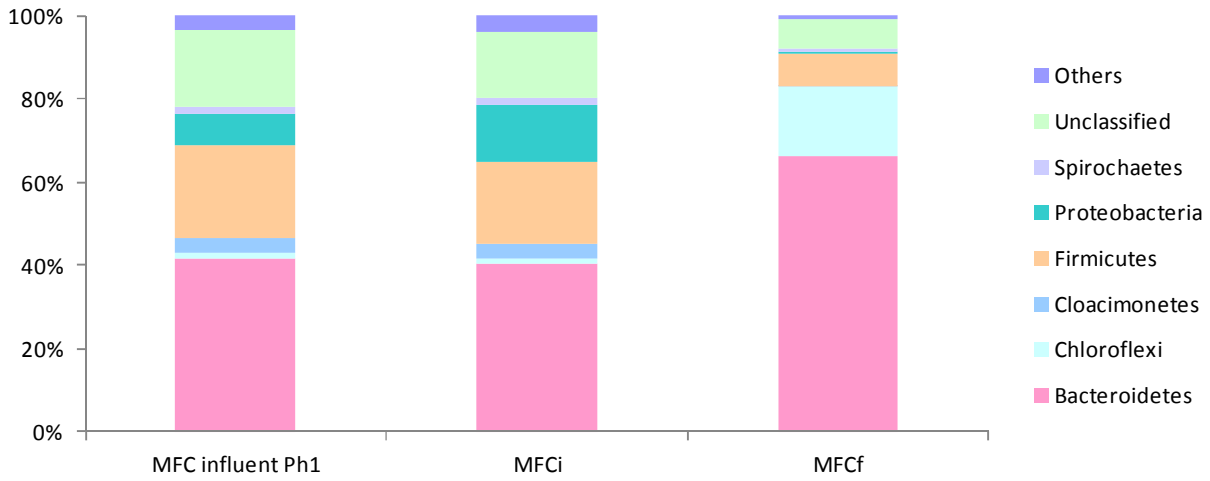

b)

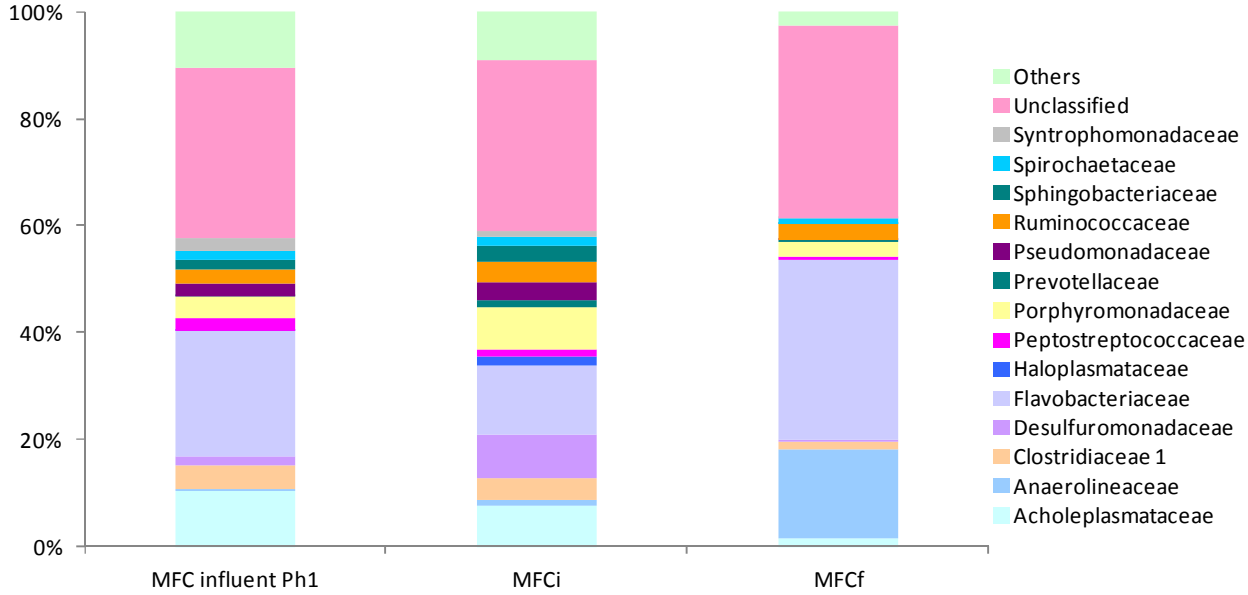

Figure 5.6 Taxonomic assignment of sequencing reads from Eubacterial community of the initial and final MFC anode biofilm (MFCi and MFCf, respectively), and the MFC influent of Phase 1, at a) phylum b) family levels. Relative abundance was defined as the number of reads (sequences) affiliated with any given taxon divided by the total number of reads per sample. Phylogenetic groups with a relative abundance lower that 1% were categorised as "others".

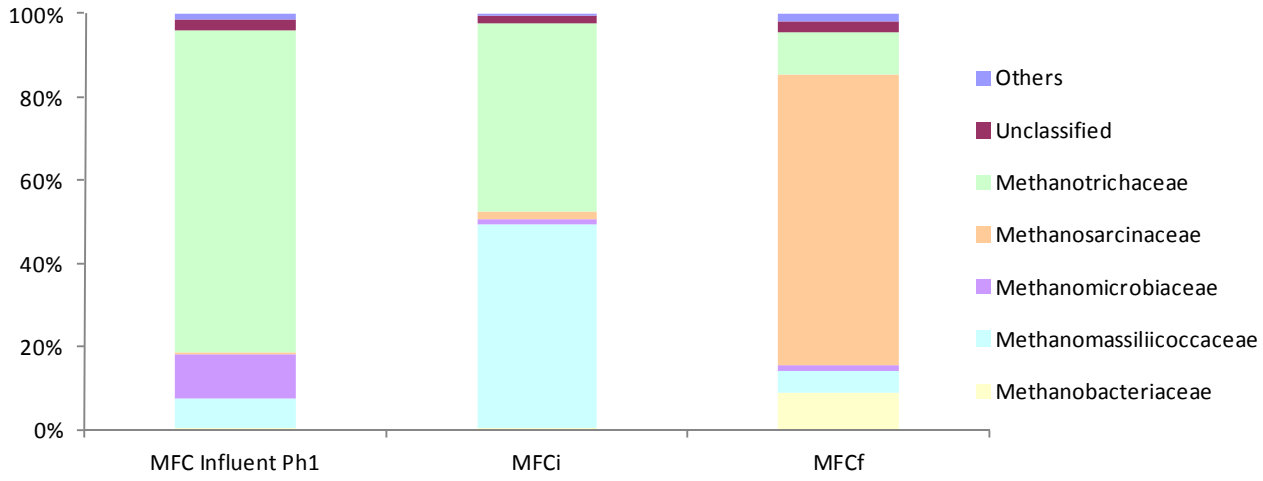

Figure 5.7 Taxonomic assignment of sequencing reads from Archaeal community of the initial and final MFC anode biofilm (MFCi and MFCf, respectively), and the MFC influent of Phase 1, at family level. Relative abundance was defined as the number of reads (sequences) affiliated with any given taxon divided by the total number of reads per sample. Phylogenetic groups with a relative abundance lower that 1% were categorised as "others".

Correspondence analysis for eubacterial and archaeal population (Figures 5.8a and 5.8b, respectively), including in this case the samples of the digested pig slurry in Phase 2a and b (AD-Ph2a and AD-Ph2b, respectively), clusters similarly in both cases. The MFC initial biofilm was clustered together with the digested pig slurry in Phase 1 (AD-Ph1), while the final biofilm was located far from this cluster and the second one formed by the digested pig slurry in Phase 2a and 2b, showing that the anode biofilm evolution is independent from the population present in the digestates feeding the MFC.

a)

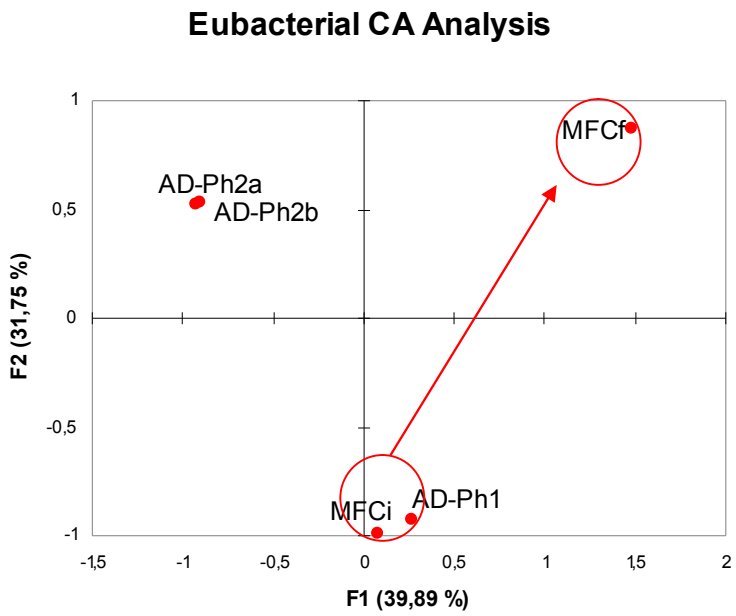

b)

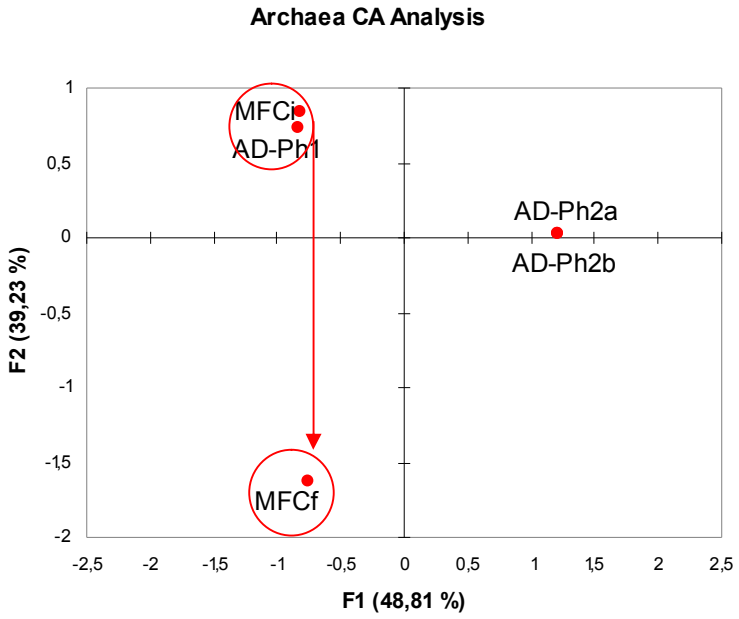

Figure 5.8 Correspondence Analysis for initial (MFC_i) and final (MFC_f) MFC anode samples and the 3 AD influents (AD-Ph1, AD-Ph2a and AD-Ph2b) regarding (a) Eubacterial and (b) Archaeal community.

5.4 Conclusions

The MFC has proven to be a useful technology to improve the effluent quality after possible malfunction of AD reactors, since it has been able to remove high levels of VFA from AD effluents, while recovering ammonia. During punctual pulses of VFA, simulating a malfunction of the AD process, the MFC showed a poor conversion of COD increase into current density. Probably other complex reactions may be taking place in the anode compartment or other electron acceptors may be present in the substrate, although VFA were totally removed. The MFC operated under a stable period of the AD achieved 10-20% of COD removal and 12-27% of ammonium removal, while when feeding with the effluent of the inhibited reactor these removal efficiencies increased to 30-40% and 14-31%, respectively. The MFC operated in serial after the anaerobic digestion of pig slurry has proven to produce a reduction of the biodiversity of the microbial population, as well as a decrease in the total population, especially of eubacteria.

5.5 References

Abrevaya, X.C., Sacco, N.J., Bonetto, M.C., Hilding-Ohlsson, A., Cortón, E. 2015. Analytical applications of microbial fuel cells. Part I: Biochemical oxygen demand. *Biosensors and Bioelectronics*, **63**, 580-590.

Aelterman, P., Versichele, M., Marzorati, M., Boon, N., Verstraete, W. 2008. Loading rate and external resistance control the electricity generation of microbial fuel cells with different three-dimensional anodes. *Bioresource Technology*, **99**(18), 8895-8902.

Angelidaki, I., Ahring, B.K. 1993. Thermophilic anaerobic digestion of livestock waste: the effect of ammonia. *Applied Microbiology and Biotechnology*, **38**(4), 560-564.

Bonmatí, A., Sotres, A., Mu, Y., Rozendal, R.A., Rabaey, K. 2013. Oxalate degradation in a bioelectrochemical system: Reactor performance and microbial community characterization. *Bioresource Technology*, **143**(0), 147-153.

Cerrillo, M., Oliveras, J., Viñas, M., Bonmatí, A. 2016a. Comparative assessment of raw and digested pig slurry treatment in bioelectrochemical systems. *Bioelectrochemistry*, **110**, 69-78.

Cerrillo, M., Viñas, M., Bonmatí, A. 2016b. Overcoming organic and nitrogen overload in thermophilic anaerobic digestion of pig slurry by coupling a microbial electrolysis cell. *Bioresource Technology*, **216**, 362-372.

Chen, Y., Cheng, J.J., Creamer, K.S. 2008. Inhibition of anaerobic digestion process: A review. *Bioresource Technology*, **99**(10), 4044-4064.

Cord-Ruwisch, R., Law, Y., Cheng, K.Y. 2011. Ammonium as a sustainable proton shuttle in bioelectrochemical systems. *Bioresource Technology*, **102**(20), 9691-9696.

De Vrieze, J., Hennebel, T., Boon, N., Verstraete, W. 2012. *Methanosarcina*: The rediscovered methanogen for heavy duty biomethanation. *Bioresource Technology*, **112**, 1-9.

Durruty, I., Bonanni, P.S., González, J.F., Busalmen, J.P. 2012. Evaluation of potato-processing wastewater treatment in a microbial fuel cell. *Bioresource Technology*, **105**(0), 81-87.

Fradler, K.R., Kim, J.R., Shipley, G., Massanet-Nicolau, J., Dinsdale, R.M., Guwy, A.J., Premier, G.C. 2014. Operation of a bioelectrochemical system as a polishing stage for the effluent from a two-stage biohydrogen and biomethane production process. *Biochemical Engineering Journal*, **85**(0), 125-131.

Ge, Z., Zhang, F., Grimaud, J., Hurst, J., He, Z. 2013. Long-term investigation of microbial fuel cells treating primary sludge or digested sludge. *Bioresource Technology*, **136**(0), 509-514.

Hansen, K.H., Angelidaki, I., Ahring, B.K. 1998. Anaerobic digestion of swine manure: inhibition by ammonia. *Water Research*, **32**(1), 5-12.

Kim, J.R., Zuo, Y., Regan, J.M., Logan, B.E. 2008. Analysis of ammonia loss mechanisms in microbial fuel cells treating animal wastewater. *Biotechnology and Bioengineering*, **99**(5), 1120-1127.

Kroeker, E.J., Schulte, D.D., Sparling, A.B., Lapp, H.M. 1979. Anaerobic treatment process stability. *Journal Water Pollution Control Federation*, **51**(4), 718-727.

Kuntke, P., Smiech, K.M., Bruning, H., Zeeman, G., Saakes, M., Sleutels, T.H.J.A., Hamelers, H.V.M., Buisman, C.J.N. 2012. Ammonium recovery and energy production from urine by a microbial fuel cell. *Water Research*, **46**(8), 2627-2636.

Mei, X., Guo, C., Liu, B., Tang, Y., Xing, D. 2015. Shaping of bacterial community structure in microbial fuel cells by different inocula. *RSC Advances*, **5**(95), 78136-78141.

Palatsi, J., Laureni, M., Andres, M.V., Flotats, X., Nielsen, H.B., Angelidaki, I. 2009. Strategies for recovering inhibition caused by long chain fatty acids on anaerobic thermophilic biogas reactors. *Bioresour Technol*, **100**(20), 4588-96.

Rodriguez Arredondo, M., Kuntke, P., Jeremiasse, A.W., Sleutels, T.H.J.A., Buisman, C.J.N., ter Heijne, A. 2015. Bioelectrochemical systems for nitrogen removal and recovery from wastewater. *Environmental Science: Water Research & Technology*, **1**(1), 22-33.

Sharma, Y., Li, B. 2010. Optimizing energy harvest in wastewater treatment by combining anaerobic hydrogen producing biofermentor (HPB) and microbial fuel cell (MFC). *International Journal of Hydrogen Energy*, **35**(8), 3789-3797.

Sotres, A., Cerrillo, M., Viñas, M., Bonmatí, A. 2015a. Nitrogen recovery from pig slurry in a two-chambered bioelectrochemical system. *Bioresource Technology*, **194**, 373-382.

Sotres, A., Díaz-Marcos, J., Guivernau, M., Illa, J., Magrí, A., Prenafeta-Boldú, F.X., Bonmatí, A., Viñas, M. 2015b. Microbial community dynamics in two-chambered microbial fuel cells: effect of different ion exchange membranes. *Journal of Chemical Technology & Biotechnology*, **90**(8), 1497-1506.

Tugtas, A.E., Cavdar, P., Calli, B. 2013. Bio-electrochemical post-treatment of anaerobically treated landfill leachate. *Bioresource Technology*, **128**(0), 266-272.

Weld, R.J., Singh, R. 2011. Functional stability of a hybrid anaerobic digester/microbial fuel cell system treating municipal wastewater. *Bioresource Technology*, **102**(2), 842-847.

Yenigün, O., Demirel, B. 2013. Ammonia inhibition in anaerobic digestion: A review. *Process Biochemistry*, **48**(5-6), 901-911.

Zhang, B., Zhao, H., Zhou, S., Shi, C., Wang, C., Ni, J. 2009. A novel UASB-MFC-BAF integrated system for high strength molasses wastewater treatment and bioelectricity generation. *Bioresource Technology*, **100**(23), 5687-5693.

Zhang, Y., Angelidaki, I. 2015. Counteracting ammonia inhibition during anaerobic digestion by recovery using submersible microbial desalination cell. *Biotechnology and Bioengineering*, **112**(7), 1478.

CHAPTER 6

Removal of volatile fatty acids and ammonia recovery from unstable anaerobic digesters with a microbial electrolysis cell

Part of the content of this chapter was published as:

Cerrillo, M., Viñas, M., Bonmatí, A. Removal of volatile fatty acids and ammonia recovery from unstable anaerobic digesters with a microbial electrolysis cell. *Bioresource Technology*, **219**, 348-356. doi:10.1016/j.biortech.2016.07.103

Abstract

Anaerobic digestion (AD) is widely used to treat various kinds of wastes. One of the main drawbacks is that the process can become unstable by organic overload and several substances that may be present in the waste stream. Furthermore, AD does not modify total N content of digestate and it usually needs correct management or further treatment. A microbial electrolysis cell (MEC) was studied as a technology to be combined with AD to overcome these limitations. Continuous assays with a MEC fed with digested pig slurry were performed to evaluate its stability and robustness to malfunction periods of the AD reactor and its feasibility as a strategy to recover ammonia. During punctual pulses of volatile fatty acids (VFA), simulating a malfunction of the AD process, an increase in the MEC current density was produced as a result of the added COD, especially when acetate was used, reaching current densities of 3500 mA m^{-2} concomitant to high levels of VFA removal. Furthermore, ammonium diffusion from the anode to the cathode compartment was enhanced during daily pulses and the removal efficiency achieved up to 60%. An AD-MEC combined system has proven to be a robust and stable configuration to obtain a high quality effluent, with a lower organic and ammonium content.

6.1 Introduction

Livestock manure can be a source of energy and nutrients if managed and processed properly. Anaerobic digestion (AD) is a biological process which converts organic substrates in a mixture of gases (biogas) –mainly methane and carbon dioxide. This energy recovering technology is well established in terms of performance, is technically and economically feasible, and is widely used to treat various kinds of wastes (Angenent et al., 2004). However, this technology presents some drawbacks. In the first place, AD does not modify total N content of digestates, and thus when it is applied to livestock manure it needs to be combined with other processes for N removal or recovery to avoid effluent management constrains, such as chemical precipitation of ammonium and phosphate as struvite (Cerrillo et al., 2015), ammonia stripping and its subsequent absorption in an acid solution (Laureni et al., 2013) or thermal concentration of the digestate (Bonmatí et al., 2003; Bonmatí and Flotats, 2003). In the second place, the process can become unstable by organic overload or inhibited by several substances that may be present in the waste stream, such as long chain fatty acids (Palatsi et al., 2009), ammonia (Yenigün and Demirel, 2013), sulphide, light metal ions (Na^+, K^+, Mg^{2+}, Ca^{2+} and Al^{3+}), heavy metals and organic compounds as chlorophenols or halogenated aliphatic compounds (Chen et al., 2008). Reactor inhibition caused by the accumulation of these substances will be indicated by reduced biogas production and/or biogas methane content, and accumulation of volatile fatty acids (VFA) such as acetate, propionate or butyrate, that may led to reactor failure. So it is interesting to find out new technologies that can help to maintain effluent quality within the desired limits.

Bioelectrochemical systems (BESs), such as Microbial Electrolysis Cells (MECs), that use microorganisms attached to one or both bioelectrode(s) in order to catalyse oxidation and/or reduction reactions, can also be coupled to AD in order to improve its performance and effluent quality (Chapter 4; Cerrillo et al., 2016). BESs offers some advantages over AD as it performs properly at low substrate concentration levels. Combining AD and MEC is a new processing strategy aiming to recover energy and nitrogen simultaneously. On the one hand, ammonium can be removed and recovered, as it is transferred through the cation exchange membrane from the anode to the cathode compartment where it can be recovered (Chapter 4; Cerrillo et al., 2016; Kuntke et al., 2014; Sotres et al., 2015; Zhang et al., 2013). And on the other hand, this system can help to produce additional energy and to polish the AD effluent, especially when malfunction of the AD system is produced due to organic overloads or inhibition process, attaining a more stable and robust performance.

The combination of BES and AD has been previously studied, although using Microbial Fuel Cell (MFC) mode and with the objective of polishing the digestate, such as the effluent of a two-stage biogas process at low organic loading (Fradler et al., 2014), digested landfill leachate

(Tugtas et al., 2013) or digested wastewater from potato-processing industries (Durruty et al., 2012). Also the long-term performance of sludge treatment has been examined in an MFC operated for almost 500 days (Ge et al., 2013). Another MFC has been coupled with a hydrogen production fermentor (Sharma and Li, 2010). It has also been described an up-flow anaerobic sludge blanket reactor-microbial fuel cell-biological aerated filter (UASB-MFC-BAF) integrated system for simultaneous bioelectricity generation and molasses wastewater treatment (Zhang et al., 2009). Finally, Chapter 4 has compared the treatment of digested pig slurry under MFC and MEC mode (Cerrillo et al., 2016).

However, a deep assessment of BES performance against an AD destabilisation has not been undertaken, neither its influence in ammonia recovery. Stability can be defined by the concepts of resistance (ability of a system to resist disturbance) and resilience (rate of recovery of a system after a disturbance) (Hashsham et al., 2000). Different studies have found a positive correlation between biodiversity and stability when working with activated sludge (Saikaly and Oerther, 2010). But stability has found to be best correlated not to population diversity *per se* but to functional redundancy (Briones and Raskin, 2003). Methanogens are represented by a low diversity compared to the more diverse fermentative bacteria (Saikaly and Oerther, 2010). In AD reactors, the lack of functional redundancy of the methanogenic group suggests that they may be less functionally stable to toxic shock loading. In BESs, microorganisms develop into a biofilm on electrodes, which confers their good resistance to toxic substances and environmental fluctuations (Borole et al., 2011) and makes the integration of BESs with AD an attractive synergic mode (Zhang et al., 2009).

The main aim of this Chapter is to assess the stability and robustness of continuous MEC operation in combination with AD, and its feasibility as a strategy to recover ammonia. MEC response to punctual and sustained organic overloads when fed in continuous with AD effluent as a result of AD failure was evaluated, regarding resistance and resilience against the perturbation, VFA removal and its capacity to absorb the higher organic load to increase current density production and ammonia removal.

6.2 Materials and methods

6.2.1 Experimental set-up

The MEC reactor was the same two chamber cell used in Chapter 4, and described in Section 3.1.1. The assays were performed after the batch assays carried out in Chapter 4.

Digested pig slurry was used as feeding solution in the anode compartment. The digestate was obtained from a mesophilic AD plant with a hydraulic retention time (HRT) of 40 days (Vila-Sana, Lleida, Spain), previously filtered through a stainless steel sieve to remove

particles larger than 125 μm and diluted with tap water to obtain the desired COD. Table 6.1 shows the main characteristics of the feeding solution. The feeding solution for the cathode chamber contained NaCl 0.1 g L^{-1} (in deionised water). The solutions of both the anode and the cathode compartment were fed in continuous with a pump working at 16.4 mL h^{-1} and mixed by recirculating them with an external pump.

6.2.2 Reactor operation

The MEC was operated in continuous for 110 days with a HRT of 30 h, while poising the anode (working electrode) potential at 0 mV vs SHE. In Phase 1, the MEC was fed for 10 days with the digestate to evaluate its performance under a stable operation of the AD reactor, with an organic loading rate (OLR) of 18.24 g COD L^{-1} d^{-1}. In Phase 2, in order to simulate an overload episode of the AD system and to study VFA degradation dynamics in the MEC, a series of pulses of diverse VFA were performed in the anode compartment in duplicate, increasing the added COD in each series; while in Phase 3 the pulses were of mixed VFA (Table 6.2). Each pulse was performed once the current density had returned to basal levels. Finally, in Phase 4, a daily pulse of mixed VFA (acetate, propionate and butyrate, as specified in Table 6.2) was applied during 5 days to the MEC cell for 2 weeks, simulating a long period of malfunction of the AD reactor. All assays were performed at room temperature (~ 23 ºC). Samples were taken from the anode and the cathode compartment prior to the pulse, and at time 1, 7, 24 and 48 h after the pulse.

Table 6.1 Characterisation of digested pig slurry and the final solution used as feeding in the MEC.

Parameter	Digested Pig Slurry	Digested Pig Slurry MEC influent*
pH (-)	8.4	8.2
COD (mg O_2 kg^{-1})	173 369	23 170
N-NH_4^+ (mg L^{-1})	4 438	2 190
TS (%)	8.39	1.44
VS (%)	6.10	0.90
Acetate (mg L^{-1})	261	110
Alkalinity (g_{CaCO3} L^{-1})	13.8	-
NH_4^+ (mg L^{-1})	3 806	1 827
Na^+ (mg L^{-1})	1 014	694
Mg^{2+} (mg L^{-1})	n.d.	n.d.
Ca^{2+} (mg L^{-1})	3 566	1 199
K^+ (mg L^{-1})	1 374	650
PO_4^{3-} (mg L^{-1})	184	n.d.
SO_4^{2-} (mg L^{-1})	3 463	972

* Digested pig slurry sieved 125 μm and diluted 50%

n.d: not detected

Table 6.2 Operational conditions for the MEC reactor during the series of VFA pulses.

Phase	Day	VFA addition (mg)			Added COD (mg)
		Acetate	Propionate	Butyrate	
1	1-10	0	0	0	-
2	11 and 12	250	0	0	267
	13 and 17	500	0	0	534
	19 and 20	0	500	0	757
	60 and 62	0	0	500	909
3	33 and 38	500	500	0	1291
	40 and 47	1000	200	85	1525
4	66 to 70 73 to 77	1000	200	85	1525

6.2.3 Analyses and calculations

Samples of the feeding solutions and the anode effluent were characterised for chemical oxygen demand (COD), total and volatile solids (TS and VS), alkalinity, volatile fatty acids (VFA), ammonium N-NH_4^+ and pH, besides dissolved methane in the anode effluent. Cathode samples were characterised for ammonium N-NH_4^+ and pH. All the analyses were performed following the methods described in Section 3.2.

In order to know the biodegradability of the remaining organic matter of the digested pig slurry (substrate) used as feed solution to the MEC, anaerobic biodegradability tests (ABT) of the digestate were performed as described in Section 3.2.11.

Current density, coulombic efficiency (CE), COD and ammonium removal efficiencies and ammonium flux were determined as described in Section 3.4.

Resilience was used as a measure of system stability, and was calculated as the time taken for VFA concentration to recover basal levels.

6.3 Results and discussion

6.3.1 Stable feeding with digested pig slurry (Phase 1)

During this phase the MEC was fed with digested pig slurry and showed a stable performance in current density (Figure 6.1), achieving a 100% reduction in VFA (an average 110 mg L^{-1} acetic acid was present in the influent and it was not detected in the effluent). The average COD removal was of 12.21±1.77%, indicating that mainly low biodegradable COD was available in the digestate. The anaerobic biodegradability assay performed in mesophilic conditions with the same digested pig slurry fed to the MEC showed an anaerobic biodegradability of 33% (data not shown). Taking this value as a reference, the MEC was able

to remove 37% of the biodegradable organic matter present in the digested pig slurry, concomitant to an ammonium removal efficiency of 11.81±1.36% (3.73±0.51 g N m^{-2} d^{-1}). The current density produced was of 425±77 mA m^{-2}. The average CE was of 3.52% (10.67% if taking into account only the biodegradable COD), and just 0.97% of the removed COD was converted into methane (the anodic effluent contained 11.40±0.72 mg_{CH4} L^{-1}). These results are in accordance with the values obtained in previous studies. Ge et al. (2013) obtained 36.2±24.4% COD removal and 2.6±1.4% CE with an MFC treating digested sludge, although with a much longer HRT (9 days) and an influent COD of 16.7±11.4 g L^{-1}. In Chapter 4 the MEC fed with digested pig slurry (8 g COD L^{-1} and 872 mg $N\text{-}NH_4^+$ L^{-1}) in discontinuous mode achieved a maximum peak of 700 mA m^{-2} when poising the anode at 0 mV, with a COD removal efficiency of nearly 20% and an ammonium removal efficiency of around 30% in 48 h assays (Cerrillo et al., 2016). Longer HRT and lower COD and ammonium concentration may have favoured these higher removal efficiencies. Higher ammonium removal efficiencies of around 30% (171.4 g N m^{-2} d^{-1}) have been reported in another study using a MEC fed with diluted urine, which may have been achieved thanks to the high current densities obtained of 14.64±1.65 A m^{-2} (Kuntke et al., 2014), which were nearly 35 times higher than the one described in the present study, and a shorter HRT of 2 h.

The pH of the anode compartment effluent was of 7.8±0.1, thus slightly lower than the influent pH (8.2±0.1). The buffering capacity of the anolyte (digested pig slurry; alkalinity 13.8 g_{CaCO3} L^{-1}) avoided a higher decrease in the anode compartment pH, despite acidification due to cation transport to the cathode compartment and proton accumulation in the anode (Rozendal et al., 2008). Regarding cathode effluent pH, it was of 10.1±0.1, a very convenient pH for ammonia recovering, since can drive ammonium to ammonia gas and favour a subsequent stripping and absorption process (Cord-Ruwisch et al., 2011; Kim et al., 2008; Kuntke et al., 2012; Sotres et al., 2015). The increase of pH in the cathode compartment was favoured as no buffer solution was used.

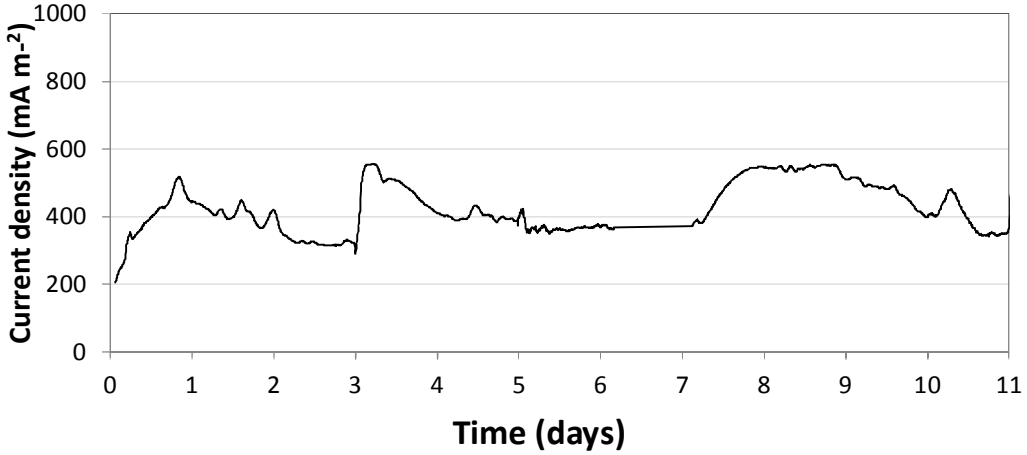

Figure 6.1 Current density during Phase 1, of stable feeding with digested pig slurry.

6.3.2 Punctual VFA pulses (Phase 2)

The response of the MEC after the pulses of acetate was an immediate increase in current density, with a peak of between 1300 and 1700 mA m^{-2} for the 250 mg pulses and between 2100 and 2600 mA m^{-2} for the 500 mg pulses; and a later decrease of it concomitant with acetate removal, achieving the total degradation in 24 h and 48 h for the 250 and 500 mg pulses, respectively (Figure 6.2a). Current density returned to levels of around 500 mA m^{-2}, similar to those obtained in Phase 1, demonstrating a high resilience to perturbation by VFA accumulation. The amount of charge produced, calculated by integrating the area under the current (A) peak, resulted in 0.65±0.03 and 1.62±0.15 mmol of electrons, equivalent to 1.94 and 2.42% of the COD added with the 250 and 500 mg pulses, respectively. Methane production increased slightly during acetate pulses, with a concentration of 12.60±2.34 mg_{CH4} L^{-1} and 14.45±2.53 mg_{CH4} L^{-1} in the anodic effluent for the 250 and 500 mg pulses, respectively although this difference was not statistically significant. A slight increase in ammonium removal was also observed, from a level of 15% before the pulse to around 20% after the pulse, in response to the increase of electron transport through the external circuit. As a result of the increase of current density, the pH of the cathode compartment was also increased during current peaks achieving a pH of 11 during 250 mg pulses and even above 12 during the 500 mg ones. The pH of the anode effluent oscillated between 7 and 8, an optimum range for microbial activity.

The response to propionate pulses was less intense than to the acetate ones: the increase in current density was observed with a slight delay, and the peak achieved 1000 mA m^{-2} (Figure 6.2b). After 24 h a level of 200 mg L^{-1} of propionate remained still in the effluent, and a small amount of acetate was detected (around 100 mg L^{-1}). Although the electrons that could potentially be delivered through propionate degradation were 1.4 fold higher than those available in the 500 mg acetate pulse (each g of acetate will produce 135.5 mmols of electrons in MEC's anode and 1 g of propionate will release 191.6 mmols of electrons), the amount of charge produced resulted in 0.45±0.05 mmols of electrons, equivalent to 0.47% of the COD added with the pulse. This behaviour could be explained because acetate was the sole VFA present in the influent of the MEC and thus the development of propionate oxidising populations, probably different to acetate oxidising populations, has not been favoured. Methane production was not statistically different to that of acetate pulses, with a concentration of 15.42±1.82 mg_{CH4} L^{-1} in the anodic effluent. As the peak current was less intense, the increase of pH in the cathode effluent was also moderate, achieving a maximum pH of 11.5. Ammonium removal was not enhanced during propionate pulses, since it was similar to the removal efficiency obtained in Phase 1.

Finally, the pulses of butyrate showed an increase in current density with a wider peak than the ones obtained with the acetate pulses, and a maximum of nearly 2500 mA m^{-2} (Figure

6.2c). Butyrate concentration in the anode effluent was of about 70 mg L^{-1} within 24 h, and acetate increased to levels between 200-360 mg L^{-1} during the peaks and decreased to basal levels after 24h. The presence of acetate, produced by butyrate degradation, explains the width of the current peak, and suggests the existence in the anode of a microbial population more efficient in the oxidation of butyrate and acetate than of propionate. The potential amount of charge that could be produced from the butyrate pulse was 1.7 fold higher than in the 500 mg acetate pulse, although the area under the peak corresponded with 1.95±0.01 mmol of electrons, only 1.2 fold higher, and 1.72% of the electrons provided by the pulse. Methane concentration in the anodic effluent 7 h after the pulse achieved levels of 20 mg_{CH4} L^{-1}. Furthermore, in response to a higher level of current production, cathode pH remained near 12 during both butyrate pulses. Anode pH, as in the preceding pulses, was maintained between 7 and 8. Ammonium removal efficiency was enhanced during the second butyrate pulse, concomitant to the current density increase, achieving nearly 28%.

From those results it can be said that the MEC has shown a high resilience against VFA increase in the influent, since the high levels of VFA have been removed, within the concentrations tested, and the effluent concentration returned to the initial level in about 48 h. Furthermore, each of the three VFA assayed had positive effect on power density. However, as shown here and consistent with previous results, acetate was the preferred substrate for electricity generation in MFC/MEC, and microbial community was less efficient in converting propionate to energy, as other studies have shown (Choi et al., 2011; Yang et al., 2015). Acetate can be directly consumed for electricity generation; however, long-chained VFAs must first be converted into acetate. In a previous study, MFC in fed batch mode with synthetic medium with the same VFA as assayed here showed that CE and power output varied with the different substrates. The acetate-fed-MFC showed the highest CE (72.3%), followed by butyrate (43.0%) and propionate (36.0%) (Chae et al., 2009). In a batch single-chambered MFC, power generated when feeding with acetate was up to 66% higher than that obtained when feeding with butyrate (Liu et al., 2005). A better performance in a MFC fed with acetate was obtained respect the ones fed with propionate or butyrate. For the same organic loading rate, the current generated with propionate or butyrate was half the produced with acetate (Freguia et al., 2010).

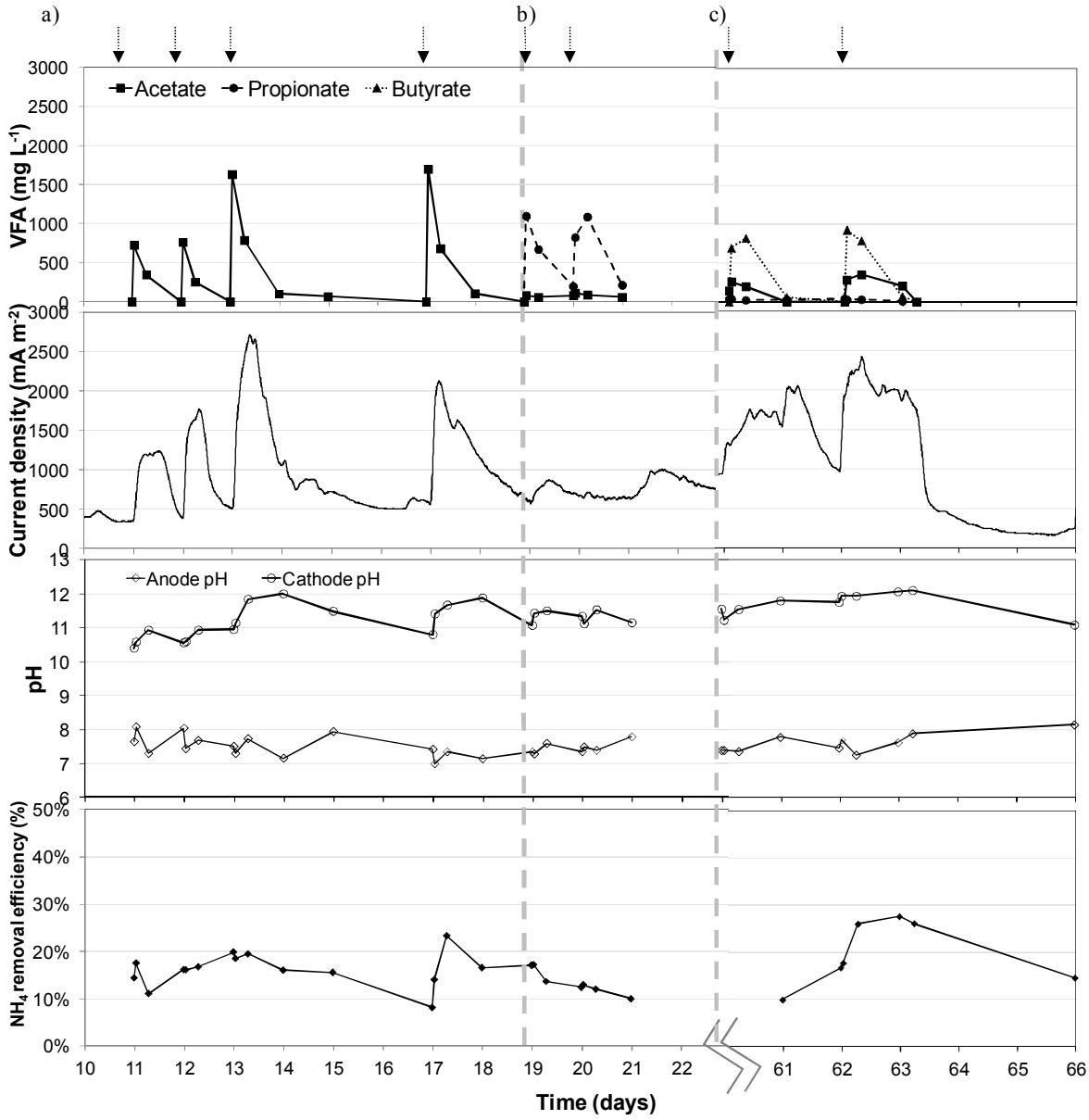

Figure 6.2 Current density, VFA concentration, ammonium removal and anode and cathode pH obtained in Phase 2 during the VFA pulses of (a) 250 and 500 mg of acetate, (b) 500 mg of propionate and (c) 500 mg of butyrate. Arrows show when each pulse was performed.

6.3.3 Punctual mixed VFA pulses (Phase 3)

Current density profiles of the pulses of mixed VFA are shown in Figure 6.3. When a pulse of acetate and propionate was applied (500 mg each one), the maximum current density achieved was between 2000 and 3000 mA m^{-2}, quite similar to that obtained when only acetate was applied, although the base of the peak was wider. The two VFA were removed at a similar rate, being undetectable 48 h after the pulse, when the current density decreased to values

below 500 mA m^{-1}. The amount of charge produced did not correspond to the addition of the charge produced during the pure VFA pulses in Phase 2, but was a value very similar to that obtained with the pulse of only acetate (1.70±0.21 mmol of electrons, 1.05% of the potential charge added with the pulse). Methane concentration in the anodic effluent was of 7.91±2.58 mg_{CH_4} L^{-1}, significantly lower to that obtained with pure 500 mg acetate pulses, although the recovery of electrons had been lower. The pH of the cathode effluent increased again up to 12, while pH of the anode effluent decreased but was always above 7. Ammonium removal followed the current density profile, being 30% the maximum removal efficiency.

Regarding the mixed VFA pulses of acetate, propionate and butyrate, Figure 6.3b shows that the current density peaks were between 3000 and 3500 mA m^{-2}, and that the bases of the peaks were the wider ones among all the pure and mixed VFA pulses performed. Current density decreased sharply when VFA were totally removed, between 48 and 55 h after the pulse, and returned to levels below 500 mA m^{-2}, similar to those obtained in Phase 1. The amount of charge produced was of 2.65±0.19 mmol of electrons, a 1.39% of the potential charge added with the pulses. As in the previous mixed VFA pulses, methane concentration in the anodic effluent (10.04±3.02 mg_{CH_4} L^{-1}) was not statistically different to that obtained with pure VFA. Showing again a very similar behaviour to the mixed VFA pulses of acetate and propionate, the pH of the cathode and the anode increased to 12 and decreased to nearly 7, respectively. Ammonium removal efficiency increased to levels up to 35%.

These results show that when mixed VFA pulses are applied, again a high resilience is shown by the MEC, since VFA and current density levels return to the initial ones in about 48 h. It has also been observed that the efficiency of the MEC in the electricity conversion is lower than when pure VFA are applied. This is in agreement with the results reported in previous studies. When food wastes were used as feedstock in an MFC, it was found that the co-existence of various VFA slowed the removal of each VFA, which indicated that anodic microbes were competing for the different substrates. Furthermore, the degradation rate of butyrate increased when short VFAs were absent in the anode chamber, indicating that these readily degradable short compounds inhibited microbial activity on large VFAs (Choi et al., 2011). Teng et al. (2010) found that although both acetate and propionate contributed positively to the power density, they had antagonistic effects when they were mixed together. Similar antagonistic effects were also obtained in that study for acetate–butyrate and propionate–butyrate, and the increase or decrease of the power density depended on the relative proportion of each VFA in the mixture.

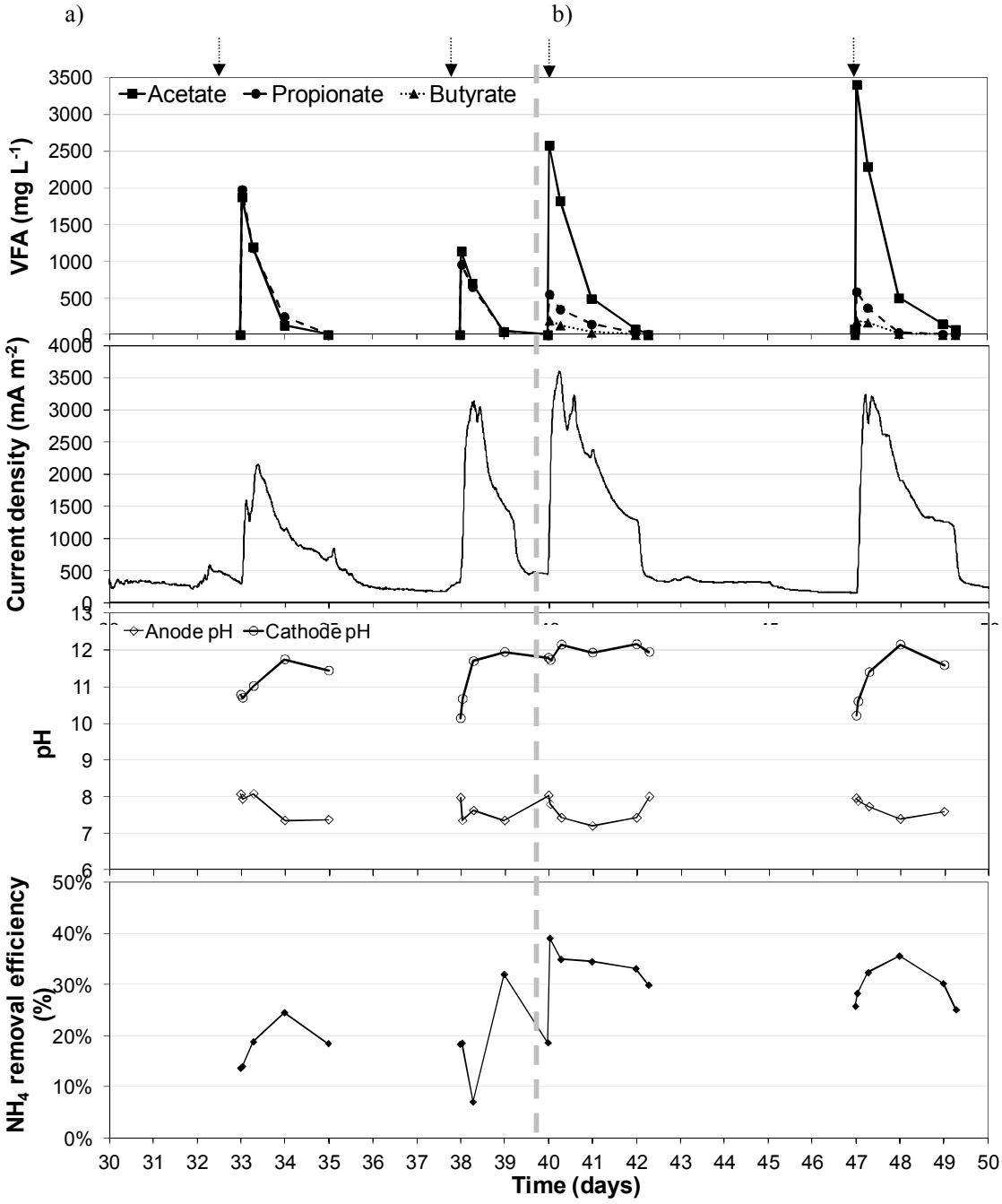

Figure 6.3 Current density, VFA concentration, ammonium removal and anode and cathode pH obtained in Phase 3 during the mixed VFA pulses of (a) 500 mg of acetate and 500 mg of propionate and (b) 1000 mg of acetate, 200 mg of propionate and 85 mg of butyrate. Arrows show when each pulse was performed.

6.3.4 Continuous daily base mixed VFA pulses (Phase 4)

During the mixed VFA daily base pulses performed in the MEC, power density was maintained on average between 1500 and 3000 mA m^{-2} (Figure 6.4). Acetate from previous pulse had not been consumed when a new pulse was added (remaining around 1000 mg L^{-1}).

But after 3 days, before starting the second series of pulses, all VFA had been removed. During the second series, the peaks of acetate were lower than in the first series.

Therefore, the MEC was able to maintain a stable production of current and reduce acetate concentration, avoiding VFA accumulation. Furthermore, methane production was maintained in the lowest levels among the different punctual pulses performed, with an average concentration in the anodic effluent of 5.09±1.45 mg_{CH4} L^{-1}. During the daily pulses, the cathode pH increased and was maintained between 12-12.5, while anode pH was stable around 7-8. A slight oscillation in the later pulses performed was shown, decreasing down to 6.5 but recovering to values higher than 7 few hours after the pulse. Furthermore, ammonium removal increased during the series of pulses to a level of 40%, achieving in the second series values up to around 60%. These values are higher than those obtained in previous studies which achieved an ammonium removal efficiency of 30%, but with 10 times higher current densities (Kuntke et al., 2014).

Sharma et al. (2014) proposed some general guidelines to meet robustness with electroactive biofilms. One of them was that electroactive biofilm should exhibit preservation of the predominant electrochemical mechanisms and metabolic constructs by which a targeted outcome was achieved (e.g. generation of electric current, a set of organic chemicals, recalcitrant COD removal, denitrification, metal reduction, etc.) after scenarios of metabolic disturbances common to BES (e.g. fluctuations in potential, pH, temperature, conductivity, substrate concentration and composition, power supply instabilities/interruptions, flow rate, dissolved oxygen). The MEC evaluated in this study has proven to be a robust system, showing a high resistance to organic overloads and also a high resilience, since after both punctual and daily VFA pulses the system has been able to recover its performance in less than 48 h after the stress.

A previous study focused in evaluating an AD-MFC hybrid system stability using a high acetic load as disturbance, reported that the hybrid system did not have increasing resilience compared to the solitary systems. However, since the low pH had a relatively delayed effect on the MFC compared to the AD, the energy output indeed was more stable in the hybrid system (Weld and Singh, 2011). By contrast, the objective of this Chapter has been to assess the stability of an AD-MEC system during a range of less severe stresses, showing that using a MEC as a post-treatment of AD can improve the quality of the effluent during AD malfunction, both at high levels of VFA and ammonia, while recovering energy.

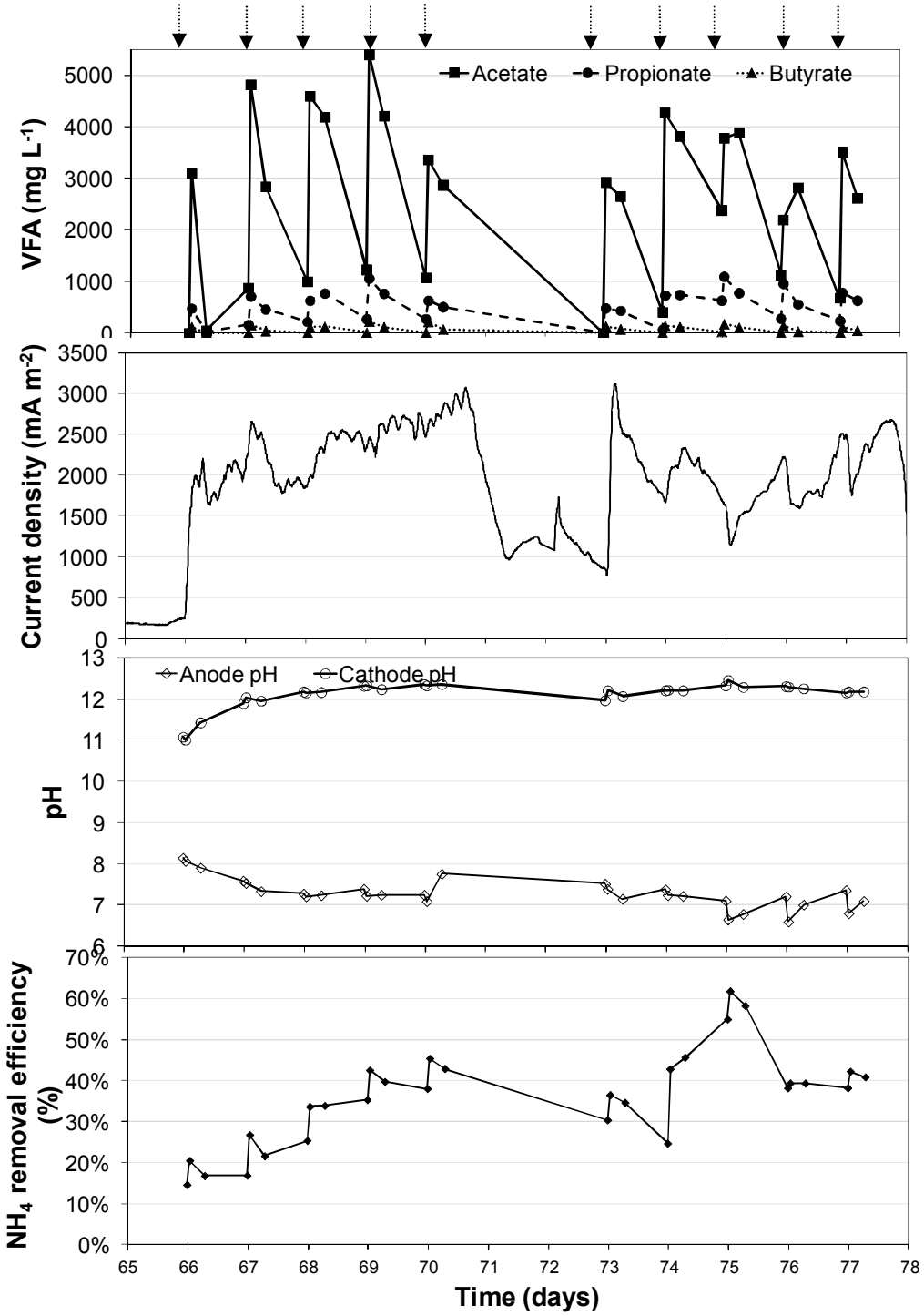

Figure 6.4 Current density, VFA concentration, ammonium removal and anode and cathode pH obtained in Phase 4, during daily pulses of 1000 mg of acetate, 200 mg of propionate and 85 mg of butyrate. Arrows show when each pulse was performed.

6.4 Conclusions

The MEC has been able to remove high levels of VFA from AD effluents and has shown to be a useful technology to correct possible malfunction of AD reactors. The MEC fed with digested pig slurry achieved 12.21±1.77% of COD removal. During punctual pulses of VFA, simulating a malfunction of the AD process, the MEC showed as a resistant and resilient system, and an increase in the current density (up to 14 times, reaching values of 3500 mA m^{-2}) was produced as a result of the added COD, especially when acetate was used. Furthermore, ammonium diffusion from anode to cathode compartment was enhanced and the removal efficiency achieved up to 60% during daily basis pulses, since electron transport is directly related to cation transport through the CEM membrane. An AD-MEC combined system has proven to be a robust and stable configuration to recover energy and obtain a high quality effluent, with a lower organic and ammonium content.

6.5 References

Angenent, L.T., Karim, K., Al-Dahhan, M.H., Wrenn, B.A., Domíguez-Espinosa, R. 2004. Production of bioenergy and biochemicals from industrial and agricultural wastewater. *Trends in Biotechnology*, **22**(9), 477-485.

Bonmatí, A., Campos, E., Flotats, X. 2003. Concentration of pig slurry by evaporation: anaerobic digestion as the key process. *Water Science and Technology*, **48**(4), 189-94.

Bonmatí, A., Flotats, X. 2003. Pig slurry concentration by vacuum evaporation: influence of previous mesophilic anaerobic digestion process. *Journal of the Air & Waste Management Association*, **53**(1), 21-31.

Borole, A.P., Reguera, G., Ringeisen, B., Wang, Z.-W., Feng, Y., Kim, B.H. 2011. Electroactive biofilms: Current status and future research needs. *Energy & Environmental Science*, **4**(12), 4813-4834.

Briones, A., Raskin, L. 2003. Diversity and dynamics of microbial communities in engineered environments and their implications for process stability. *Current Opinion in Biotechnology*, **14**(3), 270-276.

Cerrillo, M., Oliveras, J., Viñas, M., Bonmatí, A. 2016. Comparative assessment of raw and digested pig slurry treatment in bioelectrochemical systems. *Bioelectrochemistry*, **110**, 69-78.

Cerrillo, M., Palatsi, J., Comas, J., Vicens, J., Bonmatí, A. 2015. Struvite precipitation as a technology to be integrated in a manure anaerobic digestion treatment plant – Removal efficiency, crystal characterisation and agricultural assessment. *Journal of Chemical Technology & Biotechnology*, **90**, 1135-1143.

Chae, K.-J., Choi, M.-J., Lee, J.-W., Kim, K.-Y., Kim, I.S. 2009. Effect of different substrates on the performance, bacterial diversity, and bacterial viability in microbial fuel cells. *Bioresource Technology*, **100**(14), 3518-3525.

Chen, Y., Cheng, J.J., Creamer, K.S. 2008. Inhibition of anaerobic digestion process: A review. *Bioresource Technology*, **99**(10), 4044-4064.

Choi, J.-d.-r., Chang, H., Han, J.-I. 2011. Performance of microbial fuel cell with volatile fatty acids from food wastes. *Biotechnology Letters*, **33**(4), 705-714.

Cord-Ruwisch, R., Law, Y., Cheng, K.Y. 2011. Ammonium as a sustainable proton shuttle in bioelectrochemical systems. *Bioresource Technology*, **102**(20), 9691-9696.

Durruty, I., Bonanni, P.S., González, J.F., Busalmen, J.P. 2012. Evaluation of potato-processing wastewater treatment in a microbial fuel cell. *Bioresource Technology*, **105**(0), 81-87.

Fradler, K.R., Kim, J.R., Shipley, G., Massanet-Nicolau, J., Dinsdale, R.M., Guwy, A.J., Premier, G.C. 2014. Operation of a bioelectrochemical system as a polishing stage for the effluent from a two-stage biohydrogen and biomethane production process. *Biochemical Engineering Journal*, **85**(0), 125-131.

Freguia, S., Teh, E.H., Boon, N., Leung, K.M., Keller, J., Rabaey, K. 2010. Microbial fuel cells operating on mixed fatty acids. *Bioresource Technology*, **101**(4), 1233-1238.

Ge, Z., Zhang, F., Grimaud, J., Hurst, J., He, Z. 2013. Long-term investigation of microbial fuel cells treating primary sludge or digested sludge. *Bioresource Technology*, **136**(0), 509-514.

Hashsham, S.A., Fernandez, A.S., Dollhopf, S.L., Dazzo, F.B., Hickey, R.F., Tiedje, J.M., Criddle, C.S. 2000. Parallel Processing of Substrate Correlates with Greater Functional Stability in Methanogenic Bioreactor Communities Perturbed by Glucose. *Applied and Environmental Microbiology*, **66**(9), 4050-4057.

Kim, J.R., Zuo, Y., Regan, J.M., Logan, B.E. 2008. Analysis of ammonia loss mechanisms in microbial fuel cells treating animal wastewater. *Biotechnology and Bioengineering*, **99**(5), 1120-1127.

Kuntke, P., Sleutels, T.H.J.A., Saakes, M., Buisman, C.J.N. 2014. Hydrogen production and ammonium recovery from urine by a Microbial Electrolysis Cell. *International Journal of Hydrogen Energy*, **39**(10), 4771-4778.

Kuntke, P., Smiech, K.M., Bruning, H., Zeeman, G., Saakes, M., Sleutels, T.H.J.A., Hamelers, H.V.M., Buisman, C.J.N. 2012. Ammonium recovery and energy production from urine by a microbial fuel cell. *Water Research*, **46**(8), 2627-2636.

Laureni, M., Palatsi, J., Llovera, M., Bonmatí, A. 2013. Influence of pig slurry characteristics on ammonia stripping efficiencies and quality of the recovered ammonium-sulfate solution. *Journal of Chemical Technology & Biotechnology*, **88**(9), 1654-1662.

Liu, H., Cheng, S., Logan, B.E. 2005. Production of Electricity from Acetate or Butyrate Using a Single-Chamber Microbial Fuel Cell. *Environmental Science & Technology*, **39**(2), 658-662.

Palatsi, J., Laureni, M., Andres, M.V., Flotats, X., Nielsen, H.B., Angelidaki, I. 2009. Strategies for recovering inhibition caused by long chain fatty acids on anaerobic thermophilic biogas reactors. *Bioresource Technology*, **100**(20), 4588-96.

Rozendal, R.A., Sleutels, T.H., Hamelers, H.V., Buisman, C.J. 2008. Effect of the type of ion exchange membrane on performance, ion transport, and pH in biocatalyzed electrolysis of wastewater. *Water Science and Technology*, **57**(11), 1757-62.

Saikaly, P., Oerther, D. 2010. Diversity of Dominant Bacterial Taxa in Activated Sludge Promotes Functional Resistance following Toxic Shock Loading. *Microbial Ecology*, **61**(3), 557-567.

Sharma, M., Bajracharya, S., Gildemyn, S., Patil, S.A., Alvarez-Gallego, Y., Pant, D., Rabaey, K., Dominguez-Benetton, X. 2014. A critical revisit of the key parameters used to describe microbial electrochemical systems. *Electrochimica Acta*, **140**(0), 191-208.

Sharma, Y., Li, B. 2010. Optimizing energy harvest in wastewater treatment by combining anaerobic hydrogen producing biofermentor (HPB) and microbial fuel cell (MFC). *International Journal of Hydrogen Energy*, **35**(8), 3789-3797.

Sotres, A., Cerrillo, M., Viñas, M., Bonmatí, A. 2015. Nitrogen recovery from pig slurry in two chamber bioelectrochemical system. *Bioresource Technology*, **194**, 373-382.

Teng, S.-X., Tong, Z.-H., Li, W.-W., Wang, S.-G., Sheng, G.-P., Shi, X.-Y., Liu, X.-W., Yu, H.-Q. 2010. Electricity generation from mixed volatile fatty acids using microbial fuel cells. *Applied Microbiology and Biotechnology*, **87**(6), 2365-2372.

Tugtas, A.E., Cavdar, P., Calli, B. 2013. Bio-electrochemical post-treatment of anaerobically treated landfill leachate. *Bioresource Technology*, **128**(0), 266-272.

Weld, R.J., Singh, R. 2011. Functional stability of a hybrid anaerobic digester/microbial fuel cell system treating municipal wastewater. *Bioresource Technology*, **102**(2), 842-847.

Yang, N., Hafez, H., Nakhla, G. 2015. Impact of volatile fatty acids on microbial electrolysis cell performance. *Bioresource Technology*, **193**, 449-455.

Yenigün, O., Demirel, B. 2013. Ammonia inhibition in anaerobic digestion: A review. *Process Biochemistry*, **48**(5-6), 901-911.

Zhang, B., Zhao, H., Zhou, S., Shi, C., Wang, C., Ni, J. 2009. A novel UASB-MFC-BAF integrated system for high strength molasses wastewater treatment and bioelectricity generation. *Bioresource Technology*, **100**(23), 5687-5693.

Zhang, X., Zhu, F., Chen, L., Zhao, Q., Tao, G. 2013. Removal of ammonia nitrogen from wastewater using an aerobic cathode microbial fuel cell. *Bioresource Technology*, **146**(0), 161-168.

CHAPTER 7

Overcoming organic and nitrogen overload in thermophilic anaerobic digestion of pig slurry by coupling a microbial electrolysis cell

Part of the content of this chapter was published as:

Cerrillo, M., Viñas, M., Bonmatí, A. 2016. Overcoming organic and nitrogen overload in thermophilic anaerobic digestion of pig slurry by coupling a microbial electrolysis cell. *Bioresource Technology*, **216**, 362-372. doi:10.1016/j.biortech.2016.05.085

Abstract

The combination of the anaerobic digestion (AD) process with a microbial electrolysis cell (MEC) coupled to an ammonia stripping unit as a post-treatment was assessed both in series operation, to improve the quality of the effluent, and in loop configuration recirculating the effluent, to increase the AD robustness. The MEC allowed maintaining the chemical oxygen demand removal of the whole system of 46±5% despite the AD destabilisation after doubling the organic and nitrogen loads, while recovering 40±3% of ammonia. The AD-MEC system, in loop configuration, helped to recover the AD (55% increase in methane productivity) and attained a more stable and robust operation. The microbial population assessment revealed an enhancement of AD methanogenic archaea numbers and a shift in eubacterial population. The AD-MEC combined system is a promising strategy for stabilising AD against organic and nitrogen overloads, while improving the quality of the effluent and recovering nutrients for their reutilisation.

7.1 Introduction

Anaerobic digestion (AD) of livestock manure and other wastes results in organic matter stabilisation and biogas production, a biofuel containing mainly methane and carbon dioxide that can be used in power generation systems to obtain heat and electricity. This energy recovering technology is nowadays widely used to treat various kinds of wastes (Angenent et al., 2004). AD process is complex, since it involves many different groups of microorganisms, especially methanogens, that are particularly sensitive to organic overloads and diverse substances that may be present in the waste stream such as ammonia (Angelidaki and Ahring, 1993; Yenigün and Demirel, 2013). AD can mainly take place at two different ranges of temperatures, either mesophilic (25-40 ºC) or thermophilic (45-60 ºC). The later one is more favourable to obtain a high digestion rate, since high loading rates or short retention times can be applied, due to higher growth rates of bacteria at higher temperatures. Moreover, improved solids settling and destruction of microbial pathogens is attained (Angelidaki and Ahring, 1994). On the other hand, thermophilic AD has lower process stability than mesophilic AD, it being more sensitive to high ammonia concentrations since free ammonia (NH_3), the active component causing ammonia inhibition, increases with an increase in pH and temperature (Angelidaki and Ahring, 1994). Reactor upset will be indicated by a reduction in biogas production and/or biogas methane content, and the accumulation of volatile fatty acids (VFA) that may lead to reactor failure (Chen et al., 2008). At a microbiology level, and due to the complex interdependence of microbial activities for the adequate functionality of anaerobic bioreactors, the genetic expression of *mcr*A, which encodes the α subunit of methyl coenzyme M reductase –the enzyme that catalyses the final step in methanogenesis–, has been proposed as a parameter to monitor the process performance (Alvarado et al., 2014; Morris et al., 2013).

Besides monitoring the AD process by means of CH_4 production, it is interesting to explore new technologies that can help AD to maintain effluent quality within the desired limits despite AD failure. So far, different strategies for stabilising AD reactors under high organic loading rates and for controlling ammonia toxicity have been evaluated, ranging from the more classical approaches, such as co-digestion with carbon-rich substrates to equilibrate the carbon to nitrogen ratio (Chiu et al., 2013), introduction of adaptation periods (Borja et al., 1996), reduction of ammonia content of the substrates by air stripping (Bonmatí and Flotats, 2003; Laureni et al., 2013), or dilution of the substrates (Hejnfelt and Angelidaki, 2009); to more innovative ones, such as the use of an electrochemical system aimed at NH_4^+ extraction coupled to an upflow anaerobic sludge blanket (UASB) in the recirculation loop to help control ammonia toxicity with high nitrogen loading conditions (Desloover et al., 2014).

An alternative to these techniques is the use of bioelectrochemical systems (BES) in combination with an AD process. BESs are bioreactors that use microorganisms attached to

one or both electrode(s) in order to catalyse oxidation and/or reduction reactions. These systems are also useful for recovering nutrients, such as ammonium (Sotres et al., 2015a). BESs have proven to be useful as post-treatment for anaerobic digesters in order to reduce organic matter content and recover ammonium (Chapter 4; Cerrillo et al., 2016). Different AD-BES configurations have been previously studied, mainly aimed to improve biogas production in the AD (Tartakovsky et al., 2011; Zhang and Angelidaki, 2015). But more research in terms of combined system behaviour against factors that may destabilise the AD process is needed, as well as a more global approach of the AD-BES system integrating stabilisation of the process, microbial community stability, improvement of the quality of the effluent, and nutrient recovery.

Since the effluent of a BES is expected to have a lower content of organic matter and ammonium, a combined AD-BES system with a recirculation loop between both components may offer some advantages in order to increase the stability of the system, mainly improving its resistance against organic and nitrogen overloads. The combination of BES with AD, as a system to reduce ammonia inhibition, has been previously demonstrated using a submersible microbial desalination cell fed with synthetic wastewater, although in that case the BES was not exploited to reduce organic matter content (Zhang and Angelidaki, 2015). On the other hand, although combined AD-BES systems have been tested against strong perturbations (Weld and Singh, 2011), the effect of stress on microbial synergies (eubacterial and archaeal communities) is scarcely known, especially on methanogenic archaea and their evolution when operating in a coupled system under inhibited and recovered stages.

The main aim of this Chapter is to assess the combination of the AD process with a microbial electrolysis cell (MEC) both in series operation, as a system to improve the effluent quality, and in loop configuration to recirculate the effluent, as a technique to increase the stability and robustness of the AD process, while recovering ammonia with a stripping and absorption unit. Furthermore, microbial community dynamics have been assessed in both reactors to understand the reactor set-up effects, as well as microbial resilience at different operational conditions, even under an inhibited AD operation.

7.2 Materials and methods

7.2.1 Experimental set-up

A lab-scale continuous stirred tank reactor (CSTR) described in Section 3.1.3 was used to study its performance when treating pig slurry at a thermophilic temperature range. The two chamber cell MEC reactor described in Section 3.1.1, which had been previously operated in the assays performed in Chapters 4 and 6, was used, poising the anode (working electrode) potential at 0 mV vs SHE. A stripping and absorption system, described in Section 3.1.4, was

used to recover the ammonium transferred from the anode to the cathode compartment. Figure 7.1 shows the scheme of the complete AD-MEC-Stripping/Absorption combined system.

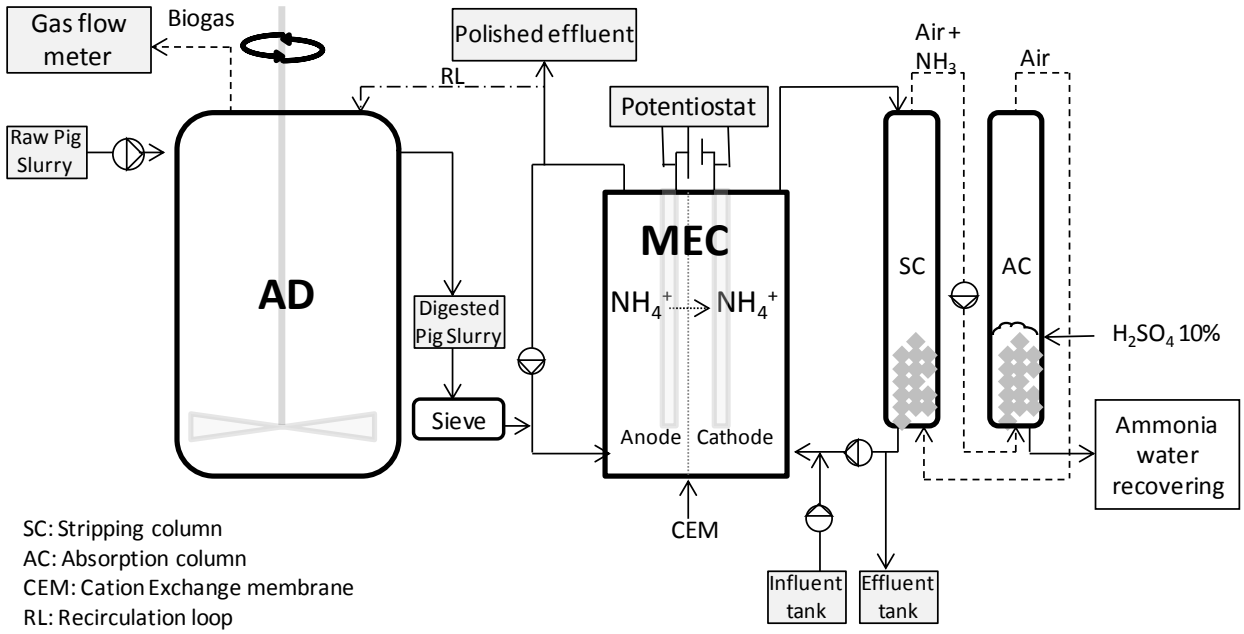

Figure 7.1 Scheme of the set up of the AD-MEC combined system coupled to the stripping and absorption unit.

7.2.2 Reactors operation

The AD was fed in a continuous mode with raw pig slurry from a farm in Vila-Sana (Lleida, Spain) with a hydraulic retention time (HRT) of 10 days. The pig slurry was diluted with tap water to obtain the desired organic load; the characteristics of the influent used can be seen in Table 7.1. The reactor was operated during 336 days in 5 different phases (Table 7.2). In Phase 1, the organic loading rate (OLR) was of 3.02±0.60 kg_{COD} m^{-3} day^{-1} and the nitrogen loading rate (NLR) was of 0.17±0.03 kg_N m^{-3} day^{-1}. In Phase 2, the previous OLR and NLR were doubled (6.25±1.05 kg_{COD} m^{-3} day^{-1}; 0.34±0.06 kg_N m^{-3} day^{-1}) to evaluate the stability of the reactor with an organic overload, and the AD effluent was used to feed the MEC from day 160, after 4 HRT, as a polishing step and a system to recover ammonia. In Phases 3, 4 and 5 a recirculation loop between the AD and the MEC was introduced, with 25%, 50% and 75% of feed flow rate recirculation, respectively, so as to study the effectiveness of this recirculation as an AD stabilisation strategy. As an effect of the recirculation, the real HRT in the AD decreased from 10 days to 8, 6.7 and 5 days (recirculation flow rates of 25, 50 and 75% of the fed flow rate, respectively). Each phase was maintained at least for 4 HRT to ensure a stable operation. Samples of the AD effluent were taken once a week.

Table 7.1 Characterisation of the diluted pig slurry used as feeding solution in the anaerobic digester (AD) in Phase 1 and Phases 2 to 5 (n=number of samples).

Parameter	Diluted pig slurry	
	Phase 1 (n=7)	Phase 2 to 5 (n=16)
pH (-)	7.49±0.36	6.98±0.21
COD (g_{O2} kg^{-1})	31.34±3.77	63.36±6.30
NTK (g L^{-1})	1.76±0.03	3.69±0.26
N-NH_4^+ (g L^{-1})	1.23±0.11	2.64±0.25
TS (g kg^{-1})	17.58±0.73	34.70±2.65
VS (g kg^{-1})	12.35±0.69	23.87±1.88

With regards to the MEC, the digested pig slurry obtained from the AD was later used as feed for the anode compartment, previously filtering it in batches through a 125 µm stainless steel sieve. Filtering removed an average of 5% of the AD influent COD, and this amount was included in the calculations of COD removal efficiency. Table 7.2 shows the average OLR and NLR for each Phase. The feeding solution for the cathode chamber contained (in deionised water) NaCl 0.1 g L^{-1}. The solutions of both the anode and the cathode compartment were fed in continuous mode at 14 mL h^{-1} and mixed recirculating them with an external pump. The stripping and absorption system was operated in Phases 2 and 3 to prove the feasibility of the full combined system. The MEC was operated at room temperature during the entire assay (~ 23 ºC). Samples were taken 3 times a week.

Table 7.2 Operational conditions for the AD reactor and the MEC.

Phase	Period (d)	AD			MEC	
		OLR (kg_{COD} m^{-3} d^{-1})	NLR (kg_N m^{-3} d^{-1})	Recirculation (% feed flow rate)	OLR (kg_{COD} m^{-3} d^{-1})	NLR (kg_N m^{-3} d^{-1})
1	1-110	3.02±0.60	0.17±0.03	0	-	-
2	110-200	6.25±1.05	0.34±0.06	0	27.80±1.40	1.76±0.02
3	200-240			25	28.50±1.80	1.73±0.09
4	240-299			50	26.10±2.90	1.68±0.09
5	299-236			75	27.00±2.20	1.94±0.03

7.2.3 Analyses and calculations

For each experimental condition of the AD, specific methane productivity rate (m^3_{CH4} m^{-3} d^{-1}) and chemical oxygen demand (COD) were determined, as well as biogas composition, alkalinity, N-NH_4^+ and VFA concentrations in the effluent. pH and N-NH_4^+ were analysed in the anode and cathode effluents of the MEC and the acidic solution of the absorption column,

besides COD and VFA of the anode effluent. All the analyses were performed following the methods described in Section 3.2.

Current density, free ammonia concentration, IA:TA ratio, COD and ammonium removal efficiencies and ammonium flux were determined as described in Section 3.4.

To better understand the results obtained, the bacterial communities present in the AD at the end of each Phase from 1 to 5, and the ones attached to the anode of the MEC at the beginning and at the end of the experiments, were analysed by culture-independent molecular techniques, such as quantitative real-time polymerase chain reaction (qPCR) and high throughput DNA sequencing (MiSeq, Illumina). Total DNA extraction, qPCR and high throughput *16S rRNA* gene sequencing (MiSeq, Illumina) were performed following the methods described in Section 3.6.1, 3.6.3, and 3.6.5, respectively. The standard curve parameters of the qPCRs performed had a high efficiency, and were as follows (for *16S rRNA* and *mcrA*, respectively): a slope of -3.407 and -3.591; a correlation coefficient of 0.999 and 0.998; and an efficiency of 97 and 90%. Data obtained from sequencing datasets were deposited in the Sequence Read Archive of the National Centre for Biotechnology Information (NCBI) under study accession number SRP063053, for eubacterial and archaeal populations.

The evaluation of the diversity of the samples and statistical multivariate analyses were performed following Section 3.6.6.

7.3 Results and discussion

7.3.1 Performance of the AD independent operation

After the start-up of the AD, in Phase 1 the COD removal efficiency increased from values in the range of 10-20% up to values in the range of 55-63% (Figure 7.2a), with COD effluent values in the range of 14.25–16.48 g kg^{-1}. When the OLR was doubled in Phase 2, the COD removal efficiency decreased down to values in the range of 20-28%, increasing the COD of the effluent up to 43.58 – 51.65 g kg^{-1}. During Phase 1, maximum methane productivity was of 0.33 m^3 m^{-3} d^{-1}, increasing to 0.56 m^3 m^{-3} d^{-1} at the beginning of Phase 2 as a response to the increase in OLR (Figure 7.2b). Nevertheless, methane productivity dropped down in the following weeks and was of only 0.12 m^3 m^{-3} d^{-1} after 80 days of operation under these new conditions, representing a 63% decrease with respect to the previous phase, as a result of a severe inhibition due to the increase of OLR and NLR. This inhibition process can also be observed with the IA:TA ratio (Figure 7.2c) found to be in the range of 0.21-0.26 at the end of Phase 1 –well below the 0.30 limit for a stable operation– but increased up to 0.52 after the stress produced by the increase of the OLR and NLR. These results are in accordance with the VFA content (Figure 7.2d), as there was an increase in values, starting under 1000 mg_{COD} L^{-1}

(585 mg_{acetic} L^{-1} and 175 $mg_{propionic}$ L^{-1}) at the end of Phase 1, and going up to a maximum of 17000 mg_{COD} L^{-1} in Phase 2, reaching values of 4808 mg_{acetic} L^{-1}, 1384 $mg_{propionic}$ L^{-1}, 794 $mg_{iso\text{-}butyric}$ L^{-1}, 1634 $mg_{n\text{-}butyric}$ L^{-1}, 838 $mg_{iso\text{-}valeric}$ L^{-1}, 686 $mg_{n\text{-}valeric}$ L^{-1} 137 $mg_{iso\text{-}caproic}$ L^{-1} and 924 $mg_{n\text{-}caproic}$ L^{-1}. This accumulation of VFA is a clear indication that the methanogenic population is inhibited, as well as of AD failure. Average values in each Phase (stable period) for COD removal efficiency, methane productivity, biogas composition, pH, alkalinity and IA:TA ratio are shown in Table 7.3.

Table 7.3 Summary of the parameters for the AD and the MEC reactors in the different phases (n=number of samples). Results for the AD correspond to the stable period of each phase. n.a.; data not available as the stripping and absorption system was disconnected.

Parameter	Phase 1	Phase 2	Phase 3	Phase 4	Phase 5
AD					
n	9	5	4	5	6
CH_4 productivity (m^3_{CH4} m^{-3} d^{-1})	0.27±0.05	0.06±0.06	0.26±0.08	0.42±0.05	0.38±0.06
CH_4 (%)	74±1	67±1	66±1	67±2	66±1
Total alkalinity ($gCaCO_3$ L^{-1})	5.23±0.41	8.42±0.31	8.63±0.19	8.66±0.43	8.92±0.34
Partial alkalinity ($gCaCO_3$ L^{-1})	3.90±0.38	4.52±0.45	4.45±0.26	5.01±0.34	5.23±0.33
IA:TA	0.26±0.03	0.50±0.04	0.49±0.03	0.41±0.03	0.42±0.02
pH (-)	7.73±0.10	7.69±0.04	7.66±0.08	7.83±0.14	7.74±0.07
COD removal efficiency (%)	47±13	30±8	31±6	35±4	42±3
MEC					
n		14	11	14	10
COD removal efficiency (%)		25±8	28±7	30±11	20±7
$N\text{-}NH_4^+$ removal efficiency (%)		40±3	31±5	22±5	17±5
$N\text{-}NH_4^+$ absorbed (%)		30±6	13±3	n.a.	n.a
Current density (A m^{-2})		2.01±0.63	1.59±0.70	0.96±0.43	0.85±0.28
Anode pH (-)		7.03±0.07	7.47±0.19	7.64±0.25	7.56±0.07
Cathode pH (-)		11.83±0.60	12.02±0.25	11.67±0.27	11.66±0.17
AD-MEC					
COD removal efficiency (%)		46±5	51±7	59±7	56±7

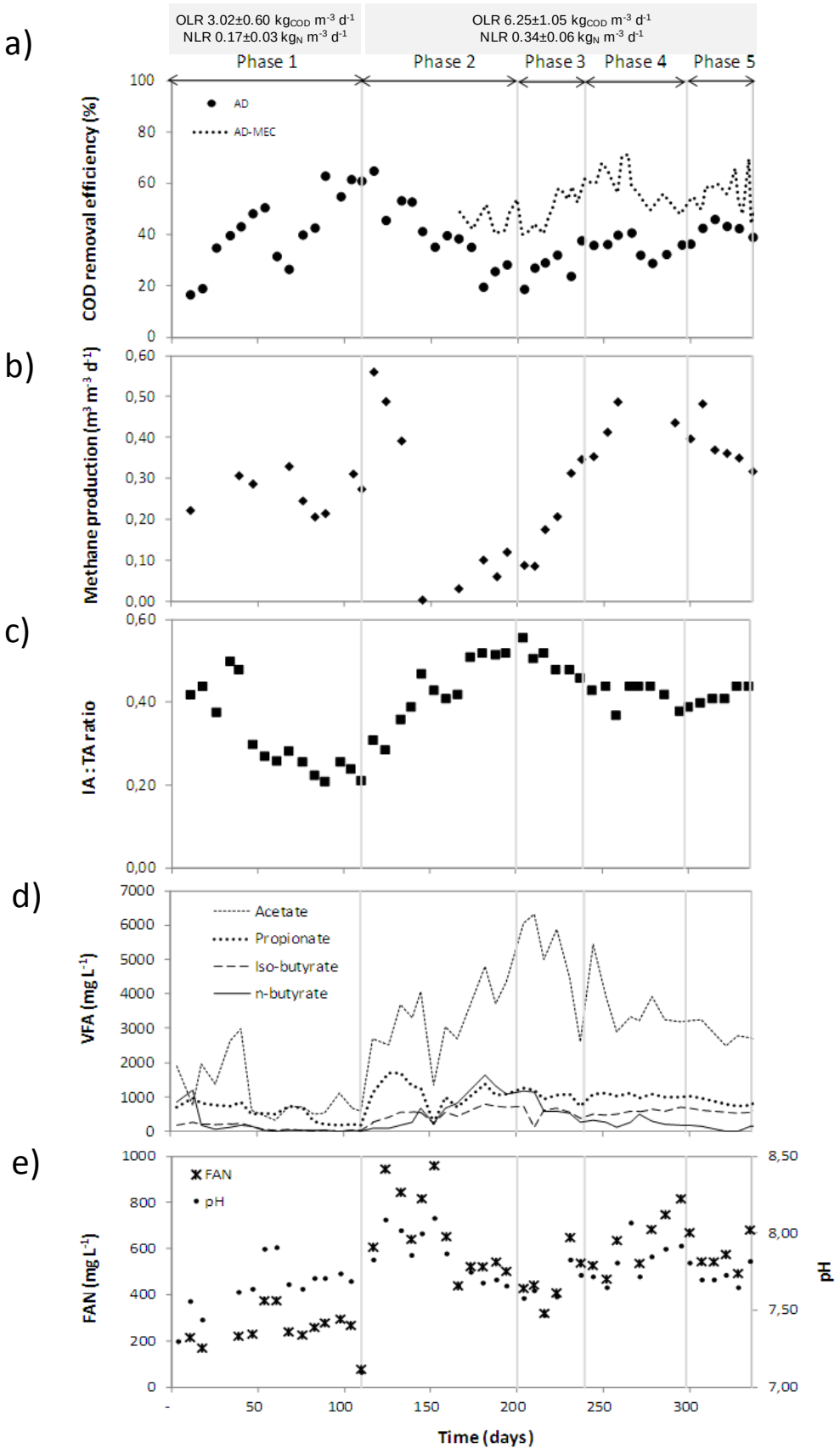

Figure 7.2 Performance of the AD regarding (a) COD removal efficiency; (b) methane productivity; (c) IA:TA ratio; (d) VFA concentration; and (e) free ammonia concentration (FAN) and pH.

Inhibition of AD by ammonia has been long studied (Yenigün and Demirel, 2013). In one of these studies, cattle manure was used as the substrate in continuously fed thermophilic laboratory scale reactors, gradually administering NH_4Cl for adaptation while the pH was kept constant. The first signs of inhibition occurred at a total ammonia nitrogen (TAN) concentration of 4000 mg L^{-1} –i.e. free ammonia nitrogen + ammonium nitrogen–, corresponding to 900 mg L^{-1} of free ammonia nitrogen (FAN). Process instability due to the presence of ammonia led to VFA accumulation, which lowered the pH. As a result, the decreased FAN concentration eventually resulted in a stable, though lowered, methane yield, called by the authors the 'inhibited steady state' (Angelidaki and Ahring, 1993). Another study investigated the digestion of swine manure in a laboratory scale batch and CSTRs –again in thermophilic conditions–, and concluded that a threshold of 1100 mg L^{-1} FAN concentration was required for introducing inhibition (Hansen et al., 1998). The values in the present study for FAN are quite below the inhibitory values indicated in those works, except at the beginning of Phase 2 (Figure 7.2e). The increase in NLR, summed to an increase in the pH of the reactor, raised the FAN concentration up to 960 mg L^{-1}. From then on, the first signs of inhibition were shown, with a decrease in COD removal efficiency and methane productivity and VFA accumulation. Later, this VFA accumulation produced a decrease in pH and in the FAN concentration, even if the reactor did not show signs of recovery. This fact can be explained because the levels of VFA, especially for propionic acid, remained high and could inhibit the activity of methanogens. Although VFA levels for which an AD reactor can show inhibition may differ from one digester to another, Wang et al. (2009) reported that acetic acid and butyric acid concentrations of 2400 and 1800 mg L^{-1}, respectively, resulted in no significant inhibition of the activity of methanogens, while a propionic acid concentration of 900 mg L^{-1} resulted in their significant inhibition. The VFA concentration of the AD was above these values, so the observed inhibition was probably produced by the combination of high ammonia and VFA concentrations.

7.3.2 Performance of the AD-MEC combined system in series operation

The MEC was fed with the effluent of the AD during Phase 2, as a polishing step and a way to buffer the malfunction period of the AD. The average COD removal efficiency achieved in the MEC was of 25±8% (Table 7.3), resulting in an effluent COD of 31.48±4.52 g kg^{-1} and a total COD removal efficiency of the combined system of 46±5%. The VFA were reduced at the effluent to a range of 6418-8804 mg_{COD} L^{-1}, maintaining acetic and propionic under 2000 and 1000 mg L^{-1}, respectively (Figure 7.3c). Furthermore, concomitant to COD removal, an average of 2.01±0.63 A m^{-2} were produced (Figure 7.3a) and 40±3% of the ammonia was transferred from the anode to the cathode compartment (12.97±2.04 g $N\text{-}NH_4^+$ d^{-1} m^{-2}) (Figure 7.3b). Those values were equivalent to the obtained in a recent work with an electrochemical system in the

recirculation loop of an UASB (Desloover et al., 2014) but lower to the 86 g $N\text{-}NH_4^+$ d^{-1} m^{-2} obtained with a submersible microbial desalination cell fed with synthetic solution (Zhang and Angelidaki, 2015). With the stripping and absorption step, up to 37% of the ammonia of the anode compartment influent was recovered in the acidic solution. Such high recovery was achieved thanks to the high cathode effluent pH (11.83±0.60), due to charge and cation transfer between the anode and cathode compartments (Chapter 4; Cerrillo et al., 2016) while the pH of the anode effluent remained neutral (7.03±0.07).

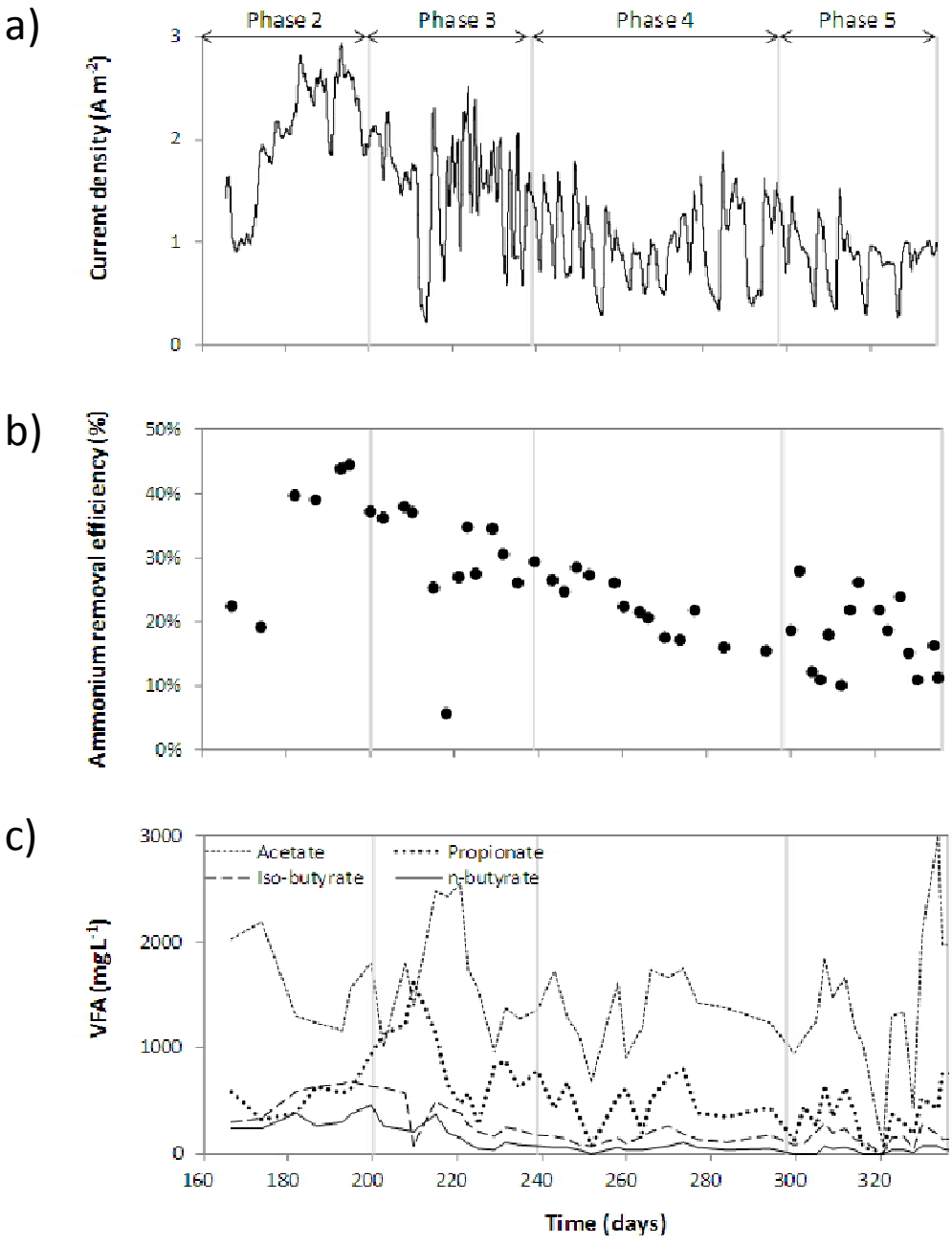

Figure 7.3 Performance of the MEC regarding (a) Current density; (b) ammonium removal efficiency; and (c) VFA concentration in the effluent.

7.3.3 Performance of the AD-MEC combined system with recirculation loop

When the recirculation loop between the AD and the MEC was established, starting with a volume of 25% of the feed flow rate in Phase 3, a clear recovery of the AD was observed. After a period of 4 HRT, the COD removal efficiency reached up to 38% and methane productivity increased up to 0.35 m^3 m^{-3} d^{-1}, equalling the productivity obtained before the inhibition (Figure 7.2b). The IA:TA ratio also showed an improvement, decreasing from 0.56 to 0.46, parallel to the VFA decrease to 11740 mg_{COD} L^{-1} (4477 mg_{acetic} L^{-1} and 1088 $mg_{propionic}$ L^{-1}). In these conditions, the MEC achieved a COD and ammonium removal efficiency of 28±7% and 31±5%, respectively (Table 7.3). The AD-MEC combined system achieved a COD removal efficiency of 51±7%, resulting in an effluent COD of 28.88±2.69 g kg^{-1}.

When the recirculation between MEC and AD was increased to 50% of the feed flow rate (Phase 4), the COD removal of the AD stabilised at an average of 35±4% and a methane productivity of 0.42±0.05 m^3 m^{-3} d^{-1}. This productivity represented a 55% increase with respect to the one obtained before the inhibition, when the OLR was a half, and a 7 fold increase with respect to inhibited state in Phase 2 (Table 7.3). The IA:TA ratio showed an improvement at the end of Phase 4, decreasing to a value of 0.38, since VFA were stabilised at around 8500 mg_{COD} L^{-1} (3200 mg_{acetic} L^{-1} and 1000 $mg_{propionic}$ L^{-1}). The MEC achieved a COD and ammonium removal efficiency of 30±11% and 22±5%, respectively (Table 7.3). This way the AD-MEC combined system achieved an overall COD removal efficiency of 59±7%, with an effluent COD of 28.10±6.04 g kg^{-1}.

Finally, in Phase 5 the recirculation volume was increased up to 75% of the feed flow rate. This time the AD showed the highest COD removal efficiency from the three recirculation phases, with an average of 42±3% (Figure 7.2). Methane productivity and IA:TA ratio were similar on average to the previous phase (0.38±0.06 m^3 m^{-3} d^{-1} and 0.42±0.02, respectively), although with a slight tendency to worsen, which can be due to the biomass wash out produced by an excess in recirculation volume. VFA were stabilised in a range of 3800 – 4150 mg_{COD} L^{-1} (2750 mg_{acetic} L^{-1} and 750 $mg_{propionic}$ L^{-1}). The MEC achieved a COD and ammonium removal efficiency of 20±7% and 17±5%, respectively (Table 7.3). The AD-MEC combined system achieved a COD removal efficiency of 56±7%, resulting in an effluent COD of 27.27±3.67 g kg^{-1}.

From these results it can be seen that MEC removal efficiencies, both for COD and for ammonium, decreased at the same time that the AD recovered its performance, and the average current density produced in Phase 5 represented only 42% of the average current density of Phase 2. This behaviour can be explained because the AD effluent decreased the COD concentration when the recirculation loop was connected, so less organic matter was available for degradation by microorganism in the MEC (especially acetate) and less electrical intensity was produced, reducing also ammonium transport between anode and cathode. In

return, removal efficiencies of the MEC were higher during the inhibition period of the AD, counterbalancing its poor performance.

The beneficial effect of the recirculation loop between the MEC and the AD can be due to different aspects. In the first place, the MEC contributes to decrease ammonia inhibition in the AD in two ways: by ammonium removal of the effluent, since it transfers from the anode to the cathode compartment, decreasing its concentration in a range of 17-31%; and by slightly decreasing the pH of the AD, and therefore the FAN level, as proton accumulation is induced in the anode compartment of the MEC due to charge and cation transport to the cathode. In the second place, the recirculation of the MEC effluent reduces also the organic load of the AD, since the MEC removes between 20 to 30% of the remaining COD. And finally, the robustness and stability of the AD may be increased thanks to the biomass connection between both reactors (Section 7.3.4.). A recent work, focused on ammonium recovery with a desalination cell to overcome AD inhibition achieved a 40.8% recovery of ammonium and helped to gradually increase methane productivity back to 83%, compared to the control, 55 days after the inhibition of the AD (Zhang and Angelidaki, 2015). In that case, synthetic wastewater was used, and the inhibition of the AD was produced only increasing the NLR; while in this work, a more complex and realistic inhibition process has been induced, increasing both OLR and NLR. Furthermore, the set up proposed by Zhang and Angelidaki (2015) does not make the most of the BES in order to reduce the COD of the AD effluent. Hence a more integrated approach is presented in this study since not just the recovery of AD, after its inhibition, is achieved, but the COD concentration in the effluent is kept low.

7.3.4 Microbial community assessment

The microbial community structure of the AD at the end of each Phase, as well as the biofilm developed on the carbon felt (anode) of the MEC reactor, at the start and at the end of the assays, were characterised by means of qPCR technique and sequenced by MiSeq.

7.3.4.1 Quantitative analysis by qPCR

Figure 7.4 shows qPCR results for all the samples. The number of bacterial *16S* rRNA gene copies g^{-1} in the AD sample at the end of Phase 1 was of $8.42 \cdot 10^{9}$, and slightly oscillated throughout the different phases, with a maximum of $1.40 \cdot 10^{10}$ (a 1.7 fold increase) at the end of Phase 3. The *mcrA* gene copy numbers quantified by qPCR revealed that the initial abundance of $4.57 \cdot 10^{7}$ copy numbers g^{-1} at the end of Phase 1, decreased gradually to a minimum at the end of Phase 4 ($9.55 \cdot 10^{6}$ copy numbers g^{-1}). The sample taken at the end of Phase 5 showed a level of *mcr*A copy numbers similar to the one obtained in Phase 2 ($2.19 \cdot 10^{7}$ copy numbers g^{-1}). These values, including those corresponding to the inhibited state, are higher than those

obtained in other studies, which quantified *mcrA* copies in different anaerobic digesters in a range of $1.04 \cdot 10^6$-$3.95 \cdot 10^6$ copy numbers mL^{-1} (Steinberg and Regan, 2009). The evolution of archaea population was found to be in great correlation with the operational parameters described in the previous sections, although a delay in the response was observed. The reduction in *mcrA* copy numbers under inhibited state, although working with lower ammonium concentrations, is similar to a previous study. qPCR in that work revealed that *mcrA* copy number decreased by one order of magnitude in the treatment with large amount of ammonium (10 g NH_4^+-N L^{-1}) but did not change much with treatments with lower NH_4^+-N content (3 and 7 g NH_4^+-N L^{-1}) compared to the control (Zhang et al., 2014). The ratio between archaea and eubacteria in the AD is under 1% in all cases, in spite of the importance of methanogenic archaea in AD, which is in agreement with previous studies (Sundberg et al., 2013). Regarding the MEC, an increase of an order of magnitude in *mcrA* copy numbers –at late stages– in the final sample, with respect to the initial one is produced, as a result of allochthonous methanogenic archaea coming from the AD. The same increase was also observed in bacterial *16S* rRNA gene copies.

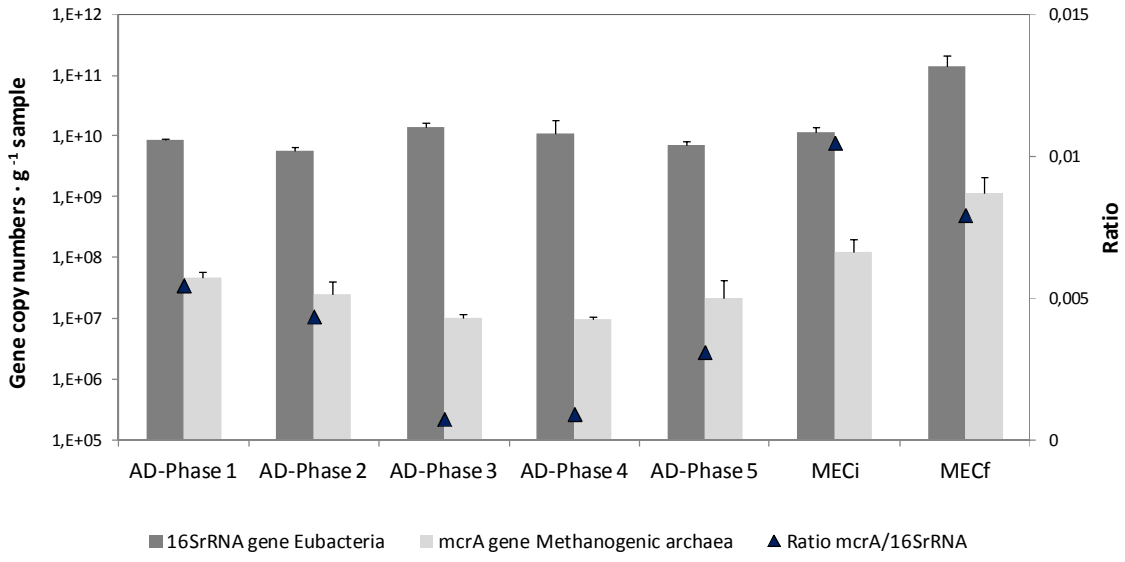

Figure 7.4 Gene copy numbers for *16S rRNA* and *mcrA* genes and ration between them, of the effluent of the AD at the five phases, and initial and final MEC anode biofilm (MECi and MECf, respectively).

7.3.4.2 MiSeq sequencing of total eubacteria and archaea, biodiversity and correspondence analysis

The reads obtained for bacteria and archaeal communities in each sample are shown in Table 7.4. Figure 7.5a shows that the dominant eubacterial *phyla* identified in the anode biofilm sample of the MEC at the start of the assay was *Bacteroidetes (31%),* followed by *Proteobacteria (21%),* while at the end of the assay a clear enrichment in the *Firmicutes* group

took place, representing 66% of the relative abundance. These three phyla have been identified in previous studies in BES (Bonmatí et al., 2013; Sotres et al., 2015b). At family level, results in Figure 7.5b revealed the dominance of *Desulfuromonadaceae* (17%), *Anaerolineaceae* (16%) and *Flavobacteriaceae* (13%) at the start of the assay, and a clear enrichment in *Clostridiaceae* (43%) and Peptostreptococcaceae (14%) once the recirculation loop with the AD was established.

Table 7.4 Diversity index for Eubacterial and Archaeal community of the MEC anode and AD effluent samples (mean±standard deviation). Data normalised to the sample with the lowest number of reads (16872 and 19235 for eubacterial and archaeal, respectively).

	Reads	**OTUs**	**Inverted Simpson**	**Shannon**
Eubacteria				
MEC_i	16872	706.00±0.00	17.50±0.00	4.27±0.00
MEC_f	22481	615.75±7.23	9.29±0.08	3.52±0.01
AD_{Phase1}	17776	489.51±2.98	15.44±0.04	3.58±0.00
AD_{Phase2}	20447	481.17±5.08	13.67±0.07	3.56±0.01
AD_{Phase3}	19778	474.51±4.95	8.03±0.05	3.21±0.01
AD_{Phase4}	20295	426.77±5.18	5.67±0.04	2.90±0.01
AD_{Phase5}	25178	520.70±7.21	12.70±0.10	3.51±0.01
Archaea				
MEC_i	56913	82.11±2.93	8.12±0.00	2.39±0.00
MEC_f	231636	26.96±0.26	1.01±0.00	0.05±0.00
AD_{Phase1}	19409	34.94±0.00	1.05±0.00	0.17±0.00
AD_{Phase2}	19235	37.00±1.47	1.06±0.00	0.20±0.01
AD_{Phase3}	25256	63.08±2.09	1.39±0.00	0.80±0.01
AD_{Phase4}	38734	35.99±0.66	1.21±0.00	0.45±0.00
AD_{Phase5}	20088	50.54±3.28	2.47±0.05	1.29±0.01

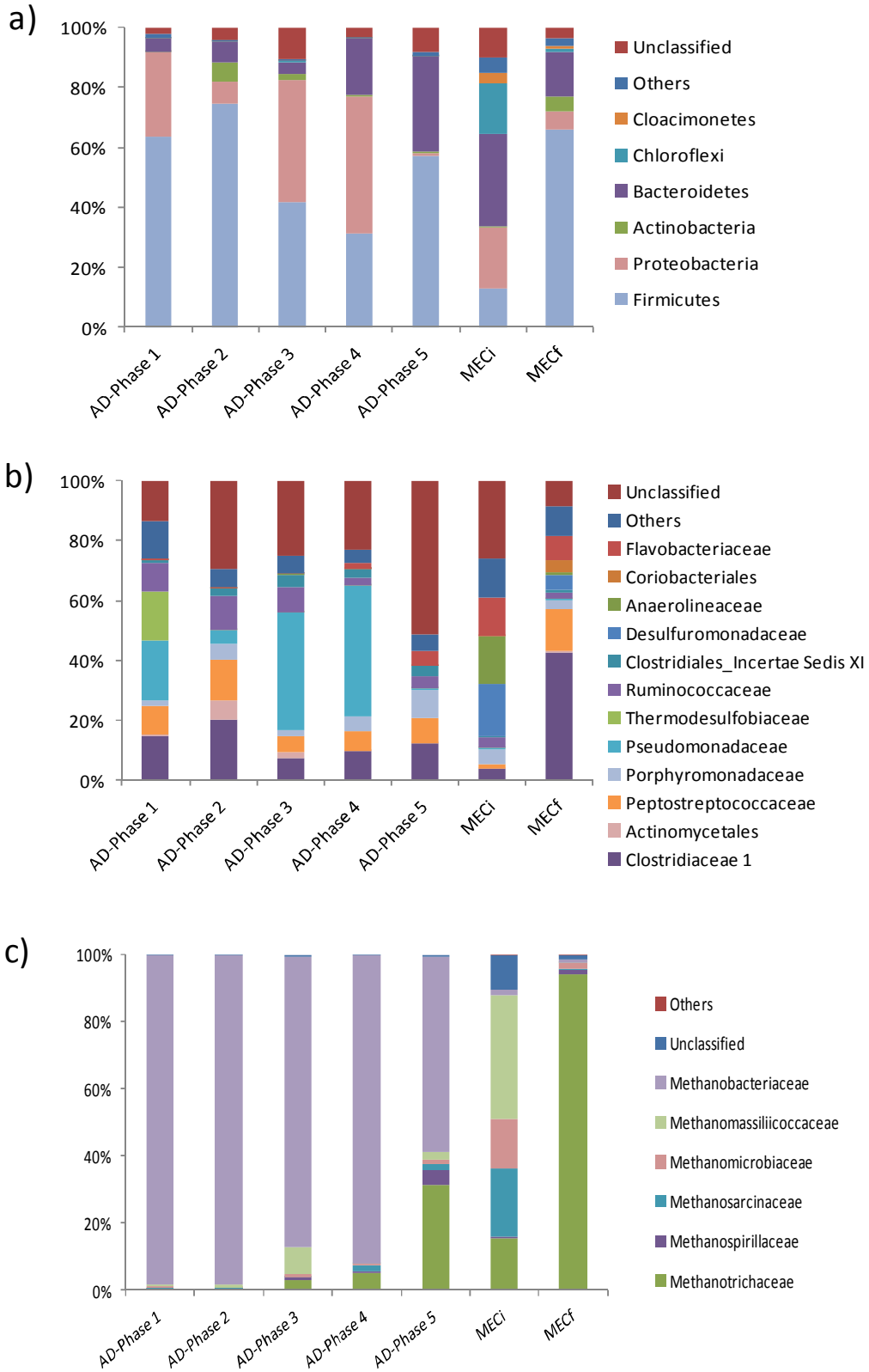

Figure 7.5 Taxonomic assignment of sequencing reads from Eubacterial community of the effluent of the AD at the five phases, and initial and final MEC anode biofilm (MECi and MECf, respectively), at a) phylum b) family levels; and c) from Archaeal community at family level. Relative abundance was defined as the number of reads (sequences) affiliated with any given taxon divided by the total number of reads per sample. Phylogenetic groups with a relative abundance lower that 1% were categorised as "others".

Regarding the samples of the AD effluent, *Firmicutes phylum* (63%) was de predominant one at the end of Phase 1, followed by *Proteobacteria* (28%). A previous study, performed also in a thermophilic AD running on swine manure by means of 454-pyrosequencing technology, also found that the *Firmicutes* phylum was the predominant one, representing 72.2% of the 16S rRNA gene sequences (Tuan et al., 2014). At the end of Phase 2, whilst the reactor was inhibited, *Firmicutes* increased its relative abundance up to 75% and *Proteobacteria* decreased to 7%. Once the recirculation loop with the MEC was established, both *phyla* equilibrated their presence at the end of Phase 3 (41%) and *Proteobacteria* surpassed *Firmicutes* in Phase 4, while at the end of Phase 5 *Firmicutes* recovered its dominance (57%). This *phylum* has been also observed to be in domination in AD under ammonia inhibition in previous studies (Niu et al., 2013). Furthermore, *Firmicutes* showed an important increase in the MEC anode, as aforementioned, it being a clear example of population sharing between both systems. Indeed, 6 OTUs belonging to the *Firmicutes phylum*, not detected in the initial MEC sample but present in the AD, increased in relative abundance in the final MEC sample after the AD-MEC combined operation (Table 7.5). On the other hand, *Bacteroidetes,* the predominant *phylum* in the MEC anode at the beginning of the assays, increased its relative abundance in the AD from 4% to 32% once the recirculation loop was established, and until Phase 5. Coincidentally, 4 new OTUs belonging to the *Bacteroidetes phylum* showed up in the AD, once the recirculation loop was connected (Table 7.6). The most abundant OTUs in the final MEC sample, three belonging to the *Firmicutes phylum* and one belonging to the *Bacteroidetes phylum*, were shared by the AD at the end of Phase 5 (Table 7.7). At family level, *Pseudomonadaceae* (20%), *Thermodesulbobiaceae* (16%) and *Clostridiaceae* (15%) were the predominant ones at the end of Phase 1. At the end of Phase 2, during the inhibition phase, Clostridiaceae increased its relative abundance (20%) with the other two families decreasing. *Peptostreptococcaceae* and *Ruminococcaceae* increased slightly their relative abundance, becoming the second and third most abundant families (14 and 11%, respectively). During Phase 3 and 4, with the recirculation loop established, *Pseudomonadaceae* showed an important increase, up to 40 and 44%, respectively, but suffered a sharp decrease at the end of Phase 5, and *Clostridiaceae*, after decreasing to 7% in Phase 3, recovered its initial relative abundance at the end of Phase 5. Finally, it is noteworthy to mention that possible syntrophic acetate-oxidising bacteria (SAOB) OTUs, such as *Syntrophaceticus* or *Tepidanaerobacter*, were detected in the AD samples, showing higher relative abundances during Phases 1, 2 and 3 (0.60, 0.51 and 0.50, respectively) than in Phases 4 and 5 (0.19 and 0.32, respectively). The high concentration of ammonia in the reactor might be favouring syntrophic acetate oxidation (SAO) coupled to a hydrogenotrophic methanogenesis route, which consists in the oxidation of methyl and carboxyl groups of acetate to CO_2, producing H_2, catalysed by the SAOB (Hattori, 2008).

Correspondence analysis for eubacterial population indicated that initial biofilm from the MEC anode evolved during the recirculation phases, approaching the composition of the AD samples, although maintaining its own specific composition. AD samples from the recirculation phases (3, 4 and 5) clustered together, moving away from samples of the phases without recirculation (1 and 2) (Figure 7.6a).

Table 7.5 Operational taxonomic units (OTUs) of eubacterial microbial community that were not detected in the initial microbial electrolysis cell (MEC) sample (MECi) but were present in the anaerobic digester and enriched in the final MEC sample (MECf) after the AD-MEC integrated operation (percentage of total 16S rRNA reads).

OTU number	Phylum	Class	Order	Family	Genus	MECi	MECf
						(% reads)	
24	*Firmicutes*	*Clostridia*	*Clostridiales*	*Ruminococcaceae*	*Ruminococcaceae*	0	0.04
41	*Firmicutes*	unclassified				0	0.11
52	*Firmicutes*	*Clostridia*	*Clostridiales*	*Clostridiales_Incertae Sedis XI*	*Tepidimicrobium*	0	0.04
56	*Firmicutes*	unclassified				0	0.10
138	*Firmicutes*	*Clostridia*	*Clostridiales*	*Clostridiales_Incertae Sedis III*	*Tepidanaerobacter*	0	0.04
637	*Firmicutes*	*Clostridia*	*Clostridiales*	*Clostridiaceae 1*	unclassified	0	0.08

Table 7.6 Operational taxonomic units (OTUs) of eubacterial microbial community that were not detected in the anaerobic digester (AD) before the connection of the recirculation loop (AD-Ph2) but were present in the microbial electrolysis cell (MEC) and enriched in the final AD sample (AD-Ph5) after the AD-MEC integrated operation (percentage of total 16S rRNA reads).

OTU number	Phylum	Class	Order	Family	Genus	AD-Ph2	AD-Ph5
						(% reads)	
107	*Bacteroidetes*	*Bacteroidia*	*Bacteroidales*	unclassified		0	0.17
161	*Bacteroidetes*	*Bacteroidia*	*Bacteroidales*	unclassified		0	0.06
359	*Bacteroidetes*	unclassified				0	0.06
561	*Bacteroidetes*	*Bacteroidia*	*Bacteroidales*	unclassified		0	0.05

Table 7.7 Operational taxonomic units (OTUs) most abundant of eubacterial microbial community in the final microbial electrolysis cell (MEC) sample (MECf) shared with the final sample of the anaerobic digester (AD-Ph5) (percentage of total 16S rRNA reads).

OTU number	Phylum	Class	Order	Family	Genus	MECf	AD-Ph5
						(% reads)	
1	*Firmicutes*	*Clostridia*	*Clostridiales*	*Peptostreptococcaceae*	*Clostridium XI*	12	7
3	*Firmicutes*	*Clostridia*	*Clostridiales*	*Clostridiaceae 1*	*Clostridium sensu stricto*	28	9
10	*Firmicutes*	*Clostridia*	*Clostridiales*	*Clostridiaceae 1*	*Clostridium sensu stricto*	7	2
5	*Bacteroidetes*	unclassified				7	4

a)

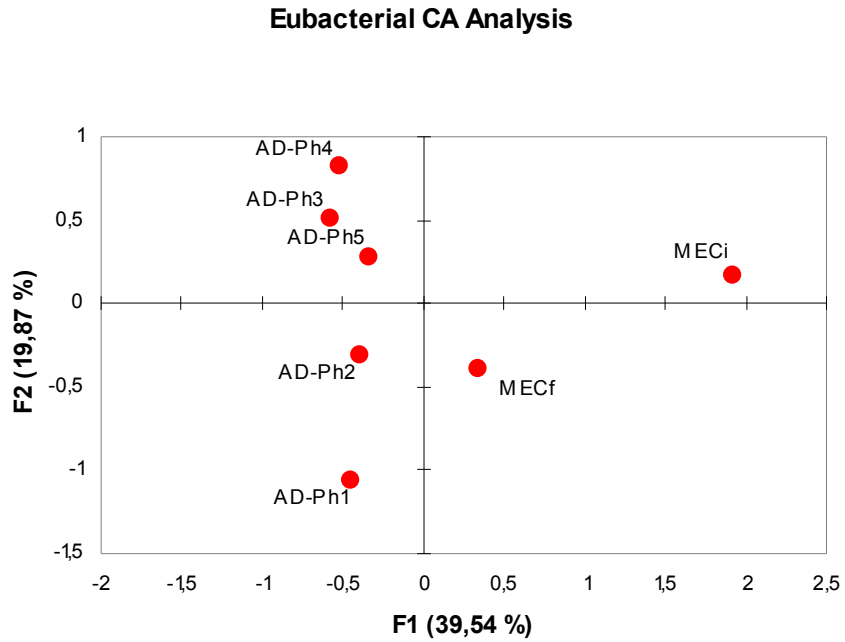

b)

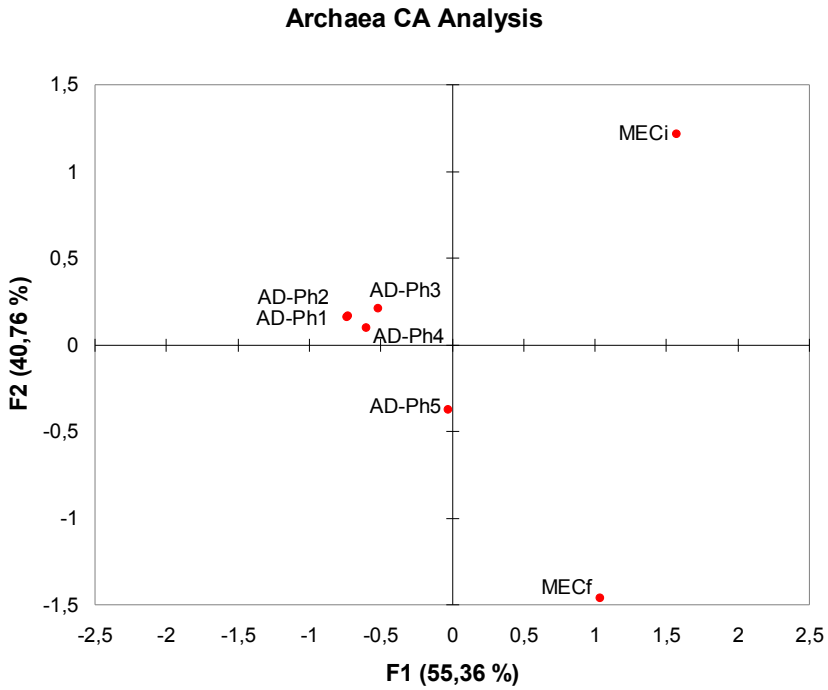

Figure 7.6 Correspondence Analysis for initial (MEC_i) and final (MEC_f) MEC anode samples and the 5 phases AD samples (AD-Ph1 to AD-Ph5) regarding (a) Eubacterial and (b) Archaeal community.

Regarding archaeal population, Figure 7.5c shows that the most abundant families in the anode of the MEC at the start of the experiments were *Methanomassiliicoccaceae* (37%), *Methanosarcinaceae* (20%), *Methanomicrobiaceae* (15%) and *Methanotrichaceae* (formerly known as *Methanosaetaceae*) (15%). The last family, of strictly acetotrophic methanogens, was clearly enriched at the end of the assays, the recirculation loop with the AD once established, achieving a relative abundance of 94%. The AD presented, at the end of Phase 1, a high dominance of the *Methanobacteriaceae* family (98%), hydrogenotrophic methanogens, dominance maintained throughout the inhibition of the reactor in Phase 2. The predominance of hydrogenotrophic methanogens could be favoured by the low HRT used in this study, since the difference in the specific growth rate between hydrogenotrophic methanogens and aceticlastic methanogens makes for a relatively short HRT to provide a more favourable environment for the first ones. Furthermore, it has been reported that *Methanobacteriaceae* became the dominant species when increasing ammonia levels in biogas reactors (Kim et al., 2014). The *Methanobacteriaceae* family was also the predominant one in a thermophilic AD running on swine manure (Tuan et al., 2014). The community of a mesophilic real scale AD fed with swine faeces was composed, up to 57.7%, of by *Methanobacteriales*, hydrogenotrophic methanogens also being the dominant methane producing archaea (more than 94% of methanogenic archaea of the reactor) (Zhu et al., 2011). Although a slight decrease in the *Methanobacteriaceae* family relative abundance was observed during Phase 3 and 4, the highest decrease was observed at the end of Phase 5 –up to 58%. In parallel with this decrease, an increase in *Methanotrichaceae* was observed, reaching up to 31% at the end of Phase 5, whilst also becoming the predominant archaea in the MEC anode, as aforementioned. An OTU shared by the MEC and the AD was the dominant one in the *Methanotrichaceae* family, either in the final MEC and the AD Phase 5 sample (Table 7.8). This shift in population towards acetotrophic methanogens can be stimulated by more favourable conditions in the AD in subsequent phases, once the ammonia concentration in the AD is reduced and the inhibition is overcome. These results correlate quite well with the ones obtained by qPCR, indicating that the inhibition of the AD regarding methane productivity and AGV increase is detected before a change in archaeal population abundance and composition is observed. Although the changes in the total population of methanogens can be used as an indicator of the performance of the AD, methanogenesis inhibition is largely due to the repression of functional gene expression (Zhang et al., 2014) and a deep study at RNA level in this sense would help to better link community structures and digester functions. Correspondence analysis for archaea population showed that initial and final biofilm from the MEC anode were far more distant in composition than in the case of the eubacteria population, and there was not a clear approach to the composition of the AD samples. AD samples were all clustered together, appreciating that the phases without recirculation (1 and 2) were quite

similar, while a slight evolution in the recirculation phases samples (3, 4 and 5) could be observed (Figure 7.6b).

Table 7.8 Operational taxonomic units (OTUs) most abundant of archaeal microbial community in the final microbial electrolysis cell (MEC) sample (MECf) shared with the final sample of the anaerobic digester (AD-Ph5) (percentage of total 16S rRNA reads).

OTU number	Phylum	Class	Order	Family	Genus	MECf (% reads)	AD-Ph5 (% reads)
1	*Euryarchaeota*	*Methanomicrobia*	*Methanosarcinales*	*Methanotrichaceae*	*Methanothrix*	94	31

Regarding biodiversity, the inverted Simpson and Shannon indices showed that the sample of the MEC at the start of the assays was the most diverse one, either for eubacteria (17.50 and 4.27, respectively) and for archaea (8.12 and 2.39, respectively) (Table 7.4). For the AD, biodiversity indices for eubacteria showed that the values corresponding to Phase 2 decreased with respect to Phase 1, but the minimum values were detected at the end of Phase 4. In Phase 5, the diversity values were near to the initial values. The AD archaea biodiversity increased over time, finishing Phase 5 with the highest values for the inverted Simpson (2.47) and Shannon (1.29). These results show that the AD diversity was increased by the parallel treatment of the substrate, and in spite of the stressful conditions in the reactor, the exchange with the MEC biomass seems to help to recover its biodiversity.

7.4 Conclusions

Coupling an inhibited AD in series, with a MEC and a stripping and absorption unit allowed for the maintenance of the effluent quality (COD removal and ammonia recovering of 46±5% and 40±3%, respectively). The AD-MEC system in loop configuration stabilised the AD after failure (55% increase in methane productivity) and enhanced methanogenic archaea recovery, concomitant to an AD biodiversity increase, while reducing it in the MEC biofilm. These results show that the AD-MEC combined system is a promising strategy to stabilise AD against organic and nitrogen overloads, while improving the quality of the effluent and recovering nutrients for their reutilisation.

7.5 References

Alvarado, A., Montáñez, L., Palacio Molina, S.L., Oropeza, R., Luevanos Escareno, M.P., Balagurusamy, N. 2014. Microbial trophic interactions and mcrA gene expression in monitoring of anaerobic digesters. *Frontiers in Microbiology*, 5.

Angelidaki, I., Ahring, B.K. 1994. Anaerobic thermophilic digestion of manure at different ammonia loads: Effect of temperature. *Water Research*, **28**(3), 727-731.

Angelidaki, I., Ahring, B.K. 1993. Thermophilic anaerobic digestion of livestock waste: the effect of ammonia. *Applied Microbiology and Biotechnology*, **38**(4), 560-564.

Angenent, L.T., Karim, K., Al-Dahhan, M.H., Wrenn, B.A., Domíguez-Espinosa, R. 2004. Production of bioenergy and biochemicals from industrial and agricultural wastewater. *Trends in Biotechnology*, **22**(9), 477-485.

Bonmatí, A., Flotats, X. 2003. Air stripping of ammonia from pig slurry: characterisation and feasibility as a pre- or post-treatment to mesophilic anaerobic digestion. *Waste Management*, **23**(3), 261-272.

Bonmatí, A., Sotres, A., Mu, Y., Rozendal, R.A., Rabaey, K. 2013. Oxalate degradation in a bioelectrochemical system: Reactor performance and microbial community characterization. *Bioresource Technology*, **143**(0), 147-153.

Borja, R., Sánchez, E., Weiland, P. 1996. Influence of ammonia concentration on thermophilic anaerobic digestion of cattle manure in upflow anaerobic sludge blanket (UASB) reactors. *Process Biochemistry*, **31**(5), 477-483.

Cerrillo, M., Oliveras, J., Viñas, M., Bonmatí, A. 2016. Comparative assessment of raw and digested pig slurry treatment in bioelectrochemical systems. *Bioelectrochemistry*, **100**, 69-78.

Chen, Y., Cheng, J.J., Creamer, K.S. 2008. Inhibition of anaerobic digestion process: A review. *Bioresource Technology*, **99**(10), 4044-4064.

Chiu, S.-F., Chiu, J.-Y., Kuo, W.-C. 2013. Biological stoichiometric analysis of nutrition and ammonia toxicity in thermophilic anaerobic co-digestion of organic substrates under different organic loading rates. *Renewable Energy*, **57**(0), 323-329.

Desloover, J., De Vrieze, J., Van de Vijver, M., Mortelmans, J., Rozendal, R., Rabaey, K. 2014. Electrochemical nutrient recovery enables ammonia toxicity control and biogas desulfurization in anaerobic digestion. *Environmental Science & Technology*, **49**(2), 948-955.

Hansen, K.H., Angelidaki, I., Ahring, B.K. 1998. Anaerobic digestion of swine manure: inhibition by ammonia. *Water Research*, **32**(1), 5-12.

Hattori, S. 2008. Syntrophic acetate-oxidizing microbes in methanogenic environments. *Microbes and Environment*, **23**(2), 118-27.

Hejnfelt, A., Angelidaki, I. 2009. Anaerobic digestion of slaughterhouse by-products. *Biomass and Bioenergy*, **33**(8), 1046-1054.

Kim, W., Shin, S., Cho, K., Han, G., Hwang, S. 2014. Population dynamics of methanogens and methane formation associated with different loading rates of organic acids along with ammonia: redundancy analysis. *Bioprocess and Biosystems Engineering*, **37**(5), 977-981.

Laureni, M., Palatsi, J., Llovera, M., Bonmatí, A. 2013. Influence of pig slurry characteristics on ammonia stripping efficiencies and quality of the recovered ammonium-sulfate solution. *Journal of Chemical Technology & Biotechnology*, **88**(9), 1654-1662.

Morris, R., Schauer-Gimenez, A., Bhattad, U., Kearney, C., Struble, C.A., Zitomer, D., Maki, J.S. 2013. Methyl coenzyme M reductase (mcrA) gene abundance correlates with activity measurements of methanogenic H2/CO2-enriched anaerobic biomass. *Microbial Biotechnology*, **7**(1), 77-84.

Niu, Q., Qiao, W., Qiang, H., Li, Y.-Y. 2013. Microbial community shifts and biogas conversion computation during steady, inhibited and recovered stages of thermophilic methane fermentation on chicken manure with a wide variation of ammonia. *Bioresource Technology*, **146**, 223-233.

Ripley, L.E., Boyle, W.C., Converse, J.C. 1986. Improved alkalimetric monitoring for anaerobic digestion of high-strength wastes. *Journal (Water Pollution Control Federation)*, **58**(5), 406-411.

Schloss, P.D., Westcott, S.L., Ryabin, T., Hall, J.R., Hartmann, M., Hollister, E.B., Lesniewski, R.A., Oakley, B.B., Parks, D.H., Robinson, C.J., Sahl, J.W., Stres, B., Thallinger, G.G., Van Horn, D.J., Weber, C.F. 2009. Introducing mothur: open-source, platform-independent, community-supported software for describing and comparing microbial communities. *Applied and Environmental Microbiology*, **75**(23), 7537-7541.

Sotres, A., Cerrillo, M., Viñas, M., Bonmatí, A. 2015a. Nitrogen recovery from pig slurry in a two-chambered bioelectrochemical system. *Bioresource Technology*, **194**, 373-382.

Sotres, A., Díaz-Marcos, J., Guivernau, M., Illa, J., Magrí, A., Prenafeta-Boldú, F.X., Bonmatí, A., Viñas, M. 2015b. Microbial community dynamics in two-chambered microbial fuel cells: effect of different ion exchange membranes. *Journal of Chemical Technology & Biotechnology*, **90**(8), 1497-1506.

Steinberg, L.M., Regan, J.M. 2009. mcrA-targeted real-time quantitative PCR method to examine methanogen communities. *Applied and Environmental Microbiology*, **75**(13), 4435-4442.

Sundberg, C., Al-Soud, W.A., Larsson, M., Alm, E., Yekta, S.S., Svensson, B.H., Sorensen, S.J., Karlsson, A. 2013. 454 pyrosequencing analyses of bacterial and archaeal richness in 21 full-scale biogas digesters. *FEMS Microbiology Ecology*, **85**(3), 612-26.

Tartakovsky, B., Mehta, P., Bourque, J.S., Guiot, S.R. 2011. Electrolysis-enhanced anaerobic digestion of wastewater. *Bioresource Technology*, **102**(10), 5685-5691.

Tuan, N.N., Chang, Y.C., Yu, C.P., Huang, S.L. 2014. Multiple approaches to characterize the microbial community in a thermophilic anaerobic digester running on swine manure: a case study. *Microbiological Research*, **169**(9-10), 717-24.

Wang, Q., Garrity, G.M., Tiedje, J.M., Cole, J.R. 2007. Naïve bayesian classifier for rapid assignment of rRNA sequences into the new bacterial taxonomy. *Applied and Environmental Microbiology*, **73**(16), 5261-5267.

Wang, Y., Zhang, Y., Wang, J., Meng, L. 2009. Effects of volatile fatty acid concentrations on methane yield and methanogenic bacteria. *Biomass and Bioenergy*, **33**(5), 848-853.

Weld, R.J., Singh, R. 2011. Functional stability of a hybrid anaerobic digester/microbial fuel cell system treating municipal wastewater. *Bioresource Technology*, **102**(2), 842-847.

Yenigün, O., Demirel, B. 2013. Ammonia inhibition in anaerobic digestion: A review. *Process Biochemistry*, **48**(5-6), 901-911.

Zhang, C., Yuan, Q., Lu, Y. 2014. Inhibitory effects of ammonia on methanogen mcrA transcripts in anaerobic digester sludge. *FEMS Microbiology Ecology*, **87**(2), 368-77.

Zhang, Y., Angelidaki, I. 2015. Counteracting ammonia inhibition during anaerobic digestion by recovery using submersible microbial desalination cell. *Biotechnology and Bioengineering*, **112**(7), 1478-1482.

Zhu, C., Zhang, J., Tang, Y., Zhengkai, X., Song, R. 2011. Diversity of methanogenic archaea in a biogas reactor fed with swine feces as the mono-substrate by mcrA analysis. *Microbiological Research*, **166**(1), 27-35.

CHAPTER 8

Unravelling the active microbial community in a thermophilic anaerobic digester-microbial electrolysis cell coupled system under different conditions

Part of the content of this chapter is in preparation to be submitted for publication as:

Cerrillo, M., Viñas, M., Bonmatí, A. Unravelling the active microbial community in a thermophilic anaerobic digester-microbial electrolysis cell coupled system under different conditions.

Abstract

Thermophilic anaerobic digestion (AD) of pig slurry coupled to a microbial electrolysis cell (MEC) with a recirculation loop was investigated at lab-scale as a strategy to increase AD stability when submitted to organic and nitrogen overloads. The system performance was studied with the recirculation loop both connected and disconnected, in terms of AD methane production, chemical oxygen demand removal (COD) and volatile fatty acids (VFA) concentration. Furthermore, microbial population was assessed quantitatively and qualitatively, through DNA and RNA-based qPCR and high throughput sequencing (MiSeq) respectively, in order to identify those active microbial populations (RNA-based) from total microbial community composition (DNA-based) both in AD and MEC reactor at different operational conditions. Suppression of the recirculation loop AD-MEC resulted in a reduction in the AD COD removal efficiency (from 40% to 22%) and in the methane production (from 0.32 to 0.03 m^3 m^{-3} d^{-1}). The restart of the recirculation increased methane production to 0.55 m^3 m^{-3} d^{-1} concomitant with maximum COD and ammonium removal efficiency of 29 and 34%, respectively in the MEC. Regarding microbial analysis, composition of AD and MEC anode populations differed from really active microorganisms. *Desulfuromonadaceae* revealed as the most active family in the MEC (18-19% of RNA relative abundance), while hydrogenotrophic methanogens (*Methanobacteriaceae*) dominated the AD biomass.

8.1 Introduction

Anaerobic digestion (AD) is a technology that has been widely used since the beginning of the twentieth century to treat animal, municipal and industrial wastes, while producing biogas, a form of renewable energy (Yenigün and Demirel, 2013). One of its weak points is the sensitivity of methanogens, one of the main groups involved in the process, to chemical and environmental stressors, especially under thermophilic conditions (Chen et al., 2008). Inhibitory substances or process conditions may lead to the anaerobic reactor upset and failure, indicated by a decrease of the methane gas production and an accumulation of volatile fatty acids (VFA). Different strategies for recovering inhibited reactors have been evaluated, such as reactor feeding patterns, dilution and addition of absorbents for fast recovery after the inhibition of AD reactor by the presence of long chain fatty acids (LCFA) (Palatsi et al., 2009) or electrochemical nutrient recovery for ammonia toxicity control (Desloover et al., 2014; Sotres et al., 2015a); dilution with distillate water, digested biomass or fresh manure have also been strategies used to recover an ammonia-inhibited thermophilic process (Nielsen and Angelidaki, 2008). Ammonia inhibition is one of the main issues when treating high strength wastes such as livestock manure, so it has been subject for a wide range of studies and reviews (Rajagopal et al., 2013; Yenigün and Demirel, 2013).

The combination of AD and bioelectrochemical systems (BES) such as microbial electrolysis cells (MEC) has been previously reported as a new processing strategy aiming to recover energy and nitrogen (Chapter 7; Cerrillo et al., 2016b). On the one hand, this system can help to produce additional energy and to polish the AD effluent, especially when malfunction of the AD reactor is produced due to organic overloads, attaining a more stable and robust system. And on the other hand, ammonium can be removed and recovered, taking advantage of this process to reduce ammonia inhibition in the AD (Chapter 7; Cerrillo et al., 2016b). In the study performed in Chapter 7, the microbial community assessment revealed that changes in biomass composition were appreciated with a certain delay with respect to the observed performance of the AD, in terms of VFA accumulation or methane production (Cerrillo et al., 2016b). This fact pointed out that RNA-based approach in AD-BES system could help us to gain insight on the active microbial key players resilient during an inhibition process. A previous work also demonstrated that the inhibition of methanogenesis by ammonia in AD was largely due to the repression of functional gene transcription rather than a decrease of the total populations of methanogenic archaea (Zhang et al., 2014). In fact, DNA only provides information about the existence of bacteria in the reactors, but it cannot provide information about their activity and gene expression, which is important to understand which groups are being enhanced by certain environmental or operational conditions. Transcription analysis enables exclusive detection of short-lived messenger RNA (mRNA) produced by active

organisms without the potential bias of DNA detection from dormant or dead cells (Munk et al., 2012). In addition, total rRNA is dependent of ribosome abundance in a bacterial cell, and it can be shifted significantly (10-100 folds) from dormant cells in comparison with growing cells (Neidhardt et al., 1996). For this reason, direct extraction of total bacterial RNA (basically mRNA and rRNA) from samples is a key procedure for subsequent application of qPCR or high throughput sequencing techniques.

The main aim of this Chapter is (1) to assess the combination of the AD process with a microbial electrolysis cell with a recirculation loop as a system to remediate AD reactors that have experienced process failure, and (2) study the microbial population in an AD-MEC system during inhibited and recovered states of the AD process, regarding presence of predominant eubacteria and archaea in the biomass, but also regarding the metabolically active populations by means of DNA and RNA-based methods.

8.2 Materials and methods

8.2.1 Experimental set-up

The anaerobic thermophilic 4 L lab-scale continuous stirred tank reactor (AD) described in Section 3.1.3 was used to study its performance when treating pig slurry. The AD reactor was connected in series with the anode compartment of the two chambered MEC described in Section 3.1.1 for ammonia recovery, and had a recirculation loop between both reactors, as it was operated in Chapter 7.

8.2.2 Reactors operation

The raw pig slurry that was used to feed the AD was collected from a farm in Vila-Sana (Lleida, Spain), and was diluted with tap water at 50% (v/v) to obtain the desired organic load (Table 8.1). The hydraulic retention time (HRT) was fixed at 10 days. The reactor was operated during 118 days in 2 different phases, with an organic loading rate (OLR) and a nitrogen loading rate (NLR) of 6.10±1.88 kg_{COD} m^{-3} day^{-1} and 0.35±0.04 kg_N m^{-3} day^{-1}, respectively (Table 8.2). The AD had been previously operated with a recirculation loop between the AD and the MEC for 37 days, with recirculation in order to reduce ammonia inhibition phenomena in Chapter 7. At the start of this study, corresponding to Phase 1, the recirculation loop was suppressed, and in Phase 2 it was again recovered (50% of the AD feed flow rate), with the objective of evaluating the effectiveness of this processing strategy to recover the AD after its failure and study the changes produced in the biomass. For each experimental condition, the specific methane yield (m^3_{CH4} d^{-1}), the specific methane production rate (m^3_{CH4} m^{-3} d^{-1}) and the COD removal efficiency

were used as control parameters, as well as the biogas composition, the alkalinity, N-NH_4^+ and the VFA concentrations in the effluent.

Regarding the MEC, the digested pig slurry obtained from the AD was used as feed in the anode compartment previous filtering it through a stainless steel sieve of 125 µm. Catholyte solution for the cathode chamber contained (in deionised water) NaCl 0.1 g L^{-1}. Samples were taken periodically to analyse the pH and N-NH_4^+ concentration in the anode and cathode effluent, besides COD and VFA of the anode effluent.

Table 8.1 Characterisation of the diluted pig slurry used as feeding in the anaerobic digester (AD) (n=number of samples).

Parameter	Value
pH (-)	7.0±0.1
COD (g_{O2} kg^{-1})	62.63±2.96
NTK (g L^{-1})	3.65±0.11
N-NH_4^+ (g L^{-1})	2.66±0.27
TS (g kg^{-1})	35.80±0.72
VS (g kg^{-1})	23.50±1.21
n	10

Table 8.2 Operational conditions for the AD reactor.

Phase	Period (d)	OLR (kg_{COD} m^{-3} day^{-1})	NLR (kg_N m^{-3} day^{-1})	Recirculation (% of feed flow rate)
1	1 - 15	6.10±1.88	0.35±0.04	0
2	16-118			50

8.2.3 Analyses and calculations

Chemical oxygen demand (COD), Kjeldahl nitrogen (NTK), ammonium (N-NH_4^+), pH, total solids (TS), volatile solids (VS), volatile fatty acids (VFAs), biogas composition (N_2, CH_4, CO_2), partial, total and intermediate alkalinity were determined as described in Section 3.2. Free ammonia nitrogen (FAN), COD and ammonium removal efficiency and current density (A m^{-2}) obtained in the MEC were calculated as described in Sections 3.3 and 3.4.

The eubacterial and archaeal communities in the AD at the end of both Phase 1 and 2, and attached to the anode on the MEC at the beginning and the end of the experiments, were analysed by culture-independent molecular techniques such as quantitative PCR (qPCR and RT-qPCR) and high throughput DNA (hereafter 16SrDNA) and cDNA (hereafter 16SrRNA) sequencing of *16S* rRNA gene libraries of eubacteria and archaea (MiSeq, Illumina). Simultaneous total genomic DNA and RNA extraction and complementary DNA (cDNA) synthesis, qPCR and high throughput 16S rRNA gene sequencing (MiSeq, Illumina) were performed following the methods described in Section 3.6.2, 3.6.3, and 3.6.5, respectively. The

standard curve parameters of the qPCRs performed prove that the reactions had a high efficiency, and were as follows (for *16S* rRNA and *mcr*A, respectively): slope of -3.515 and -3.558; correlation coefficient of 0.999 and 0.996; efficiency of 93 and 91%. The data obtained from sequencing datasets was submitted to the Sequence Read Archive of the National Center for Biotechnology Information (NCBI) under the study accession number SRP071288 for eubacterial and archaeal populations.

The evaluation of the diversity of the samples and statistical multivariate analyses were performed following Section 3.6.6.

8.3 Results and discussion

8.3.1 Inhibition of the AD with the suppression of the recirculation loop (Phase 1)

The recirculation loop between the AD and the MEC that had been operating for 37 days in a previous assay (Chapter 7) was suppressed at the beginning of Phase 1. This configuration change resulted in a failure of the AD, with a drop in the COD removal efficiency from 40% down to 22% in two weeks (Figure 8.1a), increasing the COD of the effluent from 41 to 47 g L^{-1}, and in methane production, from 0.32 to 0.03 m^3 m^{-3} d^{-1} (Figure 8.1b). The VFA concentration increased to 10140 mg_{COD} L^{-1}, especially propionic (1215 mg L^{-1}), iso and n-butyric (900 and 561 mg L^{-1}, respectively) and iso and n-valeric (561 and 918 mg L^{-1}, respectively) (Figure 8.1c), in parallel with a IA:TA ratio increase to 0.49 (Figure 8.1c). The IA:TA ratio is a parameter used as an indicator of AD stability and it is considered that values higher than 0.30 are a sign of inhibition of the reactor. On the other hand, it has been reported that a propionic acid concentration of 900 mg L^{-1} results in significant inhibition of methanogens (Wang et al., 2009). The propionic acid concentration of the AD was over this value, so the observed inhibition was probably due to VFA rather than to ammonia concentration, since the highest free ammonia nitrogen (FAN) was of 732 mg L^{-1} (data not shown), far from inhibition values of 900 mg L^{-1} (Angelidaki and Ahring, 1993). However, the FAN levels may have inhibited certain groups of methanogens, since hydrogenotrophs have a higher tolerance to FAN that acetotrophs (Angelidaki and Ahring, 1993; Lee et al., 2014).

The behaviour of the AD during this phase indicates that the recirculation loop improved the system stability and robustness, and its suppression resulted in the inhibition of the reactor. As described in Chapter 7, the beneficial effect of the recirculation loop between the MEC and the AD can be due to i) the decrease of ammonia inhibition in the AD by ammonium removal and slightly decreasing the pH of the digestate in the MEC; ii) the reduction of the organic load of the AD thanks to the MEC removing part of the remaining COD and VFA; and iii) the biomass interaction between both reactors.

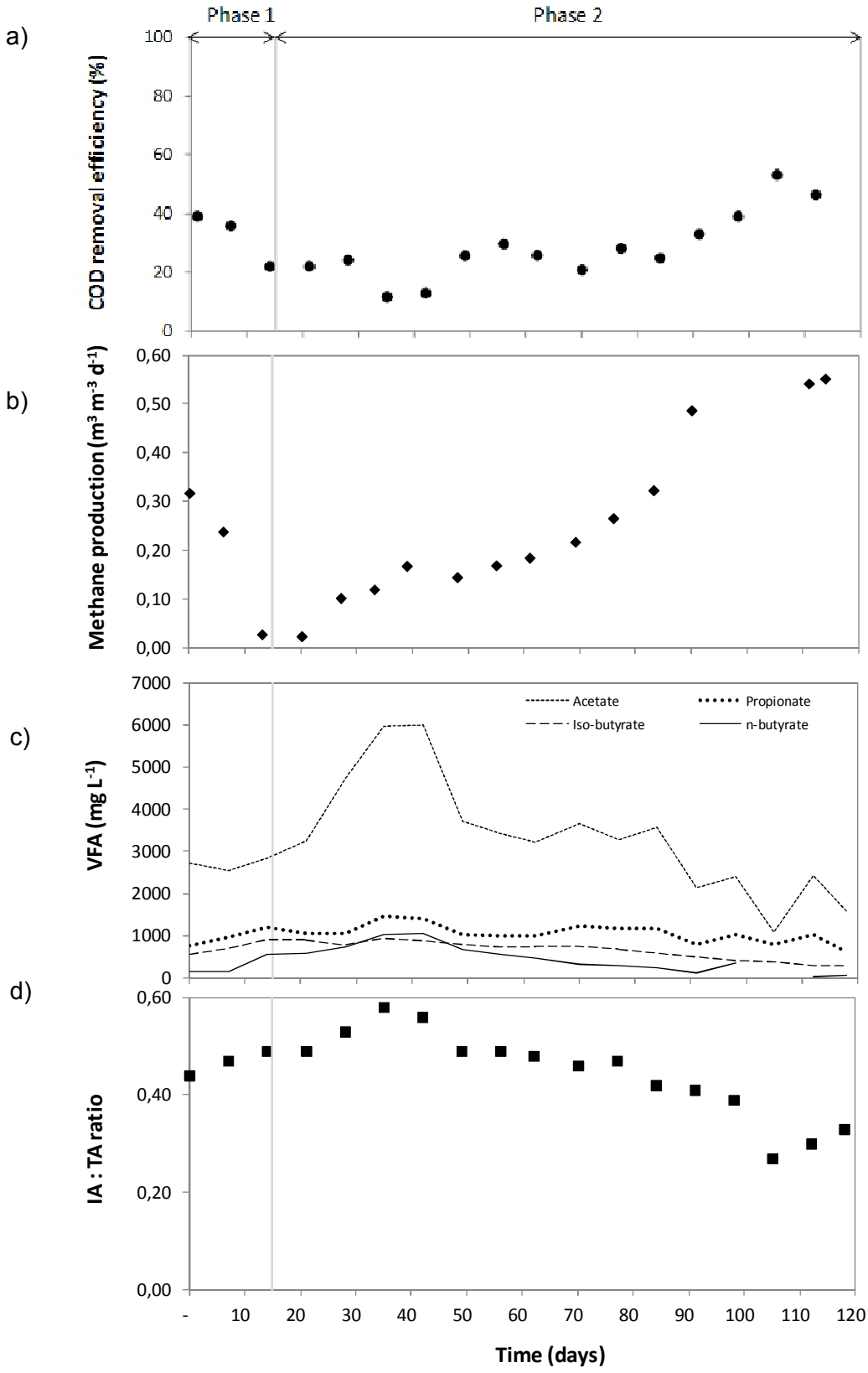

Figure 8.1 Performance of the AD regarding (a) COD removal efficiency; (b) methane production; (c) VFA concentration; and (d) IA:TA ratio.

8.3.2 Recovery of the AD after restarting the recirculation loop (Phase 2)

When the recirculation loop between the AD and the MEC was connected again, the AD showed a fast recovery in methane production, up to values of 0.55 m^3 m^{-3} d^{-1}, a 1.7 fold increase with respect to the initial value in Phase 1 (Figure 8.1b). The COD removal efficiency still decreased during 3 weeks after the restart of the recirculation, with a progressive increase afterwards up to values of 46% (effluent COD of 32 g L^{-1}), slightly higher than the initial one in Phase 1 (Figure 8.1a). Acetic acid concentration showed an increase during the same 3 weeks of lower COD removal efficiency, achieving values of 6000 mg L^{-1}, and a later decrease down to initial values for all the VFA was produced (Figure 8.1c). The same behaviour was observed regarding the IA:TA ratio (Figure 8.1d), achieving values of around 0.30 at the end of the Phase, thus improving the initial one.

The MEC achieved a maximum COD and ammonium removal efficiency of 29 and 34%, respectively, coincidentally with average current densities of around 2.5 A m^{-2} (Figure 8.2). This MEC high performance period is concurrent with the AD lowest performance period in terms of COD removal efficiency. The progressive decrease of the current density, and thus in the ammonium removal, shown in the MEC from day 80 to the end of the assay is due to the increase in the COD removal efficiency in the AD, so less organic matter is available for being converted into current in the MEC. The AD and MEC integrated system allowed this way to maintain the quality of the effluent in spite of the inhibition of the AD, keeping an overall COD removal efficiency above 35% during the poorest performance of the AD, with a maximum of 60±1% at the end of the assay (effluent COD of 25±1 g L^{-1}). This complementation between the performance of both reactors has been also described in Chapter 7, and allows not only to stabilise the AD, but also to polish the obtained effluent during AD malfunction periods. The present work has shown that the maintenance of the recirculation loop is necessary to sustain the operation of the AD under organic and nitrogen overload, suggesting that the improvement of its performance is not due to biomass acclimatisation.

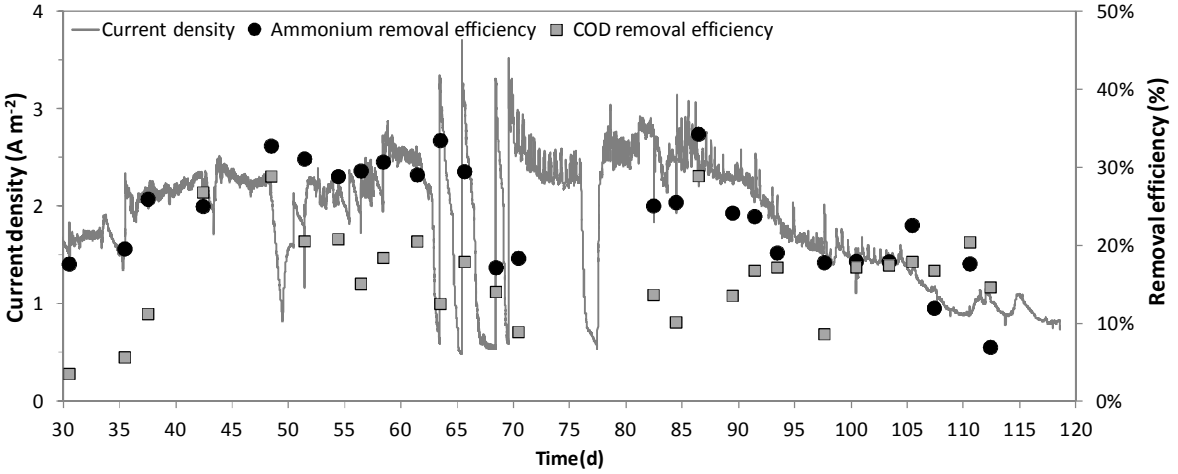

Figure 8.2 Performance of the MEC regarding current density and COD and ammonium removal efficiency (phase 2).

8.3.3 Microbial community assessment

The microbial community structure and activity of the samples taken from the AD effluent at the end of Phase 1 and 2 and from the carbon felt of the MEC reactor at the beginning and the end of the assays was characterised by means of total and active eubacteria and methanogenic archaea enumeration by means of qPCR/RT-qPCR, and 16SrDNA and 16SrRNA amplicon sequencing by means of MiSeq.

8.3.3.1 Quantitative analysis by qPCR

Figure 8.3 shows qPCR results of the four samples, regarding DNA (existence) and cDNA (active populations), for *16S* rRNA (eubacteria) and *mcr*A (methanogenic archaea) gene copy numbers. An increase in gene copy numbers regarding total eubacteria in the AD can be observed by the end of Phase 2, when the AD reactor was recovered after restarting the recirculation loop, with respect to Phase 1, or inhibited state, either in terms of DNA or cDNA for *16S* rRNA and *mcr*A genes. While *16S* rRNA gene copy numbers from DNA showed nearly a 2 fold increase in Phase 2, for *mcr*A gene the increase was of 1 order of magnitude, showing a recovery both in eubacteria and methanogenic archaea abundance in the AD. This recovery was also remarkable in the *16SrRNA* and *mcrA* transcript abundance, with a 4.5 fold raise. These results correlate well with a higher methane production of the AD in Phase 2 (Section 8.3.3). The lower *16S* rRNA gene copy numbers in Phase 1 may suggest that ammonia toxicity does not only affect methanogenic archaea but also hydrolysis and acidification processes performed by eubacteria, as stated in a previous work (El-Mashad et al., 2004).

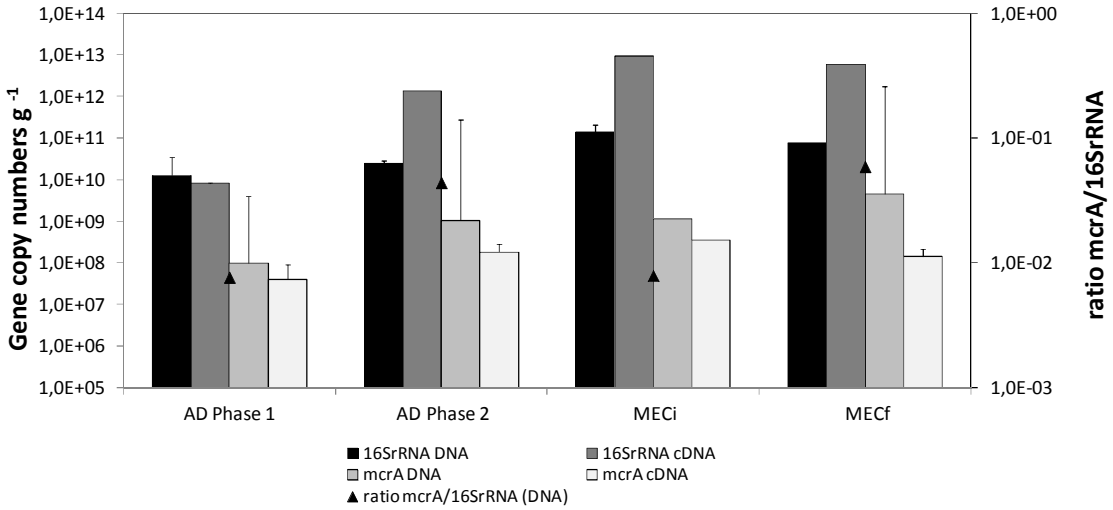

Figure 8.3 Gene copy numbers for 16S rRNA and mcrA genes and ratio between them of DNA and cDNA (gene expression), of the effluent of the AD at the end of Phases 1 and 2 and the initial and final MEC anode biofilm (MECi and MECf, respectively).

The MEC population showed similar gene copy numbers in DNA terms for both genes at the start and the end of the assay, pointing out a high stability of the anode biofilm population in spite of the changes introduced through the influent and the inhibition of the AD. The increase in *16S rRNA* abundance was concomitant to a decrease of *mcr*A transcripts (active methanogens). This fact would suggest that eubacteria population, including the exoelectrogenics group among them, are largely able to outcompete methanogenic archaea for organic substrates utilisation in these systems.

Therefore, combining simultaneous DNA and total RNA extraction has proven to be a useful technique to understand the dynamics of the biomass in the bioreactors, gaining insight in the really active population.

8.3.3.2 16SrRNA and 16SrDNA based high throughput sequencing of eubacteria and archaea

The reads and the coverage obtained for bacteria and archaeal community for each sample are shown in Table 8.3. Figure 8.4a shows that the dominant eubacterial *phylum* in the AD by the end of Phase 1 was *Firmicutes* (85%). At the end of Phase 2 its relative abundance decreased to 64%, while *Bacteroidetes* increased from 8 to 22%. However, when looking at the active populations (RNA-level), *Firmicutes* reduced its relative abundance from 81 to 35%, while *Proteobacteria* increased its activity with a relative abundance of 48% in Phase 2 (2% in Phase 1). At family level, *Clostridiaceae* (42%) and *Peptostreptococcaceae* (19%) were the predominant groups at the end of Phase 1 and Phase 2 (22 and 13% respectively), taking into account that during inhibited state or Phase 1 40% of the reads for cDNA were unclassified

sequences at 80% cut-off values according to Bayesian Classifier from RDP (Wang et al., 2007) (Figure 8.4b).

a)

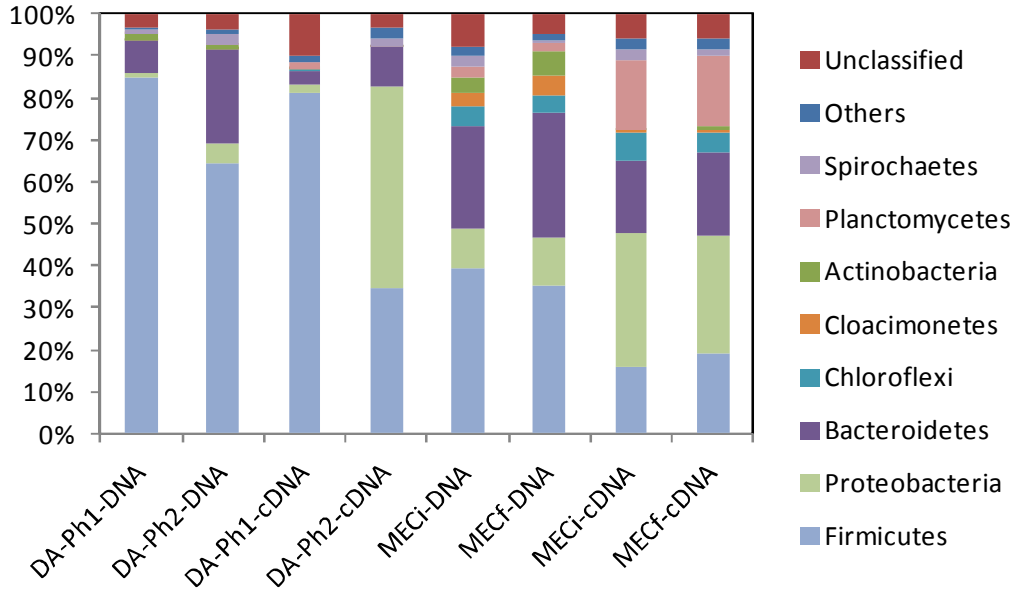

b)

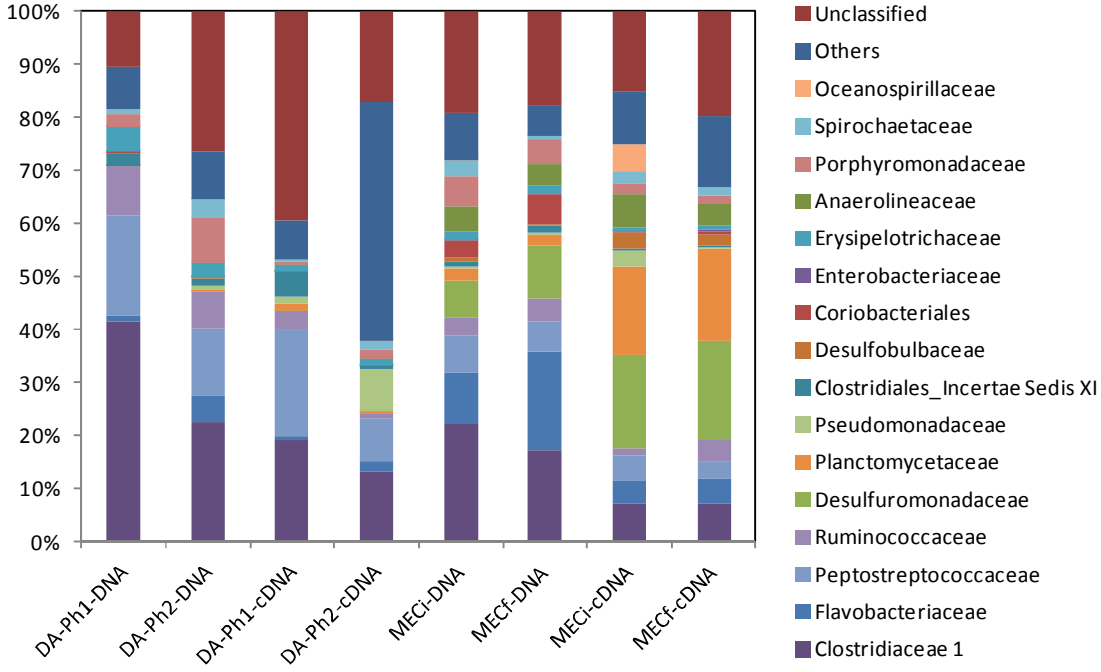

Figure 8.4 Taxonomic assignment of sequencing reads from Eubacterial community of the effluent of the AD at the end of Phases 1 (Ph1) and 2 (Ph2) and the initial and final MEC anode biofilm (MECi and MECf, respectively) for DNA and cDNA, at a) phylum b) family levels. Relative abundance was defined as the number of reads (sequences) affiliated with any given taxon divided by the total number of reads per sample. Phylogenetic groups with a relative abundance lower that 1% were categorised as “others”.

In the MEC anode biofilm, *Firmicutes* (39%) and *Bacteroidetes* (25%) were the dominant eubacterial *phyla*, followed by *Proteobacteria* (9%), with little changes between the samples at the start and the end of the assay (35, 30 and 11%, respectively, at the end of Phase 2) (Figure 8.4a). The three phyla have been identified in previous Chapters (5 and 7) and studies in BES (Bonmatí et al., 2013; Sotres et al., 2015b). When looking at active members *Proteobacteria*, *Firmicutes* and *Bacteroidetes accounted for* around 70% of *16S* rRNA relative abundance in both samples. And a new *phylum* appeared among the dominant ones, *Planctomycetes* (17% in both samples), in spite of its low relative abundance in *16S* rDNA amplicon reads (2%). *Planctomycetes phylum* is poorly known, and has been previously described in MFC focusing on Anammox processes (Li et al., 2015) or with wastewater or sludge inoculums (Kim et al., 2006; Zhang et al., 2012). At family level (Figure 8.4b), *Clostridiaceae*, *Flavobacteriaceae* and *Desulfuromonadaceae* were the predominant groups in the initial (22, 10 and 7%, respectively) and final sample (17, 19 and 10%, respectively). However, *Desulfuromonadaceae*, which is reported as an electroactive family in BES reactors (Logan, 2009) and has been enriched under MEC mode operation (Chapter 4; Cerrillo et al., 2016a), revealed as the most active family (18 and 19% relative abundance at RNA level (*16S* rRNA) in the initial and final samples, respectively), followed by *Planctomycetaceae* (17% in both samples).

Regarding archaeal community (Figure 8.5), an increase in *Methanobacteriaceae* relative abundance was observed from inhibited (73%) to stable phase (86%) in the AD, concomitant with a decrease in *Methanomicrobiaceae* (from 16 to 5%, respectively), being all the genus of both families exclusively hydrogenotrophic methanogens, such as *Methanoculleus*, *Methanobrevibacter* or *Methanothermobacter*. Changes of *mcrA* transcripts abundance in the AD have been more perceptible, accordingly to a previous study which suggested that methanogens in anaerobic sludge had a strong *mcr*A transcriptional response to ammonia stress without a change in the community structure (Zhang et al., 2014). For example, *Methanotrichaceae* (*Methanosaeta*), a minor acetotrophic family detected in DNA analysis, revealed as an active microorganism by the end of Phase 1, although suffering a sharp decrease during stable state (from 31 to 1%). This family was present in previous phases of the operation of the AD, as described in Chapter 7, so its detection in Phase 1 may reflect the evolution from this state. In turn, *Methanobacteriaceae* and *Methanomassiliicoccaceae* families, hydrogenotrophic and methylotrophic methanogens, respectively, increased their activity (*16S* rRNA) during stable operation (accounting from 15 to 36% and from 11 to 24%, respectively), while *Methanomicrobiaceae* remained stable (42 and 38% in Phase 1 and 2, respectively). Independently from the changes produced in the AD operation and methane production, the composition and activity of the biomass remained mainly dominated by hydrogenotrophic genus, probably due to the high ammonia concentration in the reactor, since acetotrophic

methanogens are usually more sensitive to the inhibitory effect of FAN (IC_{50} = 250 mg L^{-1}). FAN levels in the reactor were high enough to selectively inhibit their growth; and the low HRT of the anaerobic reactor also favoured hydrogenotrophic methanogens growth. The high concentration of ammonia in the reactor may be favouring the occurrence of potential syntrophic acetate oxidation processes (SAO) coupled to hydrogenotrophic methanogenesis route, which consist on the oxidation of methyl and carboxyl groups of acetate to CO_2, producing H_2, catalysed by the syntrophic acetate-oxidising bacteria (SAOB) (Hattori, 2008). Possible SAOB, as *Syntrophaceticus* or *Tepidanaerobacter*, were detected in the AD samples, although with a low relative abundance (0.75 and 0.48% for Phase 1 and 2, respectively). Apart from being more abundant in Phase 1, or inhibited state, they were also more active in this phase (0.29%) with respect to Phase 2 (0.05%), where the recirculation loop with the MEC was connected.

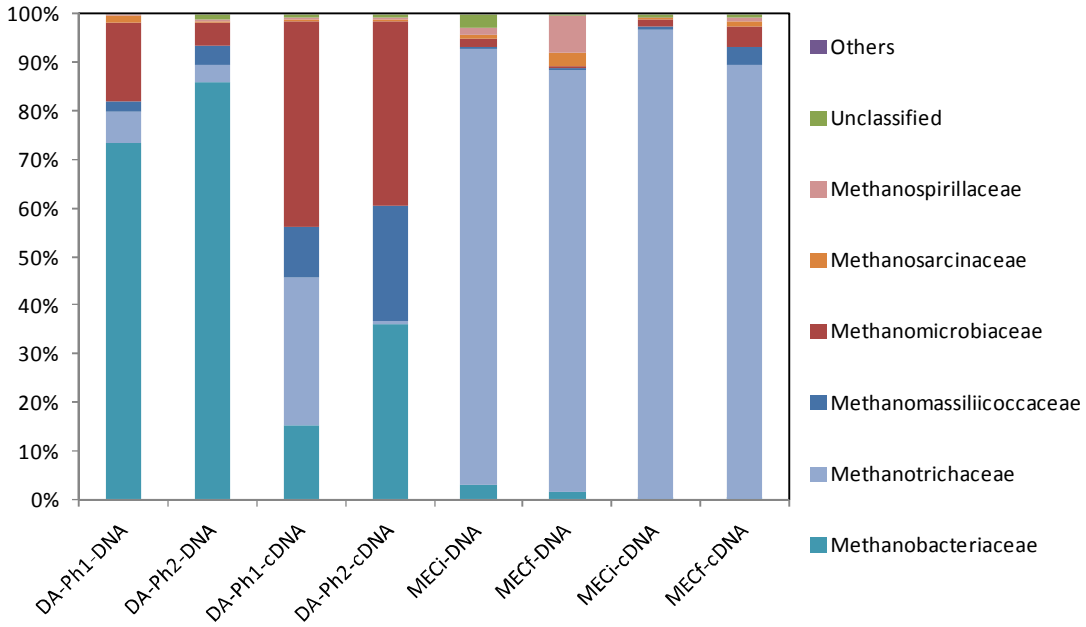

Figure 8.5 Taxonomic assignment of sequencing reads from Archaeal community of the effluent of the AD at the end of Phases 1 (Ph1) and 2 (Ph2) and the initial and final MEC anode biofilm (MECi and MECf, respectively) for DNA and cDNA at family level. Relative abundance was defined as the number of reads (sequences) affiliated with any given taxon divided by the total number of reads per sample. Phylogenetic groups with a relative abundance lower that 1% were categorised as "others".

In the case of MEC anode biofilm, the predominant and metabolically active phylotypes belonged to the archaea family of *Methanotrichaceae*, either in the initial or the final samples (90 and 87% for DNA and 97 and 89% for cDNA, respectively), showing a high stability in composition and activity in spite of changes in the influent. Contrary to these results, other studies have described the predominance of hydrogenotrophic methanogens on the BES anodes despite high concentrations of acetate in the substrate (Lu et al., 2012a; Lu et al., 2012b; Parameswaran et al., 2009; Shehab et al., 2013), and it is not clear if these archaea

were growing using hydrogen gas or electrons transferred from exoelectrogenic bacteria, since direct electron transfer from the cathode to a methanogenic biofilm has been recently described (Cheng et al., 2009). The work developed in Chapter 7 also revealed the enrichment in *Methanotrichaceae* in the MEC working in continuous with digested pig slurry, while a similar cell working in MFC mode with the same substrate evolved towards the enrichment in *Methanosarcinaceae*, able to develop the hydrogenotrophic route (Chapter 5). These results suggest that the operation mode may favour the selection of one or the other family. On the other hand, it has been recently described that *Methanothrix* (*Methanosaeta*) is capable of accepting electrons via direct interspecies electron transfer (DIET) for the reduction of carbon dioxide to methane (Rotaru et al., 2014), so additional and further assessments are necessary to better understand the role of this species in the anode of a MEC.

As a conclusion, the comparison between existing and active microorganisms through DNA and RNA extraction has revealed important differences in the obtained data and proves that analysis of *16S* rRNA at RNA level and *mcrA* transcript abundance is essential in order to evaluate the relationships and function of the different families of microorganisms.

8.3.3.3 Biodiversity analysis

Table 8.3 shows the results for the biodiversity analysis performed on AD and MEC samples. Regarding the eubacterial diversity, the inverted Simpson and Shannon indices showed that the sample of the AD at the end of Phase 2 was more diverse than in Phase 1. However, when looking at RNA-level, Phase 1 sample reveals as the most diverse one. Archaea biodiversity related to gene expression showed the opposite behaviour, with a higher biodiversity in Phase 2, while at DNA level the richness of Phase 1 sample is slightly higher. These results correlate with a better performance of the AD in Phase 2 (with connected loop), where more different archaea can be active thanks to the improvement of the conditions in the reactor.

Regarding the eubacterial diversity in the MEC anode biofilm, the initial sample showed a higher biodiversity than the final one, either in DNA or cDNA level. In Chapter 7 it was also reported a loss in biodiversity in the MEC biofilm when integrated with an AD. Biodiversity related to eubacterial *16S rRNA* (RNA level) in MEC was higher compared to both AD samples, and this fact can be of great importance to maintain the stability of the system in case of AD inhibition. Biodiversity for Archaea according to inverted Simpson and Shannon Weaver indices was very similar at DNA level, while it was higher by the end of the assay when looking at RNA-level. In this case, inversely to the behaviour detected for eubacterial biodiversity, values for *mcrA* transcripts and archaea *16S* rRNA diversity were lower in MEC than in AD samples,

confirming that methanogenic processes have less importance in MEC environments when compared to AD.

Table 8.3 Diversity index for Eubacterial and Archaeal community of the effluent of the AD at the end of Phases 1 and 2 and the initial and final MEC anode biofilm (MECi and MECf, respectively) (mean±standard deviation). Data normalised to the sample with the lowest number of reads (36854 and 62211 for eubacteria and archaea, respectively).

	Reads	Coverage	OTUs	Inverted Simpson	Shannon
Eubacteria					
AD-Ph1-DNA	50674	0.94±0.00	373±12	12.0±0.4	3.64±0.04
AD-Ph2 DNA	50751	0.91±0.00	550±15	31.1±1.1	4.52±0.03
AD-Ph1-cDNA	50897	0.94±0.00	391±12	17.2±0.5	3.88±0.03
AD-Ph2-cDNA	86842	0.94±0.00	352±12	7.3±0.3	3.34±0.04
MECi-DNA	46644	0.91±0.00	617±15	33.0±1.3	4.76±0.03
MECf-DNA	36854	0.91±0.00	549±15	19.4±0.8	4.34±0.04
MECi-cDNA	46641	0.92±0.00	533±14	27.5±1.0	4.51±0.03
MECf-cDNA	37766	0.92±0.00	535±15	17.8±0.7	4.33±0.04
Archaea					
AD-Ph1-DNA	102718	0.98±0.01	18±3	1.8±0.1	1.11±0.08
AD-Ph2 DNA	87626	0.97±0.01	23±3	1.5±0.1	0.90±0.09
AD-Ph1-cDNA	62211	0.98±0.01	26±3	4.8±0.3	2.01±0.06
AD-Ph2-cDNA	64716	0.96±0.01	33±3	7.9±0.4	2.41±0.06
MECi-DNA	112133	0.97±0.01	19±3	1.3±0.1	0.68±0.08
MECf-DNA	106114	0.98±0.01	15±3	1.4±0.1	0.70±0.07
MECi-cDNA	132548	0.98±0.01	10±2	1.1±0.0	0.34±0.06
MECf-cDNA	136706	0.98±0.01	17±3	1.3±0.0	0.58±0.07

8.3.3.4 Correspondence analysis

Correspondence analysis results for eubacteria community are shown in Figure 8.6a. MEC samples were closer together than AD samples, as it could be intuited in the sequencing analysis by the similarity of the relative abundance between the samples. Furthermore, final MEC samples moved away from AD samples, suggesting that in spite of the recirculating loop, both populations are able to evolve independently. The highest differentiation corresponded to AD samples regarding gene expression (cDNA), since the sequencing results showed a higher

population diversification, with the increase of “Others” group, composed by families with less than 1% of relative abundance.

Regarding archaea community, Figure 8.6b shows that MEC samples were clustered together, while the AD samples for DNA were well differentiated from cDNA samples. These results suggest that MEC archaea community was well established and maintained certain stability in composition in spite of slight variations in activity when influent characteristics were changed. However, AD samples showed higher differences either comparing inhibited and stable phases, or between composition and microbial activity of the community themselves. Summing up, microbial activity of the AD samples seemed to be less correlated to community composition than in the case of MEC samples.

a)

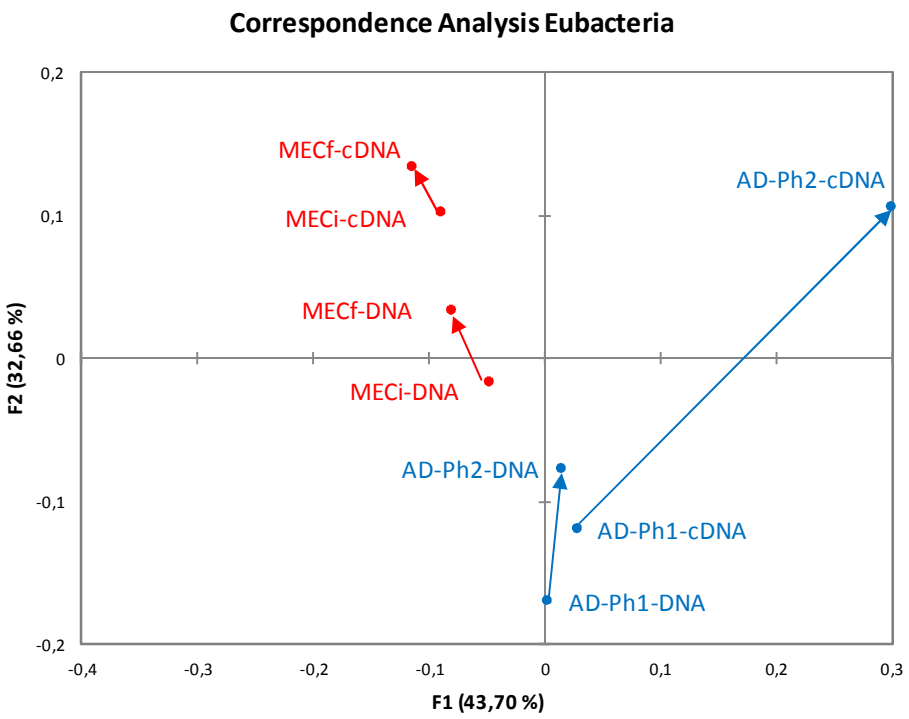

b)

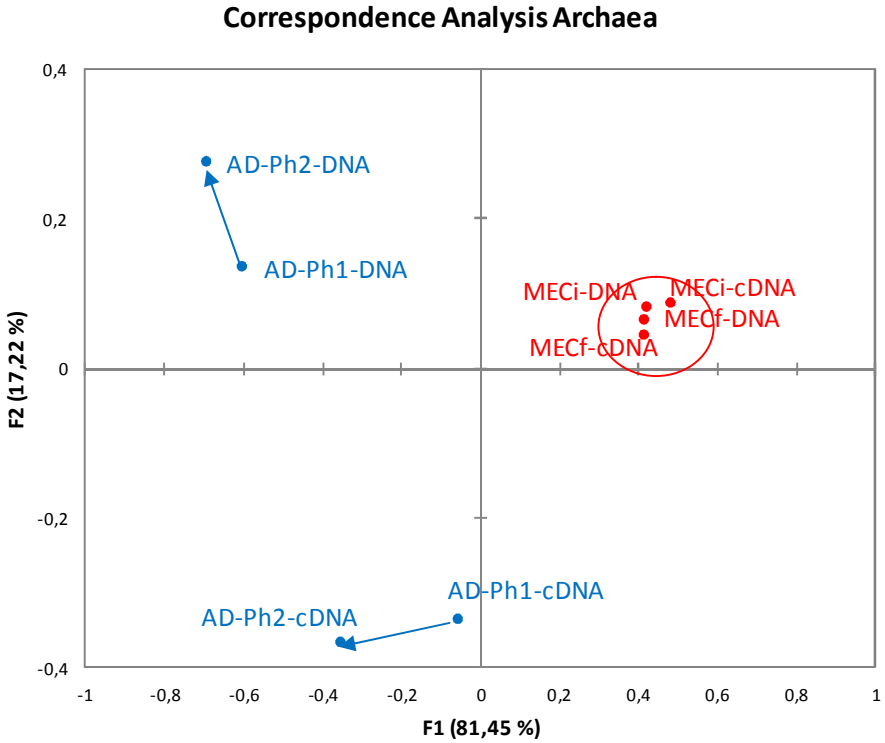

Figure 8.6 Correspondence Analysis of the effluent of the AD at the end of Phases 1 (Ph1) and 2 (Ph2) and the initial and final MEC anode biofilm (MECi and MECf, respectively) for DNA and cDNA samples regarding (a) Eubacteria and (b) Archaea community.

8.4 Conclusions

As a conclusion, the recirculation loop between the AD and the MEC allowed the first one to tolerate a high organic and nitrogen loading rate that other way would result in the inhibition of the reactor, increasing the methane production from 0.03 to 0.55 m^3 m^{-3} d^{-1}. Furthermore, the MEC process was able to improve the quality of the digestate during AD inhibition, achieving a maximum COD and ammonium removal efficiency of 29 and 34%, respectively, and overall AD-MEC COD removal efficiencies of around 60%. The microbial analysis of the AD biomass and the biofilm of the anode of the MEC showed that population composition differed from really active microorganisms according to *16S* rRNA (cDNA) amplicon sequencing. Regarding AD biomass, it was dominated by hydrogenotrophic methanogens (*Methanobacteriaceae*), as a result of the high ammonia concentrations in the reactor. MEC biofilm was stable both in diversity and activity. *Desulfuromonadaceae* revealed as the most active family in the MEC (18-19% of cDNA relative abundance in Phase 1 and 2) although not being the predominant one in DNA analysis. Furthermore, the populations of both reactors maintained well differentiated in spite of the existence of the recirculation loop, increasing the biodiversity of the system and suggesting that this configuration is more tolerant to stress than the AD operating alone. And finally, the obtained results demonstrated that AD microbial population was altered in response to the stress, while MEC consortium maintained its stability.

8.5 References

Angelidaki, I., Ahring, B.K. 1993. Thermophilic anaerobic digestion of livestock waste: the effect of ammonia. *Applied Microbiology and Biotechnology*, **38**(4), 560-564.

Bonmatí, A., Sotres, A., Mu, Y., Rozendal, R.A., Rabaey, K. 2013. Oxalate degradation in a bioelectrochemical system: Reactor performance and microbial community characterization. *Bioresource Technology*, **143**(0), 147-153.

Cerrillo, M., Oliveras, J., Viñas, M., Bonmatí, A. 2016a. Comparative assessment of raw and digested pig slurry treatment in bioelectrochemical systems. *Bioelectrochemistry*, **110**, 69-78.

Cerrillo, M., Viñas, M., Bonmatí, A. 2016b. Overcoming organic and nitrogen overload in thermophilic anaerobic digestion of pig slurry by coupling a microbial electrolysis cell. *Bioresource Technology*, *216*, 362-372.

Chen, Y., Cheng, J.J., Creamer, K.S. 2008. Inhibition of anaerobic digestion process: A review. *Bioresource Technology*, **99**(10), 4044-4064.

Cheng, S., Xing, D., Call, D.F., Logan, B.E. 2009. Direct biological conversion of electrical current into methane by electromethanogenesis. *Environmental Science & Technology*, **43**(10), 3953-3958.

Desloover, J., De Vrieze, J., Van de Vijver, M., Mortelmans, J., Rozendal, R., Rabaey, K. 2014. Electrochemical nutrient recovery enables ammonia toxicity control and biogas desulfurization in anaerobic digestion. *Environmental Science & Technology*, **49**(2), 948-955.

El-Mashad, H.M., Zeeman, G., van Loon, W.K.P., Bot, G.P.A., Lettinga, G. 2004. Effect of temperature and temperature fluctuation on thermophilic anaerobic digestion of cattle manure. *Bioresource Technology*, **95**(2), 191-201.

Hattori, S. 2008. Syntrophic acetate-oxidizing microbes in methanogenic environments. *Microbes and Environment*, **23**(2), 118-27.

Kim, G.T., Webster, G., Wimpenny, J.W.T., Kim, B.H., Kim, H.J., Weightman, A.J. 2006. Bacterial community structure, compartmentalization and activity in a microbial fuel cell. *Journal of Applied Microbiology*, **101**(3), 698-710.

Lee, J., Hwang, B., Koo, T., Shin, S.G., Kim, W., Hwang, S. 2014. Temporal variation in methanogen communities of four different full-scale anaerobic digesters treating food waste-recycling wastewater. *Bioresource Technology*, **168**, 59-63.

Li, C., Ren, H., Xu, M., Cao, J. 2015. Study on anaerobic ammonium oxidation process coupled with denitrification microbial fuel cells (MFCs) and its microbial community analysis. *Bioresource Technology*, **175**, 545-552.

Logan, B.E. 2009. Exoelectrogenic bacteria that power microbial fuel cells. *Nature Reviews Microbiology*, **7**(5), 375-381.

Lu, L., Xing, D., Ren, N. 2012a. Bioreactor performance and quantitative analysis of methanogenic and bacterial community dynamics in microbial electrolysis cells during large temperature fluctuations. *Environmental Science & Technology*, **46**(12), 6874-6881.

Lu, L., Xing, D., Ren, N. 2012b. Pyrosequencing reveals highly diverse microbial communities in microbial electrolysis cells involved in enhanced H_2 production from waste activated sludge. *Water Research*, **46**(7), 2425-2434.

Munk, B., Bauer, C., Gronauer, A., Lebuhn, M. 2012. A metabolic quotient for methanogenic Archaea. *Water Science and Technology*, **66**(11), 2311-7.

Neidhardt, F.C., C.I.R., Ingraham, J.L., Lin, E.C.C, Low, K.B., Magasanik, B., Reznikoff, W.S., Riley, M., Schaechter, M., Umbarger, H.E., eds. 1996. *Escherichia coli* and *Salmonella*: cellular and molecular biology. 2nd ed. ASM Press, Washington, D.C.

Nielsen, H.B., Angelidaki, I. 2008. Strategies for optimizing recovery of the biogas process following ammonia inhibition. *Bioresource Technology*, **99**(17), 7995-8001.

Palatsi, J., Laureni, M., Andres, M.V., Flotats, X., Nielsen, H.B., Angelidaki, I. 2009. Strategies for recovering inhibition caused by long chain fatty acids on anaerobic thermophilic biogas reactors. *Bioresource Technology*, **100**(20), 4588-96.

Parameswaran, P., Torres, C.I., Lee, H.-S., Krajmalnik-Brown, R., Rittmann, B.E. 2009. Syntrophic interactions among anode respiring bacteria (ARB) and Non-ARB in a biofilm anode: electron balances. *Biotechnology and Bioengineering*, **103**(3), 513-523.

Rajagopal, R., Massé, D.I., Singh, G. 2013. A critical review on inhibition of anaerobic digestion process by excess ammonia. *Bioresource Technology*, **143**, 632-641.

Rotaru, A.-E., Shrestha, P.M., Liu, F., Shrestha, M., Shrestha, D., Embree, M., Zengler, K., Wardman, C., Nevin, K.P., Lovley, D.R. 2014. A new model for electron flow during anaerobic digestion: direct

interspecies electron transfer to *Methanosaeta* for the reduction of carbon dioxide to methane. *Energy & Environmental Science*, **7**(1), 408-415.

Shehab, N., Li, D., Amy, G.L., Logan, B.E., Saikaly, P.E. 2013. Characterization of bacterial and archaeal communities in air-cathode microbial fuel cells, open circuit and sealed-off reactors. *Applied Microbiology and Biotechnology*, **97**(22), 9885-9895.

Sotres, A., Cerrillo, M., Viñas, M., Bonmatí, A. 2015a. Nitrogen recovery from pig slurry in a two-chambered bioelectrochemical system. *Bioresource Technology*, **194**, 373-382.

Sotres, A., Díaz-Marcos, J., Guivernau, M., Illa, J., Magrí, A., Prenafeta-Boldú, F.X., Bonmatí, A., Viñas, M. 2015b. Microbial community dynamics in two-chambered microbial fuel cells: effect of different ion exchange membranes. *Journal of Chemical Technology & Biotechnology*, **90**(8), 1497-1506.

Wang, Q., Garrity, G.M., Tiedje, J.M., Cole, J.R. 2007. Naïve bayesian classifier for rapid assignment of rRNA sequences into the new bacterial taxonomy. *Applied and Environmental Microbiology*, **73**(16), 5261-5267.

Wang, Y., Zhang, Y., Wang, J., Meng, L. 2009. Effects of volatile fatty acid concentrations on methane yield and methanogenic bacteria. *Biomass and Bioenergy*, **33**(5), 848-853.

Yenigün, O., Demirel, B. 2013. Ammonia inhibition in anaerobic digestion: A review. *Process Biochemistry*, **48**, 901-911.

Zhang, C., Yuan, Q., Lu, Y. 2014. Inhibitory effects of ammonia on methanogen mcrA transcripts in anaerobic digester sludge. *FEMS Microbiology Ecology*, **87**(2), 368-377.

Zhang, G., Zhao, Q., Jiao, Y., Wang, K., Lee, D.-J., Ren, N. 2012. Efficient electricity generation from sewage sludge using biocathode microbial fuel cell. *Water Research*, **46**(1), 43-52.

CHAPTER 9

Assessment of active methanogenic archaea in a methanol-fed upflow anaerobic sludge blanket reactor

Part of the content of this chapter has been submitted to a peer reviewed journal as:

Míriam Cerrillo, Lluís Morey, Marc Viñas, August Bonmatí. Assessment of active methanogenic archaea in a methanol-fed upflow anaerobic sludge blanket reactor

Abstract

Methanogenic archaea enrichment of a granular sludge was undertaken in an upflow anaerobic sludge blanket reactor (UASB) fed with methanol in order to enrich methylotrophic and hydrogenotrophic methanogenic populations. A microbial community assessment, in terms of microbial composition and activity –throughout the different stages of the feeding process with methanol and acetate– was performed, using specific methanogenic activity assays (SMA), quantitative real-time polymerase chain reaction (qPCR), and high throughput sequencing of 16S rRNA genes from DNA and cDNA. Distinct methanogenic enrichment was revealed by qPCR of *mcrA* gene in the methanol-fed community, being two orders of magnitude higher with respect to initial inoculum, and achieving a final *mcrA*/*16S rRNA* ratio of 0.25. High throughput sequencing analysis revealed that the resulting methanogenic population was mainly composed by methylotrophic archaea (*Methanomethylovorans* and *Methanolobus* genus*)*, being also highly active according to the RNA-based assessment. SMA confirmed that the methylotrophic pathway, with a direct conversion of methanol to CH_4, was the main step of methanol degradation in the UASB. The biomass from UASB, enriched in methanogenic archaea, may bear a great potential as further inoculum for an electromethanogenic biocathode of a microbial electrolysis cell (MEC) intended for biogas upgrading.

9.1 Introduction

Biogas production in anaerobic digestion plants is spreading due to its potential as an alternative to fossil fuels. This renewable energy carrier can be stored and used in different applications, such as heating or electricity production, or upgraded to biomethane to inject into the grid or to use as transport fuel. Raw biogas consists mainly of methane (CH_4, 40-75%) and carbon dioxide (CO_2, 15-60%), and trace amounts of other components such as water (H_2O, 5-10%), hydrogen sulphide (H_2S, 0.005-2%) or ammonia (NH_3, <1%) (Ryckebosch et al., 2011). In order to transform biogas into biomethane, a cleaning and upgrading process should be performed. Upgrading consists in the adjustment of the calorific value of the biogas –separating CH_4 from CO_2– generally performed in order to meet the standards required to use it as vehicle fuel or for injection in the natural gas grid. After biogas transformation, applying techniques for biogas upgrading, such as pressure swing adsorption, membrane separation or chemical CO_2-absorption, the final product obtained typically contains 95-97% of CH_4 and 1-3% of CO_2 (Ryckebosch et al., 2011). An alternative to these enrichment techniques, focused on CO_2 removal without changing CH_4 mass, is biological methane enrichment using hydrogenotrophic methanogenic populations capable of using CO_2 as a carbon source, and H_2 as an energy source and convert them to CH_4 (Equation 9.1) (Strevett et al., 1995), or even capable of obtaining these electrons directly from the cathode in a process known as electromethanogenesis (Cheng et al., 2009).

$$4H_2 + CO_2 \rightarrow CH_4 + H_2O \qquad (9.1)$$

Various studies about electromethanogenesis taking place in bioelectrochemical systems (BES) have been developed (Villano et al., 2011), and certain hydrogenotrophic methanogens have been identified as the key players of this process (Van Eerten-Jansen et al., 2013). Hydrogenotrophic methanogens belong to the orders *Methanobacteriales*, *Methanococcales*, *Methanomicrobiales* and *Methanosarcinales* (Karakashev et al., 2005). Thus, obtaining a biomass rich in these microorganisms to be used as inoculum could accelerate the start up of the methane producing BES.

Upflow anaerobic sludge blanket reactors (UASB) are suitable for enriching methanogenic archaea because they can be operated at low hydraulic retention times (HRT). Bhatti et al. (1996) investigated the feasibility of methanolic waste treatment in an UASB reactor and demonstrated that methanol can be converted to methane via at least three routes. Later, Vavilin (2010) developed a model for explaining the metabolic pathways for methanol degradation with ^{13}C-labeled methanol. Methanol can either be i) directly converted to methane

by methylotrophic methanogens (Equation 9.2), ii) generated via the intermediate formation of acetate (acetogenesis) and later converted to methane by acetoclastic methanogens (Equations 9.3 and 9.4), iii) or by hydrogenotrophic methanogens, with the use of H_2 and CO_2 (Equation 9.5 and 9.6).

$$4CH_3OH \rightarrow 3CH_4 + CO_2 + 2H_2O \quad (9.2)$$

$$4CH_3OH + 2H_2CO_3 \rightarrow 3CH_3COOH + 4H_2O \quad (9.3)$$

$$CH_3COOH + H_2O \rightarrow CH_4 + H_2CO_3 \quad (9.4)$$

$$CH_3OH + 2\ H_2O \rightarrow 3\ H_2 + HCO_3^- + H^+ \quad (9.5)$$

$$4\ H_2 + 2\ HCO_3^- + H^+ \rightarrow CH_4 + 3\ H_2O \quad (9.6)$$

Therefore, methanol feeding can be an alternative for the enrichment of hydrogenotrophic methanogenic archaea inoculum to CO_2/H_2 gassing or cultivation in an electrochemical bioreactor.

The main aim of this study was to assess the utilisation of a methanol-fed UASB as a system for enriching a granular sludge in methanogenic archaea and characterise the evolution of the microbial community when shifting from acetate to methanol substrate, in terms of composition and activity using quantitative real-time polymerase chain reaction (qPCR) and high throughput sequencing of *16S rDNA* and *16S rRNA*. Specific methanogenic activity tests (SMA) were also performed so as to corroborate the results obtained through the microbial community analysis regarding active methanol routes in the UASB.

9.2 Materials and methods

9.2.1 Experimental set-up

A lab-scale UASB reactor described in Section 3.1.5 was used to perform the experiment.

9.2.2 Reactor operation

The UASB was fed in continuous mode with a mineral medium, with a hydraulic retention time (HRT) fixed at 6 h. The reactor was operated for 416 days in 3 different phases (Table 9.1). The UASB was initially fed with an acetate influent for 214 days, increasing the organic loading rate (OLR) from 3 to 10 $kg_{COD}\ m^{-3}\ d^{-1}$ in order to activate the biomass and acclimate it to a high OLR (Phase 1). Having achieved high operational performance, the feed was progressively changed to methanol substrate during 21 days (Phase 2). And finally, only methanol was used as substrate for another 180 days, in order to promote the enrichment in methanogenic archaea biomass (Phase 3). The mineral medium contained acetate and/or

methanol as organic carbon source, in concentrations shown in Table 9.1 for each phase, and (per litre of deionised water): NH_4Cl, 1.33 g; $CaCl_2$, 0.04 g ; KH_2PO_4, 3 g; Na_2HPO_4, 6 g; $MgSO_4$ 0.25 g; yeast extract, 0.1 g and 1 mL of a trace mineral solution. The trace mineral solution contained (per litre of deionised water): $FeCl_3 \cdot H_2O$, 1.50 g; H_3BO_3, 0.15 g; $CuSO_4 \cdot 5H_2O$, 0.03 g; KI, 0.18 g; $MnCl_2 \cdot 4H_2O$, 0.12 g; $Na_2MoO_4 \cdot 2H_2O$, 0.06 g; $ZnSO_4 \cdot 7H_2O$, 0.12 g; $CoCl_2 \cdot 6H_2O$, 0.15 g; $NiCl_2 \cdot 6H_2O$, 0.023 g; EDTA, 10 g (Lu et al., 2006).

Table 9.1 Operational conditions of the UASB reactor.

Phase	Length (d)	OLR (kg_{COD} m^{-3} d^{-1})	Acetate concentration (g L^{-1})	Methanol concentration (g L^{-1})	Aim of the phase
1	135	3.25	1.02	0	Start-up, activation of the biomass and acclimatisation to high OLR
	7	6.05	1.89	0	
	7	8.44	2.64	0	
	65	10.08	3.15	0	
2	7	10.08	2.01	0.53	Acclimatisation of the biomass to methanol feeding
	7	10.08	1.34	1.06	
	7	10.08	0.67	1.58	
3	180	10.08	0	2.11	Enhancement of the biomass enrichment

9.2.3 Analyses and calculations

Reactor head space methane content, soluble chemical oxygen demand (CODs) and pH of the UASB effluent were used as control parameters for each experimental condition. All the analyses were performed following the methods described in Section 3.2. CODs removal efficiency was calculated as described in Section 3.4.

The SMA of the anaerobic granular sludge used as inoculum, and by the end of Phase 1 (acetate operation) and Phase 3 (methanol operation) was evaluated as described in Section 3.2.12.

A microbial community assessment in the initial UASB inoculum and in the granular sludge by the end of Phase 1 (acetate feed) and Phase 3 (methanol feed) was performed by means of both culture-independent molecular techniques such as quantitative real-time polymerase chain reaction (qPCR), and high throughput sequencing (MiSeq, Illumina) of *16S* rDNA and *16S* rRNA. Simultaneous total genomic DNA and RNA extraction and complementary DNA (cDNA) synthesis, qPCR and high throughput 16S rRNA gene sequencing (MiSeq, Illumina) were performed following the methods described in Section 3.6.2, 3.6.3, and 3.6.5,

respectively. Standard curve parameters of the qPCRs performed had a high efficiency, and were as follows (for *16S rRNA* and *mcrA*, respectively): slope of -3.515 and -3.558; correlation coefficient of 0.999 and 0.996; efficiency of 93 and 91%. Data obtained from sequencing datasets were deposited in the Sequence Read Archive of the National Centre for Biotechnology Information (NCBI) under study accession number SRP071847, for eubacterial and archaeal populations.

The evaluation of the diversity of the samples and statistical multivariate analyses were performed following Section 3.6.6.

9.3 Results and discussion

9.3.1 Operation performance

Average COD removal efficiencies and methane content in the biogas for each phase are shown in Table 9.2. The COD removal efficiency by the end of Phase 1 was of 82±12%, gradually increasing during the acetate shift to methanol, up to an average value of 97±1% by the end of Phase 3. It was in the range of the 86-98% obtained with a similar OLR as the one previously described by Badshah et al. (2012). These values are also comparable or even higher than those described in previous studies with higher OLR, such as 97.1% and 92.5% with an OLR of 30 and 48 kg_{COD} m^{-3} d^{-1}, respectively (Kobayashi et al., 2011; Lu et al., 2015); showing high adaptation of the UASB biomass to the methanol feeding. Methane content in the head space of the reactor increased from 68±14%, when using acetate as feed, to 85±1% during the methanol fed phase. The low methane content during Phase 1 was partly due to operational problems with the outlet of the reactor, which led to air flowing into the head space.

Table 9.2 Average performance of the UASB reactor in the different operational phases.

Phase	Carbon source (% COD)		OLR (kg_{COD} m^{-3} d^{-1})	COD removal efficiency (%)	Biogas CH_4 content (%)
	Acetate	Methanol			
1	100	0	3.25	73±9	22±8
			6.05	74±1	41±1
			8.44	82±3	32±1
			10.08	82±12	68±14
2	75	25	10.08	70±16	70±0
	50	50	10.08	93±13	81±8
	50	75	10.08	96±1	81±3
3	0	100	10.08	97±1	85±1

9.3.2 Metabolic pathways and granular sludge activity

To better understand the metabolic pathways of methanol in the UASB (Vavilin, 2010), and assess the activity of the biomass in the UASB reactor, both the SMA of the granules used as inoculum and from the samples taken at the end of Phase 1, of activation with acetate, and Phase 3, of methanol feed, were determined with different substrates (VFA mix, acetate, H_2, and methanol). Table 9.3 shows that by the end of Phase 3, the granular sludge had a high SMA for methanol, acetate and VFA mix (470; 239 and 220 mg COD_{CH4} g^{-1} VSS d^{-1}, respectively), while being 20-40 fold lower for H_2 (12 mg COD_{CH4} g^{-1} VSS d^{-1}). Nevertheless, this later value increased 6 times with respect to the one corresponding to the acetate feeding phase (2 mg COD_{CH4} g^{-1} VSS d^{-1}). Again, the VFA mix and acetate SMA showed values 70 times higher than those of the H_2 assay. These results suggest that in spite of the long term operation of the reactor with methanol as the sole carbon source (180 days), the granular sludge did not completely lose its acetate utilisation capacity. Other studies have reported the loss of acetic activity after long periods of methanol feeding (Paulo et al., 2003). A recent study stated that after operating an UASB with methanol for 143 days, the granules presented an acetate SMA of 150 mg COD_{CH4} g^{-1} VSS d^{-1}, losing completely this capacity after 300 days of operation (Lu et al., 2015). In this same study, higher SMA values were achieved for H_2 and methanol (0.08 and 2.11 g COD_{CH4} g^{-1} VSS d^{-1}, respectively) than those obtained in the present study. From the SMA results, it can be concluded that the main pathway in the UASB reactor for methanol conversion to methane is more likely methylotrophic methanogenesis, although the conservation of the acetate activity suggests that the acetogenesis-acetoclastic route may be taking place as well. Finally, such a low hydrogenotrophic activity indicates that the methanol oxidation followed by hydrogenotrophic methanogenesis was not promoted in the operational conditions applied in the UASB, the hydrogenotrophic methanogenic enrichment not taking place. Nevertheless, these hypotheses should be confirmed by the microbial community assessment simultaneously performed.

Table 9.3 Specific methanogenic activity (SMA) of the inoculum and Phase 1 and 3 granular sludge fed with different substrates. n.d: not determined.

Phase	SMA (mg COD_{CH4} / g VSS d)			
	VFA Mix	Acetate	H_2	Methanol
Inoculum	107	125	40	n.d.
1	138	149	2	n.d.
3	220	239	12	470

9.3.3 Microbial community assessment

The microbial community structure and the activity of the samples taken from the initial inoculum and the biomass in the UASB by the end of Phase 1 (acetate feeding) and 3 (methanol feeding) were characterised by means of qPCR technique and high throughput sequencing of 16S rRNA gene of total and active eubacteria and archaea by MiSeq.

9.3.3.1 Quantitative analysis by qPCR

qPCR results of the 3 samples, regarding DNA (present microorganisms) and cDNA (active microbial populations), for *16S* rRNA (eubacteria) and *mcr*A (methanogenic archaea) gene copy numbers showed a progressive increase in *mcr*A gene copy numbers from the inoculum to the biomass sample by the end of Phase 3 (Figure 9.1). This result correlates with the increase in methane content in the biogas in the UASB (Section 9.3.1). An increase of two orders of magnitude of *mcrA* gene (at DNA level) in Phase 3 in comparison to the initial inoculum ($1.13 \cdot 10^{10}$ and $1.25 \cdot 10^{8}$ gene copy numbers g^{-1}, respectively) was revealed, while the *mcrA* expression (cDNA level) in Phase 3 was twice the obtained in Phase 1 ($4.76 \cdot 10^{8}$ and $2.46 \cdot 10^{8}$ gene copy numbers g^{-1}, respectively). On the contrary, *16S* rRNA gene copy numbers remained in the same order of magnitude in both Phases and initial inoculum. As a consequence, the highest *mcr*A/*16S* rRNA gene ratio achieved was of 0.25, by the end of Phase 3. These quantitative results prove that a progressive enrichment in methanogenic archaea was taking place in the reactor biomass, and that its activity was coincident with an enhancement of methane production. Since the ratio between methanogenic archaea and eubacteria in the biomass clearly increased during the methanol feeding phase of the UASB, it may harbour a great potential as inoculum for an electromethanogenic biocathode MEC intended for biogas upgrading.

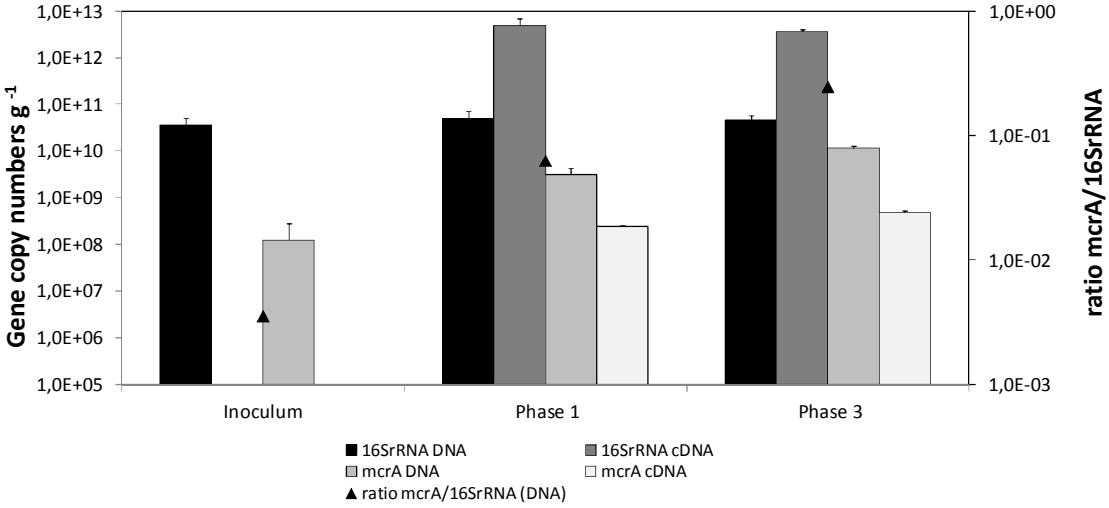

Figure 9.1 Gene copy numbers for *16S* rRNA and *mcr*A genes and ratio between them of DNA and mRNA (cDNA), of the initial inoculum and the biomass of the UASB at the end of Phases 1 (acetate feeding) and 3 (methanol feeding).

9.3.3.2 Sequencing results for eubacteria and archaea

In the high throughput sequencing analysis (MiSeq) 2,770 and 483 OTUs were detected for eubacteria and archaea, respectively, with 50,466-64,777 reads for eubacteria and 66,226-121,706 reads for archaea. Figure 9.2a shows the relative abundance of eubacterial *phyla* in the inoculum and the anaerobic granular sludge of the UASB at the end of Phase 1 (acetate feeding) and 3 (methanol feeding), both at DNA and RNA (cDNA) level. Although *Proteobacteria* was the predominant *phylum* in the inoculum (39%), *Bacteroidetes*, *Firmicutes* and *Synergistetes* grew into the most abundant in Phase 1 (40, 26 and 14%, respectively) and Phase 3 samples (61, 14 and 8%, respectively). At gene expression level (cDNA), relative abundance of the predominant *phylum* was consistent with the obtained for DNA, except for an increase up to 22% in *Proteobacteria* in Phase 1 sample and a general reduction of *Synergistetes phylum*. At family level, between 24% and 74% of the OTUS were unclassified, Phase 3 sample showing the highest values (Figure 9.2b). Of the classified OTUs, *Pseudomonadaceae* accounted for 37% of the relative abundance in the inoculum, it being below 1% in the granular sludge of the UASB in Phase 1 and Phase 3. *Porphyromonadaceae*, *Ruminococcaceae* and *Synergistaceae* were the predominant families in Phase 1 (28, 13 and 14%, respectively), though less abundant in Phase 3 (14, 6 and 8%, respectively). The first family, *Porphyromonadaceae,* maintained its predominance as an active group (cDNA level) in Phase 1 (19%), and *Desulfobulbaceae* revealed itself as a highly active family (15%) in spite of its low relative abundance (2%) at DNA level. Finally, regarding Phase 3 sample, no clear

dominant active families were highlighted, due to the high number of unclassified OTUs (74%). 78% of the unclassified OTUs obtained in Phase 3 cDNA sample correspond to *Bacteroidetes* phylum, and 21% to *Firmicutes*. These OTUs that cannot be assigned to a known family could be novel taxa or perhaps still poorly defined in the RDP database.

As for archaea population, Figure 9.3 shows a clear *Methanosarcinaceae* family enrichment in the UASB, particularly in Phase 3, both in community composition and activity (52 and 64% of relative abundance, respectively). On the contrary, *Methanotrichaceae*, an acetotrophic family formerly known as *Methanosaetaceae*, was clearly reduced during Phase 3, due to methanol feeding, and although maintaining 19% of relative abundance at DNA level, solely represented 3% of all OTUs at cDNA level. Nevertheless, its presence is relevant as correlates well with the results obtained in the SMA test, in which the acetic activity of the granular sludge was high (Section 9.3.2) when acetate was used as feed. The fact that the *Methanotrichaceae (Methanosaeta)* family was still active after 180 days of methanol feeding as the sole carbon source suggest that the homoacetogenic route may be responsible of methanol transformation to acetate. Bicarbonate plays an important role in the anaerobic conversion of methanol, as a required co-substrate in the acetogenic breakdown. Although bicarbonate was not added to the medium used in this assay in order to avoid the acetogenic route, it is produced when methanol is converted into methane (Equation 9.4). According to stoichiometry, up to one third of the methanol can potentially be consumed by acetogens from the endogenous methanogenic supplied bicarbonate (Florencio et al., 1997). Indeed, the methylotrophic acetogenic eubacteria *Sporomusa* was active in the granular sludge with a low relative abundance (0.2 %), and may be involved in the conversion of methanol to acetate. In Phase 1, the *Methanotrichaceae* family accounted for the highest relative abundance at cDNA level (60%), demonstrating its high activity during acetate feeding, in spite of presenting a lower relative abundance at DNA level (39%). However, according to a recent study, it seems that *Methanothrix* (*Methanosaeta*) is capable of accepting electrons via direct interspecies electron transfer (DIET) to reduce carbon dioxide to methane (Rotaru et al., 2014) and not being strictly aceticlastic. To what extend it could have a role in the hydrogenotrophic route in Phase 3 should be analysed in depth. *Methanobacteriaceae* and *Methanoregulaceae*, families where most of its members obtain energy from the reduction of CO_2 with H_2, decreased their relative abundance during Phase 3 (10% and not detected, respectively), thus suggesting that the enrichment in the hydrogenotrophic methanogenic group, aim of this work, was not achieved. Conversely, genus *Methanomethylovorans* and *Methanolobus*, both part of the *Methanosarcinaceae* family and defined as methylotrophs (Jiang et al., 2005; Mochimaru et al., 2009), were the predominant and most active groups. These were followed by the *Thermoplasmatales* genus (*Methanossiliicoccaceae* family), which is also capable of using methanol as a substrate

(Poulsen et al., 2013). The predominance of methylotrophic groups agrees with the results of the SMA test, which showed a high activity with methanol substrate.

a)

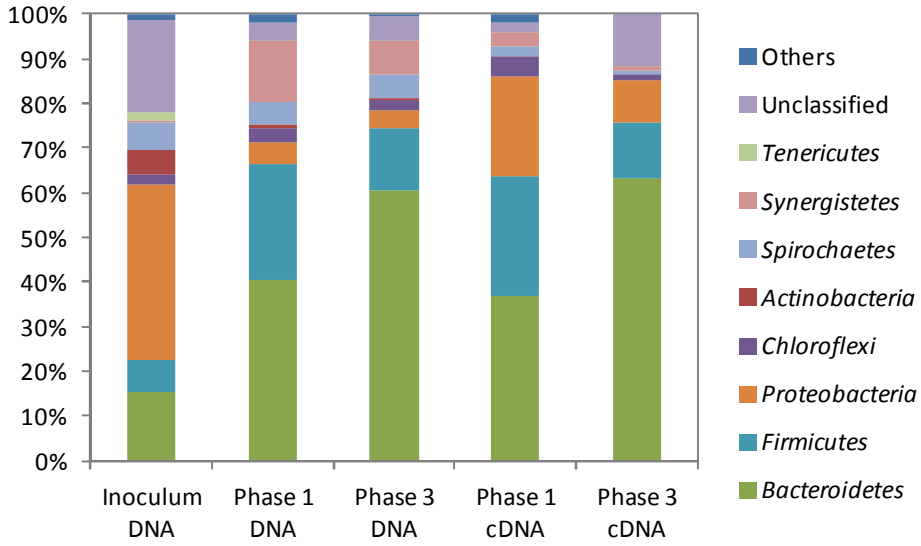

b)

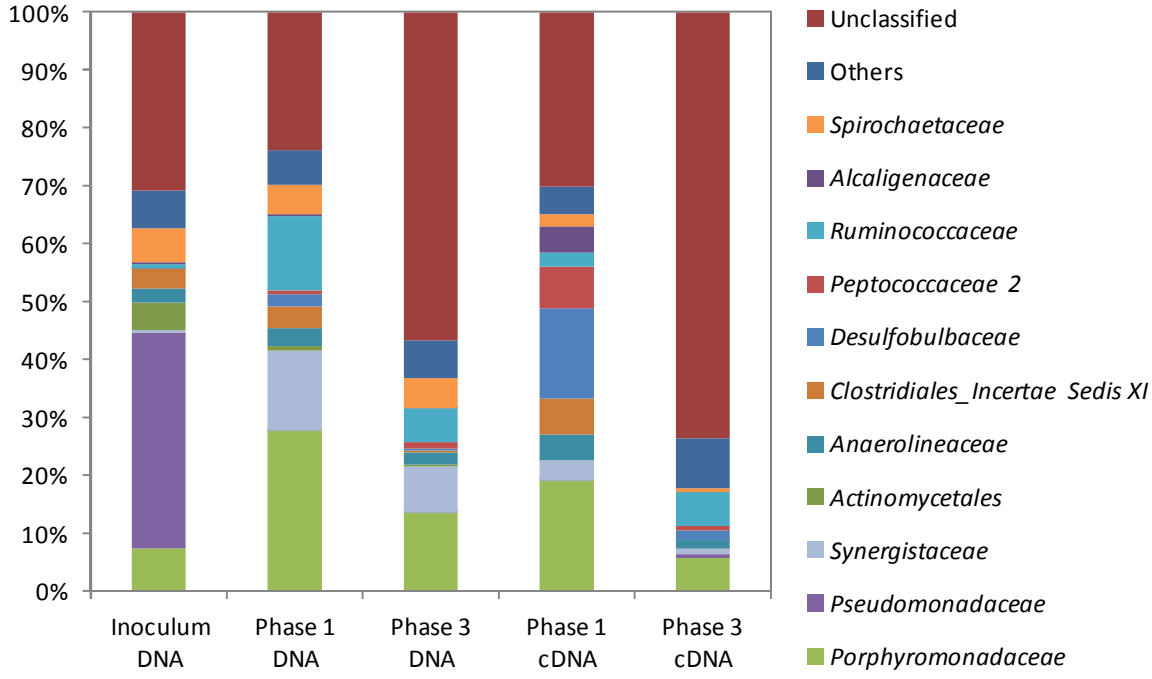

Figure 9.2 Taxonomic assignment of sequencing reads from Eubacterial community of the initial inoculum and the biomass of the UASB at the end of Phases 1 (acetate feeding) and 3 (methanol feeding) for genomic DNA and RNA (cDNA) level , at a) phylum b) family levels. Relative abundance was defined as the number of reads (sequences) affiliated with any given taxon divided by the total number of reads per sample. Phylogenetic groups with a relative abundance lower that 1% were categorised as “others”.

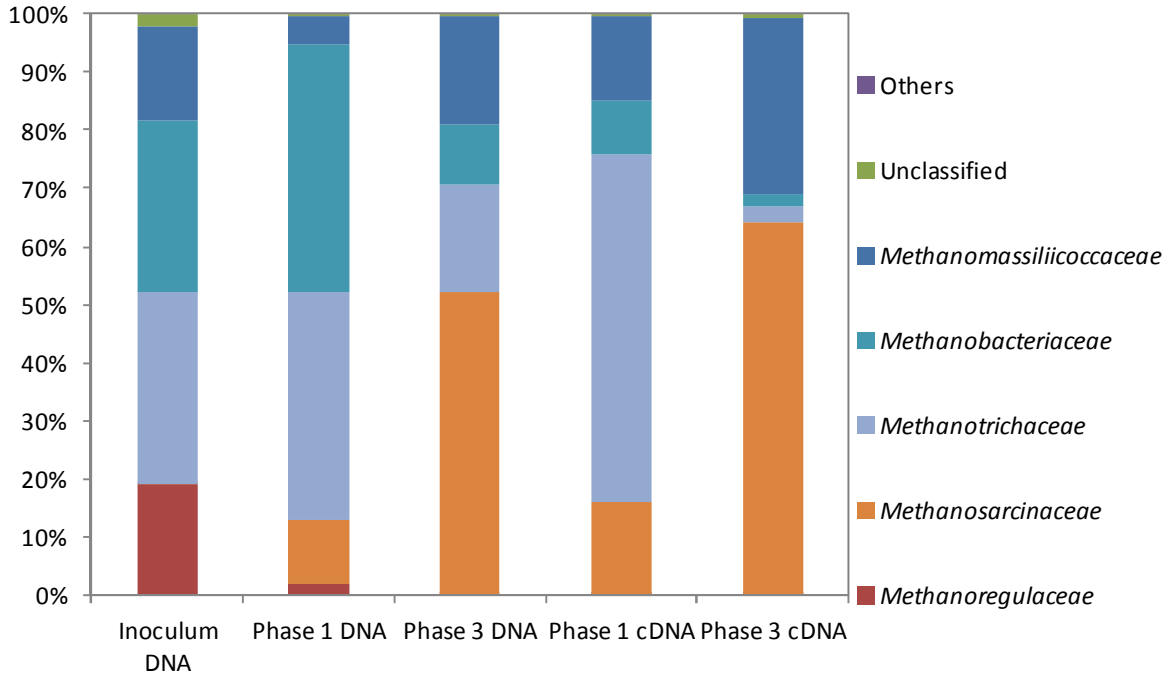

Figure 9.3 Taxonomic assignment of sequencing reads from Archaeal community of the initial inoculum and the biomass of the UASB at the end of Phases 1 (acetate feeding) and 3 (methanol feeding) for genomic DNA and RNA (cDNA) at family level. Relative abundance was defined as the number of reads (sequences) affiliated with any given taxon divided by the total number of reads per sample. Phylogenetic groups with a relative abundance lower that 1% were categorised as "others".

Although methanol is a simple compound with only one carbon, it can support a very complex food chain under anaerobic conditions (Florencio et al., 1994). The methylotrophic population enriched in this study may have been favoured by the pH in operation, which was maintained between 6.9 and 7.0. A slightly more acidic pH would have stimulated the hydrogenotrophic pathway, according to Bhatti et al. (1996), who established that at pH values close to 7.0, methanol will either be converted directly to methane (by methylotrophic methanogens), via the intermediate formation of acetate (by acetoclastic methanogens), or through a combination of both. Hydrogenotrophic methanogens will be mainly responsible for this conversion, by utilising H_2 and CO_2, only at pH values between 5.0 and 6.0.

9.3.3.3. Biodiversity analysis

Table 9.4 shows the results for the biodiversity analysis performed on UASB granular sludge samples. Inverted Simpson and Shannon indices for archaea population decreased throughout the entire operation time of the UASB, and when the change of feed from acetate to methanol was carried out, suggesting that Phase 3 promoted the enrichment of certain groups of methanogenic microorganism, reducing the biomass biodiversity of the granular sludge. The inoculum was the most diverse sample, followed by Phase 1 and Phase 3 samples. This

biodiversity reduction in Phase 3 is observed at community composition level, and also at activity level. For eubacterial population, both indices showed that the inoculum sample was the least diverse community. The highest biodiversity was harboured by the Phase 1 sample, according to the Shannon index but, according to the Inverted Simpson index, it was harboured by the Phase 3 sample. On the contrary, both indices were the highest in Phase 1 when it comes to gene expression (cDNA), suggesting that acetate feeding promoted that more eubacteria species were active in the granular sludge than with methanol feeding. So it can be concluded that the use of methanol as carbon source induced a reduction in biomass biodiversity due to the high predominance of the methylotrophic route for its degradation.

Table 9.4 Diversity index for Eubacteria and Archaea community of the inoculum and the biomass of the UASB at the end of Phases 1 (acetate feeding) and 3 (methanol feeding) for DNA and cDNA samples (mean±standard deviation). Data normalised to the sample with the lowest number of reads (50466 and 66226 for eubacterial and archaeal, respectively).

	Coverage	**Inverted Simpson**	**Shannon**
Eubacteria			
Inoculum	1.00±0.00	8.35±0.03	3.66±0.00
Phase 1-DNA	0.99±0.00	15.06±0.00	4.01±0.00
Phase 3-DNA	0.99±0.00	15.27±0.04	3.75±0.00
Phase 1-cDNA	0.99±0.00	9.80±0.02	3.66±0.00
Phase 3-cDNA	0.99±0.00	5.44±0.02	2.94±0.01
Archaea			
Inoculum	1.00±0.00	5.92±0.02	2.33±0.00
Phase 1-DNA	1.00±0.00	4.12±0.01	1.95±0.00
Phase 3-DNA	1.00±0.00	2.83.±0.00	1.63±0.00
Phase 1-cDNA	1.00±0.00	3.37±0.01	1.99±0.01
Phase 3-cDNA	1.00±0.00	2.97±0.01	1.85±0.01

9.3.3.4 Correspondence analysis

Correspondence analysis results for eubacteria community are shown in Figure 9.4a. A clear evolution in population was evidenced with the change of feed, from the inoculum to Phase 1 sample, using acetate, and from Phase 1 to Phase 3 sample, with methanol as a substrate. DNA (16S rDNA) and cDNA samples (16S rRNA) for each phase were clustered together, suggesting that few differences could be found between existing and active microorganisms. Therefore, the distribution of the samples agrees with the discussion of the sequencing results (Section 9.3.3.2). Regarding archaea correspondence analysis (Figure 9.4b), Phase 1 sample remained near to the inoculum when looking at DNA composition but moved away when looking at gene expression. Phase 3 samples, as in the case of eubacteria community, were clustered together and far from the 3 other samples.

These results confirm that a clear population shift in UASB microbial communities was promoted during the operation of the reactor, obtaining specialised acetotrophic and methylotrophic communities in Phase 1 and Phase 3, respectively, due to the different feeding strategies applied.

a)

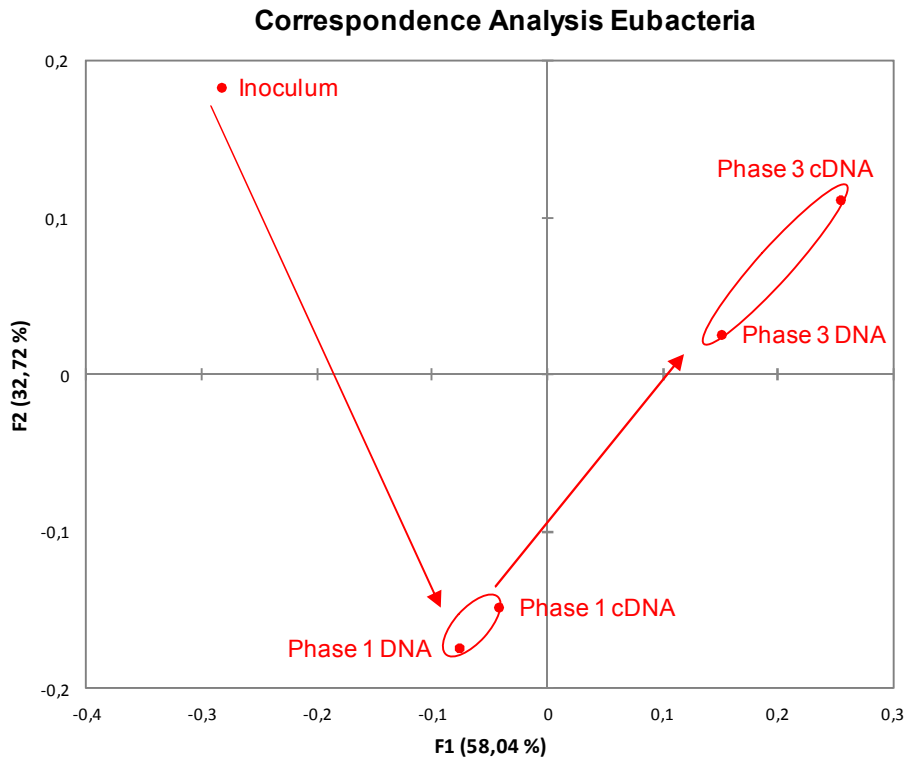

b)

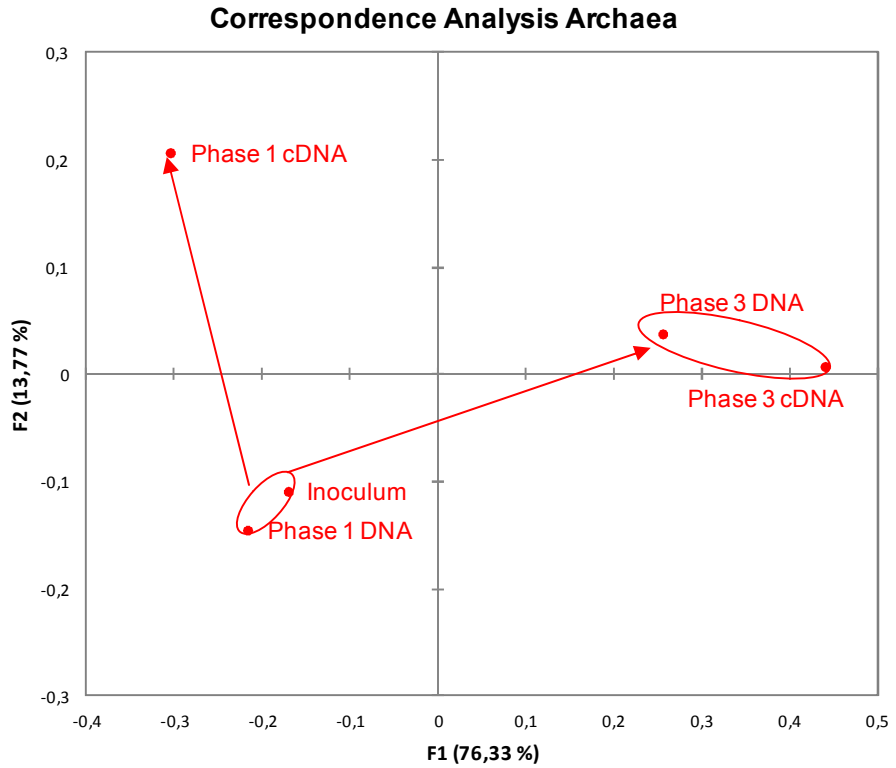

Figure 9.4 Correspondence Analysis of the initial inoculum and the biomass of the UASB at the end of Phases 1 (acetate feeding) and 3 (methanol feeding) for DNA and cDNA samples regarding (a) Eubacteria and (b) Archaea community.

9.4 Conclusions

The anaerobic granular sludge used as inoculum in the UASB was activated during the acetate feeding phase, and later progressively adapted to a methanol substrate, achieving high COD removal efficiencies (97±1%). From the different metabolic pathways known for methanol, the methylotrophic methanogenic (by the genus *Methanomethylovorans* and *Methanoglobus*) was the predominant pathway by the end of the UASB operation, followed by the aceticlastic one (by the genus *Methanothrix (Methanosaeta*) while the hydrogenotrophic route presented a low activity. The ratio between methanogenic archaea and eubacteria in the biomass showed a distinct increase during the methanol feeding phase of the UASB, so it may harbour a great potential as inoculum for an electromethanogenic biocathode MEC intended for biogas upgrading.

9.5 References

Badshah, M., Parawira, W., Mattiasson, B. 2012. Anaerobic treatment of methanol condensate from pulp mill compared with anaerobic treatment of methanol using mesophilic UASB reactors. *Bioresource Technology*, **125**, 318-327.

Bhatti, Z.I., Furukawa, K., Fujita, M. 1996. Feasibility of methanolic waste treatment in UASB reactors. *Water Research*, **30**(11), 2559-2568.

Cheng, S., Xing, D., Call, D.F., Logan, B.E. 2009. Direct biological conversion of electrical current into methane by electromethanogenesis. *Environmental Science & Technology*, **43**(10), 3953-3958.

Florencio, L., Field, J.A., Lettinga, G. 1997. High-rate anaerobic treatment of alcoholic wastewaters. *Brazilian Journal of Chemical Engineering*, 14.

Florencio, L., Field, J.A., Lettinga, G. 1994. Importance of cobalt for individual trophic groups in an anaerobic methanol-degrading consortium. *Applied and Environmental Microbiology*, **60**(1), 227-234.

Jiang, B., Parshina, S.N., van Doesburg, W., Lomans, B.P., Stams, A.J.M. 2005. Methanomethylovorans thermophila sp. nov., a thermophilic, methylotrophic methanogen from an anaerobic reactor fed with methanol. *International Journal of Systematic and Evolutionary Microbiology*, **55**(6), 2465-2470.

Karakashev, D., Batstone, D.J., Angelidaki, I. 2005. Influence of Environmental Conditions on Methanogenic Compositions in Anaerobic Biogas Reactors. *Applied and Environmental Microbiology*, **71**(1), 331-338.

Kobayashi, T., Yan, F., Takahashi, S., Li, Y.-Y. 2011. Effect of starch addition on the biological conversion and microbial community in a methanol-fed UASB reactor during long-term continuous operation. *Bioresource Technology*, **102**(17), 7713-7719.

Lu, H., Oehmen, A., Virdis, B., Keller, J., Yuan, Z. 2006. Obtaining highly enriched cultures of Candidatus Accumulibacter phosphates through alternating carbon sources. *Water Research*, **40**(20), 3838-3848.

Lu, X., Zhen, G., Chen, M., Kubota, K., Li, Y.-Y. 2015. Biocatalysis conversion of methanol to methane in an upflow anaerobic sludge blanket (UASB) reactor: Long-term performance and inherent deficiencies. *Bioresource Technology*, **198**, 691-700.

Mochimaru, H., Tamaki, H., Hanada, S., Imachi, H., Nakamura, K., Sakata, S., Kamagata, Y. 2009. *Methanolobus profundi* sp. nov., a methylotrophic methanogen isolated from deep subsurface sediments in a natural gas field. *International Journal of Systematic and Evolutionary Microbiology*, **59**(4), 714-718.

Paulo, P.L., Villa, G., Bernardus van Lier, J., Lettinga, G. 2003. The anaerobic conversion of methanol under thermophilic conditions: pH and bicarbonate dependence. *Journal of Bioscience and Bioengineering*, **96**(3), 213-218.

Poulsen, M., Schwab, C., Borg Jensen, B., Engberg, R.M., Spang, A., Canibe, N., Højberg, O., Milinovich, G., Fragner, L., Schleper, C., Weckwerth, W., Lund, P., Schramm, A., Urich, T. 2013. Methylotrophic methanogenic Thermoplasmata implicated in reduced methane emissions from bovine rumen. *Nat Commun*, **4**, 1428.

Rotaru, A.-E., Shrestha, P.M., Liu, F., Shrestha, M., Shrestha, D., Embree, M., Zengler, K., Wardman, C., Nevin, K.P., Lovley, D.R. 2014. A new model for electron flow during anaerobic digestion: direct interspecies electron transfer to *Methanosaeta* for the reduction of carbon dioxide to methane. *Energy & Environmental Science*, **7**(1), 408-415.

Ryckebosch, E., Drouillon, M., Vervaeren, H. 2011. Techniques for transformation of biogas to biomethane. *Biomass and Bioenergy*, **35**(5), 1633-1645.

Strevett, K.A., Vieth, R.F., Grasso, D. 1995. Chemo-autotrophic biogas purification for methane enrichment: mechanism and kinetics. *The Chemical Engineering Journal and the Biochemical Engineering Journal*, **58**(1), 71-79.

Van Eerten-Jansen, M.C.A.A., Veldhoen, A.B., Plugge, C.M., Stams, A.J.M., Buisman, C.J.N., Ter Heijne, A. 2013. Microbial Community Analysis of a Methane-Producing Biocathode in a Bioelectrochemical System. *Archaea*, 2013, 12.

Vavilin, V.A. 2010. Equation for isotope accumulation in products and biomass as a way to reveal the pathways in mesophilic methanol methanization by microbial community. *Ecological Modelling*, **221**(24), 2881-2886.

Villano, M., Monaco, G., Aulenta, F., Majone, M. 2011. Electrochemically assisted methane production in a biofilm reactor. *Journal of Power Sources*, **196**(22), 9467-9472.

CHAPTER 10

Start-up of electromethanogenic microbial electrolysis cells with two different biomass inocula

Part of the content of this chapter is in preparation to be submitted for publication as:

Cerrillo, M., Viñas, M., Bonmatí, A. Start-up of electromethanogenic microbial electrolysis cells with two different biomass inocula.

Abstract

The performance and biomass enrichment of the biocathode of a pair of lab-scale two-chambered microbial electrolysis cells (MEC) were assessed during 95 days as a technology for upgrading the biogas produced in anaerobic digesters, converting CO_2 into CH_4 through the electromethanogenic process. Two different inocula were compared: i) a mixture of biomass from the anode of a MEC and anaerobic granular sludge (BC1); ii) biomass enriched in a methanol-fed upflow anaerobic sludge blanket reactor (UASB) (BC2). Quantitative and qualitative microbial community assessment of the enrichment process on the biocathodes from initial inocula was performed by means of high throughput sequencing of 16S rDNA and 16S rRNA based massive libraries, as well as RT-qPCR of *16S* rRNA and *mcrA* genes. Results showed that, although BC2 had a faster increase in current density than BC1, there were no significant differences neither in the average CH_4 production (0.23±0.01 and 0.22±0.05 L m^{-3} d^{-1} for BC1 and BC2, respectively), or in the cathodic methane recovery efficiency (65±8 and 79±17%, respectively). Furthermore, independently from the origin of the inoculum, archaeal microbial community in both biocathodes were highly dominant, both in presence and activity, in hydrogenotrophic methanogenic archaea, especially belonging to *Methanobacteriaceae* family (mainly *Methanobrevibacter* genus) (84-98% of both 16S rDNA and 16S rRNA relative abundance).

10.1 Introduction

Biogas is a renewable energy carrier gas consisting mainly of methane (CH_4, 40-75%) and carbon dioxide (CO_2, 15-60%) (Ryckebosch et al., 2011) that is obtained from the anaerobic digestion of bio-degradable materials such as manure, energy crops, household and industry wastes. So far, heating and electricity generation are the main applications of biogas, which are spreading its use as an alternative to fossil fuels. Moreover, it has more efficient uses, such as the injection in the existent natural gas grid or the utilisation as transport fuel. For the latter purposes raw biogas needs some treatments prior to its use intended to remove undesired compounds (cleaning) and adjust the calorific value separating CH_4 from CO_2 (upgrading), obtaining biomethane. Conventional techniques for biogas upgrading, that are focused on CO_2 removal without changing CH_4 mass, include pressure swing adsorption, membrane separation or chemical CO_2-absorption, obtaining a final product with 95-97% of CH_4 and 1-3% of CO_2 (Ryckebosch et al., 2011). An alternative to these enrichment techniques that has recently emerged is the use of microbial electrolysis cells (MEC), in which external energy is supplied to promote a thermodynamic no spontaneous reaction such as the bioelectrochemical CO_2 conversion into methane in a process known as electromethanogenesis (Cheng et al., 2009; Van Eerten-Jansen et al., 2013; Villano et al., 2011). This way, the methane yield from anaerobic digestion could be increased (Van Eerten-Jansen et al., 2011; Xu et al., 2014). The key players of the electromethanogenesis process are hydrogenotrophic methanogenic archaea that develop in the cathode compartment of the MEC (biocathode). Previous studies have demonstrated that methane obtaining from CO_2 can be achieved through two different mechanisms of extracellular electron transfer, i) indirectly, through the intermediate abiotic electrochemical and/or microbially catalysed production of hydrogen in the cathodic compartment (Equation 10.1 and 10.2); or ii) directly, by taking the electrons from the cathode and using them to reduce CO_2 to methane (Equation 10.3) (Cheng et al., 2009; Van Eerten-Jansen et al., 2013; Villano et al., 2011).

$$2\ H^+ + 2\ e^- \rightarrow H_2 \quad (10.1)$$

$$4\ H_2 + CO_2 \rightarrow CH_4 + H_2O \quad (10.2)$$

$$CO_2 + 8\ H^+ + 8\ e^- \rightarrow CH_4 + 2\ H_2O \quad (10.3)$$

The cathode potential required to enhance the electromethanogenic process due to potential losses is in the range from -650 to -750 mV (vs. the standard hydrogen electrode, SHE), since at more negative potentials also acetate may be produced simultaneously with CH_4 and H_2 in a microbial biocathode based on mixed cultures (Jiang et al., 2013). However, acetate

has been coproduced with methane at a fixed cathode potential as low as -590 mV (vs, SHE) in another study (Marshall et al., 2012).

Obtaining a biomass rich in hydrogenotrophic methanogenic archaea in order to be used as inoculum could accelerate the start up of the methane producing MECs and improve methane production rates, being CO_2/H_2 gassing (Jiang et al., 2014; Villano et al., 2010) or cultivation in an electrochemical bioreactor (Hou et al., 2015; Jiang et al., 2013) the most common enrichment methods. A recently proposed alternative enrichment method was the utilisation of a methanol-fed upflow anaerobic sludge blanket reactor (UASB), providing that hydrogenotrophic methanogenesis is one of the possible routes for methanol degradation, besides the predominant methylotrophic route (Chapter 9). The effectiveness of this latter method to increase the performance of an electromethanogenic biocathode needs to be further evaluated. Furthermore, a deep study of the biomass harboured by methanogenic biocathodes is needed, applying new techniques such as simultaneous DNA and RNA extraction, quantification and high throughput sequencing, in order to disclose which microorganisms are really active among the ones that might be present in the biofilm (Chapter 8).

The main aim of this Chapter was to assess the performance and biomass enrichment of the biocathode of a lab-scale MEC to convert CO_2 into CH_4 as a technology for upgrading the biogas produced in anaerobic digesters, comparing two different inocula: i) a mixture of biomass from the anode of a MEC and anaerobic granular sludge; ii) biomass enriched in a methanol-fed upflow anaerobic sludge blanket reactor (UASB). The microbial enrichment on the biocathodes was assessed in terms of composition and activity using quantitative real-time polymerase chain reaction (qPCR) and high throughput sequencing of 16S rDNA and 16S rRNA massive libraries.

10.2 Materials and methods

10.2.1 Experimental set-up

A pair of identical two chamber cell described in Section 3.1.2 (BC1 and BC2) were operated.

10.2.2 Reactor operation

The MECs were operated in continuous for 95 days poising the cathode potential at -800 mV vs SHE. One of the MECs (BC1) was inoculated, both the anode and the cathode compartment, with 30 mL of a mixture 3.6:1 of the biomass of the anode of the MEC operated in Chapter 8 and granular biomass from a full-scale AD, with a volatile suspended solids (VSS) content of 16 g L^{-1}. The cathode of the second MEC (BC2) was inoculated with 30 mL of a resuspension (VSS content of 33 g L^{-1}) of the anaerobic granular sludge of the UASB that was operated in Chapter 9 with methanol in order to enrich the biomass with methanogenic archaea.

The resuspension was done by vortex mixing during 10 minutes in a 50 mL tube containing 30 g of granular sludge and 25 mL of Ringer 1/4 sterilised solution. The two MEC were operated in continuous mode, the influent solutions of both the anode and the cathode compartment were fed in continuous with a pump at 40 mL h^{-1} and mixed by recirculating them by an external pump. The hydraulic retention time of each compartment (HRT) was of 6.8 h (with respect to the net volume of each compartment), and the organic loading rate (OLR) of the anode compartment was established at 7.83 kg_{COD} m^{-3} day^{-1}. The MECs were operated at room temperature during the entire assay (23±2 ºC).

10.2.3. Analyses and calculations

Samples of the effluent of each compartment were analysed for pH, besides chemical oxygen demand (COD) in the anode compartment samples and dissolved methane in the cathode samples, following the methods described in Section 3.2. Methane production was normalised to the net volume of the cathode compartment (0.265 L). COD removal efficiency in the MECs was calculated as described in Section 3.4.1.

The current density (A m^{-3}) of the MECs was calculated as described in Section 3.3. The Coulombic efficiency (CE), or the fraction of electrons obtained from the consumption of COD that are available for methane production at the cathode; the energy efficiency relative to electrical input recovered as methane (EE_e); the energy efficiency relative to the energy content of the substrate (EE_s); the energy efficiency with respect to the energy input and the energy in the substrate (EE_{e+s}); and the cathodic methane recovery efficiency (R_{cat}), defined as the fraction of electrons reaching the cathode that are recovered as methane, were calculated as described in Section 3.4.3.

Cyclic voltammetries (CV) in turnover conditions were performed at the start (day 0) and the end (day 95) of the assays in each biocathode, following the methodology described in Section 3.3.

The bacterial communities in the 2 different inoculums used for the cathodes of BC1 and BC2 and the biofilm harboured in the same electrodes at the end of the assay were analysed by culture-independent molecular techniques such as (RT) quantitative PCR (RT-qPCR) and high throughput sequencing (MiSeq, Illumina) of *16S* rDNA and *16S* rRNA. Simultaneous total genomic DNA and RNA extraction and complementary DNA (cDNA) synthesis, qPCR and high throughput 16S rRNA gene sequencing (MiSeq, Illumina) were performed following the methods described in Section 3.6.2, 3.6.3, and 3.6.5, respectively. The standard curve parameters of the qPCRs were as follows (for *16S* rRNA and *mcr*A, respectively): slope of -3.244 and -3.532; correlation coefficient of 0.998 and 0.999; efficiency of 103 and 92%; showing that the reactions performed had a high efficiency. The data obtained from sequencing datasets for eubacterial

and archaeal populations was submitted to the Sequence Read Archive of the National Center for Biotechnology Information (NCBI) under the study accession number SRP072511.

The evaluation of the diversity of the samples and statistical multivariate analyses were performed following Section 3.6.6.

10.3 Results and discussion

10.3.1 Operation performance

The current densities produced by the BC1 and the BC2 during the 95 days of operation are shown in Figure 10.1a and 1b, respectively. The BC2 achieved current densities between 150 and 200 A m^{-3} after 5 days of operation, while the BC1 showed a more progressive increase (the low current densities between days 8 and 14 are due to a MEC destabilisation after the performance of a cyclic voltammetry). However, the BC1 maintained a current density between 100 and 150 A m^{-3} from day 50 on, while the BC2 produced a current density around 80 A m^{-3}. The decrease in current density on day 10, 41 and 60 of the BC2 was due to a failure in the potentiostat that did not allowed to maintain the cathode poised at -800 mV. Nevertheless, the average methane production was similar in both MECs, 0.22-0.23 m^3 m^{-3} d^{-1} (Table 10.1). It is noteworthy that the obtained values are twenty-fold and ten-fold higher, in terms of current density and methane production respectively than those reported previously in a dual-chamber methanogenic MEC using graphite granules as electrodes, with current density generation and methane production rate of 9.3 A m^{-3} and 0.018 m^3 m^{-3} d^{-1}, respectively (Villano et al., 2011); also higher than those achieved from a spiral-wound-electrode MEC with an applied voltage of 1.2 V, with a current density generation and methane production rate of 109 A m^{-3} and 0.16 m^3 m^{-3} d^{-1}, respectively (Hou et al., 2015). Even 0.28 m^3 m^{-3} d^{-1} were achieved in a MEC with a semi-batch fed cathode (Villano et al., 2013).

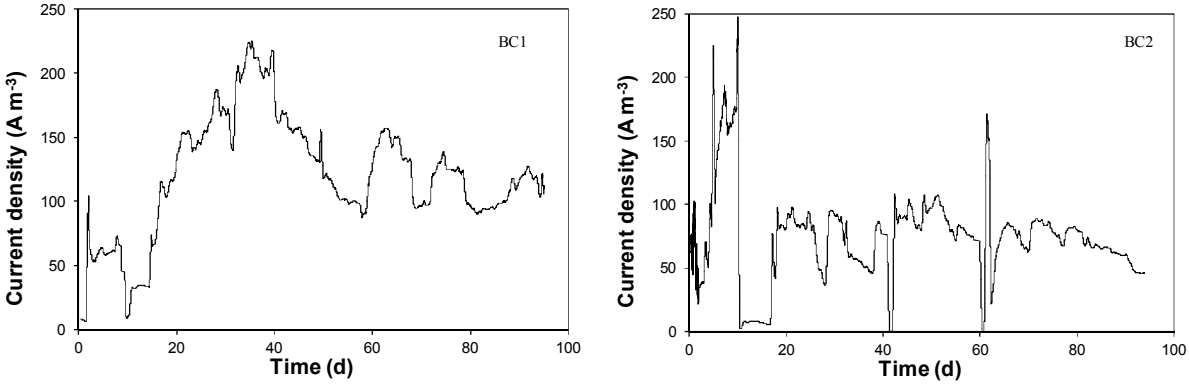

Figure 10.1 Current density profiles obtained for (a) BC1 and (b) BC2.

Table 10.1 Performance of BC1 and BC2 (average±standard deviation).

Parameter	BC1	BC2
CH_4 production ($m^3\ m^{-3}\ d^{-1}$)	0.23±0.01	0.22±0.05
CE (%)	33±10	25±12
R_{cat} (%)	65±8	79±17
EE_e (%)	57±17	61±16
EE_s (%)	23±6	54±34
EE_{e+s} (%)	17±2	33±18

Regarding the cathodic methane recovery efficiency (R_{cat}) and energy efficiencies (EE_e, EE_s and EE_{e+s}), the values obtained for the BC2 are higher than those of the BC1, but due to their higher variability the differences cannot be considered as significant (Table 10.1). Previous works with a two-chambered MEC using graphite granules as electrodes have achieved an energy efficiency related to the electrical energy input (EE_e) and of electrical input and substrate (EE_{e+s}) of 57% and 30%, respectively, in batch mode (Villano et al., 2011), values very similar to these obtained in this study. On the contrary, the achieved CE (33±10 for BC1 and 25±12 for BC2) are lower than those previously reported, such as 72-80% (Zeppilli et al., 2014). Finally, the obtained R_{cat} (65±8 for BC1 and 79±17 for BC2) are below the 96% previously reported by Cheng et al. (2009) or the 84-86% obtained by Zeppilli et al. (2014), but much higher than the 23.1% achieved by Van Eerten-Jansen et al. (2001) or the 24.2 ± 4.7% reported by Zhen et al. (2015).

Figure 10.2 shows the cyclic voltammograms obtained in both biocathodes at the start (day 0) and the end (day 95) of their operation. The curves obtained at the start of the operation showed a low response to the different applied potentials, as a result of the recent inoculation. At the end of the assay the curves showed that the biofilm was established in both biocathodes, with a better performance of BC2 at potentials lower than -330 mV vs. SHE. However, current densities obtained during continuous operation of the MECs were lower than those achieved in the cyclic voltammetries, especially in BC2. Catalytic current for both biocathodes had an onset at approximately -300 mV, that could be related to the reduction of CO_2 to methane (*E'* = -237 to -303 mV for pH 7-8) or acetate (*E'* = -287 to -352 mV for pH 7-8), in the case that this product was generated in the cathode compartment (Xafenias and Mapelli, 2014). A second onset appeared at a potential near -800 mV, which might be related to the hydrogen evolution reaction ($2H^+ + 2e^- \rightarrow H_2$) (Fu et al., 2015), so it is possible that H_2 was formed at the biocathode and immediately consumed by hydrogenotrophic methanogens.

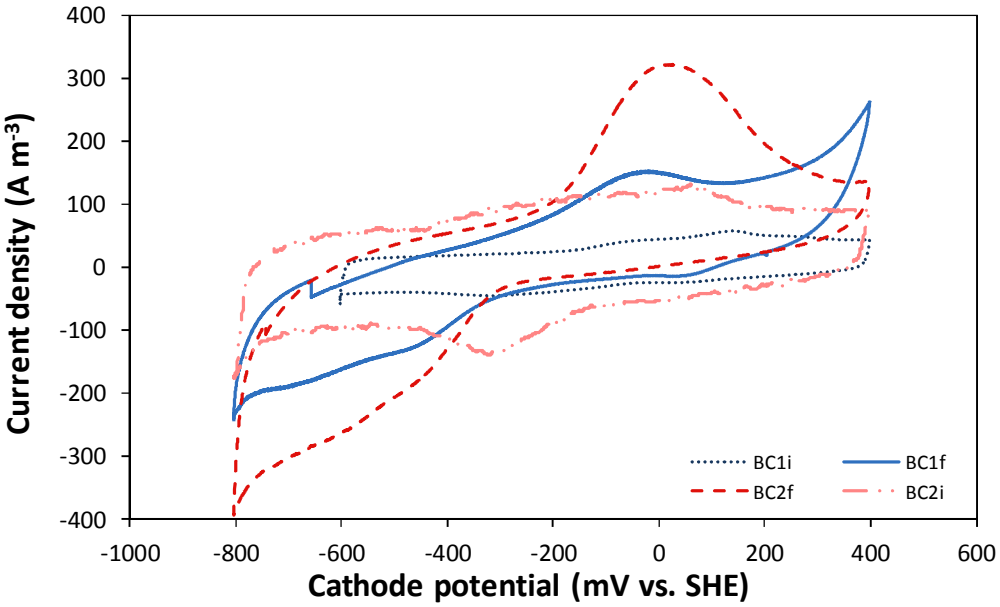

Figure 10.2 Cyclic voltammograms obtained for BC1 and BC2 at the start (BC1i and BC2i) and the end (BC1f and BC2f) of the assay.

10.3.2 Evaluation of the electromethanogenic MEC as a biogas upgrading technology

With the obtained results of methane conversion from CO_2 (0.23 m^3 m^{-3} d^{-1}), the performance of the electromethanogenic MEC as a biogas upgrading technology was assessed. Assuming a typical biogas composition of 60% CH_4 and 40% CO_2, a volume of biogas of 0.58 m^3 m^{-3} d^{-1} could be treated in this biocathode to obtain near 100% CH_4. And for example 1 m^3 m^{-3} d^{-1} of biogas could be treated to obtain a composition of 83% CH_4 and 17% CO_2. When compared to the existing biogas upgrading technologies, that achieve a methane purity of 95-97% (Ryckebosch et al., 2011), it has to be taken into account that these technologies remove CO_2, without changing CH_4 mass, so the final volume of gas obtained is reduced. That is, for each m^3 of biogas treated on traditional biogas upgrading technologies, about 0.6 m^3 of CH_4 would be recovered, while in the biocathode the obtained volume would be of 0.9 m^3. As higher cathodic methane recovery efficiencies have been achieved in previous studies (Cheng et al., 2009), and the designs and materials for biocathodes are constantly improving (Hou et al., 2015), a better performance for this new biogas upgrading technology can be expected in the future, so its scaling up must be undertaken.

10.3.3 Microbial community assessment

The microbial community structure and activity of the samples taken from the inoculums of the cathodes of BC1 and BC2 and the biofilm harboured on the electrodes at the end of the assay was characterised by means of qPCR and high throughput sequencing by Miseq of 16SrRNA/16SrDNA-based massive libraries.

10.3.3.1 Quantitative evolution of cathode biomass

qPCR results of the 4 samples, regarding DNA (present microorganisms) for both *16S* rRNA (eubacteria) and *mcr*A (methanogenic archaea) showed higher gene copy numbers in the final BC2 biofilm than in BC1, although of the same order of magnitude (Figure 10.3). However, when looking at cDNA (active microorganisms), methanogenic archaea in BC1 biofilm revealed themselves more active than in BC2, with more than one order of magnitude increase ($2.95 \cdot 10^5$ and $9.86 \cdot 10^3$ *mcr*A transcript copy numbers g^{-1}, respectively), while eubacteria 16S rRNA gene copy numbers in the BC2 biofilm were 3.2 times higher than in BC1. In spite of the quantitative differences in methanogenic archaea between both biocathodes, no significant differences were observed related to methane production, so other mechanisms may be affecting the performance of the biomass. It could be possible that the higher number of active eubacteria in the BC2 increased the synergies with archaea that could help to overcome their lower number in comparison with BC1, as will be discussed in the following section.

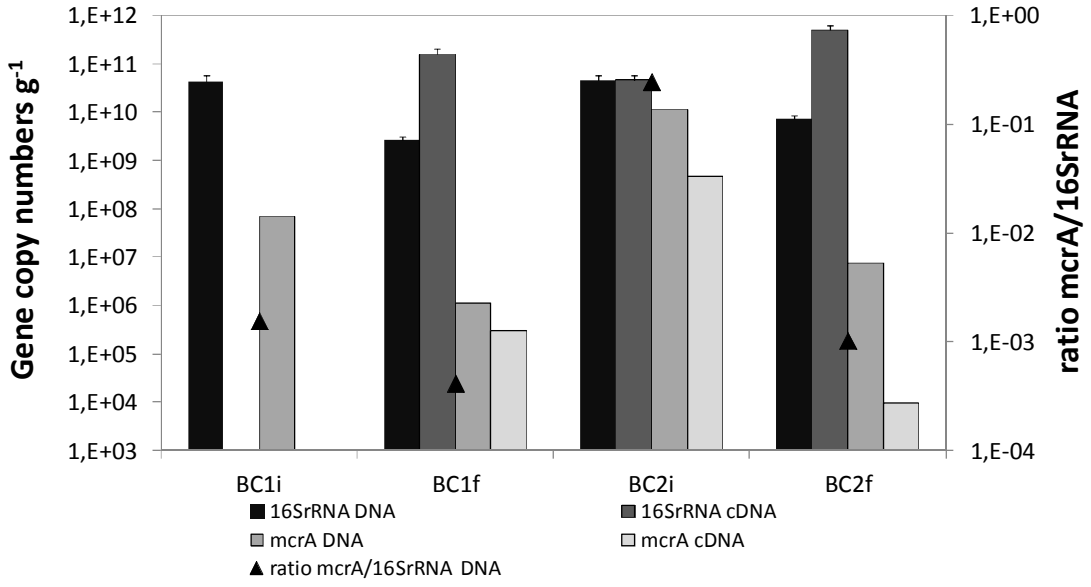

Figure 10.3 Gene copy numbers and transcripts of *16S* rRNA and *mcr*A genes from initial inoculum of BC1 and BC2 (i) and the final enrichment on each biocathode (f).

10.3.3.2 Sequencing results for eubacteria and archaea

Table 10.2 shows the number of reads obtained for the inoculums and the final biofilm of the biocathodes for eubacteria (3538 OTUS) and archaea (725 OTUS). Figure 10.4a shows the relative abundance of eubacterial *phyla* for the four samples, regarding DNA (present microorganisms) and cDNA (active microorganisms) forms. Both inoculums had a different composition, with a higher relative predominance of *Proteobacteria* (57%) and in *Bacteroidetes* (61%) in the inoculums of BC1 and BC2, respectively, while at the end of the assays the biofilms where enriched the opposite (45% for *Bacteroidetes* and 58% for *Proteobacteria* in BC1 and BC2, respectively). The most active *phyla* in BC1 biofilm were, according to cDNA results, *Bacteroidetes* (37%), *Firmicutes* (33%) and *Proteobacteria* (27%), while *Proteobacteria phylum* (73%) was highly active in BC2 biofilm. A previous study also found that *Proteobacteria* was the most predominant *phylum* (54% of the clones in the library) (Kobayashi et al., 2013). At family level (Figure 10.4b), *Cyclobacteriaceae* was the predominant one in the BC1 biofilm (30%) in spite of being *Pseudomonadaceae* the most abundant in the inoculum (46%). In the BC2 biofilm four families accounted for the same relative abundance (11%): *Desulfovibrionaceae, Cyclobacteriaceae*, *Pseudomonadaceae* and *Rhodocyclaceae,* when they had a low relative abundance in the inoculum (below 3% for *Desulfovibrionaceae* and below 0.25% for the other three families).

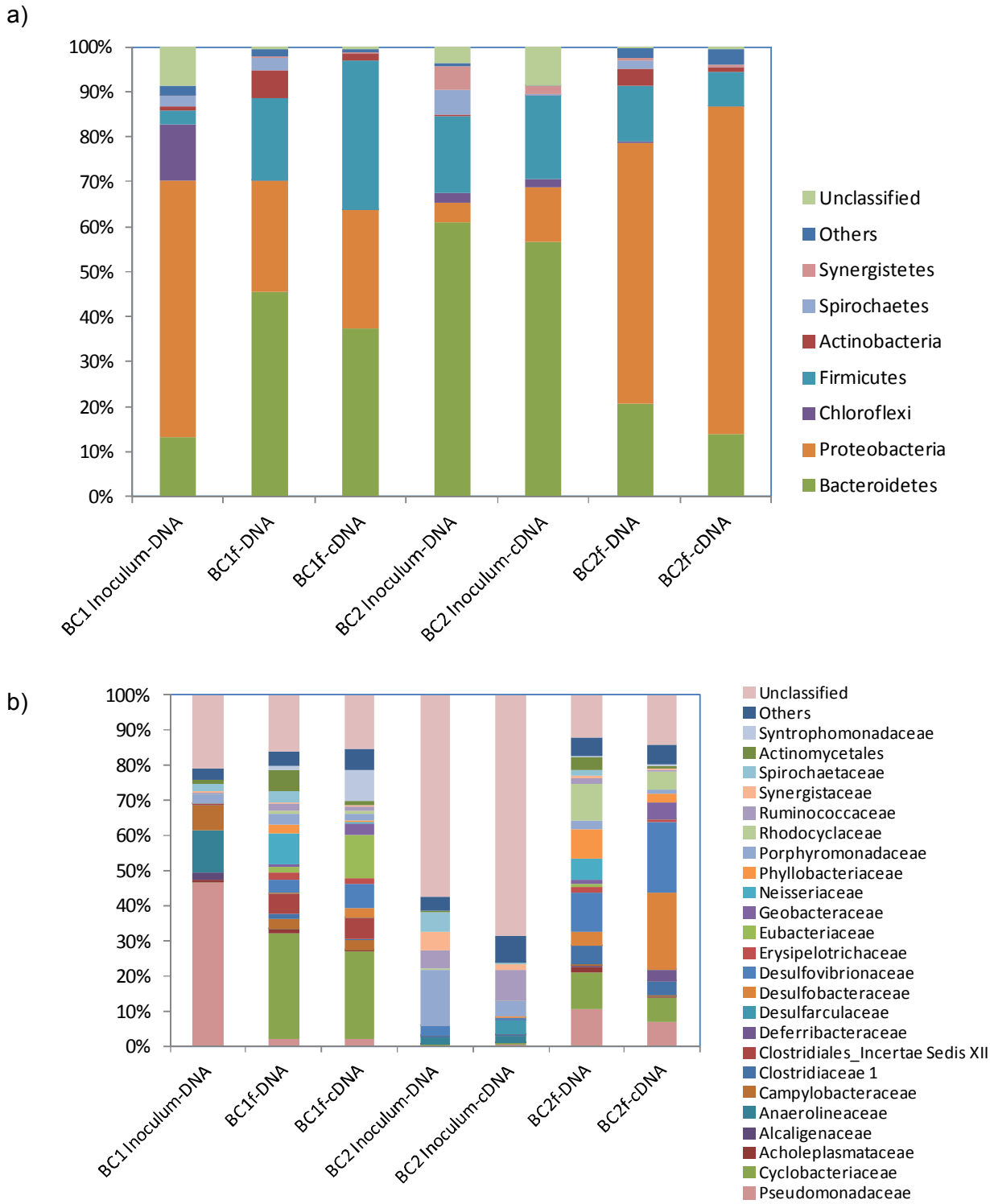

Figure 10.4 Taxonomic assignment of sequencing reads from Eubacterial community of the inoculum of BC1 and BC2 and the final sample of each cathode for DNA (total population) and cDNA (active populations), at a) phylum b) family levels. Relative abundance was defined as the number of reads (sequences) affiliated with any given taxon divided by the total number of reads per sample. Phylogenetic groups with a relative abundance lower that 1% were categorised as “others”.

When looking at the cDNA form, and thereby active microorganisms, the *Cyclobacteriaceae* family maintained its higher relative abundance (25%), accompanied by *Eubacteriaceae* (13%) in the BC1 biofilm. However, the most active families in the BC2 biofilm where *Desulfobacteraceae* and *Desulfovibrionaceae* (22 and 20%, respectively), although being practically inactive in the inoculum. Therefore, these results suggest on the one hand that the active groups of microorganisms differ from the most abundant ones; and on the second hand, the enrichment of eubacteria on the electromethanogenic biocathodes under the same operational conditions may be different, which is consistent with a recent work (Siegert et al., 2015b). Some of the genera identified in the biocathodes with a higher relative abundance belonged to *Pseudomonas* (2 and 7% of active microorganisms in BC1 and BC2, respectively), *Geobacter* (3 and 4% of active microorganisms in BC1 and BC2, respectively), *Desulfovibrio* (7 and 20% of active microorganisms in BC1 and BC2, respectively) or *Acetobacterium* (11 and 0.1% of active microorganisms in BC1 and BC2, respectively), which have been identified previously in methanogenic cathodes (Siegert et al., 2015a; Siegert et al., 2015b; Van Eerten-Jansen et al., 2013). *Acetobacterium* is a typical cathodic acetogen (Marshall et al., 2012), and its presence could indicate that electrons were not exclusively directed to methanogenesis, explaining the obtained cathodic methane recovery below 100% of both biocathodes. This hypothesis is reinforced by the fact that small amounts of acetate were detected in the cathode effluent (<33 mg L^{-1}). In turn, *Geobacter* and *Desulfovibrio* are able to catalyse bioelectrochemical hydrogen production at the cathode (Aulenta et al., 2012; Geelhoed and Stams, 2011), and may be involved in the production of methane through the microbially catalysed production of hydrogen (equation 10.1 and 10.2). As the latter family is more abundant in BC2, it could be the reason for its similar methane production to BC1 in spite of the lower copy number of active *mcr*A gene obtained by qPCR.

Regarding archaea population, Figure 10.5 shows a clear enrichment in the *Methanobacteriaceae* family in both biocathodes, especially in BC2 (90% of relative abundance), belonging mainly to *Methanobrevibacter* genus. A part from its high relative abundance, it also revealed itself as the most active family (87 and 98% in BC1 and BC2, respectively). Previous work also determined that *Methanobacteriaceae* was the predominant family on methanogenic biocathodes, although identifying *Methanobacterium* as the predominant species (Van Eerten-Jansen et al., 2013; Xu et al., 2014; Zhen et al., 2015). An abundance of 86.7% for *Methanobacterium* was determined using fluorescent in situ hybridisation (FISH) in a two-chamber electrochemical reactor containing an abiotic anode and a biocathode for methane production (Cheng et al., 2009); and it represented more than 93% of the total sequenced active archaeal reads in a MEC with concomitant production of acetate, methane and hydrogen (Marshall et al., 2012). *Methanobacterium* dominated also on the

biocathodes, with lesser members of *Methanobrevibacter*, in MECs inoculated with either anaerobic bog sediment where hydrogenotrophic methanogens were detected or anaerobic digestion sludge dominated by the acetoclastic *Methanosaeta* (Siegert et al., 2015a). Instead, *Methanobrevibacter* was found to dominate the biofilms developed on platinum cathodes (81-100%), while *Methanobacterium* abounded on the other cathode materials assayed (median of 97% in abundance of all archaea), when the inoculum used contained primarily the genus *Methanosaeta* (95%) (Siegert et al., 2015b). *Methanobacterium*, *Methanobrevibacter* and *Methanocorpusculum* dominated the biocathode of another MEC at an applied voltage of 0.7 V (Jiang et al., 2014), and *Methanobrevibacter* and *Methanosarcina* were observed in a MEC with a cathode of graphite granules (Zeppilli et al., 2014). Therefore, regardless of the initial composition of the inoculums, in the present study a convergent enrichment towards hydrogenotrophic methanogenic families was clear, especially in the case of the inoculum of BC2, which was initially enriched in methylotrophic methanogenic archaea (Methanomassiliicoccaceae, 24% (Poulsen et al., 2013) and Methanosarcinaceae, 50%, genus *Methanomethylovorans* and *Methanolobus* (Jiang et al., 2005; Mochimaru et al., 2009)). *Methanobrevibacter* genus, along with *Methanobacterium* found in other studies, seem to be especially adapted for growth in electromethanogenic MECs, as stated in a previous work (Siegert et al., 2015b), differentiating from other hydrogenotrophic methanogens under poised potentials.

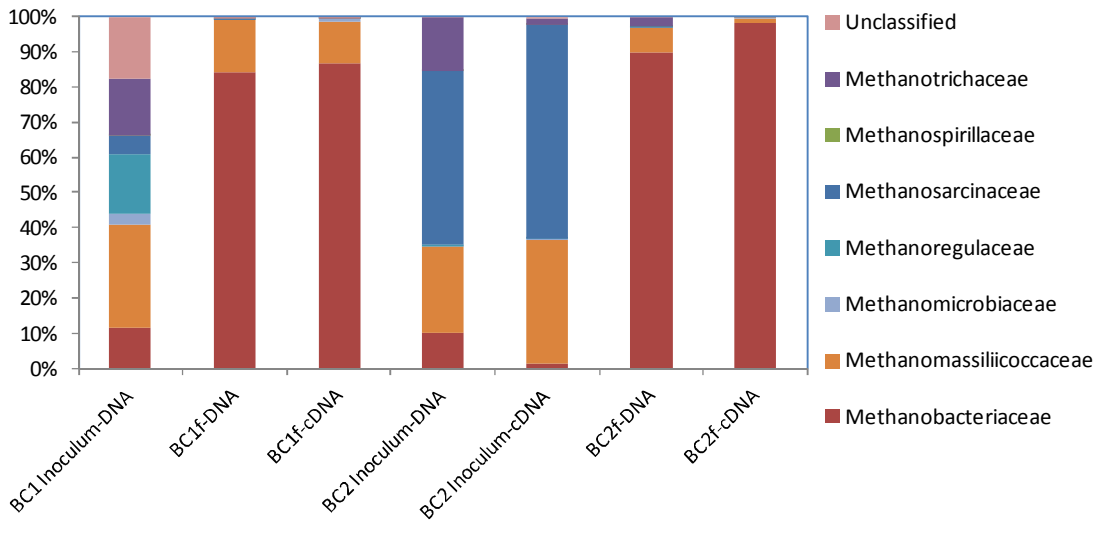

Figure 10.5 Taxonomic assignment of sequencing reads from Archaeal community of the inoculum of BC1 and BC2 and the final sample of each cathode for DNA (total population) and cDNA (active populations) at family level. Relative abundance was defined as the number of reads (sequences) affiliated with any given taxon divided by the total number of reads per sample. Phylogenetic groups with a relative abundance lower that 1% were categorised as "others".

10.3.3.3. Biodiversity analysis

Table 10.2 shows the results for the biodiversity analysis performed on inoculums and final biocathode biofilm samples. The Inverted Simpson and Shannon indices for eubacteria and archaea population showed that in general biodiversity decreased when looking at the really active population in biofilms with respect to the present one. Eubacteria population in the final biofilm of BC2 was the richest, either in presence or in activity according to the Inverted Simpson index (16.36 and 9.90, respectively), while archaea population was richer in the final biofilm of BC1 (2.46 and 2.30 for DNA and cDNA, respectively). These results agree with the high relative abundance of *Methanobacteriaceae* in BC2 found in the Miseq 16S-based sequencing analysis, which reduces its biodiversity. On the other hand, the final biocathode biofilms showed a lower biodiversity compared to the inoculums regarding archaea community, as a result of their high enrichment in *Methanobrevibacter*, while eubacteria increased its biodiversity in BC2 compared to the inoculum, which disagree with the results of a previous work that found the opposite behaviour (Siegert et al., 2015b).

Table 10.2 Diversity indices for Eubacteria and Archaeal community of the inoculums and the final biofilm of BC1 and BC2 (BC1f and BC2f, respectively) for 16S rRNA (cDNA) and 16S rDNA (DNA) massive libraries (mean±standard deviation). Data normalised to the sample with the lowest number of reads (104277 and 93126 for eubacterial and archaeal, respectively)

	Reads	Coverage	Inverted Simpson	Shannon
Eubacteria				
Inoculum BC1-DNA	110431	1.00±0.00	9.20±0.01	3.67±0.00
BC1f-DNA	104277	1.00±0.00	9.02±0.00	3.62±0.00
Inoculum BC2-DNA	114481	1.00±0.00	13.66±0.02	3.56±0.00
BC2f-DNA	174367	1.00±0.00	16.36±0.04	3.90±0.00
BC1f-cDNA	206865	1.00±0.00	6.73±0.02	3.51±0.00
Inoculum BC2-cDNA	243660	1.00±0.00	5.69±0.02	3.22±0.00
BC2f-cDNA	112853	1.00±0.00	9.90±0.01	3.33±0.00
Archaea				
Inoculum BC1-DNA	93126	1.00±0.00	13.04±0.00	3.17±0.00
BC1f-DNA	177146	1.00±0.00	2.46±0.01	1.51±0.00
Inoculum BC2-DNA	223995	1.00±0.00	3.86±0.01	2.54±0.00
BC2f-DNA	212931	1.00±0.00	2.21±0.00	1.45±0.00
BC1f-cDNA	192016	1.00±0.00	2.30±0.01	1.48±0.00
Inoculum BC2-cDNA	175828	1.00±0.00	3.97±0.01	2.34±0.00
BC2f-cDNA	230930	1.00±0.00	1.91±0.00	1.05±0.00

10.3.3.4 Correspondence analysis

Correspondence analysis results for eubacteria and archaea community are shown in Figure 10.6a and 6b. The evolution from the inoculums to the final biocathode biofilms was similar for both populations. Results show a clear differentiation between BC1 and BC2 inoculums but, in spite of their diverse initial composition, their populations evolved on the biocathodes towards consortiums that were clearly clustered together at the end of the assay, as a clear example of convergent microbial enrichment. Furthermore, DNA and cDNA for each sample were prochain, indicating that the active populations were similar to the existing ones, in spite of the differences detected by the MiSeq sequencing. These results corroborate that a very specific archaea population was obtained under the strict operation conditions of both biocathodes, and that the different inocula used had little influence on the final composition and

activity, as was also suggested by the results obtained regarding methane production and operation performance.

a)

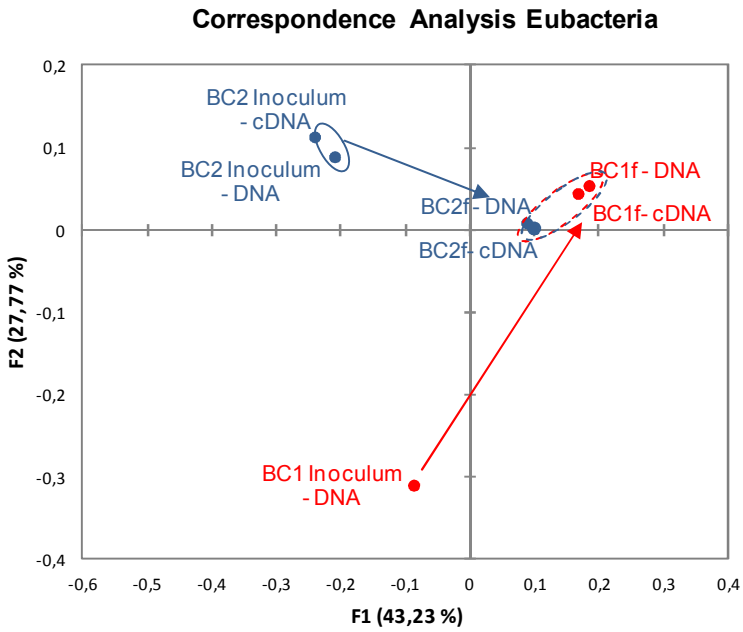

b)

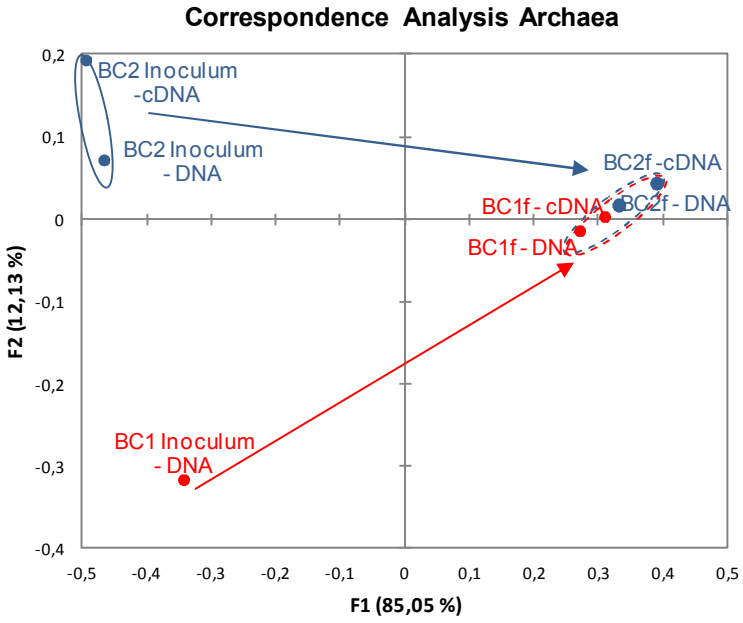

Figure 10.6 Correspondence Analysis (CA) of the inoculum of BC1 and BC2 and the final sample of each cathode for 16SrDNA and 16SrRNA (cDNA) regarding (a) Eubacteria and (b) Archaea community on the basis of MiSeq-16S based profile (OTU level).

10.4 Conclusions

Results showed that, although BC2 achieved a higher current density faster than BC2, there were no significant differences in the average CH_4 production (0.23±0.01 and 0.22±0.05 m^3 m^{-3} d^{-1} for BC1 and BC2, respectively) or cathodic methane recovery efficiency (65±8 and 79±17%, respectively), suggesting that the origin of the biomass had little influence on the performance of the biocathode. Furthermore, also independently from the inocula, the obtained archaeal communities on both biocathodes at the end of the assay were very similar, highly dominated by hydrogenotrophic methanogenic archaea, especially in *Methanobacteriaceae* family (84-90% of DNA relative abundance), being also the most active (87-98% of RNA relative abundance) belonging mainly to *Methanobrevibacter*. From the obtained results it has been proved that the electromethanogenic biocathode MEC is a promising technology for biogas upgrading, as it is based on CO_2 conversion into CH_4, that would be able to compete in the future with the existing technology, based on CO_2 removal.

10.5 References

Aulenta, F., Catapano, L., Snip, L., Villano, M., Majone, M. 2012. Linking bacterial metabolism to graphite cathodes: electrochemical insights into the H2-producing capability of Desulfovibrio sp. *ChemSusChem*, **5**(6), 1080-1085.

Cheng, S., Xing, D., Call, D.F., Logan, B.E. 2009. Direct biological conversion of electrical current into methane by electromethanogenesis. *Environmental Science & Technology*, **43**(10), 3953-3958.

Fu, Q., Kuramochi, Y., Fukushima, N., Maeda, H., Sato, K., Kobayashi, H. 2015. Bioelectrochemical analyses of the development of a thermophilic biocathode catalyzing electromethanogenesis. *Environmental Science & Technology*, **49**(2), 1225-1232.

Geelhoed, J.S., Stams, A.J.M. 2011. Electricity-assisted biological hydrogen production from acetate by Geobacter sulfurreducens. *Environmental Science & Technology*, **45**(2), 815-820.

Hou, Y., Zhang, R., Luo, H., Liu, G., Kim, Y., Yu, S., Zeng, J. 2015. Microbial electrolysis cell with spiral wound electrode for wastewater treatment and methane production. *Process Biochemistry*, **50**(7), 1103-1109.

Jiang, B., Parshina, S.N., van Doesburg, W., Lomans, B.P., Stams, A.J.M. 2005. Methanomethylovorans thermophila sp. nov., a thermophilic, methylotrophic methanogen from an anaerobic reactor fed with methanol. *International Journal of Systematic and Evolutionary Microbiology*, **55**(6), 2465-2470.

Jiang, Y., Su, M., Li, D. 2014. Removal of sulfide and production of methane from carbon dioxide in microbial fuel cells–microbial electrolysis cell (MFCs–MEC) coupled system. *Applied Biochemistry and Biotechnology*, **172**(5), 2720-2731.

Jiang, Y., Su, M., Zhang, Y., Zhan, G., Tao, Y., Li, D. 2013. Bioelectrochemical systems for simultaneously production of methane and acetate from carbon dioxide at relatively high rate. *International Journal of Hydrogen Energy*, **38**(8), 3497-3502.

Kobayashi, H., Saito, N., Fu, Q., Kawaguchi, H., Vilcaez, J., Wakayama, T., Maeda, H., Sato, K. 2013. Bio-electrochemical property and phylogenetic diversity of microbial communities associated with bioelectrodes of an electromethanogenic reactor. *Journal of Bioscience and Bioengineering*, **116**(1), 114-117.

Marshall, C.W., Ross, D.E., Fichot, E.B., Norman, R.S., May, H.D. 2012. Electrosynthesis of commodity chemicals by an autotrophic microbial community. *Applied and Environmental Microbiology*, **78**(23), 8412-8420.

Mochimaru, H., Tamaki, H., Hanada, S., Imachi, H., Nakamura, K., Sakata, S., Kamagata, Y. 2009. Methanolobus profundi sp. nov., a methylotrophic methanogen isolated from deep subsurface sediments in a natural gas field. *International Journal of Systematic and Evolutionary Microbiology*, **59**(4), 714-718.

Poulsen, M., Schwab, C., Borg Jensen, B., Engberg, R.M., Spang, A., Canibe, N., Højberg, O., Milinovich, G., Fragner, L., Schleper, C., Weckwerth, W., Lund, P., Schramm, A., Urich, T. 2013. Methylotrophic methanogenic Thermoplasmata implicated in reduced methane emissions from bovine rumen. *Nat Commun*, **4**, 1428.

Ryckebosch, E., Drouillon, M., Vervaeren, H. 2011. Techniques for transformation of biogas to biomethane. *Biomass and Bioenergy*, **35**(5), 1633-1645.

Siegert, M., Li, X.-f., Yates, M.D., Logan, B.E. 2015a. The presence of hydrogenotrophic methanogens in the inoculum improves methane gas production in microbial electrolysis cells. *Frontiers in Microbiology*, **5**.

Siegert, M., Yates, M.D., Spormann, A.M., Logan, B.E. 2015b. Methanobacterium dominates biocathodic archaeal communities in methanogenic microbial electrolysis cells. *ACS Sustainable Chemistry & Engineering*, **3**(7), 1668-1676.

Van Eerten-Jansen, M.C.A.A., Heijne, A.T., Buisman, C.J.N., Hamelers, H.V.M. 2011. Microbial electrolysis cells for production of methane from CO2: long-term performance and perspectives. *International Journal of Energy Research*, **36**(6), 809-819.

Van Eerten-Jansen, M.C.A.A., Veldhoen, A.B., Plugge, C.M., Stams, A.J.M., Buisman, C.J.N., Ter Heijne, A. 2013. Microbial community analysis of a methane-producing biocathode in a bioelectrochemical system. *Archaea*, **2013**, 12.

Villano, M., Aulenta, F., Ciucci, C., Ferri, T., Giuliano, A., Majone, M. 2010. Bioelectrochemical reduction of CO2 to CH4 via direct and indirect extracellular electron transfer by a hydrogenophilic methanogenic culture. *Bioresource Technology*, **101**(9), 3085-3090.

Villano, M., Monaco, G., Aulenta, F., Majone, M. 2011. Electrochemically assisted methane production in a biofilm reactor. *Journal of Power Sources*, **196**(22), 9467-9472.

Villano, M., Scardala, S., Aulenta, F., Majone, M. 2013. Carbon and nitrogen removal and enhanced methane production in a microbial electrolysis cell. *Bioresource Technology*, **130**, 366-371.

Xafenias, N., Mapelli, V. 2014. Performance and bacterial enrichment of bioelectrochemical systems during methane and acetate production. *International Journal of Hydrogen Energy*, **39**(36), 21864-21875.

Xu, H., Wang, K., Holmes, D.E. 2014. Bioelectrochemical removal of carbon dioxide (CO2): An innovative method for biogas upgrading. *Bioresource Technology*, **173**, 392-398.

Zeppilli, M., Villano, M., Aulenta, F., Lampis, S., Vallini, G., Majone, M. 2014. Effect of the anode feeding composition on the performance of a continuous-flow methane-producing microbial electrolysis cell. *Environmental Science and Pollution Research*, **22**(10), 7349-7360.

Zhen, G., Kobayashi, T., Lu, X., Xu, K. 2015. Understanding methane bioelectrosynthesis from carbon dioxide in a two-chamber microbial electrolysis cells (MECs) containing a carbon biocathode. *Bioresource Technology*, **186**, 141-148.

CHAPTER 11

Anaerobic digestion and electromethanogenic microbial electrolysis cell integrated system: increased stability and recovery of ammonia and methane

Part of the content of this chapter is in preparation to be submitted for publication as:

Cerrillo, M., Viñas, M., Bonmatí, A. Anaerobic digestion and electromethanogenic microbial electrolysis cell integrated system: increased stability and recovery of ammonia and methane.

Abstract

The integration of anaerobic digestion (AD) and a microbial electrolysis cell (MEC) with an electromethanogenic biocathode is proposed here to increase the stability and robustness of the AD process against organic and nitrogen overloads; to keep the effluent quality; to recover ammonium; and to upgrade the biogas. The methane production of the AD could be recovered after the inhibition of the reactor due to the doubling of the organic and nitrogen loading rate thanks to the connection of a recirculation loop with the MEC effluent. Ammonium removal in the anode compartment of the MEC achieved 14.46 g $N\text{-}NH_4^+$ m^{-2} d^{-1}, while obtaining on average 79 L CH_4 m^{-3} d^{-1} through the conversion of CO_2 in the cathode compartment. The microbial analysis showed that methylotrophic *Methanossiliicoccaceae* family (*Methanomassiliicoccus* genus) was the most abundant among active archaea in the AD during the inhibited state; while on the cathode *Methanobacteriaceae* family (*Methanobrevibacter* and *Methanobacterium* genus), usually found to be the most abundant in methanogenic biocathodes, shared dominance with *Methanomassiliicoccaceae* and *Methanotrichaceae* families (*Methanomassiliicoccus* and *Methanothrix* genus, respectively).

11.1 Introduction

The combination of anaerobic digestion (AD) and bioelectrochemical systems (BES) is attracting attention in recent years as an integrated strategy that can be implemented with different objectives. On the one hand, nutrients can be recovered from ammonium-rich wastewater such as pig slurry or digested pig slurry thanks to cation or anion transport through exchange membranes that takes places in BESs. The main example of this application is the recovery of ammonium (Chapter 4 to 8), which can be reused as fertiliser (Cerrillo et al., 2016a; Kuntke et al., 2012; Sotres et al., 2015a; Zhang et al., 2013). Otherwise, the AD effluent would need to be processed or managed properly due to its high nutrient content. Ammonia recovery has been demonstrated in various BESs including microbial fuel cells (MFCs) and microbial electrolysis cells (MECs). In MECs, a higher current density would greatly enhance ammonium recovery, and thus MECs exhibit a better performance for ammonium recovery than MFCs (Liu et al., 2016). On the second hand, BESs can operate with low organic loading rates and may be used to polish the effluent of the AD (Chapter 5; Durruty et al., 2012; Ge et al., 2013) or even to absorb higher organic concentrations in the digestates due to AD destabilisation or inhibition (Chapter 6). On the third place, the combination of the previous advantages can be applied to increase the stability of the AD process through the use of a submersible microbial desalination cell (Zhang and Angelidaki, 2015) or the establishment of a recirculation loop with the BES (Chapter 7 and 8). The latter strategy has proven to be effective for the control of AD inhibition due to organic and nitrogen overloads, while recovering ammonia and maintaining the effluent quality and the methane production of the AD (Chapter 6). Finally, BES have been applied to increase the methane content of the biogas produced in the AD by the use of MECs with electromethanogenic biocathodes (Chapter 10; Xu et al., 2014). Since biogas consists mainly of methane (CH_4, 40-75%) and carbon dioxide (CO_2, 15-60%) it needs upgrading prior to its use as vehicle fuel or for injection in the natural gas grid intended to adjust the calorific value. Conventional techniques for biogas upgrading focus on CO_2 removal without changing CH_4 mass (Ryckebosch et al., 2011), while electromethanogenesis performed in MECs allows for the conversion of CO_2 into CH_4 (Cheng et al., 2009; Van Eerten-Jansen et al., 2013; Villano et al., 2011). MECs for CO_2 conversion to methane have been operated mainly with synthetic medium (Hou et al., 2015; Zeppilli et al., 2014), and there is a lack of studies with real wastewater feed for the anode compartment.

The multiple ways of AD and BES combination suggest that a more comprehensive strategy can help to settle most of the limitations of the AD process, which up to now has not been assessed. An integrated AD-MEC system could be designed with a multiple purpose: i) to increase the stability and robustness of the AD process against organic and nitrogen overloads, ii) to keep the effluent quality, iii) to recover nutrients, and iv) to upgrade the biogas.

Furthermore, further study on the active microbial populations enriched in the bioanode and biocathode of the BES is needed to gain insight on potential resilience strategies as well as to complement previous studies (Zeppilli et al., 2014). An special focus on active biomass is lacking, since usual studies are centred so far on the description of existent microorganisms on methanogenic biocathodes (Cheng et al., 2009; Marshall et al., 2012; Van Eerten-Jansen et al., 2013; Xu et al., 2014; Zhen et al., 2015).

The main aim of this Chapter was to assess the performance of a lab-scale AD-MEC integrated system as a strategy to stabilise a pig slurry thermophilic AD under an organic and nitrogen overload, recover ammonia and increase the methane content of the biogas produced by the AD, in terms of chemical oxygen demand and ammonia removal, methane yield and energy efficiency of the process. The evolution of the active microbial community of the AD and the MEC bioelectrodes (both the anode and the cathode) was evaluated in terms of composition and activity by means of high throughput sequencing (16S rRNA /16SrDNA based Miseq) and quantifying total and active populations (16SrRNA and mcrA gene and transcripts) by qPCR.

11.2 Materials and methods

11.2.1 Experimental set-up

A 4 L lab-scale thermophilic anaerobic continuous stirred tank reactor (AD) described in Section 3.1.3 was used in the assays. The AD reactor was connected in series with the anode compartment of a two-chambered MEC (described in Section 3.1.2) and had a recirculation loop between both reactors. The cathode compartment of the MEC was inoculated with 30 mL of a resuspension of the anaerobic granular sludge of the UASB (volatile suspended solids content of 33 g L^{-1}) that had been operated with methanol in order to enrich the biomass in methanogenic archaea, in Chapter 9. The resuspension was done by vortex mixing during 10 minutes in a 50 mL tube containing 30 g of granular sludge and 25 mL of Ringer 1/4 sterilised solution.

11.2.2 Reactor operation

The AD was fed with pig slurry (Table 11.1) and operated for 222 days in three different phases, with a hydraulic retention time (HRT) of 10 days (Table 11.2). In Phase 1, the organic loading rate (OLR) and nitrogen loading rate (NLR) were established at 3.92 kg_{COD} m^{-3} day^{-1} and 0.22 kg_N m^{-3} day^{-1}, respectively. In Phase 2, the OLR and NLR were doubled to force the inhibition of the reactor. And finally, in Phase 3 the OLR and NLR were the same as those of the previous phase and the recirculation loop with the MEC was connected (50% of the AD feed flow rate) to recover the AD. Samples of the AD effluent were taken once a week in order to assess the operation of the reactor.

The MEC was operated in continuous in series with the AD poising the cathode potential at -800 mV *vs* SHE. The solutions of both the anode and the cathode compartment were fed in continuous with a pump at 20 mL h^{-1} and mixed recirculating them by an external pump. The HRT was of 32.4 h and 14.1 h for de anode and cathode compartment, respectively (with respect to the net volume of each compartment). The OLR and NLR of the anode compartment for each phase are specified in Table 11.2. The MEC was operated at room temperature during the entire assay (23±2 ºC).

Table 11.1 Characterisation of the raw pig slurry used as feeding solution in the anaerobic digester (AD) in Phase 1 and Phases 2 and 3 (n=number of samples; mean±standard deviation).

Parameter	**Raw pig slurry**	
	Phase 1 (n=6)	**Phase 2 and 3** (n=12)
pH (-)	7.1±0.1	6.8±0.2
COD (g_{O2} kg^{-1})	43.96±2.04	80.55±6.40
NTK (g L^{-1})	2.41±0.00	4.29±0.17
N-NH_4^+ (g L^{-1})	1.59±0.08	2.97±0.25
TS (g kg^{-1})	24.40±0.52	47.95±2.53
VS (g kg^{-1})	16.37±0.43	32.79±1.88

Table 11.2 Operational conditions of the AD reactor and the MEC (mean±standard deviation).

Phase	**Period (d)**	**AD**			**MEC**	
		OLR (kg_{COD} m^{-3} d^{-1})	**NLR (kg_N m^{-3} d^{-1})**	**Recirculation (% feed flow rate)**	**OLR (kg_{COD} m^{-3} d^{-1})**	**NLR (kg_N m^{-3} d^{-1})**
1	1 - 78	3.92±0.61	0.22±0.03	0	7.87±0.76	0.74±0.04
2	78 - 126	7.39±1.36	0.40±0.06	0	43.12±3.58	2.42±0.13
3	126 - 222			50		

11.2.3 Analyses and calculations

Samples were analysed for pH, chemical oxygen demand (COD), ammonium (N-NH_4^+), methane content (biogas produced by the AD and dissolved methane in the cathode effluent samples), partial alkalinity (PA), total alkalinity (TA) and intermediate alkalinity (IA) accordingly to the methods described in Section 3.2. COD and ammonium removal efficiency in the MEC were calculated as described in Section 3.4.1.

The current density (A m^{-2}) of the MEC was calculated as described in Section 3.3. The Coulombic efficiency (CE), or the fraction of electrons obtained from the consumption of COD

that are available for methane production at the cathode, the energy efficiency relative to electrical input recovered as methane (EE_e), the energy efficiency relative to the energy content of the substrate (EE_s), the energy efficiency with respect to the energy input and the energy in the substrate (EE_{e+s}) and the cathodic methane recovery efficiency (R_{cat}), defined as the fraction of electrons reaching the cathode that are recovered as methane, were calculated as described in Section 3.4.3.

Cyclic voltammetries (CV) in turnover conditions were performed after the cathode inoculation (day 0) and at the end of Phase 2 and 3 (day 78 and 222 of the assays, respectively), following the methodology described in Section 3.3.

The bacterial communities in the biofilm harboured in the bioanode and the biocathode of the MEC at the end of Phase 2 and 3 and in the AD biomass at the end of each Phase (1, 2 and 3) were analysed by culture-independent molecular techniques such as quantitative PCR (qPCR) and high throughput sequencing (MiSeq, Illumina) of partial *16S* rDNA and *16S* rRNA massive libraries. Simultaneous total genomic DNA and RNA extraction and complementary DNA (cDNA) synthesis, qPCR and high throughput 16S rRNA gene sequencing (MiSeq, Illumina) were performed following the methods described in Section 3.6.2, 3.6.3, and 3.6.5, respectively. The standard curve parameters of the qPCRs were as follows (for *16S* rRNA and *mcr*A, respectively): a slope of -3.244 and -3.532; a correlation coefficient of 0.998 and 0.999; and an efficiency of 103 and 92%. The data obtained from sequencing datasets for eubacterial and archaeal populations was submitted to the Sequence Read Archive of the National Center for Biotechnology Information (NCBI) under the study accession number SRP072956.

The inoculum of the cathode and the biofilm settled up on the anode had been characterised in Chapters 9 and 8, respectively. Briefly, regarding eubacteria, the cathode inoculum was dominated by *Bacteroidetes*, *Firmicutes* and *Synergistetes* (61, 14 and 8%, respectively); *Methanosarcinaceae* (52%) was the predominant archaea family (methylotrophs genus, *Methanomethylovorans* and *Methanolobus*). In the case of MEC anode biofilm, *Firmicutes, Bacteroidetes* and *Proteobacteria* were the dominant eubacterial *phyla* (35, 30 and 11%, respectively), and the predominant archaea family was *Methanotrichaceae* (87%).

The evaluation of the diversity of the samples and statistical multivariate analyses were performed following Section 3.6.6.

11.3 Results and discussion

11.3.1 Performance of the AD independent operation

The AD showed a stable operation during Phase 1 (Figure 11.1), with an average COD removal efficiency of 54±8% and a methane production of 0.45±0.06 m^3 m^{-3} d^{-1} (Table 11.3). The IA:TA ratio was kept below 0.3, corroborating the stability of the reactor. When the OLR and NLR of the AD were doubled in Phase 2, the reactor showed a fast inhibition, reducing the value of COD removal to 18% and the methane production to 0.23 m^3 m^{-3} d^{-1}, 50% of the obtained in the previous phase (Figure 11.1a and b). VFA accumulated, reaching values of 5670 mg L^{-1} for acetate, 1850 mg L^{-1} for propionate and over 1000 mg L^{-1} for butyrate (Figure 11.1c), and the IA:TA ratio increased to 0.44 (Figure 11.1d) confirming the instability of the AD reactor.

Table 11.3 Summary of the main parameters of the AD and the MEC reactors in the different phases. Results for the AD correspond to the stable period of each phase (mean±standard deviation).

Parameter	Phase 1	Phase 2	Phase 3
AD			
CH_4 production (m^{-3} m^{-3} d^{-1})	0.45±0.06	0.27±0.04	0.38±0.04
COD removal efficiency (%)	54±8	28±8	22±5
IA:TA	0.22±0.04	0.40±0.08	0.50±0.03
pH	7.8±0.1	7.8±0.1	7.6±0.1
MEC			
COD removal efficiency (%)	24±8	14±5	21±6
N-NH_4^+ removal efficiency (%)	30±6	18±5	20±5
CE (%)	3.5±1.8	2.1±1.4	1.5±0.5
CH_4 production (L m^{-3} d^{-1})	79±34	63±15	78±29
R_{cat} (%)	45±37	61±18	59±13
EE_e (%)	50±41	62±17	85±23
EE_s (%)	4.2±2.3	3.0±1.5	1.4±0.7
EE_{e+s} (%)	3.6±1.4	2.9±1.4	1.4±0.7
AD-MEC			
COD removal efficiency (%)	-	42±6	41±6

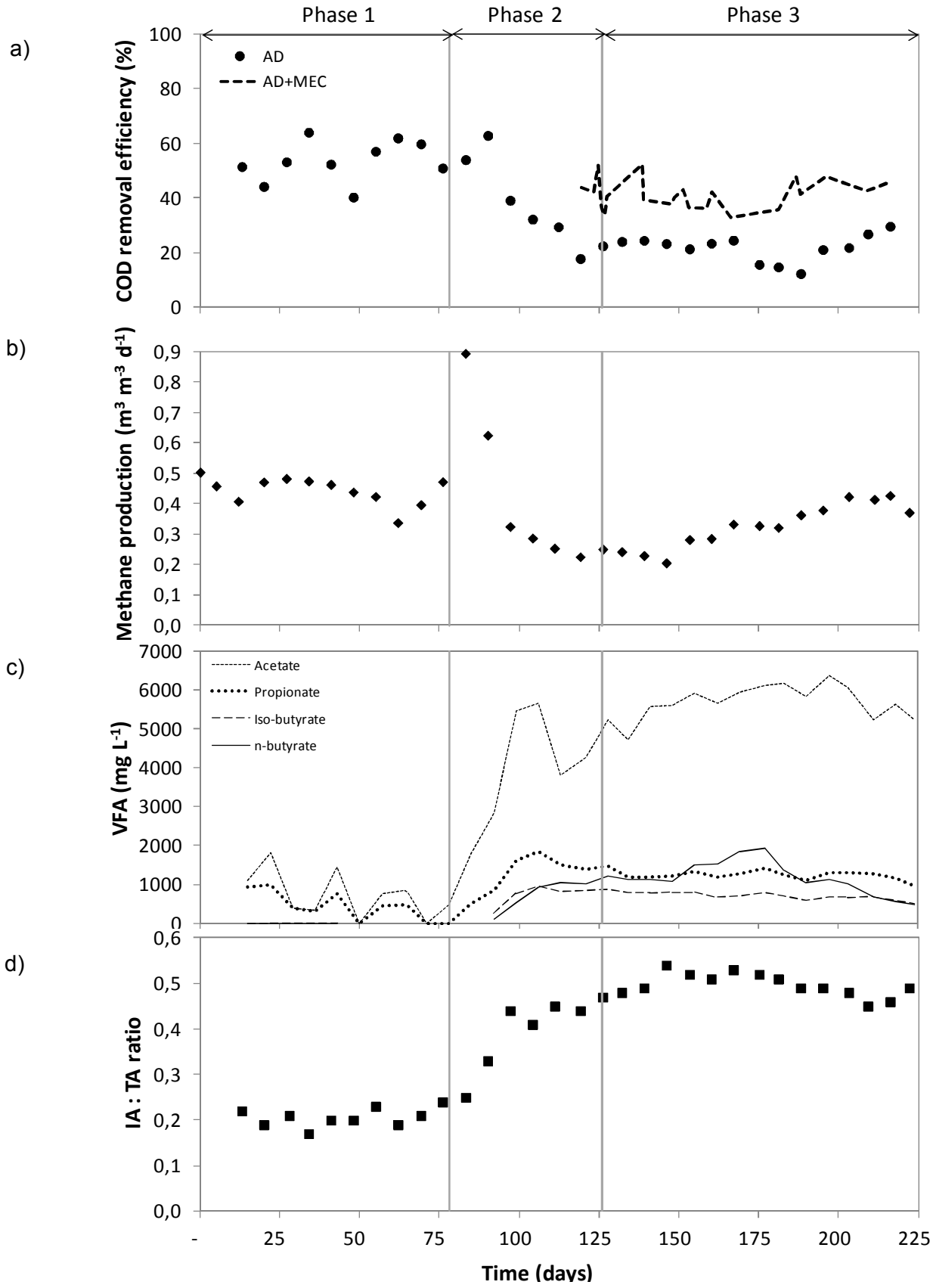

Figure 11.1 Performance of the AD regarding (a) COD removal efficiency; (b) methane production; (c) VFA concentration; and (d) IA:TA ratio.

11.3.2 Performance of the AD-MEC combined system in series operation

The MEC fed with the effluent of the AD during Phase 1 showed a stable performance regarding current density production during the first 30 days of operation, with an average current density of 0.4 A m^{-2} (Figure 11.2). Afterwards, the current density production became unstable, showing peaks of up to 4.5 A m^{-2} (average of 1.5 A m^{-2}) and was drastically reduced from day 64 onward due to the degradation of the stainless steel mesh used as electron collector in the anode compartment (data corresponding to the unstable period was not considered for calculations). The mesh was replaced at the beginning of Phase 2. This change produced some period of instability at the beginning of Phase 2, but afterwards the MEC showed a current density production similar to the obtained in Phase 1. The COD removal efficiency of the MEC in Phase 1 was of 24±8%, with a maximum removal of 3.2 kg_{COD} m^{-3} d^{-1}, and the CE was of 3.5±1.8% (Table 11.3). In Phase 2 the COD removal efficiency and the CE decreased to 14±5% and 2.1±1.4%, respectively. Since CE is related with the substrate concentration, the increase in COD of the influent resulted in a decrease in CE (Zhang et al., 2015). The ammonium removal efficiency in Phase 1 was of 30±6%, corresponding to 6.64 g N-NH_4^+ m^{-2} d^{-1}. The removal efficiency decreased to 18±5% during Phase 2, although the absolute flux was higher (12.87 g N-NH_4^+ m^{-2} d^{-1}) as a result of the increased NLR. Previous work performed with the same MEC but with an abiotic cathode fed with NaCl (0.1 g L^{-1}) and higher organic and nitrogen loading rates (28.50±1.80 kg_{COD} m^{-3} day^{-1} and 1.73±0.09 kg_N m^{-3} day^{-1}, respectively) achieved a nitrogen removal rate of 12.97±2.04 g N-NH_4^+ m^{-2} d^{-1}, similar to the one obtained in Phase 2 and almost doubling the rate obtained in Phase 1 in this study (Chapter 7). And values as high as 86 g N-NH_4^+ m^{-2} d^{-1} were reported with a submersible microbial desalination cell fed with synthetic solution (Zhang and Angelidaki, 2015).

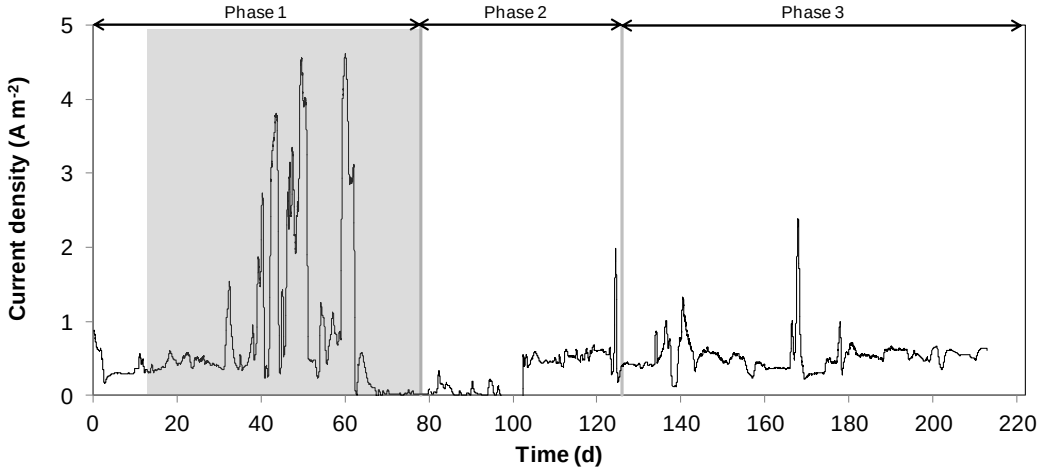

Figure 11.2 Current density profile obtained during the operation of the MEC. Data corresponding to the unstable period (shaded) was not considered for calculations.

11.3.3 Performance of the AD-MEC combined system with recirculation loop

When the recirculation loop with the MEC was connected in Phase 3, the performance of the AD started to recover. COD removal values achieved 30% (below 20% in the end of Phase 2) and maximum methane production was 0.43 m^3 m^{-3} d^{-1}, representing a 100% increase with respect to the production at the end of Phase 2, and nearly recovering the values achieved in Phase 1. However, the VFA concentration and the IA:TA ratio were similar to the previous phase. Interestingly, the overall performance of the AD-MEC integrated system maintained the COD removal in a range of 33-52%, in spite of the poorer performance of the AD, concomitant to an ammonium removal of 20±5% (14.46 g $N\text{-}NH_4^+$ m^{-2} d^{-1}). The MEC showed a current density production similar to the obtained at the beginning of Phase 1. The CE of the MEC decreased with respect to Phase 1, as described in Phase 2. The low CEs obtained are to be expected when working with complex substrates where other electron acceptors may be present (Catal et al., 2011; Liu et al., 2004; Min et al., 2005), while in Chapter 10 the methanogenic biocathode MEC, working with acetate medium, the CE achieved 33%. Much higher CEs have been previously reported, such as 72-80% (Zeppilli et al., 2014).

11.3.4 Biocathode operation performance

Methane production in the cathode compartment was around 0.079 m^3 m^{-3} d^{-1}. A volume of biogas of 0.2 m^3 m^{-3} d^{-1} could be treated in this MEC with biocathode, assuming a typical biogas composition of 60% of CH_4 and 40% of CO_2, to obtain methane with a purity prochain to 100%. Higher productions have been achieved in previous works, such as 0.16 m^3 m^{-3} d^{-1} (Hou et al., 2015), 0.23 m^3 m^{-3} d^{-1} (Chapter 10) or 0.28 m^3 m^{-3} d^{-1} (Villano et al., 2013).

The highest R_{cat} was achieved in Phase 2 (61±18%), although the high variability of the obtained results makes the observed differences between phases not to be significant (Table 11.3). The obtained results for R_{cat} are below the 96% previously reported by Cheng et al. (2009) or the 84-86% obtained by Zeppilli et al. (2014), but much higher than the 23.1% achieved by Van Eerten-Jansen et al. (2001) or the 24.2 ± 4.7% reported by Zhen et al. (2015).

The EEe was between 50 and 85%, values similar to the obtained in Chapter 10 with the anode fed with synthetic medium (57-61%) or in batch mode with a two-chambered MEC using graphite granules as electrodes (57%) (Villano et al., 2011). The low CE achieved in this MEC made also the obtained EEs (between 1.4 and 3.6%) to be low in comparison with the previous work (between 23 and 54%).

Figure 11.3 shows the cyclic voltammograms obtained after the cathode inoculation and at the end of Phases 2 (78 days) and 3 (222 days). The curve obtained at the start of the operation showed a low response to the different applied potentials, as a result of the recent

inoculation. The performance of the biocathode increased at the voltage of -800 mV at the end of the assay (Phase 3), coincidently with the period of the best EE_e.

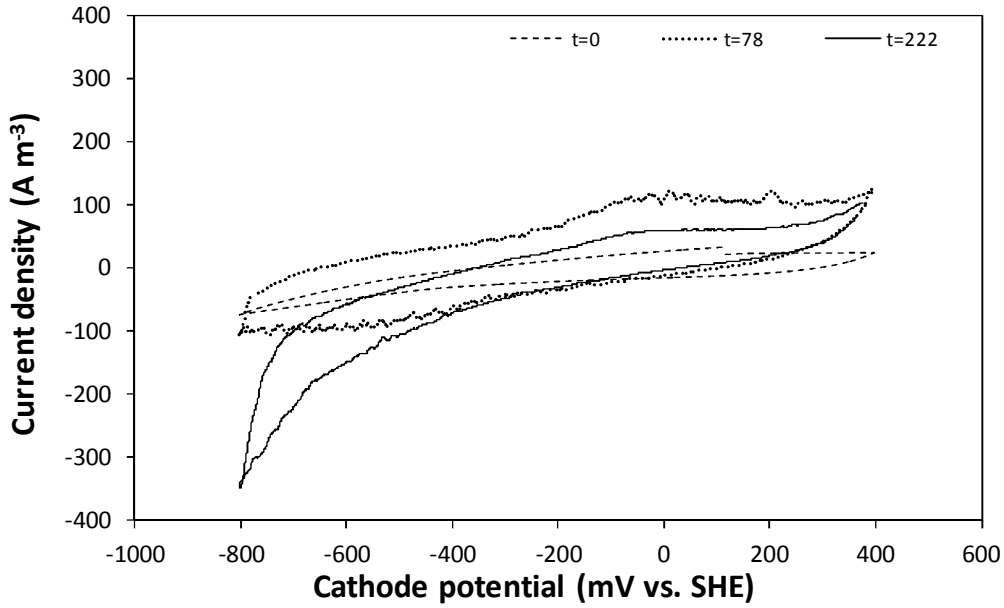

Figure 11.3 Cyclic voltammograms of the MEC after the cathode inoculation (t=0 d) and at the end of Phase 2 and 3 ((t=78 d and t=222 d, respectively).

11.3.3 Microbial community assessment

The microbial community structure and activity of the samples taken from the AD and the biofilm harboured on the electrodes of the MEC was characterised by means of qPCR technique and sequenced by MiSeq.

11.3.3.1 Quantitative analysis by qPCR

Figure 11.4 shows qPCR results for *16S* rRNA and *mcr*A gene copy numbers of the seven samples analysed, either for DNA (present microorganisms) and cDNA (active microorganisms). In the AD samples eubacteria remained in the same order of magnitude for *16S* rRNA gene copy numbers g^{-1} during the stable, inhibited and recovered states; while showed a decrease of one order of magnitude for *mcr*A (from $1.26 \cdot 10^8$ to $2.18 \cdot 10^7$ gene copy numbers g^{-1}) at the end of Phase 2 due to the inhibition caused by doubling the OLR and NLR. The connexion of the recirculation loop reduced the inhibition and helped to recover the methanogenic population and return to levels similar to those existing prior to the inhibition ($1.38 \cdot 10^8$ gene copy numbers g^{-1}). The same behaviour was observed at cDNA-based qPCR, showing a decrease of one order of magnitude for *mcr*A transcripts copy numbers in the AD sample of the end of Phase 2 and confirming that the methanogenic population was suffering inhibition. The magnitude of the reduction in *mcr*A gene copy numbers when the AD was

submitted to inhibition by an organic and nitrogen overload was similar to the described in Chapter 8 and other previous work (Zhang et al., 2014). In Phase 1 free ammonia nitrogen (FAN) concentration was in the range of 400-670 mg L^{-1}. Concentrations of FAN above 900 mg L^{-1} were reached during Phase 2, when the OLR and NLR were doubled, with a maximum of 1186 mg FAN L^{-1} at the end of the Phase. At these levels the first signs of inhibition may occur according to previous studies (Angelidaki and Ahring, 1993; Hansen et al., 1998). Once the recirculation loop was established in Phase 3, FAN levels remained in a range of 365-740 mg L^{-1}.

Regarding the MEC, gene copy numbers for *16S* rRNA for the anode and cathode biofilm were of the same order of magnitude both for Phase 2 and 3 samples, either in DNA or in cDNA forms. On the contrary, *mcrA* gene copy numbers of the anode sample increased at the end of the recirculation phase, probably due to the parallel increase of methanogenic population in the AD. In the case of the cathode biofilm, *mcrA* gene copy numbers g^{-1} for DNA-based qPCR at the end of the assay were within 10^6 gene copy numbers g^{-1}, coincidently with the values obtained in Chapter 10. While a total methanogenic population decrease was observed from the initial cathode to the final sample (DNA level), *mcrA* expression belonging to methanogenic archaea increased one order of magnitude (from $1.40 \cdot 10^5$ to $2.63 \cdot 10^6$ transcript copy numbers g^{-1}).

From these results, it is clear that the AD methanogenic population decreased due to the organic and nitrogen overload and then could be recovered thanks to the establishment of the recirculation loop with the MEC. Furthermore, the methanogenic cathode of the MEC was progressively enriched in metabolically active methanogenic archaea.

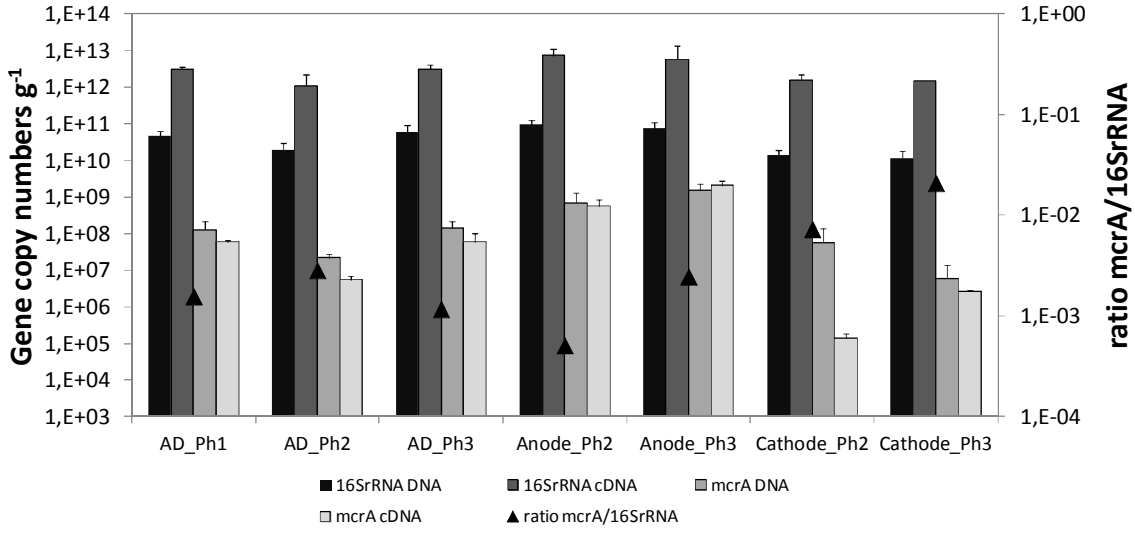

Figure 11.4 Gene copy numbers for *16S* rRNA and *mcr*A genes and ratio between them of DNA and cDNA, of the AD effluent at the end of Phases 1, 2 and 3, and the biofilm harboured on the anode and cathode of the MEC at the end of Phase 2 and 3.

11.3.3.2 High Throughput Sequencing (16S-based MiSeq) results for eubacteria and archaea

Table 11.4 shows the number of reads obtained for the AD samples and the anode and cathode biofilms of the MEC for eubacteria (6822 OTUs) and archaea (900 OTUs). Figure 11.5a shows the relative abundance of eubacterial *phyla* for the seven samples, regarding DNA (present microorganisms) and cDNA (metabolically active microorganisms) forms. The three AD samples showed a similar eubacterial composition at DNA level, dominated by *Firmicutes*, *Bacteroidetes* and *Proteobacteria*, with relative abundances in the ranges of 64-68%, 12-18% and 5-10%, respectively. Previous studies, performed also in a thermophilic AD running on pig slurry, found that the *Firmicutes phylum* was the predominant one (Chapter 7; Cerrillo et al., 2016b; Tuan et al., 2014). The sample from the end of Phase 2 showed a decrease in *Firmicutes* and *Proteobacteria phyla* with respect to Phase 1 and the sample at the end of Phase 3, while *Bacteroidetes* increased slightly. At cDNA level, although *Firmicutes* was still the predominant *phylum* (46-75% of relative abundance), *Proteobacteria* active microorganisms clearly surpassed *Bacteroidetes* (19-40% and 1-5%, respectively) and were increasingly more abundant over time, while *Firmicutes* showed the opposite tendency. *Bacteroidetes* was the predominant *phylum* in the anode of the MEC both in Phase 2 and 3 samples (34 and 41%, respectively), according to DNA-based sequencing, while *Proteobacteria* revealed as the most active one in Phase 2 sample (65%) and *Bacteroidetes* and *Proteobacteria* shared dominance in the final sample (18 and 16%, respectively). These three phyla have been identified in previous studies in BES (Bonmatí et al., 2013; Sotres et al., 2015b; Sotres et al., 2016). In the case of the cathode biofilm, the domination of *Firmicutes* at DNA level in Phase 2 and 3 samples (56 and 31%, respectively), shared by *Proteobacteria* in Phase 3 sample (33%), shifted to a clear dominance of *Proteobacteria* in both samples at cDNA level (59 and 68%).

At family level *Clostridiaceae 1* and *Peptostreptococcaceae* were the most present and active groups in the three AD samples (Figure 11.5b). *Porphyromonadaceae*, which was the third more abundant family (6-9%) at DNA level, showed a low activity according to cDNA sequencing (below 1%). *Planococcaceae* and *Pseudomonadaceae* revealed as active families at the end of Phase 2 (21 and 12%, respectively), as *Campylobacteraceae* at the end of Phase 2 (13%), although they were below 3% in DNA form abundance. Regarding the samples of the MEC anode, *Planctomyceraceae* and *Porphyromonadaceae* stood out in the Phase 2 sample when looking at DNA sequencing results (12 and 16%, respectively), but were replaced by *Desulfuromonadaceae* and *Pseudomonadaceae* families according to cDNA (21 and 18%, respectively). In Phase 3 anode sample *Porphyromonadaceae* and *Planctomycetaceae* were the most abundant families at DNA (12%) and cDNA (14%) levels, respectively. Finally, the cathode biofilm was dominated by *Clostridiaceae* in Phase 2 and 3 samples at DNA level (34

and 12%, respectively), but by metabolically active *Phodocyclaceae* and *Desulfovibrionaceae* according to cDNA results (14 and 37%, respectively). Thus, a clear differentiation between total eubacteria and active eubacterial microorganisms, especially in the biomass harboured by the MEC electrodes, has been shown.

a)

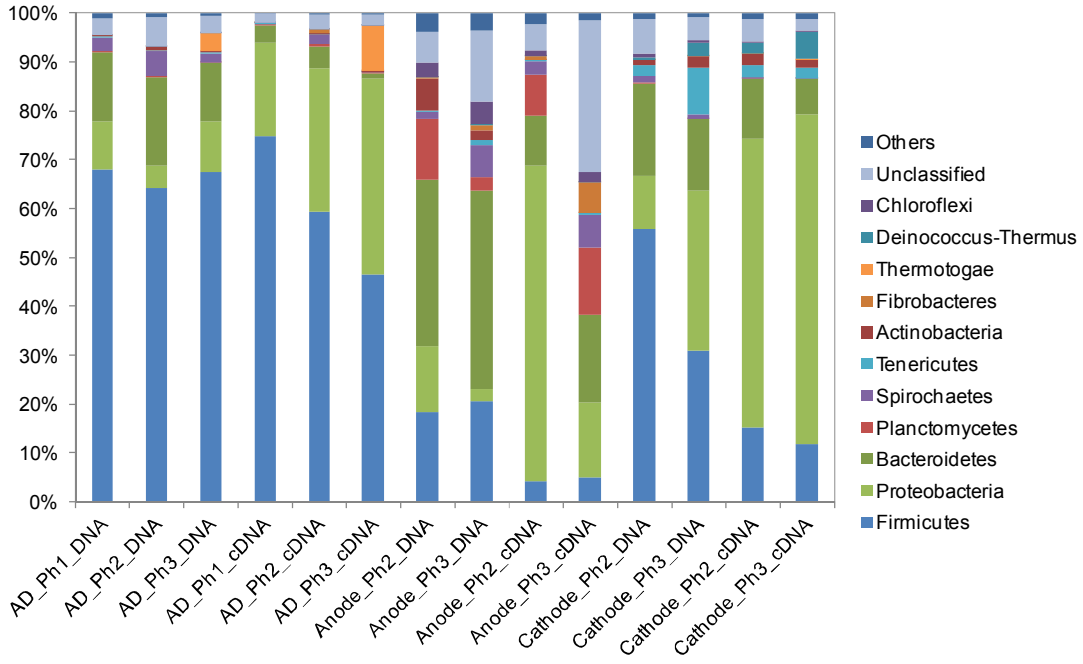

b)

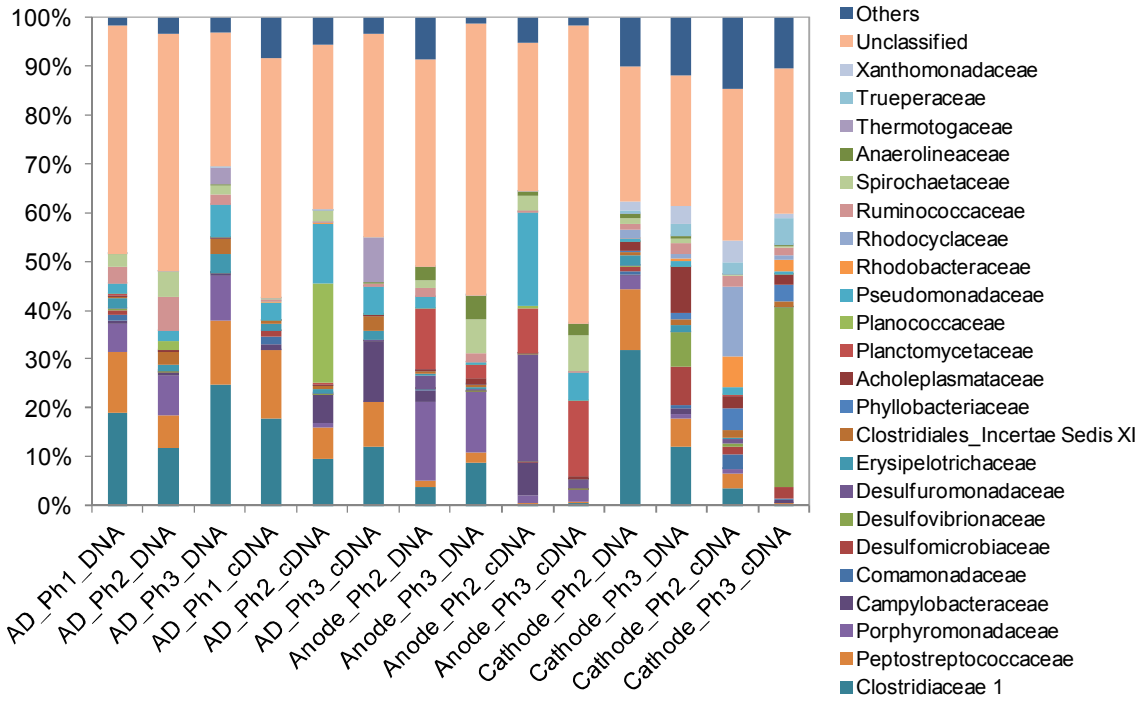

Figure 11.5 Taxonomic assignment of sequencing reads from Eubacterial community of the AD effluent at the end of Phases 1, 2 and 3, and the biofilm harboured on the anode and cathode of the MEC at the end of Phase 2 and 3 for DNA and cDNA, at a) phylum and b) family levels. Relative abundance was defined as the number of reads (sequences) affiliated with any given taxon divided by the total number of reads per sample. Phylogenetic groups with a relative abundance lower that 1% were categorised as “others”.

Figure 11.6 shows the relative abundance of archaea families of the seven samples. Although *Methanobacteriaceae* showed a high abundance in the three AD samples (74-86%), the most active archaeal populations were *Methanomicrobiaceae* in Phase 1 and Phase 3 AD samples (58 and 56%, respectively) and Methanossiliicoccaceae in Phase 2 sample (54%). Members of the *Methanomassiliicoccaceae* family have recently been described as obligate hydrogen-consuming methanogens, reducing methanol and methylamines instead of carbon dioxide (Borrel et al., 2013; Dridi et al., 2012). A recent study has reported an increase of this family at high OLR, and concluded that an additional methanogenic pathway might contribute to methane production at high OLR (Moestedt et al., 2016). It has also been reported that this family emerged in the recovery process of a thermophilic AD after an organic overload (Hori et al., 2015), since methanol could be produced fermentatively from lactate by a kind of *Clostridium* species. Methanogenic population in the AD showed higher differences between existing vs active composition than eubacteria. On the contrary, *Methanotrichaceae*, the predominant family on the MEC anode Phase 2 and 3 samples in presence (75 and 48%, respectively) was also active (74 and 31%, respectively), independently of being on a low relative abundance in the AD. On the other hand, *Methanossiliicoccaceae* and *Methanomicrobiaceae* increased in presence and activity over time, probably due to the high activity of these families in the AD. When looking at the cathode biofilm, *Methanotrichaceae* (genus *Methanothrix*, formerly known as *Methanosaeta*) was the dominant family at the Phase 2 sample either in presence and activity (53 and 68%, respectively), while in the Phase 3 sample it dominated at DNA but not at cDNA level (36% and 0.3%, respectively). *Methanothrix* (*Methanosaeta) genus* was also detected in a methanogenic cathode by Xu et al. (2014). It has been recently described that *Methanothrix (Methanosaeta)* is capable of accepting electrons via direct interspecies electron transfer (DIET) for the reduction of carbon dioxide to methane (Rotaru et al., 2014), so a deeper study is necessary to understand the role of these species in the cathode biofilm of the methanogenic MEC. *Methanomassiliicoccaceae* (genus *Methanomassiliicoccus*) and *Methanobacteriaceae* (genus *Methanobacterium* and *Methanobrevibacter*) were also families with high relative abundances at DNA level (15-31%), being the most active ones in the Phase 3 sample (57 and 33%, respectively) as well. Previous works have showed a clear dominance of *Methanobacteriaceae* family in methanogenic biocathodes (Chapter 10; Cheng et al., 2009; Marshall et al., 2012; Van Eerten-Jansen et al., 2013; Xu et al., 2014; Zhen et al., 2015), differing from the results obtained in this study. The high relative abundance of the methylotrophic *Methanomassiliicoccaceae* family among the active archaea suggests that methanol must be present in the cathode compartment, although it was not monitored in the present study. Methanol produced in the anode compartment due to the fermentation of organic compounds could migrate to the cathode compartment through the

CEM. Methanol could be also produced at very low O_2 partial pressure, from methane by ammonia oxidising bacteria (AOB) which can partially oxidise CH_4 to methanol when using ammonia as an energy source (Taher and Chandran, 2013). The genera *Nitrosomonas*, a well known AOB, was present in the biocathode samples, although at low relative abundance (<0.01%). Besides, some methane oxidising archaea and bacteria can also carry out anaerobic oxidation of methane (Ge et al., 2014), although so far they are poorly known and it cannot be determined if they are present in the biocathode.

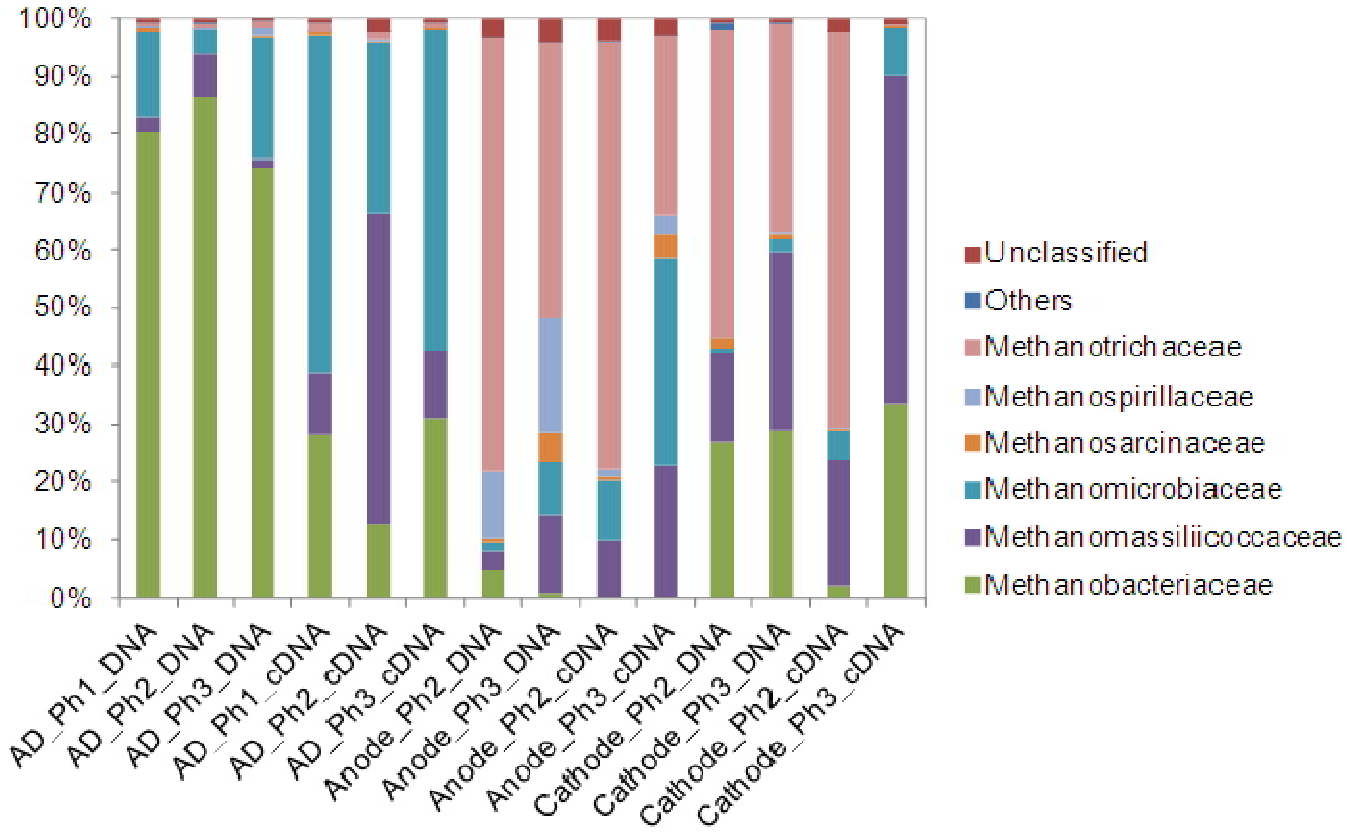

Figure 11.6 Taxonomic assignment of sequencing reads from Archaeal community of the AD effluent at the end of Phases 1, 2 and 3, and the biofilm harboured on the anode and cathode of the MEC at the end of Phase 2 and 3 for DNA and cDNA, at family level. Relative abundance was defined as the number of reads (sequences) affiliated with any given taxon divided by the total number of reads per sample. Phylogenetic groups with a relative abundance lower that 1% were categorised as "others".

11.3.3.3 Biodiversity analysis

Table 11.4 shows the results for the biodiversity analysis performed on the AD samples and the anode and cathode biofilms of the MEC samples. The Inverted Simpson and Shannon indices of the AD samples for eubacteria at DNA level decreased during Phase 2 and recovered

in Phase 3, showing the opposite behaviour for archaea. The biodiversity of the bioanode and the biocathode increased regarding archaeal population, either in total (DNA) or in metabolically active (cDNA). The previous work performed in Chapter 10 with a similar MEC but in synthetic medium found the opposite behaviour for the biocathode diversity, since a great enrichment in *Methanobacteriaceae* took place. On the contrary, eubacteria decreased its biodiversity, result that agrees with the trend observed in other studies (Siegert et al., 2015).

11.3.3.4 Correspondence analysis

Correspondence analysis results for eubacteria and archaea community are shown in Figure 11.7a and 11.7b, respectively. Regarding eubacteria, AD samples were clustered together, especially in the case of DNA, while for cDNA form the samples were more disperse and detached from the first ones. This cluster included the Phase 2 DNA sample of the cathode biofilm, which separated lately at the end of the assay. When looking at the Phase 2 sample for active microorganisms (cDNA), it was nearer to the anode samples, although the Phase 3 sample differentiated completely from all the samples analysed. Finally, the anode samples clustered clearly in two groups, one for DNA and a second one for cDNA, showing that the metabolically active population (cDNA sequencing) was different from total population (DNA sequencing).

Archaeal results for the AD biomass showed that the three DNA samples were prochain, so little differences in composition were detected between inhibited and stable states. On the contrary, cDNA samples, related to the active microorganisms, were distant from DNA samples and Phase 1 and 3 samples were clustered together while Phase 2 sample moved away from them. This means that active microorganisms in the initial sample shifted to a different active community during Phase 2 due to the inhibition and, once recovered with the recirculation loop, went back to the previous composition. Regarding the anode and cathode communities, Phase 2 DNA and cDNA samples resembled and an evolution was observed for the Phase 3 samples, moving away from the initial composition, especially for cDNA. Interestingly, the biocathode cDNA Phase 3 sample approached to the cDNA AD sample of Phase 2, suggesting that the active population of the cathode resembled the AD population under inhibition.

Table 11.4 Diversity index for Eubacteria and Archaea community of the AD effluent at the end of Phases 1, 2 and 3, and the biofilm harboured on the anode and cathode of the MEC at the end of Phase 2 and 3 for DNA and cDNA samples (mean±standard deviation). Normalised to the lowest number of reads (56424 and 59671 for eubacteria and archaea, respectively)

	Reads	Inverted Simpson	Shannon
Eubacteria			
ADPh1-DNA	116316	14.67±0.07	3.94±0.01
ADPh2-DNA	142940	13.00±0.07	3.85±0.01
ADPh3-DNA	117089	13.61±0.08	4.02±0.01
Anodei-DNA	95391	38.16±0.22	4.90±0.01
Anodef-DNA	96879	34.12±0.20	4.87±0.01
Cathodei-DNA	65906	16.12±0.06	4.29±0.00
Cathodef-DNA	61741	35.48±0.09	4.57±0.00
ADPh1-cDNA	163191	7.55±0.03	3.07±0.01
ADPh2-cDNA	152610	7.26±0.04	3.39±0.01
ADPh3-cDNA	214052	6.54±0.03	2.78±0.01
Anodei-cDNA	147740	8.58±0.05	3.71±0.01
Anodef-cDNA	171251	9.24±0.05	3.54±0.01
Cathodei-cDNA	56424	3.65±0.00	4.53±0.00
Cathodef-cDNA	93469	5.22±0.02	3.01±0.01
Archaea			
ADPh1-DNA	97511	2.87±0.01	1.67±0.01
ADPh2-DNA	59777	3.41±0.00	2.10±0.00
ADPh3-DNA	71736	3.33±0.01	1.84±0.00
Anodei-DNA	183422	1.58±0.00	1.18±0.01
Anodef-DNA	140800	2.83±0.01	1.90±0.01
Cathodei-DNA	220361	1.77±0.01	1.44±0.01
Cathodef-DNA	92290	4.92±0.02	2.40±0.01
ADPh1-cDNA	59671	3.95±0.00	2.26±0.00
ADPh2-cDNA	82628	5.97±0.02	2.61±0.00
ADPh3-cDNA	91203	6.75±0.02	2.54±0.00
Anodei-cDNA	125143	2.02±0.01	1.60±0.01
Anodef-cDNA	99696	6.35±0.02	2.55±0.01
Cathodei-cDNA	99324	2.37±0.01	1.76±0.01
Cathodef-cDNA	64740	4.61±0.01	2.23±0.00

a)

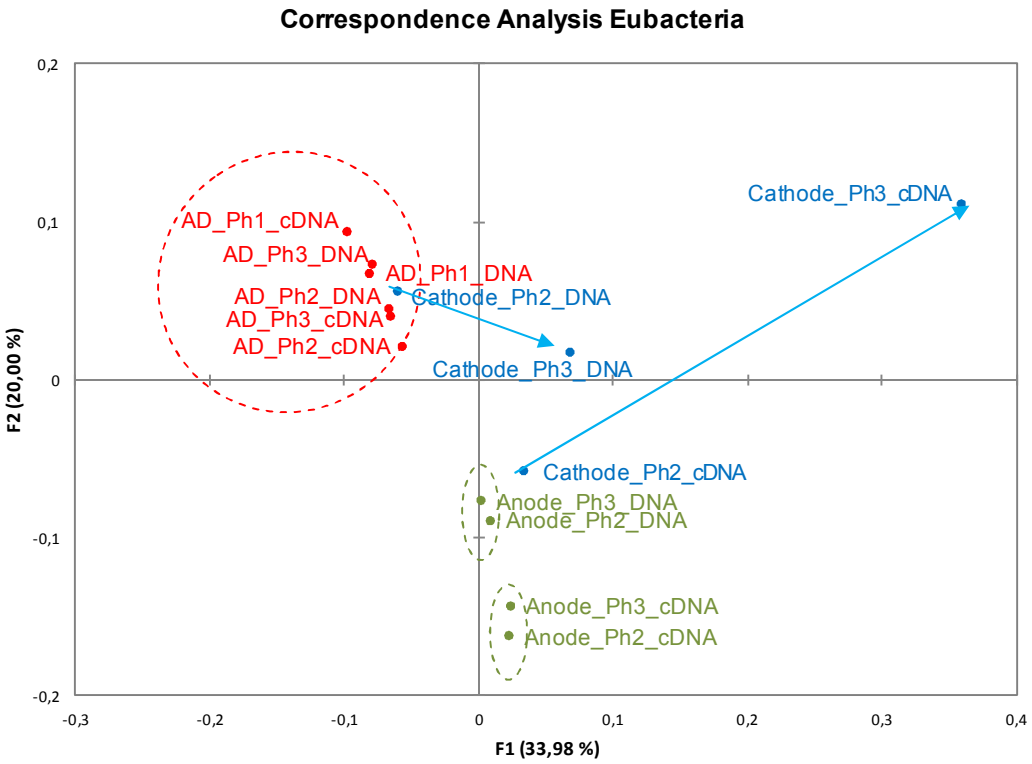

b)

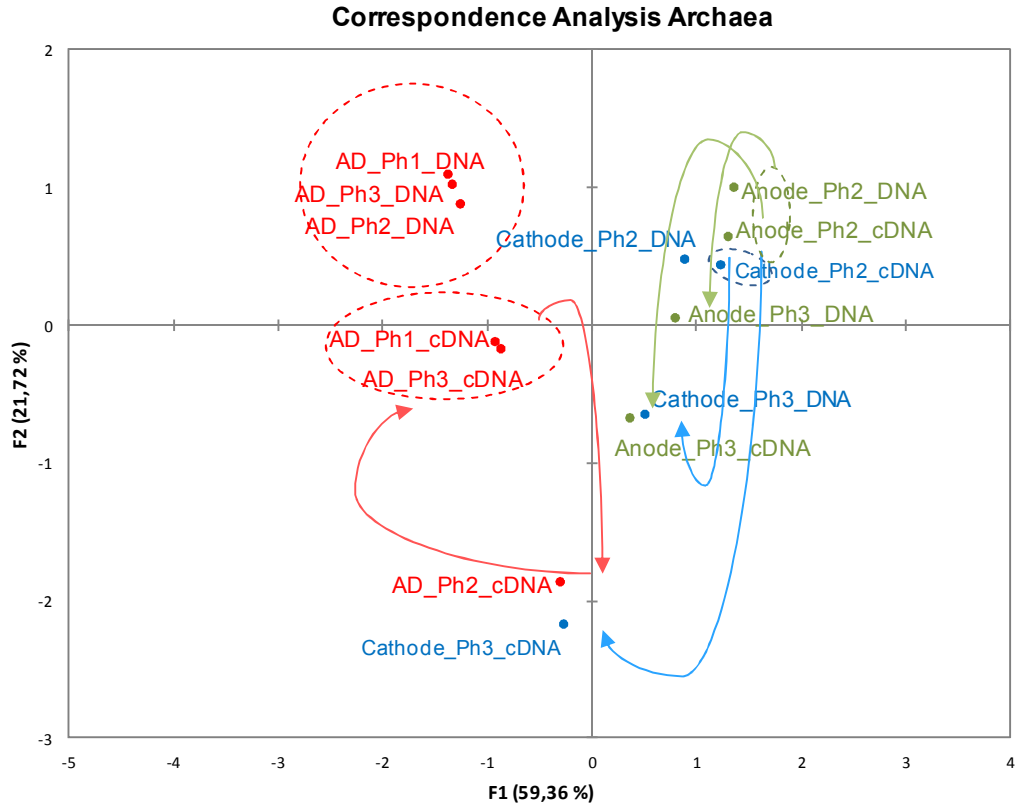

Figure 11.7 Correspondence Analysis of the AD effluent at the end of Phases 1, 2 and 3, and the biofilm harboured on the anode and cathode of the MEC at the end of Phase 2 and 3 for DNA and cDNA samples regarding (a) Eubacteria and (b) Archaea community.

11.4 Conclusions

The integration of anaerobic digestion (AD) and a microbial electrolysis cell (MEC) with a methanogenic biocathode has proven to be a promising strategy to treat high strength wastewaters. The methane production of the AD could be recovered after the inhibition of the reactor due to the doubling of the organic and nitrogen loading rate thanks to the connexion of a recirculation loop with the MEC. Ammonium removal in the anode compartment of the MEC achieved 14.46 g $N\text{-}NH_4^+$ m^{-2} d^{-1}, while obtaining on average 79 L CH_4 m^{-3} d^{-1} through the conversion of CO_2 in the cathode compartment. The microbial analysis showed that methylotrophic *Methanossiliicoccaceae* family (*Methanomassiliicoccus* genus) was the most abundant among active archaea in the AD during the inhibited state. On the other hand, in the cathode *Methanobacteriaceae* family (*Methanobrevibacter* and *Methanobacterium* genus), usually found to be the most abundant in methanogenic biocathodes, shared dominance with *Methanomassiliicoccaceae* (*Methanomassiliicoccus* genus) and *Methanotrichaceae* (*Methanothrix* genus) families.

11.5 References

Angelidaki, I., Ahring, B.K. 1993. Thermophilic anaerobic digestion of livestock waste: the effect of ammonia. *Applied Microbiology and Biotechnology*, **38**(4), 560-564.

Bonmatí, A., Sotres, A., Mu, Y., Rozendal, R.A., Rabaey, K. 2013. Oxalate degradation in a bioelectrochemical system: Reactor performance and microbial community characterization. *Bioresource Technology*, **143**(0), 147-153.

Borrel, G., O'Toole, P.W., Harris, H.M.B., Peyret, P., Brugère, J.-F., Gribaldo, S. 2013. Phylogenomic Data Support a Seventh Order of Methylotrophic Methanogens and Provide Insights into the Evolution of Methanogenesis. *Genome Biology and Evolution*, **5**(10), 1769-1780.

Catal, T., Cysneiros, D., O'Flaherty, V., Leech, D. 2011. Electricity generation in single-chamber microbial fuel cells using a carbon source sampled from anaerobic reactors utilizing grass silage. *Bioresource Technology*, **102**(1), 404-410.

Cerrillo, M., Oliveras, J., Viñas, M., Bonmatí, A. 2016a. Comparative assessment of raw and digested pig slurry treatment in bioelectrochemical systems. *Bioelectrochemistry*, **110**, 69-78.

Cerrillo, M., Viñas, M., Bonmatí, A. 2016b. Overcoming organic and nitrogen overload in thermophilic anaerobic digestion of pig slurry by coupling a microbial electrolysis cell. *Bioresource Technology*, **216**, 362-372.

Cheng, S., Xing, D., Call, D.F., Logan, B.E. 2009. Direct biological conversion of electrical current into methane by electromethanogenesis. *Environmental Science & Technology*, **43**(10), 3953-3958.

Dridi, B., Fardeau, M.-L., Ollivier, B., Raoult, D., Drancourt, M. 2012. *Methanomassiliicoccus luminyensis* gen. nov., sp. nov., a methanogenic archaeon isolated from human faeces. *International Journal of Systematic and Evolutionary Microbiology*, **62**(8), 1902-1907.

Durruty, I., Bonanni, P.S., González, J.F., Busalmen, J.P. 2012. Evaluation of potato-processing wastewater treatment in a microbial fuel cell. *Bioresource Technology*, **105**(0), 81-87.

Ge, X., Yang, L., Sheets, J.P., Yu, Z., Li, Y. 2014. Biological conversion of methane to liquid fuels: Status and opportunities. *Biotechnology Advances*, **32**(8), 1460-1475.

Ge, Z., Zhang, F., Grimaud, J., Hurst, J., He, Z. 2013. Long-term investigation of microbial fuel cells treating primary sludge or digested sludge. *Bioresource Technology*, **136**(0), 509-514.

Hansen, K.H., Angelidaki, I., Ahring, B.K. 1998. Anaerobic digestion of swine manure: inhibition by ammonia. *Water Research*, **32**(1), 5-12.

Hori, T., Haruta, S., Sasaki, D., Hanajima, D., Ueno, Y., Ogata, A., Ishii, M., Igarashi, Y. 2015. Reorganization of the bacterial and archaeal populations associated with organic loading conditions in a thermophilic anaerobic digester. *Journal of Bioscience and Bioengineering*, **119**(3), 337-344.

Hou, Y., Zhang, R., Luo, H., Liu, G., Kim, Y., Yu, S., Zeng, J. 2015. Microbial electrolysis cell with spiral wound electrode for wastewater treatment and methane production. *Process Biochemistry*, **50**(7), 1103-1109.

Kuntke, P., Smiech, K.M., Bruning, H., Zeeman, G., Saakes, M., Sleutels, T.H.J.A., Hamelers, H.V.M., Buisman, C.J.N. 2012. Ammonium recovery and energy production from urine by a microbial fuel cell. *Water Research*, **46**(8), 2627-2636.

Liu, H., Ramnarayanan, R., Logan, B.E. 2004. Production of electricity during wastewater treatment using a single chamber microbial fuel cell. *Environmental Science & Technology*, **38**(7), 2281-2285.

Liu, Y., Qin, M., Luo, S., He, Z., Qiao, R. 2016. Understanding Ammonium Transport in Bioelectrochemical Systems towards its Recovery. *Scientific Reports*, **6**, 22547.

Marshall, C.W., Ross, D.E., Fichot, E.B., Norman, R.S., May, H.D. 2012. Electrosynthesis of commodity chemicals by an autotrophic microbial community. *Applied and Environmental Microbiology*, **78**(23), 8412-8420.

Min, B., Kim, J., Oh, S., Regan, J.M., Logan, B.E. 2005. Electricity generation from swine wastewater using microbial fuel cells. *Water Research*, 39(20), 4961-4968.

Moestedt, J., Müller, B., Westerholm, M., Schnürer, A. 2016. Ammonia threshold for inhibition of anaerobic digestion of thin stillage and the importance of organic loading rate. *Microbial Biotechnology*, **9**(2), 180-194.

Rotaru, A.-E., Shrestha, P.M., Liu, F., Shrestha, M., Shrestha, D., Embree, M., Zengler, K., Wardman, C., Nevin, K.P., Lovley, D.R. 2014. A new model for electron flow during anaerobic digestion: direct interspecies electron transfer to Methanosaeta for the reduction of carbon dioxide to methane. *Energy & Environmental Science*, **7**(1), 408-415.

Ryckebosch, E., Drouillon, M., Vervaeren, H. 2011. Techniques for transformation of biogas to biomethane. *Biomass and Bioenergy*, **35**(5), 1633-1645.

Siegert, M., Yates, M.D., Spormann, A.M., Logan, B.E. 2015. Methanobacterium dominates biocathodic archaeal communities in methanogenic microbial electrolysis cells. *ACS Sustainable Chemistry & Engineering*, **3**(7), 1668-1676.

Sotres, A., Cerrillo, M., Viñas, M., Bonmatí, A. 2015a. Nitrogen recovery from pig slurry in a two-chambered bioelectrochemical system. *Bioresource Technology*, **194**, 373-382.

Sotres, A., Díaz-Marcos, J., Guivernau, M., Illa, J., Magrí, A., Prenafeta-Boldú, F.X., Bonmatí, A., Viñas, M. 2015b. Microbial community dynamics in two-chambered microbial fuel cells: effect of different ion exchange membranes. *Journal of Chemical Technology & Biotechnology*, **90**(8), 1497-1506.

Sotres, A., Tey, L., Bonmatí, A., Viñas, M. 2016. Microbial community dynamics in continuous microbial fuel cells fed with synthetic wastewater and pig slurry. *Bioelectrochemistry*, **111**, 70-82.

Taher, E., Chandran, K. 2013. High-Rate, High-Yield Production of Methanol by Ammonia-Oxidizing Bacteria. *Environmental Science & Technology*, **47**(7), 3167-3173.

Tuan, N.N., Chang, Y.C., Yu, C.P., Huang, S.L. 2014. Multiple approaches to characterize the microbial community in a thermophilic anaerobic digester running on swine manure: a case study. *Microbiological Research*, **169**(9-10), 717-24.

Van Eerten-Jansen, M.C.A.A., Heijne, A.T., Buisman, C.J.N., Hamelers, H.V.M. 2011. Microbial electrolysis cells for production of methane from CO2: long-term performance and perspectives. *International Journal of Energy Research*, **36**(6), 809-819.

Van Eerten-Jansen, M.C.A.A., Veldhoen, A.B., Plugge, C.M., Stams, A.J.M., Buisman, C.J.N., Ter Heijne, A. 2013. Microbial community analysis of a methane-producing biocathode in a bioelectrochemical system. *Archaea*, **2013**, 12.

Villano, M., Monaco, G., Aulenta, F., Majone, M. 2011. Electrochemically assisted methane production in a biofilm reactor. *Journal of Power Sources*, **196**(22), 9467-9472.

Villano, M., Scardala, S., Aulenta, F., Majone, M. 2013. Carbon and nitrogen removal and enhanced methane production in a microbial electrolysis cell. *Bioresource Technology*, **130**, 366-371.

Xu, H., Wang, K., Holmes, D.E. 2014. Bioelectrochemical removal of carbon dioxide (CO2): An innovative method for biogas upgrading. *Bioresource Technology*, **173**, 392-398.

Zeppilli, M., Villano, M., Aulenta, F., Lampis, S., Vallini, G., Majone, M. 2014. Effect of the anode feeding composition on the performance of a continuous-flow methane-producing microbial electrolysis cell. *Environmental Science and Pollution Research*, **22**(10), 7349-7360.

Zhang, C., Yuan, Q., Lu, Y. 2014. Inhibitory effects of ammonia on methanogen mcrA transcripts in anaerobic digester sludge. *FEMS Microbiology Ecology*, **87**(2), 368-77.

Zhang, X., He, W., Ren, L., Stager, J., Evans, P.J., Logan, B.E. 2015. COD removal characteristics in air-cathode microbial fuel cells. *Bioresource Technology*, **176**(0), 23-31.

Zhang, X., Zhu, F., Chen, L., Zhao, Q., Tao, G. 2013. Removal of ammonia nitrogen from wastewater using an aerobic cathode microbial fuel cell. *Bioresource Technology*, **146**(0), 161-168.

Zhang, Y., Angelidaki, I. 2015. Counteracting ammonia inhibition during anaerobic digestion by recovery using submersible microbial desalination cell. *Biotechnology and Bioengineering*, **112**(7), 1478-1482.

Zhen, G., Kobayashi, T., Lu, X., Xu, K. 2015. Understanding methane bioelectrosynthesis from carbon dioxide in a two-chamber microbial electrolysis cells (MECs) containing a carbon biocathode. *Bioresource Technology*, **186**, 141-148.

CHAPTER 12

General conclusions

12.1 General conclusions

The main objective of this Thesis was to study the integration of AD and BES in order to optimise energy production and nitrogen recovery, as well as the resilience of the combined process, during the treatment of a complex waste stream (pig slurry). This chapter summarises the main conclusions obtained from the research performed.

1. Regarding the energy production optimisation of an integrated AD-BES system with ammonia recovery by a stripping and absorption system, both in MFC and MEC mode operation the main conclusions are:

1.1 In batch assays, the AD-MEC integrated system achieved the maximum COD removal efficiency (60%). The use of NaCl solution as catholyte increased the pH (>10), which favours ammonium recovering in a subsequent stripping and absorption process. However, the highest ammonia removal efficiencies were achieved in MFC mode (40%).

Desulfuromonadaceae was highly enriched in MEC mode on the anode, whereas phylotypes belonging to the potential methylotrofic-hydrogenotrophic methanogen *Thermoplasmatales* were also more favoured than acetotrophic *Methanosaetaceae*.

1.2 In an integrated AD-MFC system the COD and ammonium removal was enhanced during the inhibition of the AD reactor with respect to the stable phase, with maximums of 40% and 31%, respectively.

A reduction of the biodiversity of the microbial populations was observed in the MFC anode. Main enriched populations in the anode (MFC) belonged to Bacteroidetes (*Flavobacteriaceae), Chloroflexi* (fermentative bacteria *Anaerolineaceae), Methanosarcinaceae* and hydrogenotrophic methanogens belonging to *Methanobacteriaceae* family.

1.3 Ammonium diffusion from the anode to the cathode compartment was enhanced during AD malfunction episodes (VFA pulses) in an integrated AD-MEC system, similarly to the behaviour observed with the AD-MFC. VFA were fast removed, concomitant with an increase in current density after the pulse, especially when acetate was added.

1.4 The AD-MEC combined system in series achieved COD removal and ammonia recovering of 46% and 40%, respectively. The methane productivity of the AD increased 55% with a recirculation loop configuration, after doubling the OLR and NLR.

Methanogenic populations increased when AD-MEC was connected with a loop configuration, whereas a clear shift in eubacterial population promoting *Proteobacteria* family relative prevalence was revealed. AD increased in biodiversity, while the MEC biofilm showed a reduction in biodiversity, as it was observed previously with the MFC, although in this case it was enriched in *Methanotrichaceae* family.

1.5 The assessment of metabolically active populations by means of simultaneous DNA and RNA-based method showed the stability of the MEC consortium in spite of the alteration of the AD microbial population due to the stress. Although *Methanobacteriaceae* dominated among population present in the AD, *Methanomicrobiaceae* revealed as the most active family. *Desulfuromonadaceae* was the most active family in the MEC anode, although not being the predominant one in total population.

2. Regarding the study of the conversion of CO_2 into CH_4 by the electromethanogenic process operating a MEC with a biocathode in combination with AD the main conclusions are:

2.1 The operation of the UASB with methanol feed resulted in a biomass enrichment with methanogenic archaea. The methylotrophic methanogenic metabolic pathway (represented by the genus *Methanomethylovorans* and *Methanoglobus*) seems to be the predominant pathway at the end of the UASB operation, followed by the acetoclastic one (owned by the genus *Methanothrix (Methanosaeta*)) while the hydrogenotrophic route showed a low activity.

2.2 The origin of the biomass used as inoculum in the biocathodes had little influence on CH_4 production or cathodic methane recovery efficiency.

Despite the different composition of the two initial inocula, the archaeal communities on both biocathodes at the end of the assay were very similar, highly dominated by hydrogenotrophic methanogenic archaea, especially in *Methanobacteriaceae* family (belonging mainly to well known hydrogenotrophic *Methanobrevibacter*), being also the most active one.

2.3 The integration of AD and a MEC with a methanogenic biocathode removed 14.46 g N-NH_4^+ m^{-2} d^{-1} from the anode compartment of the MEC, while obtaining on average 79 L CH_4 m^{-3} d^{-1} through the conversion of CO_2 in the cathode compartment.

The methylotrophic *Methanossiliicoccaceae* family (*Methanomassiliicoccus* genus) was the most abundant among active archaea in the AD during the inhibited state. In the biocathode, *Methanobacteriaceae* family (*Methanobrevibacter* and *Methanobacterium* genus), shared relative dominance with *Methanotrichaceae* and *Methanomassiliicoccaceae* families.

Considering these conclusions, the integration of AD with BES technology could be an alternative strategy to optimise energy and nutrients recovery from complex waste streams. The inhibition of the AD due to organic or nitrogen overload can be prevented or corrected, and the digestate would maintain its quality whenever the AD became unstable. Ammonium can be recovered for its reuse as fertiliser. The biogas produced by the AD could achieve the purity requirements for the injection in the gas natural grid or the use as transport fuel. And finally, microbial composition of each reactor maintains well differentiated in spite of the connexion, and the increase in biodiversity in the integrated system may increase its resilience to stress.

12.2 Future work

In this Thesis it has been shown that BES can be integrated with AD to overcome some of the limitations that AD presents. In order to achieve an efficient technology suitable for future full scale application, further work has to be undertaken.

In the first place, the results obtained from the different assays performed can be useful to develop a mathematical model, in order to predict volatile fatty acids (VFA), chemical oxygen demand (COD) or ammonia removal in a BES. Even its integration with an AD with a recirculation loop could be modelled as a valuable tool to predict the AD evolution with different recirculation rates.

Secondly, the set up and operation of a pilot scale AD-MEC-Stripping system would be need as a proof of concept to demonstrate the feasibility of this configuration to optimise energy and ammonia recovery from complex streams. The information obtained in this operation would be highly valuable in order to implement this technology at full scale.

RNA-based high throughput sequencing and quantification of microbial populations has to be further assessed in order to be used as a tool to predict the behaviour of the reactors under different conditions.

BES could be employed to recover other nutrients present in the digestates, such as phosphates. Further research is needed to integrate this application with AD and combine the recovery of different nutrients at the same time.

Methane production and recovery in the MEC with electromethanogenic biocathode has to be optimised. The study of the generation of other products, such as VFA, is needed to understand the different processes that take place at the biocathode.

Besides, the assays developed with the integrated AD-MEC-biocathode systems have been performed with the utilisation of buffered medium as catholyte. Since the use of a buffered medium limits the increase of pH in the cathode compartment (Chapter 4), the recovery of ammonia by stripping and absorption would be reduced. In order to improve ammonia recovery from the cathode compartment, removal of the buffer from the catholyte has to be assessed, especially regarding the effect the increase of pH could have over electromethanogenic biomass.

Finally, metatranscriptomic techniques can give information about which physiological processes are active and which bacteria are carrying them out. This analysis will increase the knowledge about syntrophic relations and active pathways for the biosynthesis of organic compounds at the cathode.